TESIS DOCTORAL

Analysis and numerical simulation of Network of Noisy Leaky Integrate and Fire neuron models

Programa de doctorado de Física y Matemáticas (FisyMat)

**UNIVERSIDAD
DE GRANADA**

Ricarda Schneider

Directores:

María J. Cáceres y José Miguel Mantas

Granada, 2017

A mi abuelo
Manfred, q.d.e.p.

La doctoranda Ricarda Schneider y los directores de la tesis María J. Cáceres y José Miguel Mantas garantizamos, al firmar esta tesis doctoral, que el trabajo ha sido realizado por el doctorando bajo la dirección de los directores de la tesis y hasta donde nuestro conocimiento alcanza, en la realización del trabajo, se han respetado los derechos de otros autores a ser citados, cuando se han utilizado sus resultados o publicaciones.
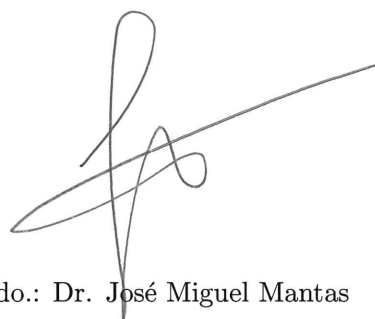
Granada, 16 Noviembre 2017

La doctoranda

Fdo.: Ricarda Schneider

Los directores

Fdo.: Dr. María J. Cáceres   Fdo.: Dr. José Miguel Mantas

The doctoral candidate Ricarda Schneider and the thesis supervisors guarantee, by signing this doctoral thesis, that the work has been done by the doctoral candidate under the direction of the thesis supervisor/s and, as far as our knowledge reaches, in the performance of the work, the rights of other authors to be cited (when their results or publications have been used) have been respected.
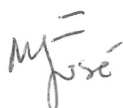
Granada, 16 Noviembre 2017

Doctoral Candidate

Fdo.: Ricarda Schneider

Thesis supervisors

Fdo.: Dr. María J. Cáceres   Fdo.: Dr. José Miguel Mantas

x

Agradecimientos

Contents

Introducción

El cerebro es uno de los órganos más perfectos, complejos y a la vez fascinantes de nuestro cuerpo. Gracias a él, entre otros, tomamos consciencia de nosotros mismos, experimentamos todo tipo de emociones, usamos el lenguaje, transformamos nuestro entorno y entendemos el porqué del mundo que nos rodea. Usando la potente herramienta que nos proporciona, hemos descifrado una parte importante de los complejos mecanismos biológicos, químicos, físicos, etc, subyacentes a los acontecimientos de la naturaleza, lo cual nos ha permitido desarrollar medicinas, construir impresionantes infraestructuras, crear la inteligencia artificial, etc. Por otro lado, en el cerebro también hay cabida para disciplinas menos científicas, y más inherentes al ser humano, como lo son la cultura, la música, la creación de obras de arte, la literatura, la religión y demás humanidades. En esta dirección le debemos, además, la capacidad única de expresarnos mediante el lenguaje y de suprimir o/y controlar nuestros instintos más ancestrales para vivir en sociedad de forma pacífica.

Sin embargo, aunque cada vez se entiende mejor el complicadísimo mecanismo que usa el cerebro para abarcar todas estas áreas, aún quedan muchas preguntas abiertas. Descifrar totalmente su funcionamiento no sólo nos ayudará a entendernos a nosotros mismos y nuestro lugar en el universo un poco mejor, sino que también proporcionará alivio a todas aquellas personas aquejadas de diversas patologías cerebrales: depresión, trastornos obsesivos compulsivos, epilepsia, Alzheimer, etc.

La investigación para continuar desvelando el enigma del cerebro (y del sistema nervioso en general) se lleva a cabo desde diversas perspectivas. La parte experimental es crucial para alcanzar este objetivo, pero también el modelado desempeña un papel importante. En concreto, existen numerosos modelos que se aplican habitualmente en neurociencia para traducir el comportamiento biológico de una red neuronal a una ecuación matemática. Este procedimiento permite determinar la evolución a lo largo del tiempo de dicha red por medio del análisis de las soluciones de la ecuación matemática resultante. Por lo tanto, aquí es donde las matemáticas aportan sus granos de arena a la duna que suponen todas las investigaciones relacionadas con el cerebro y el sistema nervioso en general.

Centrándonos ahora más en el análisis de los modelos matemáticos, que es la cuestión que se pretende abordar en esta tesis, podemos decir que este estudio generalmente se lleva a cabo tanto desde el punto de vista analítico como numérico. Además, distinguiremos entre modelos microscópicos y modelos mesoscópicos. Los primeros describen la evolución de la red a partir del comportamiento de cada una de las neuronas que la forman. En consecuencia, consisten en sistemas de ecuaciones, con frecuencia de tipo estocástico, donde cada una de las ecuaciones describe el comportamiento de una de las neuronas de la red. Sin embargo, aunque hay muchos trabajos que realizan simulaciones numéricas directamente para los modelos microscópicos usando el método de Monte-Carlo [21, 23, 69, 70, 80, 82, 84, 89], desde el punto de vista computacional es complicado manejar estos modelos para redes neuronales integradas por un gran número de neuronas. Surge, por lo tanto, la necesidad de deducir modelos mesoscópicos, los cuales permiten determinar la evolución de la red por medio de funciones de densidad que son soluciones de una (o pocas) Ecuaciones en Derivadas Parciales (EDPs). Este procedimiento se lleva

a cabo, p.e., en [7, 32, 46, 47, 52, 58, 71, 72, 99, 105]. Además, con los modelos mesoscópicos se pueden recuperar cantidades macroscópicas como lo son, p.e., la tasa de disparo global de la red, que permiten comparar los resultados obtenidos con los de los modelos microscópicos por medio de dichas magnitudes.

En esta tesis se pretende estudiar el comportamiento de las soluciones de algunos de estos modelos mesoscópicos en esa doble vertiente: analítica y numérica. En concreto, nos centraremos en el modelo No Lineal de Integración y Disparo (sus siglas en inglés NNLIF) que mediante EDPs de tipo Fokker-Planck determina a nivel mesoscópico la evolución en tiempo del comportamiento de una red neuronal cuyas neuronas están descritas a nivel microscópico por el modelo de Integración y Disparo (IF, en inglés).

Para entender bien este modelo comenzaremos explicando el funcionamiento de las neuronas, descrito a través de varios modelos microscópicos. Después deduciremos el modelo NNLIF a partir del modelo microscópico subyacente. Una vez entendido el modelo que estudiaremos en este trabajo, ofreceremos un amplio repaso a la literatura relacionada para dejar claro el punto de partida de nuestra investigación. Finalmente, concluiremos esta introducción con los aspectos más relevantes de los resultados obtenidos en esta tesis.

0.1   Fisiología de las neuronas

La neurona es una célula altamente especializada que se encarga de la recepción y propagación de impulsos nerviosos. Para enviar un impulso nervioso las neuronas generan *potenciales de acción*, que son impulsos eléctricos que aparecen en respuesta a los estímulos que reciben: bien el inicio del potencial de acción se crea en la neurona o bien la neurona sólo se encarga de propagar el impulso nervioso que recibe de otra neurona. Estos impulsos llegan a las neuronas por las dentritas, viajan por el axón y pasan de unas a otras por medio de las *sinapsis*, gracias a la acción de los neurotransmisores. Hay que tener en cuenta que el envío y recepción del impulso nervioso de una neurona a otra no es un proceso inmediato, sino que desde que la señal sale de la neurona presináptica hasta que llega a la neurona postsináptica transcurre un pequeño periodo de tiempo conocido como *retraso sináptico*. Por otro lado, las señales que reciben de otras neuronas pueden ser *excitadoras* o *inhibidoras* dependiendo de si incrementan o disminuyen la probabilidad de que ocurra un potencial de acción.

Veamos ahora con detalle cuál es el mecanismo subyacente que hace aparecer los potenciales de acción [36, 51, 101]. En el interior de la neurona, entre otros, se encuentran diferentes iones, como lo son el sodio Na^+ y el potasio K^+. La membrana de las neuronas es impermeable frente a estos iones, pero presenta unos *canales iónicos* que, en ciertas situaciones, permiten el paso de iones desde el interior de la membrana al exterior o viceversa. Muchos de estos canales son altamente selectivos, como los del sodio y potasio, y sólo permiten el paso de un tipo de ion. En ausencia de señales, el *potencial de membrana* $V(t)$, que se define como la diferencia de potencial entre el interior de la membrana $V_{int}(t)$ y el exterior $V_{ext}(t)$: $V(t) = V_{int}(t) - V_{ext}(t)$, tiende a un *potencial de equilibrio o reposo* V_{eq}.

El potencial de equilibrio suele encontrarse en torno a $V_{eq} \sim -70mV$. Vemos entonces que en el estado de equilibrio hay un exceso de carga negativa en el interior de la membrana. En este estado, la membrana crea una *capacitancia* que es la capacidad de mantener la diferencia de potencial que da lugar al equilibrio. Esto se consigue gracias a *bombas de iones*, que pasan los iones de un lado a otro de la membrana, según sea necesario. Las bombas de iones necesitan energía para funcionar.

Ahora bien, si aplicamos una corriente a una neurona en forma de impulso nervioso, se pierde el

potencial de reposo. En primer lugar, en respuesta al estímulo, se abren los canales de sodio, de manera que el sodio entra en la neurona a través de la membrana por atracción eléctrica. En consecuencia, aumenta el valor del voltaje del potencial de la membrana. Si llega a alcanzar un cierto valor umbral, V_F, se emite el potencial de acción. Cabe resaltar que si no se alcanza el valor umbral, no se emite un potencial de acción. Además, mientras se abren los canales de sodio, más lentamente se abren los de potasio. En consecuencia, sale potasio de la membrana por la diferencia de concentración, ya que suele haber una concentración de potasio más alta dentro de la célula que en el exterior. La salida del potasio hace que el potencial vuelva a ser negativo. Por último, la bomba de sodio-potasio devuelve a cada ion a su lugar, reestableciendo el potencial de reposo o equilibrio. Además, una vez emitido el potencial de acción, la neurona entra durante un breve espacio de tiempo en un *estado refractario* τ, durante el cual no responde a los estímulos externos.

Veamos ahora cómo podemos traducir este comportamiento a un modelo matemático [36, 60, 51]. La evolución del potencial de membrana V se puede modelar como un circuito eléctrico

$$C_m \frac{dV}{dt}(t) = I(t),$$

donde $I(t)$ es la intensidad de la corriente aplicada. Sin embargo, como en una neurona hay una gran cantidad de canales iónicos activos que influyen directamente sobre el valor del potencial de membrana, tenemos que ampliar la ecuación como sigue:

$$C_m \frac{dV}{dt}(t) = -g_{N_a}(V(t) - V_{N_a}) - g_K(V(t) - V_K) - g_L(V(t) - V_L) + I(t), \tag{1}$$

donde g_i es la *conductancia* del canal asociado al ion i y V_i es el *potencial reverso o de equilibrio* del canal i. Definimos como conductancia la facilidad con la que la carga eléctrica atraviesa el canal, y como potencial reverso el valor del potencial que corresponde a un equilibrio entre los flujos, que van hacia el exterior e interior. Así, si tenemos un canal con potencial reverso V_i y el potencial de membrana es V, si $V > V_i$ las corrientes positivas fluyen hacia fuera a través del canal produciendo una disminución del potencial de membrana y viceversa si $V < V_i$. Además, en el término $I_L(t) := g_L(V(t) - V_L)$, que llamaremos *corriente de fuga* agrupamos todas las aportaciones de los demás iones, distintos al sodio y potasio. Las constantes g_L y V_L se ajustan hasta que coincidan con la conductancia y el potencial reverso restantes de la membrana.

El **modelo de Hodgkin-Huxley (HH)**, obtenido a partir de la observación del axón del calamar por Hodgkin y Huxley en 1952 [54, 55], usa la ecuación (1) para describir la evolución del potencial de membrana unida a tres Ecuaciones Diferenciales Ordinarias (EDOs) que determinan el "estado" en el que se encuentran los canales de sodio y potasio:

$$\begin{aligned}
C_m \frac{dV}{dt}(t) &= -g_{N_a}(V(t) - V_{N_a}) - g_K(V(t) - V_K) - g_L(V(t) - V_L) + I(t), \\
\frac{dh}{dt}(t) &= \alpha_h(V)(1 - h) - \beta_h(V)h, \\
\frac{dm}{dt}(t) &= \alpha_m(V)(1 - m) - \beta_m(V)m, \\
\frac{dn}{dt}(t) &= \alpha_n(V)(1 - n) - \beta_n(V)n,
\end{aligned}$$

3

donde $g_{N_a} = \bar{g}_{N_a} m^3 h$, $g_K = \bar{g}_K n^4$ y g_L son las conductancias del sodio, potasio y de la corriente de fugas, respectivamente, y n, m y h las variables de activación. Los valores de $\alpha_i(V)$ y $\beta_i(V)$ para $i = h, m, n$ son constantes y se obtienen mediante la regresión de datos experimentales.

El **modelo de integración y disparo (IF)**, que se basa en el modelo de Lapicque propuesto en 1907 [48, 60], se obtiene al incluir las corrientes iónicas del sodio y potasio también en el término que agrupa las corrientes de fuga $I_L(t)$. En consecuencia, este modelo supone una simplifación del modelo HH, quedando la ecuación (1) reducida a

$$C_m \frac{dV}{dt}(t) = -g_L(V(t) - V_L) + I(t).$$

Hay otros modelos que son simplificaciones del modelo HH, como lo son el modelo HH para dos dimensiones [44], el modelo de Morris-Lecar [68] y el modelo de Fitzhugh-Nagumo [45], cuya aproximación macroscópica se ha estudiado, p.e, en [2, 67]. Aquí nos hemos centrado en la descripción del modelo simplificado de IF, ya que proporciona la descripción a nivel microscópico del funcionamiento de las neuronas sobre la que se basan los modelos NNLIF que estudiaremos en esta tesis.

0.2   Deducción del modelo NNLIF completo

Con el fin de proporcionar el marco conceptual, matemático y biológico dentro del cual desarrollaremos nuestro trabajo, en esta sección explicamos la obtención de las ecuaciones (EDPs y EDOs) que representan el modelo NNLIF completo a nivel mesoscópico, a partir del modelo biológico que describe el funcionamiento de las neuronas a nivel microscópico. Antes de seguir, referenciamos a [12, 85, 95, 10, 88, 11, 94, 41, 48, 101, 51] para la persona interesada en obtener un conocimiento extenso acerca de diferentes versiones del modelo de IF y su validación como modelo adecuado para ser usado en neurociencia.

Consideramos una red neuronal con n neuronas (n_E excitadoras y n_I inhibidoras) descrita por el modelo IF, que detalla la actividad del potencial de membrana. La evolución en tiempo del potencial de membrana $V_\alpha(t)$ de una neurona inhibidora ($\alpha = I$) o una excitadora ($\alpha = E$) está dada por la siguiente ecuación (véase la sección anterior y [11, 12] para los detalles)

$$C_m \frac{dV^\alpha}{dt}(t) = -g_L(V^\alpha(t) - V_L) + I^\alpha(t), \tag{2}$$

donde C_m es la capacitancia de la membrana, g_L es la conductancia de fugas, V_L es el potencial de fugas reverso y $I^\alpha(t)$ es la corriente sináptica de entrada, que modela todas las interacciones de la neurona con otras neuronas. En ausencia de interacción con otras neuronas ($I^\alpha(t) = 0$), el potencial de membrana tiende hacia un valor de descanso V_L. Sin embargo, la interacción con otras neuronas provoca que la neurona dispare, es decir, que emita un potencial de acción (disparo) cuando $V^\alpha(t)$ alcance su umbral o valor de disparo V_F, y que el potencial de membrana se relaje hacia un valor de reinicio V_R. (Nótese que $V_L < V_R < V_F$). Cada neurona recibe C_{ext} conexiones de neuronas excitadoras que están fuera de la red, y $C = C_E + C_I$ conexiones de neuronas de la red; $C_E = \epsilon\, n_E$ de neuronas excitadoras y $C_I = \epsilon\, n_I$ de neuronas inhibidoras. Estas conexiones se consideran escogidas aleatoriamente, y la red se supone escasamente conectada, en concreto, $\epsilon = \frac{C_E}{n_E} = \frac{C_I}{n_I} << 1$, véase

[11]. La corriente sináptica $I^\alpha(t)$ toma la forma del siguiente proceso estocástico

$$I^\alpha(t) = J_E^\alpha \sum_{i=1}^{\bar{C}_E} \sum_j \delta(t - t_{Ej}^i - D_E^\alpha) - J_I^\alpha \sum_{i=1}^{C_I} \sum_j \delta(t - t_{Ij}^i - D_I^\alpha), \qquad \alpha = E, I,$$

donde $D_E^\alpha \geq 0$, $D_I^\alpha \geq 0$ son los retrasos sinápticos, t_{Ej}^i y t_{Ij}^i son los tiempos del j-disparo procedente de la i-neurona presináptica para neuronas excitadoras e inhibidoras, respectivamente, $\bar{C}_E = C_E + C_{ext}$, y J_k^α, para $\alpha, k = E, I$ son las fuerzas de las sinapsis. El carácter estocástico está contenido en la distribución de los tiempos de disparo de las neuronas. Las secuencias de potenciales de acción de la red se suponen descritas por procesos de Poisson con una tasa de disparo instantánea común, $\nu_\alpha(t)$, $\alpha = E, I$. Estos procesos se supone que son independientes [11, 15]. Usando estas hipótesis, el valor medio de la corriente, $\mu_C^\alpha(t)$, y su varianza, $\sigma_C^{\alpha 2}(t)$, toman la forma para $\alpha = E, I$

$$\begin{align}
\mu_C^\alpha(t) &= C_E J_E^\alpha \nu_E(t - D_E^\alpha) - C_I J_I^\alpha \nu_I(t - D_I^\alpha), \tag{3}\\
\sigma_C^{\alpha 2}(t) &= C_E (J_E^\alpha)^2 \nu_E(t - D_E^\alpha) + C_I (J_I^\alpha)^2 \nu_I(t - D_I^\alpha), \tag{4}
\end{align}$$

donde se necesita la hipótesis de que $C_{ext} = C_E$, para que esten bien definidos.

Muchos autores [11, 12, 65, 73] aproximan ahora la corriente sináptica de entrada por un proceso estocástico de tipo Ornstein-Uhlenbeck continuo en tiempo, que tiene la misma media y varianza que los procesos de Poison de las secuencias de potenciales de acción. En concreto, $I^\alpha(t)$ se aproxima por

$$I^\alpha(t)dt \approx \mu_C^\alpha(t) \ dt + \sigma_C^\alpha(t) \ dB_t, \qquad \alpha = E, I, \tag{5}$$

donde B_t es el movimiento Browniano estándar.

En resumen, la aproximación al modelo de ecuaciones diferenciales estocásticas (2), (donde por simplicidad se toman las unidades de voltaje y tiempo de manera que $C_m = g_L = 1$), finalmente produce

$$dV^\alpha(t) = (-V^\alpha(t) + V_L + \mu_C^\alpha(t)) \ dt + \sigma_C^\alpha(t) \ dB_t, \qquad V^\alpha \leq V_F, \qquad \alpha = E, I, \tag{6}$$

con el proceso de salto $V^\alpha(t_0^+) = V_R$, $V^\alpha(t_0^-) = V_F$, siempre que en t_0 el voltaje alcance el valor umbral V_F.

La tasa de disparo o probabilidad de disparar por unidad de tiempo de la secuencia de potenciales de acción de tipo Poisson, $\nu_\alpha(t)$, se calcula en [85] como

$$\nu_\alpha(t) = \nu_{\alpha,ext} + N_\alpha(t), \qquad \alpha = E, I,$$

donde $\nu_{\alpha,ext}$ es la frecuencia del input externo y $N_\alpha(t)$ es la tasa de disparo media de la población α. Además $\nu_{I,ext} = 0$ ya que las conexiones externas se producen con neuronas excitadoras.

Volviendo a (6), se puede escribir un sistema acoplado de ecuaciones en derivadas parciales para la evolución de las densidades de probabilidad $\rho_\alpha(v, t)$, donde $\rho_\alpha(v, t)$ denota la densidad de probabilidad de encontrar una neurona de la población α, con un voltaje $v \in (-\infty, V_F]$ en un tiempo $t \geq 0$. En [11, 12, 65, 73, 87] tomando límite en $n \to \infty$ y usando la regla de Itô transforman las ecuaciones estocásticas (2) y (5) en un sistema acoplado de tipo Fokker-Planck o ecuaciones de Kolmogorov hacia

atrás con fuentes

$$\begin{cases} \frac{\partial \rho_I}{\partial t}(v,t) + \frac{\partial}{\partial v}[h^I(v, N_E(t-D_E^I), N_I(t-D_I^I))\rho_I(v,t)] - a_I(N_E(t-D_E^I), N_I(t-D_I^I))\frac{\partial^2 \rho_I}{\partial v^2}(v,t) \\ \qquad\qquad\qquad\qquad\qquad\qquad\qquad\qquad\qquad\qquad\qquad = M_I(t)\delta(v-V_R), \\ \\ \frac{\partial \rho_E}{\partial t}(v,t) + \frac{\partial}{\partial v}[h^E(v, N_E(t-D_E^E), N_I(t-D_I^E))\rho_E(v,t)] - a_E(N_E(t-D_E^E), N_I(t-D_I^E))\frac{\partial^2 \rho_E}{\partial v^2}(v,t) \\ \qquad\qquad\qquad\qquad\qquad\qquad\qquad\qquad\qquad\qquad\qquad = M_E(t)\delta(v-V_R), \end{cases} \tag{7}$$

siendo $h^\alpha(v, N_E(t-D_E^\alpha), N_I(t-D_I^\alpha)) = -v + V_L + \mu_C^\alpha$ y $a_\alpha(N_E(t-D_E^\alpha), N_I(t-D_I^\alpha)) = \frac{\sigma_C^{\alpha 2}}{2}$. Las partes derechas de (7) representan el hecho de que las neuronas, cuando alcanzan el valor umbral V_F, emiten un disparo o potencial de acción sobre la red, reinician su potencial de membrana al valor de reinicio V_R y permanecen algún tiempo en un periodo refractario, notado por τ_α. Se pueden considerar diferentes elecciones de $M_\alpha(t)$: $M_\alpha(t) = N_\alpha(t-\tau_\alpha)$, estudiado en [11] o $M_\alpha(t) = \frac{R_\alpha(t)}{\tau_\alpha}$ propuesto en [17]. En consecuencia, el sistema (7) se completa con dos EDOs para $R_\alpha(t)$, las probabilidades de encontrar una neurona de la población α en estado refractario

$$\frac{dR_\alpha(t)}{dt} = N_\alpha(t) - M_\alpha(t), \quad \forall \alpha = E, I, \tag{8}$$

y con las condiciones de contorno de Dirichlet y los datos iniciales

$$\rho_\alpha(-\infty, t) = 0, \ \rho_\alpha(V_F, t) = 0, \ \rho_\alpha(v, 0) = \rho_\alpha^0(v) \geq 0, \quad R_\alpha(0) = R_\alpha^0 \geq 0 \quad \alpha = E, I. \tag{9}$$

Para simplificar la notación, notamos $d_k^\alpha = C_k(J_k^\alpha)^2 \geq 0$ y $b_k^\alpha = C_k J_k^\alpha \geq 0$ para $k, \alpha = E, I$, y la variable v se cambia por otra usando el cambio $\bar{v} = v + V_L + b_E^E \nu_{E,ext}$. Observemos que mantenemos la misma notación para los otros valores involucrados (V_R, V_F) y también v para la variable nueva. Con esta nueva variable de voltaje y usando las expresiones (3) y (4) para $\mu_C^\alpha(t)$ y $\sigma_C^\alpha(t)$, los coeficientes de deriva y difusión se convierten en

$$h^\alpha(v, N_E(t-D_E^\alpha), N_I(t-D_I^\alpha)) = -v + b_E^\alpha N_E(t-D_E^\alpha) - b_I^\alpha N_I(t-D_I^\alpha) + (b_E^\alpha - b_E^E)\nu_{E,ext}, \tag{10}$$
$$a_\alpha(N_E(t-D_E^\alpha), N_I(t-D_I^\alpha)) = d_E^\alpha \nu_{E,ext} + d_E^\alpha N_E(t-D_E^\alpha) + d_I^\alpha N_I(t-D_I^\alpha), \quad \alpha = E, I. \tag{11}$$

El acoplamiento del sistema (7) está escondido en estos dos términos ya que las tasas de disparo medias N_α obedecen a

$$N_\alpha(t) = -a_\alpha(N_E(t), N_I(t))\frac{\partial \rho_\alpha}{\partial v}(V_F, t) \geq 0, \quad \alpha = E, I. \tag{12}$$

Además, (12) da lugar a la no-linealidad del sistema (7), ya que las tasas de disparo están definidas en términos de funciones de distribución ρ_α. Por otro lado, ya que R_E, R_I, son probabilidades y ρ_E y ρ_I representan densidades de probabilidad, la masa total deber ser conservada:

$$\int_{-\infty}^{V_F} \rho_\alpha(v,t)\,dv + R_\alpha(t) = \int_{-\infty}^{V_F} \rho_\alpha^0(v)\,dv + R_\alpha^0 = 1 \quad \forall\, t \geq 0, \quad \alpha = E, I.$$

0.3 Otros modelos

Una vez detallado el modelo NNLIF completo, conviene mencionar que hay una gran cantidad de modelos matemáticos que comparten con el modelo NNLIF el objetivo de describir el comportamiento de redes neuronales a través de EDPs. A continuación se presentan algunos de los modelos en los que se ha empezado a trabajar con perspectiva de investigaciones futuras a llevar a cabo tras la finalizacin de esta tesis, ya que mantienen un estrecho lazo con el modelo NNLIF. Entre otros, se pretende establecer relaciones entre ellos, siguiendo las ideas de, p.e., [42].

- **Modelos estructurados por edad o de Pakdaman, Perthame y Salort (PPS).** En este modelo la dinámica de una red neuronal a nivel mesoscópico se describe a través de una EDP que recuerda a los modelos estructurados por edad, aplicados habitualmente en ecología y exhaustivamente estudiados, p. e., en [77]. La incógnita es una densidad de probabilidad $n(s,t)$ que determina la probabilidad de encontrar una neurona de "edad" s en el instante de tiempo t. En este caso la "edad" se refiere al tiempo transcurrido desde el último disparo. El modelo, ampliamente estudiado en [74], [75] y [76], responde a:

$$\begin{cases} \frac{\partial}{\partial t}n(s,t) + \frac{\partial}{\partial s}n(s,t) + p\left(s, X(t)\right)n(s,t) = 0, \\[2mm] X(t) = J\int_0^t \alpha(s)N(t-s)\,ds \text{ si hay retraso}, \\[2mm] X(t) = JN(t) \text{ si no hay retraso}, \\[2mm] N(t) := n(0,t) = \int_0^\infty p\left(s, X(t)\right)n(s,t)\,ds, \end{cases}$$

donde las funciones no-negativas $\alpha(s)$ y $p(s,x)$ tienen que satisfacer las siguientes hipótesis de modelado

$$\int_0^\infty \alpha(s)\,ds = 1, \qquad \alpha(.) \geq 0,$$

$$\frac{\partial}{\partial s}p(s,x) \geq 0, \quad p(s,x) = 0 \text{ para } s \in (0, s^*(x)), \quad p(s,x) > 0 \text{ para } s > s^*(x), \quad p(s,x) \xrightarrow[s\to\infty]{} 1,$$

$$\frac{\partial}{\partial x}p(s,x) \geq 0, \qquad p(s,x) \xrightarrow[x\to\infty]{} 1.$$

El significado biológico de las funciones y el parámetro que aparecen en este modelo son:

  - $N(t)$ es la densidad de neuronas que disparan en tiempo t,
  - $\alpha(s) \geq 0$ es la función de retraso distribuida,
  - $X(t)$ es la actividad neuronal global en el tiempo t,
  - $p(s, X)$ es la tasa de disparo de las neuronas en estado s y con actividad global X,
  - $J \geq 0$ representa la conectividad de la red.

Algunos aspectos relevantes que se estudian en los trabajos citados consisten en analizar el comportamiento de las soluciones en función de los parámetros y funciones variables del modelo: estados estacionarios, existencia de solución, convergencia hacia un estado estacionario y oscilaciones periódicas espontáneas. Estos resultados teóricos se ilustran y complementan con simulaciones numéricas. Además, en [42] se encuentra una transformada integral que permite

reescribir una solución del modelo PPS como una solución del modelo NNLIF para un término de deriva de la forma $h(v, N) = \mu - v$ con $\mu \in \mathbb{R}$ constante y un término de difusión constante $a(N) = \frac{\sigma^2}{2}$, que evitan la no-linealidad del modelo.

Por otro lado, hay varios trabajos que relacionan el modelo PPS con su versión a nivel microscópico. Esto es interesante, puesto que para algunos modelos microscópicos se ha podido probar que se ajustan estadísticamente a los datos de secuencias de potenciales de acción reales [79, 86]. En concreto, en [34] se relacionan diversos modelos microscópicos (Poisson, Wold, Hawkes) con el modelo PPS y en [33] se obtiene que el modelo PPS es el límite de campo medio (mean-field) de n procesos de campo medio de tipo Hawkes estructurados por edad que interactúan.

- **Modelos de densidad de población de neuronas de IF con saltos.** Este modelo, que fue presentado inicialmente en [73] para facilitar la simulación numérica del comportamiento de poblaciones de neuronas a nivel mesoscópico, surge de la misma aproximación a nivel microscópico que el modelo NNLIF y, por lo tanto, su incógnita ρ se refiere a una densidad de probabilidad similar a las del modelo NNLIF. En concreto, ρ es la densidad para la probabilidad de encontrar una neurona con potencial v en el tiempo t. Sin embargo, la forma concreta de la EDP que representa a estos modelos varía, ya que para llegar a ella se realizan menos aproximaciones:

$$
\begin{cases}
\frac{\partial}{\partial t}\rho(t,v) - \frac{\partial}{\partial v}\left(v\rho(t,v)\right) = \sigma(t)\left(\rho(t, v-h) - \rho(t,v)\right) + \delta(v-V_R)r(t), \\[2mm]
\sigma(t) := \sigma_0(t) + J\ r(t) \text{ sin retraso sináptico, o,} \\[2mm]
\sigma(t) := \sigma_0(t) + J\int_0^t \alpha(u)r(t-u)\ du \text{ con retraso sináptico,} \\[2mm]
r(t) = \sigma(t)\int_{1-h}^1 \rho(t,w)\ dw, \\[2mm]
\rho(t,1) = 0, \\[2mm]
\rho(0,.) = \rho_0 \in L^1_+(0,1),
\end{cases}
$$

donde

- h es el "tamaño" del salto que se produce en el potential v cuando la neurona recibe un impulso nervioso en una de sus sinapsis,
- $\alpha(u)$ es la función de densidad del retraso, cumpliendo, por lo tanto, que $\int_0^\infty \alpha(u)\ du = 1$,
- V_R es el valor de reinicio,
- $\sigma(t)$ es la tasa de recepción de cada neurona,
- $r(t)$ es la tasa de disparo de la población,
- $\sigma_0(t)$ es la influencia externa que viene de una población excitadora,
- J es el número medio de neuronas presinápticas por neurona.

Desde el punto de vista teórico se ha estudiado entre otros en [41, 40, 39]. El resultado más destacado de [41] es que se demuestra que la tasa de disparo explota en tiempo finito en ciertas

situaciones (*blow-up*) y el de [40] consiste en probar que esta explosión desaparece si incluimos un retraso. En [39], entre otros, se estudia la existencia, unicidad y estabilidad de los estados estacionarios para ciertos valores del parámetro de conectividad.

- **Modelo NNLIF con conductancia.** Este modelo supone una versión aún mas realista del modelo NNLIF presentado en (7), ya que se incluye una variable más: la conductancia. Esta es necesaria para tener en cuenta receptores post-sinápticos lentos [84]. En consecuencia, la incógnita de la EDP que representa este modelo, es una densidad de probabilidad $\rho(v, g, t)$ que describe la probabilidad de encontrar una neurona en el tiempo t con un potencial de membrana $v \in [V_R, V_F]$ y una conductancia $g > 0$. La ecuación resultante, deducida en [23, 22] y [83] es esta:

$$\frac{\partial \rho(v, g, t)}{\partial t} + \frac{\partial[(-g_L v + g(V_E - v))\rho(v, g, t)]}{\partial v} + \frac{\partial}{\partial g}\left[\frac{g_{in}(t) - g}{\sigma_E}\rho(v, g, t)\right] - \frac{a(t)}{\sigma_E}\frac{\partial^2 \rho(v, g, t)}{\partial g^2} = 0,$$

que se completa con estos datos iniciales

$$\rho^0(v, g) \geq 0, \quad \text{tal que} \quad \int_0^{V_F}\int_0^\infty \rho^0(v, g) \; dv \; dg = 1.$$

La no-linealidad de esta ecuación se debe a los término $g_{in}(t)$ y $a(t)$, que dependen de la tasa de disparo total $\mathcal{N} > 0$, que se define como sigue

$$N(g, t) := [-g_L V_F + g(V_E - V_F)]\rho(V_F, g, t) \geq 0, \qquad \mathcal{N} := \int_0^\infty N(g, t)dg,$$

donde $N(g, t)$ representa la tasa de disparo dependiente de g y

$$\begin{aligned} g_{in}(t) &= f_E \nu(t) + S_E \mathcal{N}(t), \\ a(t) &= \frac{1}{2\sigma_E}\left(f_E^2 \nu(t) + \frac{S_E^2}{N_E}\mathcal{N}\right). \end{aligned}$$

Los parámetros que aparecen en la ecuación tienen las siguientes interpretaciones:

- V_E es el potencial reverso excitador,
- V_F es el potencial umbral,
- el reinicio se produce en V_R y consideramos que $0 = V_R < V_F < V_E$,
- $\sigma_E > 0$ denota la constante de decaimiento de la conductancia excitadora,
- $g_L > 0$ denota la conductancia de fuga,
- $g_{in}(t) \geq 0$ es la conductancia inducida por corrientes de entrada,
- $a(t) = a(\mathcal{N}, t) > 0$ representa la intensidad del ruido sináptico,
- $S_E \geq 0$ denota la fuerza sináptica del acoplamiento excitador de la red,
- $\nu(t)$ es la aportación externa,
- $f_E > 0$ denota la fuerza sináptica de $\nu(t)$,
- N_E proporciona la normalización total de la fuerza de los acoplamientos.

Este modelo se ha estudiado desde el punto de vista analítico, entre otros, en [78], donde se ha analizado sobre todo si aparece el fenómemo del *blow-up*. Se obtienen varias cotas a priori sobre ρ y la tasa de disparo, que permiten concluir que dicho fenómeno no se presenta. Por otro lado, en [16] se presenta un resolutor numérico determinista para este modelo, se realizan diversas simulaciones y se comparan los resultados deterministas con simulaciones hechas con Monte Carlo.

0.4 Punto de partida

En esta sección hacemos un repaso a la literatura para dejar claro el punto de partida de la investigación de esta tesis. Inicialmente, en [11] se dedujo el modelo NNLIF completo, incluyendo todas las propiedades biológicas descritas anteriormente. Sin embargo, este modelo es bastante complejo de estudiar desde el punto de vista matemático. Con lo que, para iniciar el análisis matemático, en [15] se propuso un modelo simplificado que considera una red neuronal formada por una sola población de neuronas, que puede ser en media excitadora o inhibidora. Este hecho queda reflejado en el signo de uno de los parámetros del modelo, conocido como *parámetro de conectividad*. Además, se supuso que las neuronas no entran en estado refractario y que tampoco hay un retraso sináptico en la transmisión de la señal nerviosa. Desde el punto de vista matemático, este modelo consiste en una EDP de tipo Fokker-Planck no lineal que ha sido ampliamente estudiada en [15], [29] y [26].

Los resultados más destacados de [15] son el estudio del número de estados estacionarios en función de los valores de los parámetros y la prueba de la existencia de ciertos valores de los parámetros y/o condiciones iniciales para el caso excitador, para los que las soluciones no existen para todo tiempo (*blow-up*). Además, las simulaciones numéricas mostradas sugieren que esto se debe a que la tasa de disparo explota en tiempo finito.

En [29] se proporciona un criterio para determinar el tiempo maximal de existencia de solución para dicho modelo simplificado. Éste asegura que la solución existe, y es única, siempre que la tasa de disparo sea finita, corroborando, por lo tanto, las observaciones numéricas del trabajo anterior. Además, usando este criterio se demuestra la existencia para todo tiempo de una única solución para el caso inhibidor. Esto nos permite deducir entonces que, para las poblaciones de neuronas en media inhibidoras, el fenómeno del *blow-up* no puede aparecer.

En [26] se demuestra la convergencia con velocidad exponencial de las soluciones al equilibrio cuando el parámetro de conectividad es pequeño, en valor absoluto, usando una desigualdad de tipo Poincaré y el método de disipación de entropía. También se recupera el resultado de existencia global para el caso inhibidor, usando el criterio de tiempo maximal de existencia combinado con un concepto de super-solución. Este concepto permitirá por otro lado, obtener unas cotas a priori para la tasa de disparo.

Posteriormente, en [17] se consideró un modelo más completo, añadiendo el estado refractario al modelo simplificado inicial de [15]. Entre otros, se estudia el modelo siguiendo las líneas de [15] y se analizan los cambios en el comportamiento de las soluciones: p.e. en el modelo anterior había casos donde no hay equilibrios, y para este modelo más completo existe siempre al menos un equilibrio. Se prueba, además, que el fenómeno del *blow-up* sigue apareciendo bajo las mismas condiciones que las dadas en [15].

Por otro lado, se han desarrollado también algunos trabajos que estudian las redes neuronales de IF a nivel microscópico, a través de ecuaciones estocásticas. Entre ellos se encuentran [37] y [38]. En [37] al igual que en [15], se considera que las neuronas no presentan estado refractario ni retraso sináptico.

Aquí, entre otras, los autores prueban que el *blow-up* queda reflejado a nivel microscópico. En [38] se incluye el retraso sináptico en el modelo, pero no el estado refractario. El resultado más destacado es que se demuestra que el fenómeno de *blow-up* desaparece. Esto inmediamente nos hace pensar que este hecho probablemente quede plasmado también en el nivel mesoscópico.

Hay una gran cantidad de trabajos que tratan de incluir el retraso sináptico en modelos neuronales. Entre otros, podemos encontrar los trabajos de Touboul [96, 98, 97] donde se tiene en cuenta también la distribución espacial de las poblaciones de neuronas.

Esto, junto con los resultados sobre el retraso para el modelo de Omurtag-Dumont de [40], es el punto de partida, a partir del cual arranca el trabajo realizado en esta tesis. El objetivo ahora es realizar el estudio de modelos simplificados cada vez más completos hasta llegar al análisis del modelo más realista (7), derivado en [11].

0.5 Resumen de resultados

Los resultados obtenidos para el modelo NNLIF completo, y para algunas de sus simplificaciones, se exponen en tres capítulos. Los capítulos esán ordenados de manera creciente, según la completitud del modelo que estudian. Así, en el primer capítulo se trata el modelo NNLIF para una sola población de neuronas, con retraso sináptico y sin estado refractario; en el segundo capítulo se considera el modelo NNLIF para dos poblaciones, pero sin estados refractarios ni retrasos sinápticos; y en el tercer capítulo se exponen los resultados para el modelo NNLIF completo: dos poblaciones, con estados refractarios y retrasos sinápticos. Además, se ha implementado un resolutor numérico, usado para ilustrar gran parte de los resultados teóricos y también para aclarar los aspectos que no se han podido abordar desde el punto de vista analítico debido a su gran complejidad. Esta memoria se completa con un apéndice en el que se detallan los esquemas numéricos y técnicas de implementación aplicadas para obtener dicho resolutor.

Antes de proceder a explicar en detalle los resultados, vamos a aclarar la notación y los acrónimos usados a lo largo de esta tesis. Para $1 \leq p < \infty$, $L^p(\Omega)$ es el espacio de funciones tal que f^p es integrable Ω, $L^\infty(\Omega)$ es el espacio de funciones esencialmente acotadas en Ω, $L^\infty_+(\Omega)$ representa el espacio de funciones no-negativas esencialmente acotadas en Ω, $C^p(\Omega)$ es el conjunto de las funciones p veces diferenciables en Ω, $C^\infty(\Omega)$ es el conjunto de funciones infinitamente diferenciables en Ω, $L^1_{loc,+}(\Omega)$ denota el conjunto de funciones no-negativas que son localmente integrables en Ω y el espacio de Sobolev $H^p = W^{p,2}$ es el subconjunto de las funciones f en $L^p(\mathbb{R})$ tal que la función f y sus derivadas débiles hasta orden k tienen norma L^p finita. El significado de los acrónimos se especifica en la Tabla 1.

0.5.1 Resultados principales del capítulo 1

En el primer capítulo, que se basa en el trabajo [18], consideramos un modelo NNLIF simplificado, que retrata una sola población de neuronas con retraso sináptico, $D \geq 0$, y sin estado refractario. El sistema asociado es más simple que (7), ya que sólo consta de una EDP:

$$\frac{\partial \rho}{\partial t}(v,t) + \frac{\partial}{\partial v}[(v - \mu(t-D))\rho(v,t)] - a\frac{\partial^2 \rho}{\partial v^2}(v,t) = N(t)\delta(v - V_R), \qquad v \leq V_F = 0, \qquad (13)$$

donde $\rho(v,t)$ es la función de densidad para la probabilidad de encontrar una neurona de la población con un valor de voltaje v en el instante t. El término de la deriva μ y la tasa de disparo N están dados

Acrónimo	Significado
NNLIF	Nonlinear Noisy Leaky Integrate and Fire
IF	Integrate and Fire
EDP	Ecuación en Derivadas Parciales
EDO	Ecuación Diferencial Ordinaria
WENO	Weighted Essentially Non-Oscillatory
CFL	Courant-Friedrich-Lewy
TVD	Total Variation Diminishing
MPI	Message Passing Interface
IVP	Initial Value Problem
RHS	Right Hand Side

Tabla 1: Tabla de acrónimos.

por

$$\mu(t) = b_0 + bN(t) \quad \text{siendo} \quad N(t) = -a\frac{\partial \rho}{\partial v}(V_F, t) \geq 0, \tag{14}$$

donde b es el pámetro de conectividad que determina el tipo de red considerado: excitadora ($b > 0$) o inhibidora ($b < 0$) y el b_0 es el parámetro que controla la fuerza de los estímulos externos y puede ser tanto positivo como negativo. La EDP (13) ha de completarse con condiciones iniciales y de contorno

$$N(t) = N^0(t) \geq 0, \quad \forall \, t \in [-D, 0), \quad \rho(v, 0) = \rho^0(v) \geq 0, \quad \rho(V_F, t) = 0, \quad \rho(-\infty, t) = 0. \tag{15}$$

Además, como ρ es una densidad de probabilidad, la masa total se conserva

$$\int_{-\infty}^{V_F} \rho(v, t) \, dv = \int_{-\infty}^{V_F} \rho^0(v) \, dv = 1, \qquad \forall \, t \geq 0.$$

EL resultado principal de este capítulo consiste en probar que las soluciones de (13)-(14)-(15) existen para todo tiempo para el caso excitador si incluimos el retraso sináptico, tal y como se había observado en [38] a nivel microscópico. En consecuencia, desaparece el fenómeno de explosión en tiempo finito para el caso excitador que se había observado para este mismo modelo sin retraso sináptico en [15] para ciertos valores de los parámetros y para determinados datos iniciales. Como subproducto, obtenemos la existencia global de solución también para el caso inhibidor con retraso. Esto era de esperar, ya que en [29] se probó que para el caso inhibidor las soluciones existen para todo tiempo si no hay retraso sináptico. El resultado es este:

Teorema 0.5.1 (Existencia global - caso excitador e inhibidor) *Sea (ρ, N) una solución clásica local de (13)-(14)-(15) para $b_0 = 0$ y $D > 0$ para la condición inicial no-negativa (ρ^0, N^0), donde $N^0 \in C^0([-D, 0))$ está acotado y $\rho^0 \in L^1((-\infty, V_F)) \cap C^1((-\infty, V_R) \cup (V_R, V_F]) \cap C^0((-\infty, V_F])$ siendo $\rho^0(V_F) = 0$. Supongamos, además, que ρ^0 admite derivadas laterales finitas en V_R y que ρ y $(\rho^0)_v$ decrecen a cero cuando $v \to 0$. Entonces, el tiempo maximal de existencia para la solución (ρ, N) es $T^* = +\infty$.*

Obtener este resultado es complicado, tenemos que combinar argumentos y técnicas de [26] con las

de [29] y adoptar una estrategia apropiada para tratar el retraso. Comenzamos transformando (13)-(14)-(15) en un problema de tipo Stefan con frontera libre y parte derecha no estándar. Para ello, realizamos dos cambios de variables conocidos, (ampliamente estudiados en [30]) y unos cómputos para traducir adecuadamente el retraso sináptico:

- El *primer cambio de variables* viene dado por

$$y = e^t v, \qquad \tau = \frac{1}{2}(e^{2t} - 1).$$

En consecuencia,

$$v = y\alpha(\tau), \qquad t = -\log(\alpha(\tau)),$$

donde $\alpha(\tau) = (\sqrt{2\tau + 1})^{-1}$, y definimos

$$w(y, \tau) = \alpha(\tau)\rho(y\alpha(\tau), -\log(\alpha(\tau))),$$

Derivando obtenemos la ecuación

$$w_\tau(y, \tau) = w_{yy}(y, \tau) - \alpha(\tau)\mu(t - D)w_y(y, \tau) + M(\tau)\delta\left(y - \frac{V_R}{\alpha(\tau)}\right), \tag{16}$$

donde $M(\tau) = -w_y(0, \tau) = \alpha^2(\tau)N(t)$.

- El *segundo cambio de variables:*

$$x = y - \int_0^\tau \mu(t - D)\alpha(s)\ ds = y - b_0(\sqrt{2\tau + 1} - 1) - b\int_0^\tau N(t - D)\alpha(s)\ ds,$$

se hace para eliminar el término en w_y en (16), considerando

$$u(x, \tau) = w(x + \int_0^\tau \mu(t - D)\alpha(s)\ ds, \tau).$$

De este modo obtenemos el siguiente sistema para u_τ:

$$\begin{cases} u_\tau(x, \tau) = u_{xx}(x, \tau) + M(\tau)\delta(x - s_1(\tau)), & x < s(\tau), \tau > 0, \\ s_1(\tau) = s(\tau) + \frac{V_R}{\alpha(\tau)}, & \tau > 0, \\ s(\tau) = -b_0(\sqrt{2\tau + 1} - 1) - b\int_0^\tau N(t - D)\alpha(s)\ ds, & \tau > 0, \\ M(\tau) = -u_x(s(\tau), \tau), & \tau > 0, \\ N(t) = N(0), & t \in (-D, 0], \\ u(-\infty, \tau) = u(s(\tau), \tau) = 0, & \tau > 0, \\ u(x, 0) = u_I(x), & x < 0. \end{cases} \tag{17}$$

- *Traduciendo el retraso.* Necesitamos eliminar la dependencia explícita de t en (17) en el término $N(t - D)$. Para ello recordamos que t y τ están relacionados a través del cambio de variables $\tau = \frac{1}{2}(e^{2t} - 1)$, $t = \frac{1}{2}\log(2\tau + 1)$. En consecuencia, si consideramos el tiempo $t - D$, hay un τ_D relacionado: $\tau_D = \frac{1}{2}(e^{2(t-D)} - 1)$, que hace difícil manejar D. Para trabajar con el retraso de una forma más cómoda, proponemos la siguiente estrategia. Como $D \geq 0$, $\tau_D \leq \tau$, y entonces, existe

un $\bar{D} > 0$ tal que $\tau_D = \tau - \bar{D}$. Mediante cálculos directos obtenemos que $\bar{D} = \frac{1}{2}e^{2t}(1 - e^{-2D}) > 0$. Sustituyendo ahora t por el τ relacionado y definiendo $\hat{D} = (1 - e^{-2D})$, finalmente concluimos que $\bar{D} = \hat{D}(\tau + \frac{1}{2})$.

Este resultado nos permite escribir apropiadamente la siguiente relación

$$\begin{aligned} N(t - D) &= \alpha^{-2}(\tau_D)M(\tau_D) = \alpha^{-2}(\tau - \bar{D})M(\tau - \bar{D}) \\ &= \alpha^{-2}\left((1 - \hat{D})\tau - \frac{1}{2}\hat{D}\right)M\left((1 - \hat{D})\tau - \frac{1}{2}\hat{D}\right). \end{aligned} \tag{18}$$

De este modo, el retraso sináptico inicial D se traduce al retraso $\hat{D}$, que se reescala entre 0 y 1, siendo $\hat{D} = 0$ si $D = 0$ y $\hat{D} = 1$ si $D = \infty$.

- La *ecuación equivalente de tipo Stefan*. Usando (18) podemos reescribir $s(\tau)$ de (17) en términos de $M(\tau)$, evitando su dependencia de t a través de $N(t)$

$$\begin{aligned} s(\tau) &= -b_0(\sqrt{2\tau + 1} - 1) - b\int_0^\tau N(t - D)\alpha(s)\ ds \\ &= -b_0(\sqrt{2\tau + 1} - 1) - b\int_0^\tau \alpha^{-2}((1 - \hat{D})s - \frac{1}{2}\hat{D})M((1 - \hat{D})s - \frac{1}{2}\hat{D})\alpha(s)\ ds. \end{aligned}$$

Un simple cambio de variables produce

$$s(\tau) = -b_0(\sqrt{2\tau + 1} - 1) - \frac{b}{\sqrt{1 - \hat{D}}}\int_{-\frac{1}{2}\hat{D}}^{(1 - \hat{D})\tau - \frac{1}{2}\hat{D}} M(s)\alpha^{-1}(s)\ ds.$$

Notando $t = \tau$ y $D = \hat{D}$ finalmente llegamos a la siguiente ecuación equivalente de tipo Stefan

$$\begin{cases} u_t(x, t) = u_{xx}(x, t) + M(t)\delta(x - s_1(t)), & x < s(t), t > 0, \\ s_1(t) = s(t) + \frac{V_R}{\alpha(t)}, & t > 0, \\ s(t) = -b_0(\sqrt{2t + 1} - 1) - \frac{b}{\sqrt{1 - D}}\int_{-\frac{1}{2}D}^{(1 - D)t - \frac{1}{2}D} M(s)\alpha^{-1}(s)\ ds, & t > 0, \\ M(t) = -u_x(s(t), t), & t > 0, \\ M(t) = M(0), & t \in (-D, 0], \\ u(-\infty, t) = u(s(t), t) = 0, & t > 0, \\ u(x, 0) = u_I(x), & x < 0, \end{cases} \tag{19}$$

donde $D \in [0, 1)$ y $\alpha(t) = \frac{1}{\sqrt{2t + 1}}$. Nótese que este problema está bien definido ya que $\alpha(t) \in \mathbb{R}^+ \ \forall\ t > -\frac{1}{2}$.

Una vez obtenido el sistema equivalente de tipo Stefan, realizando unos tediosos cómputos, podemos obtener una formulación integral implícita para M:

$$\begin{aligned} M(t) &= -2\int_{-\infty}^{V_R} G(s(t), t, \xi, 0)u_I'(\xi)d\xi - 2\int_{V_R}^0 G(s(t), t, \xi, 0)u_I'(\xi)d\xi \\ &\quad + 2\int_0^t M(\tau)G_x(s(t), t, s(\tau), \tau)d\tau - 2\int_0^t M(\tau)G_x(s(t), t, s_1(\tau), \tau)d\tau, \end{aligned} \tag{20}$$

14

donde G es la función de Green para la ecuación del calor en la recta real

$$G(x,t,\xi,\tau) = \frac{1}{[4\pi(t-\tau)]^{\frac{1}{2}}} e^{-\frac{|x-\xi|^2}{4(t-\tau)}}.$$

Esta formulación integral será crucial para poder desarrollar gran parte de los cómputos realizados en este capítulo. En primer lugar, mediante un argumento de punto fijo, nos permitirá obtener un resultado de existencia local de solución para el problema (19). Este resultado, además, proporciona una estimación del tiempo de existencia de la solución local:

Teorema 0.5.2 *Sea $u_I(x)$ una función no-negativa de clase $C^0((-\infty,0]) \cap C^1((-\infty,V_R) \cup (V_R,0]) \cap L^1((-\infty,0))$ tal que $u_I(0) = 0$. Supongamos, además, que u_I, $(u_I)_x$ decrecen hacia cero cuando $x \to -\infty$ y que las derivadas laterales en V_R son finitas. Entonces existe un tiempo $T > 0$ tal que $M(t)$, definida por la formulación integral (20), existe para todo $t \in [0,T]$ y es única en $C^0([0,T])$. El tiempo de existencia T satisface*

$$T \leq \left(\sup_{x \in (-\infty,V_R) \cup (V_R,0]} |u_I'(x)| \right)^{-1}.$$

Por completitud tenemos que mostrar cómo el Teorema 0.5.2, se traduce a nuestra ecuación inicial. En primer lugar, como en [49], una vez M es conocida, la ecuación para u se desacopla, y se puede resolver mediante una fórmula de Duhamel. En consecuencia, la existencia local queda reflejada también para el sistema (19). A continuación, ρ se recupera a partir de u deshaciendo los cambios de variables, por lo que, finalmente, tenemos existencia local para (13).

El resultado de existencia local es la herramienta fundamental para demostrar un criterio que determina el tiempo maximal de existencia de la solución en función del crecimiento de la tasa de disparo, el cual, a su vez, será la clave para derivar el resultado principal de este capítulo (Teorema 0.5.1).

Teorema 0.5.3 (Tiempo maximal de existencia) *Supongamos que estamos en las hipótesis del Teorema 0.5.2. Entonces la solución u se puede extender hasta un tiempo maximal $0 < \bar{T} \leq \infty$ dado por*

$$\bar{T} = \sup\{t > 0 : M(t) < \infty\}.$$

Traduciendo de nuevo este resultado a (13) por el mismo procedimiento que para la existencia local, podemos decir que se asegura que las soluciones existen siempre que la tasa de disparo, N, sea finita. Para probar el resultado de existencia global usando este criterio necesitamos el concepto de super-solución:

Definición 0.5.4 *Sea $T \in \mathbb{R}_+^*$, $(\bar{\rho},\bar{N})$ es una super-solución (clásica) en $[0,T]$ si para todo $t \in [0,T]$ tenemos que $\bar{\rho}(V_F,t) = 0$ y*

$$\partial_t \bar{\rho} + \partial_v[(-v + b\bar{N}(t-D))\bar{\rho}] - a\partial_{vv}\bar{\rho} \geq \delta_{v=V_R}\bar{N}(t), \quad \bar{N}(t) = -a\partial_v\bar{\rho}(V_F,t).$$

en $(-\infty,V_F] \times [0,T]$ en el sentido de las distribuciones y en $(-\infty,V_F] \setminus V_R \times [0,T]$ en sentido clásico, con valores arbitrarios para $\bar{N}$ en $[-D,0)$.

Éste nos permitirá calcular una familia de super-soluciones, que proporcionarán el control necesario sobre la tasa de disparo para poder aplicar el criterio de tiempo maximal de existencia de la solución, a través de este teorema:

Teorema 0.5.5 *Sea $T < D$. Sea (ρ, N) una solución clásica del modelo* (13)*-*(14)*-*(15) *para $b_0 = 0$ en* $(-\infty, V_F] \times [0, T]$*para el dato inicial (ρ^0, N^0) y sea $(\bar{\rho}, \bar{N})$ una super-solución clásica en* $(-\infty, V_F] \times [0, T]$*. Supongamos que*

$$\forall v \in (-\infty, V_F], \quad \bar{\rho}(v, 0) \geq \rho^0(v) \qquad \text{y} \qquad \forall t \in [-D, 0), \quad \bar{N}(t) = N^0(t).$$

Entonces,

$$\forall (v, t) \in (-\infty, V_F] \times [0, T], \quad \bar{p}(v, t) \geq p(v, t) \qquad \text{y} \qquad \forall t \in [0, T], \quad \bar{N}(t) \geq N(t).$$

Nótese que para este modelo no es necesario realizar el estudio del número de estados estacionarios, ya que el resultado presentado en [15], que, p. e., asegura unicidad de equilibrio para b pequeño en valor absoluto, es válido también para el modelo (13).

0.5.2 Resultados principales del capítulo 2

El contenido del capítulo segundo se corresponde a la publicación [19], abordando una versión aún más completa del modelo, ya que considera una red neuronal formada por dos poblaciones, lo cual da lugar a dos EDPs no lineales de tipo Fokker-Planck acopladas. Para reducir la complejidad, sin embargo, consideramos que no hay retrasos ni estado refractarios. El modelo resultante responde a este sistema:

$$\begin{cases} \frac{\partial \rho_I}{\partial t}(v, t) + \frac{\partial}{\partial v}[h^I(v, N_E(t), N_I(t))\rho_I(v, t)] - a_I(N_E(t), N_I(t))\frac{\partial^2 \rho_I}{\partial v^2}(v, t) = N_I(t)\delta(v - V_R), \\[2mm] \frac{\partial \rho_E}{\partial t}(v, t) + \frac{\partial}{\partial v}[h^E(v, N_E(t), N_I(t))\rho_E(v, t)] - a_E(N_E(t), N_I(t))\frac{\partial^2 \rho_E}{\partial v^2}(v, t) = N_E(t)\delta(v - V_R), \end{cases} \quad (21)$$

que se completa con condiciones de contorno de tipo Dirichlet y dos datos iniciales

$$\rho_\alpha(-\infty, t) = 0, \ \rho_\alpha(V_F, t) = 0, \ \rho_\alpha(v, 0) = \rho_\alpha^0(v) \geq 0, \quad \alpha = E, I. \quad (22)$$

Los coeficientes de deriva y difusión vienen dados por

$$\begin{align} h^\alpha(v, N_E(t), N_I(t)) &= -v + b_E^\alpha N_E(t) - b_I^\alpha N_I(t) + (b_E^\alpha - b_E^E)\nu_{E,ext}, \quad (23) \\ a_\alpha(N_E(t), N_I(t)) &= d_\alpha + d_E^\alpha N_E(t) + d_I^\alpha N_I(t), \quad \alpha = E, I, \quad (24) \end{align}$$

siendo $d_\alpha > 0$, $d_i^\alpha \geq 0$, $b_i^\alpha > 0$, $D_i^\alpha \geq 0$ para $\alpha, i = E, I$. Las tasas de disparo N_α responden a

$$N_\alpha(t) = -a_\alpha(N_E(t), N_I(t))\frac{\partial \rho_\alpha}{\partial v}(V_F, t) \geq 0, \quad \alpha = E, I. \quad (25)$$

Por otro lado, ya que ρ_E y ρ_I representan densidades de probabilidad, la masa total se conserva:

$$\int_{-\infty}^{V_F} \rho_\alpha(v, t) \, dv = \int_{-\infty}^{V_F} \rho_\alpha^0(v) \, dv = 1 \quad \forall \, t \geq 0, \quad \alpha = E, I.$$

El concepto de solución débil con el que trabajamos es el siguiente:

Definición 0.5.6 *Una solución débil de* (21)*-*(25) *es una cuadrupla de funciones no-negativas* $(\rho_E, \rho_I, N_E, N_I)$ *donde* $\rho_\alpha \in L^\infty(\mathbb{R}^+; L^1_+((-\infty, V_F)))$ *y* $N_\alpha \in L^1_{loc,+}(\mathbb{R}^+) \; \forall \; \alpha = E, I$, *satisfacen*

$$\int_0^T \int_{-\infty}^{V_F} \rho_\alpha(v,t) \left[-\frac{\partial \phi}{\partial t} - \frac{\partial \phi}{\partial v} h^\alpha(v, N_E(t), N_I(t)) - a_\alpha(N_E(t), N_I(t)) \frac{\partial^2 \phi}{\partial v^2} \right] dv \; dt$$

$$= \int_0^T N_\alpha(t)[\phi(V_R, t) - \phi(V_F, t)]dt + \int_{-\infty}^{V_F} \rho_\alpha^0(v)\phi(v, 0)dv - \int_{-\infty}^{V_F} \rho_\alpha(v, T)\phi(v, T)dv, \qquad \alpha = E, I,$$

para cualquier función test $\phi(v,t) \in C^\infty((-\infty, V_F] \times [0,T])$ *tal que* $\frac{\partial^2 \phi}{\partial v^2}, \; v\frac{\partial \phi}{\partial v} \in L^\infty((-\infty, V_F] \times (0,T))$.

Comenzamos el análisis de este modelo estudiando el fenómeno del *blow-up*. Éste aparece bajo ciertas hipótesis, a pesar de haber una población inhibidora en la población. Recuérdese que en [29] se probó que el modelo NNLIF para una red neuronal en media inhibidora, presenta existencia global de solución, es decir, no puede aparecer el fenómeno del *blow-up*. Esto nos hizo pensar inicialmente que, quizás, la presencia de la población inhibidora podría ayudar a evitar este *blow-up* para el modelo de dos poblaciones. Sin embargo, esto no ocurre, como enuncia este teorema:

Teorema 0.5.7 *Supongamos que*

$$h^E(v, N_E, N_I) + v \geq b_E^E N_E - b_I^E N_I,$$

$$a_E(N_E, N_I) \geq a_m > 0,$$

$\forall v \in (-\infty, V_F]$ *and* $\forall \; N_I, N_E \geq 0$. *Supongamos además que existe* $M > 0$ *tal que*

$$\int_0^t N_I(s) \; ds \leq M \, t, \qquad \forall \, t \geq 0.$$

Entonces, una solución débil del sistema (21)*-*(25) *no puede ser global-en-tiempo en los siguientes casos:*

1. $b_E^E > 0$ *lo suficientemente grande, para* ρ_E^0 *fijo.*

2. ρ_E^0 *está 'lo suficientemente concentrado' alrededor de* V_F:

$$\int_{-\infty}^{V_F} e^{\mu v} \rho_E^0(v) \; dv \geq \frac{e^{\mu V_F}}{b_E^E \mu}, \qquad \text{para un cierto } \mu > 0$$

para $b_E^E > 0$ *fijo.*

A continuación estudiamos el número de estados estacionarios en función de los valores de los parámetros, lo cual para este modelo es bastante más complejo que en [15] (donde se llevó a cabo este estudio para una sola población), obteniendo además una gran variedad de comportamientos: casos de unicidad de equilibrio, casos de un número par o impar de estados estacionarios, e, incluso, situaciones de su ausencia. De hecho, desde el punto de vista numérico se han localizado casos de tres equilibrios, los cuales para modelos NNLIF de una sola población no se han detectado. Además, por otro lado, los resultados numéricos sugieren que para los casos de ausencia de equilibrios, se produce el fenómeno del *blow-up*. Este teorema resume con precisión los resultados teóricos relativos a este estudio:

Teorema 0.5.8 *Supongamos que los parámetros de conectividad b_I^E y b_E^I no se hacen cero (b_I^E, $b_E^I >$ 0), a_α es independiente de N_E y N_I, $a_\alpha(N_E, N_I) = a_\alpha$, y $h^\alpha(v, N_E, N_I) = V_0^\alpha(N_E, N_I) - v$ con $V_0^\alpha(N_E, N_I) = b_E^\alpha N_E - b_I^\alpha N_I + (b_E^\alpha - b_E^E)v_{E,ext}$ para todo $\alpha = E, I$. Entonces:*

1. *Hay un número par o no hay estado estacionario para (21)-(25) si:*

$$(V_F - V_R)^2 < (V_F - V_R)(b_E^E - b_I^I) + b_E^E b_I^I - b_I^E b_E^I. \tag{26}$$

   Si b_E^E es lo suficientemente grande en comparación con el resto de parámetros de conectividad, no hay estados estacionarios.

2. *Hay un número impar de estados estacionarios para (21)-(25) si:*

$$(V_F - V_R)^2 > (V_F - V_R)(b_E^E - b_I^I) + b_E^E b_I^I - b_I^E b_E^I.$$

   Si b_E^E es lo suficientemente pequeño en comparación con el resto de parámetros de conectividad, hay un único estado estacionario.

Una vez aclarada la cuestión del número de estados estacionarios, analizamos el comportamiento a largo plazo de las soluciones para las que los parámetros de conectividad son pequeños, en valor absoluto. Observamos que las soluciones convergen al único estado estacionario con velocidad exponencial si el dato inicial está lo suficientemente cerca de éste. Para obtener este resultado usamos el método de disipación de entropía, considerando la entropía total del sistema:

$$E[t] = \int_{-\infty}^{V_F} \left[\rho_E^\infty(v) \left(\frac{\rho_E(v,t)}{\rho_E^\infty(v)} - 1 \right)^2 + \rho_I^\infty(v) \left(\frac{\rho_I(v,t)}{\rho_I^\infty(v)} - 1 \right)^2 \right] dv.$$

Para controlar la producción de entropía empleamos una desigualdad de tipo Poincaré, llegando finalmente al resultado:

Teorema 0.5.9 *Supongamos que a_α es constante para $\alpha = E, I$, que los parámetros de conectividad b_E^E, b_E^I, b_I^E y b_I^I son lo suficientemente pequeños y que el dato inicial (ρ_E^0, ρ_I^0) es tal que*

$$E[0] < \frac{1}{2 \max\left(b_E^E + b_I^E, b_E^I + b_I^I\right)}.$$

Entonces, para soluciones de (21)-(25) con decaimiento rápido, hay una constante $\mu > 0$, tal que, para todo $t \geq 0$

$$E[t] \leq e^{-\mu t} E[0].$$

En consecuencia, para $\alpha = E, I$

$$\int_{-\infty}^{V_F} \rho_\alpha^\infty(v) \left(\frac{\rho_\alpha(v,t)}{\rho_\alpha^\infty(v)} - 1 \right)^2 dv \leq e^{-\mu t} E[0].$$

Al final del capítulo ilustramos todos los resultados teóricos con resultados numéricos. También proporcionamos el estudio numérico de la estabilidad de los equilibrios para algunos de los casos de dos y tres estados estacionarios. Todos estos resultados numéricos se han obtenido usando un esquema numérico (detallado en el apéndice) que usa una aproximación de tipo *Weighted Essentially Non-Oscillatory* (WENO) para el témino de la deriva, diferencias finitas de segundo orden para la difusión

y un método Runge-Kutta *Total Variation Diminishing* (TVD) explícito junto con una condición Courant-Friedrich-Lewy (CFL) para la evolución en tiempo. El código que ejecuta este esquema numérico se ha programado en paralelo sobre dos núcleos debido a la complejidad de la simulación.

0.5.3 Resultados principales del capítulo 3

El tercer capítulo que se apoya sobre el trabajo [20], trata el modelo NNLIF completo (7), incluyendo, por lo tanto, dos poblaciones, estados refractarios y retrasos sinápticos, véase Sección 0.2. Empezamos definiendo una solución débil para este modelo, siguiendo la línea del capítulo previo:

Definición 0.5.10 *Sea $\rho_\alpha \in L^\infty(\mathbb{R}^+; L^1_+((-\infty, V_F)))$, $N_\alpha \in L^1_{loc,+}(\mathbb{R}^+)$ y $R_\alpha \in L^\infty_+(\mathbb{R}^+)$ para $\alpha = E, I$. Entonces $(\rho_E, \rho_I, R_E, R_I, N_E, N_I)$ es una solución débil de (7)-(12) si para cualquier función test $\phi(v,t) \in C^\infty((-\infty, V_F] \times [0, T])$ y tal que $\frac{\partial^2 \phi}{\partial v^2}$, $v \frac{\partial \phi}{\partial v} \in L^\infty((-\infty, V_F) \times (0, T))$ se cumple la siguiente relación*

$$\int_0^T \int_{-\infty}^{V_F} \rho_\alpha(v,t) \left[-\frac{\partial \phi}{\partial t} - \frac{\partial \phi}{\partial v} h^\alpha(v, N_E(t - D_E^\alpha), N_I(t - D_I^\alpha)) - a_\alpha(N_E(t - D_E^\alpha), N_I(t - D_I^\alpha)) \frac{\partial^2 \phi}{\partial v^2} \right] dv dt$$

$$= \int_0^T [M_\alpha(t)\phi(V_R, t) - N_\alpha(t)\phi(V_F, t)] dt + \int_{-\infty}^{V_F} \rho_\alpha^0(v)\phi(v, 0) dv - \int_{-\infty}^{V_F} \rho_\alpha(v, T)\phi(v, T) \, dv,$$

para $\alpha = E, I$, y donde R_α, para $\alpha = E, I$, son soluciones de las EDOs

$$\frac{dR_\alpha(t)}{dt} = N_\alpha(t) - M_\alpha(t).$$

Una vez definido el concepto de solución débil, estudiamos si aparece el fenónemo del *blow-up* para este modelo. Vemos que si hay estado refractario y retraso entre todas las sinápsis excepto entre las neuronas excitadoras, las soluciones no son globales en tiempo en algunos casos. Es decir, que el fenómeno del *blow-up* aparace también si hay retraso y estado refractario, siempre que el retraso de las conexiones excitadora-excitadora sea cero. Posiblemente, si este retraso es no cero, se evite la explosión en tiempo finito, como se ha mostrado en el primer capítulo para el caso de una sola población excitadora. El resultado de *blow-up* para este modelo es este:

Teorema 0.5.11 *Supongamos que*

$$h^E(v, N_E, N_I) + v \geq b_E^E N_E - b_I^E N_I,$$

$$a_E(N_E, N_I) \geq a_m > 0,$$

$\forall v \in (-\infty, V_F]$, y $\forall N_I, N_E \geq 0$. Supongamos también que $D_E^E = 0$ y que existe algún $C > 0$ tal que

$$\int_0^t N_I(s - D_I^E) \, ds \leq C\, t, \qquad \forall\, t \geq 0.$$

Entonces, una solución débil del sistema (7)-(12) no puede ser global-en-tiempo debido a una de las siguientes razones:

- *$b_E^E > 0$ es lo suficientemente grande, para ρ_E^0 fijo.*

- ρ_E^0 está 'lo suficientemente concentrado' alrededor de V_F:

$$\int_{-\infty}^{V_F} e^{\mu v} \rho_E^0(v) \ dv \geq \frac{e^{\mu V_F}}{b_E^E \mu}, \qquad para \ un \ cierto \ \mu > 0$$

y para $b_E^E > 0$ fijo.

También estudiamos los estados estacionarios para este modelo, observando que siempre hay un número impar y, por lo tanto, existe siempre al menos uno, que es único en ciertas situaciones. Recordemos que para el modelo sin estado refractario estudiado en el capítulo previo, había ciertos valores de los parámetros para los cuales no hay equilibrios. El estudio de los equilibrios queda resumido en este teorema:

Teorema 0.5.12 *Supongamos que $b_I^E > 0$, $b_E^I > 0$, $\tau_E > 0$, $\tau_I > 0$, $a_\alpha(N_E, N_I) = a_\alpha$ constante, y $h^\alpha(v, N_E, N_I) = V_0^\alpha(N_E, N_I) - v$ con $V_0^\alpha(N_E, N_I) = b_E^\alpha N_E - b_I^\alpha N_I + (b_E^\alpha - b_E^E)v_{E,ext}$ para $\alpha = E, I$. Siempre hay un número impar de estados estacionarios para el sistema (7)-(12).*

Además, si b_E^E es lo suficientemente pequeño o τ_E es lo suficientemente grande (en comparación con el resto de parámetros), entonces hay un único equilibrio para (7)-(12).

A continuación analizamos el comportamiento a largo plazo de las soluciones para parámetros de conectividad pequeños, en valor absoluto, y sin retrasos. Obtenemos que las soluciones convergen al único equilibrio con velocidad exponencial si los datos iniciales se encuentran lo suficientemente cerca del estado estacionario. La prueba de este resultado usa el método de disipación de entropía y emplea una desigualdad de tipo Poincaré adaptada a la presencia del estado refractario para controlar la producción de entropía. Para aplicar el método de disipación de entropía tenemos que identificar la función de entropía total. Para dos poblaciones está dada por:

$$\mathcal{E}[t] := \int_{-\infty}^{V_F} \rho_E^\infty(v) \left(\frac{\rho_E(v) - \rho_E^\infty(v)}{\rho_E^\infty(v)} \right)^2 \ dv + \int_{-\infty}^{V_F} \rho_I^\infty(v) \left(\frac{\rho_I(v) - \rho_I^\infty(v)}{\rho_I^\infty(v)} \right)^2 \ dv$$
$$+ \frac{(R_E(t) - R_E^\infty)^2}{R_E^\infty} + \frac{(R_I(t) - R_I^\infty)^2}{R_I^\infty}.$$

Finalmente, el teorema que determina el comportamiento a largo plazo de las soluciones es este:

Teorema 0.5.13 *Consideremos el sistema (7)-(12) para $M_\alpha(t) = \frac{R_\alpha(t)}{\tau}$. Supongamos que los parámetros de conectividad b_i^α son lo suficientemente pequeños, los términos de difusión $a_\alpha > 0$ constantes, los retrasos sinápticos D_i^α se hacen cero ($\alpha = I, E$, $i = I, E$), y los datos iniciales (ρ_E^0, ρ_I^0) están lo suficientemente cerca del único equilibrio $(\rho_E^\infty, \rho_I^\infty)$:*

$$\mathcal{E}[0] < \frac{1}{2 \max \left(b_E^E + b_I^E, b_E^I + b_I^I \right)}.$$

Entonces, para soluciones de decaimiento rápido, hay una constante $\mu > 0$ de manera que para todo $t \geq 0$

$$\mathcal{E}[t] \leq e^{-\mu t} \mathcal{E}[0].$$

En consecuencia, para $\alpha = E, I$

$$\int_{-\infty}^{V_F} \rho_\alpha^\infty(v) \left(\frac{\rho_\alpha(v) - \rho_\alpha^\infty(v)}{\rho_\alpha^\infty(v)} \right)^2 dv + \frac{(R_\alpha(t) - R_\alpha^\infty)^2}{R_\alpha^\infty} \leq e^{-\mu t} \mathcal{E}[0].$$

La demostración de este teorema de comportamiento a largo plazo, también se puede extender a retrasos pequeños, es decir valores de $D_i^\alpha \geq 0$ pequeños. Para ello, hay que usar unas estimaciones a priori de tipo L^2 sobre las tasas de disparo. Éstas se pueden obtener siguiendo las ideas de [26] [Sección 3]. Además, el Teorema 0.5.13 también es válido para el modelo NNLIF de una población con estado refractario y sin retraso, o con un retraso pequeño.

Completamos el estudio presentando un resolutor numérico mejorado con respecto al implementado en el capítulo previo y el de [15, 17]: incluye una aproximación WENO de tipo *flux-splitting* y permite simular el modelo completo tanto para una como para dos poblaciones, con estados refractarios y retrasos. A nuestro conocimiento, este resolutor es el primer resolutor determinista que describe el comportamiento del modelo NNLIF completo, que involucra todos los fenómenos característicos de redes reales. Desarrollar resolutores numéricos eficientes que incluyen todos los fenómenos relevantes, es esencial para proponer estrategias que, por un lado, den respuestas a las preguntas que aún quedan abiertas; y, por otro lado, ayuden a implementar resolutores para otros modelos de gran escala, ya que estos son cada vez más frecuentes en neurociencia computacional [56, 63, 81, 92, 93, 100]. Además, se muestran estrategias para el guardado y recuperación de valores a la hora de tener en cuenta el retraso sináptico en las simulaciones. En esta dirección proporcionamos resultados numéricos novedosos, que suponen una interesante línea de trabajo para futuras investigaciones: para ambos modelos (una y dos poblaciones) con estados refractarios y retrasos parece que no hay explosión para ningún espacio de parámetros, y las soluciones o van al equilibrio o se hacen periódicas.

En resumen, los problemas más relevantes estudiados en este trabajo son: problemas de existencia, análisis del número de estados estacionarios, comportamiento a largo plazo de las soluciones y estudio numérico. El análisis numérico se ha usado, por un lado, para estudiar ciertos comportamientos de las soluciones, probados analíticamente y, por otro lado, para aclarar algunos de los aspectos que, debido a su complejidad, no han podido ser abordados desde la perspectiva teórica: la estabilidad de los equilibrios cuando hay más de uno, la desaparición del *blow-up* cuando hay un retraso en las sinapsis excitadora-excitadora, la aparición de soluciones periódicas, etc.

Las principales herramientas empleadas en esta tesis desde el punto de vista analítico son: la transformación del modelo NNLIF de una población con retraso a un problema de Stefan con una parte derecha no estándar, argumentos de punto fijo y la noción de super-solución global, que permitieron probar la existencia de solución para todo tiempo para este modelo; para el comportamiento asintótico el método de disipación de entropía y para controlar la producción de entropía varias desigualdades, siendo la más destacada una desigualdad de tipo Poincaré; y diferentes estrategias aplicadas para determinar el número de estados estacionarios.

Desde un punto de vista numérico, las principales técnicas aprendidas son el método WENO (flux splitting) de quinto orden usado para aproximar las derivas, y el método Runge-Kuttta TVD de tercer orden combinado con una condición CFL para simular la evolución en tiempo de las soluciones. Además, todos los códigos se han programado en C++, combinado, a veces, con técnicas de programación en paralelo usando MPI. Por lo tanto, el aprendizaje de estas técnicas y lenguajes de programación también es parte de la formación obtenida durante el desarrollo de este trabajo.

Nuestros resultados analíticos y numéricos contribuyen a respaldar que el modelo NNLIF es un modelo adecuado para describir fenómenos neurofisiológicos bien conocidos, como lo son la sincronización/asincronización de la red (como en [11] llamaremos *asíncronos* a los estados donde la

tasa de disparo tiende a ser constante en tiempo y *síncrono* a cualquier otro estado), ya que la explosión en tiempo finito quizás represente una sincronización de parte de la red, mientras que la presencia de un único estado estacionario asintóticamente estable describe un asincronización de la red. Asimismo, la abundancia del número de estados estacionarios, en función de los valores de los parámetros de conectividad, que puede ser observada para estos modelos simplificados (Teorema 0.5.8 y Teorema 0.5.12), probablemente nos ayude a caracterizar situaciones de multiestabilidad para otros modelos más completos, como p.e., los que incluyen variables de conductancia [16]. En [17] se mostró que si incluimos un estado refractario en el modelo, hay situaciones de multiestabilidad, con dos estados estables y uno inestable. En [16] se han descrito fenómenos de biestabilidad numéricamente. Redes bi- y multiestables están relacionadas, p. e., con la percepción visual y la toma de decisiones [50, 3], la memoria de trabajo a corto plazo [104] e integradores oculomotores [59]. Por otro lado, las soluciones periódicas u oscilantes se usan para modelar estados síncronos y oscilaciones observadas, p.e., durante el procesado cortical [50, 53].

Introduction

The brain is one of the most perfect, complex and at the same time fascinating organs of our body. Thanks to it, among others, we become aware of ourselves, experience all kind of emotions, use the language, transform our environment and understand the why of the world around us. Using the powerful tool that it provides, we have decoded an important part of the complex biological, chemical, physical, etc, mechanisms underlying the events of nature, which has allowed us to develop medicaments, to construct impressive infrastructures, to create the artificial intelligence, etc. On the other hand, in the brain there is also room for disciplines that are less scientific, and more inherent to the human being, as it are the culture, the music, the creation of artworks, the religion and the rest of humanities. In that direction, thanks to the brain, moreover, we have the unique ability to express ourselves through the language and also to control/suppress our most ancestral instincts to live in society in a peaceful way.

Nevertheless, although the very complex mechanism that uses the brain to cover all this areas is every time better understood, there are still many open questions. Decoding totally how the brain works, not only will allow us to understand ourselves and our place in the universe a bit better, but also it will provide relief to all that people that suffer brain pathologies: depression, obsessive-compulsive disorder, epilepsy, Alzheimer, etc.

The investigation to continue revealing the enigma of the brain (and the nervous system in general) is tackled from different perspectives. The experimental part is crucial to reach this aim, but also the modeling plays an important role. Specifically, there are several models that are usually used in neuroscience to translate the biological behavior of a neural network into a mathematical equation. This procedure allows to determine the time evolution of the network through the analysis of the solutions of the resulting mathematical equation. Thus, here is the place where the mathematics make their contribution to the large amount of investigations related to the brain and the nervous system in general.

Focusing now on the analysis of the mathematical models, which is the question that will be tackled in this thesis, we remark that this study usually is carried out both from the analytical and the numerical point of view. Moreover, we will distinguish between microscopic models and mesoscopic models. The first ones describe the evolution of the network based on the behavior of each neuron that belongs to it. As a consequence, they consist of systems of equations, often of stochastic type, where every equation describes the behavior of one of the network's neurons. Nevertheless, although there are many works that perform numerical simulations directly for the microscopic models using the Monte-Carlo method [21, 23, 69, 70, 80, 82, 84, 89], from a computational point of view, it is complicated to handle this models for networks composed of a large number of neurons. Thus, it appears the need to derive mesoscopic models, which allow to determine the evolution of the network through density functions that are solutions of one (or few) Partial Differential Equations (PDEs). This procedure is applied, e.g., in [7, 32, 46, 47, 52, 58, 71, 72, 99, 105]. Usually, the mesoscopic

models permit to recover macroscopic quantities as it are, e.g., the global firing rate of the network, which allow to compare the obtained results with the ones of the microscopic models by means of this magnitudes.

In this thesis, we aim to study the behavior of the solutions of some of this mesoscopic models in the mentioned two directions: analytical and numerical. Specifically, we will focus on the Network of Noisy Leaky Integrate and Fire Neuron (NNLIF) model. It consists of Fokker-Planck like PDEs and determines at mesoscopic level the behavior of a neural network whose neurons are described at microscopic level by the leaky Integrate and Fire (IF) model.

In order to understand properly this model, we will start explaining the physiology of neurons, described by means of several microscopic models. Afterwards we will derive the NNLIF model from the underlying microscopic model. Once the model that we will study in this work has been understood, we will offer a wide review of the related literature in order to make clear the starting point of our investigation. We will finish the introduction summarizing the main aspects of the results obtained in this thesis.

0.1   Physiology of a neuron

Neurons are highly specialized cells which are in charge of the reception and propagation of the nerve impulses. In order to send a nerve impulse, neurons generate *action potencials (or spikes)*, which are electric impulses that appear as a reply to the stimuli they receive: either the beginning of the spike can be created within the neuron or the neuron only propagates the nerve impulse that it receives from another neuron. These impulses arrive at the neuron by the dentrites, travel through the axon and pass from one to another by means of the *synapses*, thanks to the action of the neurotransmitters. We have to take into account that the sending and reception of the nerve impulse is not an instantaneous process: since the signal leaves the presynaptic neuron until it reaches the postsynaptic one, it passes a small period of time known as *synaptic delay*. On the other hand, the signals that they receive from other neurons can be *excitatory* or *inhibitory*, depending on whether they increase or decrease the probability of occurrence of an action potential.

Let us decribe now in detail the underlying mechanism that provokes the appearance of the action potentials [36, 101, 51]. Inside the neuron, among others, there are different ions, as it are sodium Na^+ and potassium K^+. The neuron membrane is impermeable to this ions, but it has some *ionic channels* that, in certain situations, allow the crossing of ions from inside the membrane to the outside or vice versa. Many of this channel are highly selective, as it are the sodium and potassium ones, and only allow the crossing of one ion type. Without signals, the *membrane potential* $V(t)$, which is defined as the potential difference between inside the membrane $V_{int}(t)$ and the outside $V_{ext}(t)$: $V(t) = V_{int}(t) - V_{ext}(t)$, relaxes towards a *equilibrium or resting potential* V_{eq}.

The value of the resting potencial usually is situated around $V_{eq} \sim -70mV$. Thus, in the equilibrium state there is an excess of negative charge inside the membrane. This is achieved thanks to *ionic pumps*, which move the ions from one side of the membrane to the other one, as necessary. The ionic bombs need energy in order to operate.

However, if we apply a current to a neuron in form of a nerve impulse, the resting potential gets lost. First, as a reply to the stimulus, the sodium channels are opened, so that sodium enters the neuron through the membrane due to the electrical attraction. As a consequence, the value of the voltage of the membrane potential increases. If it reaches a certain threshold value, V_F, an action potential is emitted. Let us point out that if the threshold value is not reached, the action potential

is not emitted. Moreover, while the sodium channels are opened, the potassium channels are opened slower. Thus, potassium gets out of the cell due to the concentration difference, since usually there is a higher sodium concentration inside the neuron than outside. The exit of potassium makes the membrane potential negative again. Finally, the sodium-potassium pumps return every ion to its place, reestablishing the resting potential. Moreover, once the action potential has been emitted, the neuron remains some time in a *refractory period*, and does not respond to stimuli.

Let us show now how this behavior is translated into a mathematical model [36, 60, 51]. The time evolution of the membrane potential can be modeled as an electrical circuit

$$C_m \frac{dV}{dt}(t) = I(t),$$

where $I(t)$ is the intensity of the applied current. Nevetheless, as in a neuron there are several active ionic channels that influence directly the value of the membrane potential, we have to extend the equation as follows:

$$C_m \frac{dV}{dt}(t) = -g_{N_a}(V(t) - V_{N_a}) - g_K(V(t) - V_K) - g_L(V(t) - V_L) + I(t), \qquad (1)$$

where g_i is the *conductance* of the channel associated to the ion i and V_i is the *reversal or equilibrium potential* of the channel i. We define the conductance as the ease with which the ions cross the channel and as reversal potential the value of the potential that corresponds to an equilibrium between the inside and outside fluxes. Thus, if we have a channel with reversal potential V_i and the membrane potential is V, if $V > V_i$ then the positive currents flow outside through the channels yielding a decrease of the membrane potential and vice versa if $V < V_i$. Moreover, in the term $I_L(t) := g_L(V(t) - V_L)$, which is called *leak current*, we join all the contributions of the other ions, distinct from sodium and potassium. The constants g_L amd V_L are adjusted until they match the remaining conductance and reversal potential of the membrane.

The **Hodgkin-Huxley (HH) model**, obtained from the observations of the squid's axon by Hodgkin and Huxley in 1952 [55, 54], uses equation (1) to describe the time evolution of the membrane potential coupled to three Ordinary Differential Equations (ODEs) that determine the "state" of the sodium and potassium channels:

$$\begin{aligned}
C_m \frac{dV}{dt}(t) &= -g_{N_a}(V(t) - V_{N_a}) - g_K(V(t) - V_K) - g_L(V(t) - V_L) + I(t), \\
\frac{dh}{dt}(t) &= \alpha_h(V)(1-h) - \beta_h(V)h, \\
\frac{dm}{dt}(t) &= \alpha_m(V)(1-m) - \beta_m(V)m, \\
\frac{dn}{dt}(t) &= \alpha_n(V)(1-n) - \beta_n(V)n,
\end{aligned}$$

where $g_{N_a} = \bar{g}_{N_a} m^3 h$, $g_K = \bar{g}_K n^4$ and g_L are the conductances of sodium, potassium and of the leak current, respectively, and n, m and h are the activation variables. The values of $\alpha_i(V)$ and $\beta_i(V)$ for $i = h, m, n$ are constant and obtained by means of the regression of experimental data.

The **Integrate and Fire (IF) model**, which is based on Lapicque's model proposed in 1907 [48, 60], is obtained if we include the ionic currents of sodium and potassium also in the term that

groups the leaky currents $I_L(t)$. As a consequence, this model is a simplification of the HH model, being equation (1) reduced to

$$C_m \frac{dV}{dt}(t) = -g_L(V(t) - V_L) + I(t).$$

There are other models which are simplifications of the HH model, as it are the HH model for two dimensions [44], the Morris-Lecar model [68] and the Fitzhugh-Nagumo model [45], whose macroscopic approximation has been studied, e.g., in [2, 67]. Here we have focused our attention on the description of the simpliflied IF model, since it provides the microscopic description of the physiology of neurons on which are based the NNLIF models that are analyzed in this thesis.

0.2   Deriving the full NNLIF model

In order to provide the conceptual, mathematical and biological framework of our work, in this section we explain how the equations (PDEs and ODEs) that represent the full NNLIF model at microscopic level are derived, starting from the biological model that describes the behavior of the neurons at microscopic level. Before continuing we refer to [12, 85, 95, 10, 88, 11, 94, 41, 48, 101, 51] for the reader interested in obtaining a wider knowledge of different versions of the IF model and its validation as an suitable model to be used in neuroscience.

We consider a neural network with n neurons (n_E excitatory and n_I inhibitory) described by the Integrate and Fire model, which depicts the activity of the membrane potential. The time evolution of the membrane potential $V_\alpha(t)$ of an inhibitory neuron ($\alpha = I$) or an excitatory one ($\alpha = E$) is given by the following equation (see the previous section and [11, 12] for details)

$$C_m \frac{dV^\alpha}{dt}(t) = -g_L(V^\alpha(t) - V_L) + I^\alpha(t), \tag{2}$$

where C_m is the capacitance of the membrane, g_L is the leak conductance, V_L is the leak reversal potential and $I^\alpha(t)$ is the incoming synaptic current, which models all the interactions of the neuron with other neurons. In the absence of interactions with other neurons ($I^\alpha(t) = 0$), the membrane potential relaxes towards a resting value V_L. However, the interaction with other neurons provokes the neuron to fire, that is, it emits an action potential (spike) when $V^\alpha(t)$ reaches its threshold or firing value V_F, and the membrane potential relaxes to a reset value V_R. (Let us remark that $V_L < V_R < V_F$). Each neuron receives C_{ext} connections from excitatory neurons outside the network, and $C = C_E + C_I$ connections from neurons in the network; $C_E = \epsilon \, n_E$ from excitatory neurons and $C_I = \epsilon \, n_I$ from inhibitory neurons. These connections are assumed to be randomly choosen, and the network to be sparsely connected, namely, $\epsilon = \frac{C_E}{n_E} = \frac{C_I}{n_I} << 1$, see [11]. The synaptic current $I^\alpha(t)$ takes the form of the following stochastic process

$$I^\alpha(t) = J_E^\alpha \sum_{i=1}^{\bar{C}_E} \sum_j \delta(t - t_{Ej}^i - D_E^\alpha) - J_I^\alpha \sum_{i=1}^{C_I} \sum_j \delta(t - t_{Ij}^i - D_I^\alpha), \qquad \alpha = E, I,$$

where $D_E^\alpha \geq 0$, $D_I^\alpha \geq 0$ are the synaptic delays, t_{Ej}^i and t_{Ij}^i are the times of the jth-spike coming from the ith-presynaptic neuron for excitatory and inhibitory neurons, respectively, $\bar{C}_E = C_E + C_{ext}$, and J_k^α, for $\alpha, k = E, I$ are the strengths of the synapses. The stochastic character is enclosed in

the distribution of the spike times of the neurons. The spike trains of all neurons in the network are supposed to be described by Poisson processes with a common instantaneous firing rate, $\nu_\alpha(t)$, $\alpha = E, I$. These processes are supposed to be independent [11, 15]. By using these hypotheses, the mean value of the current, $\mu_C^\alpha(t)$, and its variance, $\sigma_C^{\alpha 2}(t)$, take the form

$$
\begin{align}
\mu_C^\alpha(t) &= C_E J_E^\alpha \nu_E(t - D_E^\alpha) - C_I J_I^\alpha \nu_I(t - D_I^\alpha), \tag{3} \\
\sigma_C^{\alpha 2}(t) &= C_E (J_E^\alpha)^2 \nu_E(t - D_E^\alpha) + C_I (J_I^\alpha)^2 \nu_I(t - D_I^\alpha), \tag{4}
\end{align}
$$

where we need the hypothesis $C_{ext} = C_E$ in order to have them well defined. Many authors [11, 12, 65, 73] then approximate the incoming synaptic current by a continuous in time stochastic process of Ornstein-Uhlenbeck type which has the same mean and variance as the Poissonian spike-train process. Specifically, $I^\alpha(t)$ is approached by

$$
I^\alpha(t) dt \approx \mu_C^\alpha(t) \ dt + \sigma_C^\alpha(t) \ dB_t, \qquad \alpha = E, I, \tag{5}
$$

where B_t is the standard Brownian motion.

Summing up, the approximation to the stochastic diferential equation model (2), taking the voltage and time units so that $C_m = g_L = 1$, finally yields

$$
dV^\alpha(t) = (-V^\alpha(t) + V_L + \mu_C^\alpha(t)) \ dt + \sigma_C^\alpha(t) \ dB_t, \qquad V^\alpha \le V_F, \qquad \alpha = E, I, \tag{6}
$$

with the jump process $V^\alpha(t_0^+) = V_R$, $V^\alpha(t_0^-) = V_F$, whenever at t_0 the voltage reaches the threshold value V_F.

The firing rate or probability of firing per unit time of the Poissonian spike train, $\nu_\alpha(t)$, is calculated in [85] as

$$
\nu_\alpha(t) = \nu_{\alpha, ext} + N_\alpha(t), \qquad \alpha = E, I,
$$

where $\nu_{\alpha, ext}$ is the frequency of the external input and $N_\alpha(t)$ is the mean firing rate of the population α. Also $\nu_{I, ext} = 0$ since the external connections are with excitatory neurons.

Going back to (6), a system of coupled partial differential equations for the evolution of the probability densities $\rho_\alpha(v, t)$ can be written, where $\rho_\alpha(v, t)$ denotes the probability of finding a neuron in the population α, with a voltage $v \in (-\infty, V_F]$ at a time $t \ge 0$. In [11, 12, 65, 73, 87] taking the limit $n \to \infty$ and using Itô's rule transform the stochastic equations (2) and (5) into a system of coupled Fokker-Planck or backward Kolmogorov equations with sources

$$
\begin{cases}
\frac{\partial \rho_I}{\partial t}(v, t) + \frac{\partial}{\partial v}[h^I(v, N_E(t - D_E^I), N_I(t - D_I^I)) \rho_I(v, t)] - a_I(N_E(t - D_E^I), N_I(t - D_I^I)) \frac{\partial^2 \rho_I}{\partial v^2}(v, t) \\
\qquad\qquad\qquad\qquad\qquad\qquad\qquad\qquad\qquad\qquad\qquad\qquad = M_I(t) \delta(v - V_R), \\
\\
\frac{\partial \rho_E}{\partial t}(v, t) + \frac{\partial}{\partial v}[h^E(v, N_E(t - D_E^E), N_I(t - D_I^E)) \rho_E(v, t)] - a_E(N_E(t - D_E^E), N_I(t - D_I^E)) \frac{\partial^2 \rho_E}{\partial v^2}(v, t) \\
\qquad\qquad\qquad\qquad\qquad\qquad\qquad\qquad\qquad\qquad\qquad\qquad = M_E(t) \delta(v - V_R),
\end{cases} \tag{7}
$$

with $h^\alpha(v, N_E(t - D_E^\alpha), N_I(t - D_I^\alpha)) = -v + V_L + \mu_C^\alpha$ and $a_\alpha(N_E(t - D_E^\alpha), N_I(t - D_I^\alpha)) = \frac{\sigma_C^{\alpha 2}}{2}$. The right hand sides in (7) represent the fact that when neurons reach the threshold potential V_F, they emit a spike over the network, reset their membrane potential to the reset value V_R and remain some time in a refractory period, denoted τ_α. Different choices of $M_\alpha(t)$ can be considered: $M_\alpha(t) = N_\alpha(t - \tau_\alpha)$, as

27

studied in [11] or $M_\alpha(t) = \frac{R_\alpha(t)}{\tau_\alpha}$ as proposed in [17]. Thus, system (7) is completed with two ODEs for $R_\alpha(t)$, the probabilities to find a neuron from population α in the refractory state

$$\frac{dR_\alpha(t)}{dt} = N_\alpha(t) - M_\alpha(t), \quad \forall \alpha = E, I, \tag{8}$$

Dirichlet boundary conditions and initial data

$$\rho_\alpha(-\infty, t) = 0, \; \rho_\alpha(V_F, t) = 0, \; \rho_\alpha(v, 0) = \rho_\alpha^0(v) \geq 0, \quad R_\alpha(0) = R_\alpha^0 \geq 0 \quad \alpha = E, I. \tag{9}$$

In order to simplify the notation, we denote $d_k^\alpha = C_k(J_k^\alpha)^2 \geq 0$ and $b_k^\alpha = C_k J_k^\alpha \geq 0$ for $k, \alpha = E, I$, and the variable v is translated with the factor $V_L + b_E^E \nu_{E,ext}$. Let us remark that we keep the same notation for the other involved values $(V_R, \; V_F)$ and also v for the new variable. With the new voltage variable and using expressions (3) and (4) for $\mu_C^\alpha(t)$ and $\sigma_C^\alpha(t)$, the drift and diffusion coefficients become

$$h^\alpha(v, N_E(t - D_E^\alpha), N_I(t - D_I^\alpha)) = -v + b_E^\alpha N_E(t - D_E^\alpha) - b_I^\alpha N_I(t - D_I^\alpha) + (b_E^\alpha - b_E^E)\nu_{E,ext}, \tag{10}$$
$$a_\alpha(N_E(t - D_E^\alpha), N_I(t - D_I^\alpha)) = d_E^\alpha \nu_{E,ext} + d_E^\alpha N_E(t - D_E^\alpha) + d_I^\alpha N_I(t - D_I^\alpha), \quad \alpha = E, I. \tag{11}$$

The coupling of the system (7) is hidden in these two terms, since the mean firing rates N_α obey to

$$N_\alpha(t) = -a_\alpha(N_E(t), N_I(t))\frac{\partial \rho_\alpha}{\partial v}(V_F, t) \geq 0, \quad \alpha = E, I. \tag{12}$$

Moreover, (12) gives rise to the nonlinearity of the system (7), since firing rates are defined in terms of boundary conditions on distribution functions ρ_α. On the other hand, since R_E and R_I represent probabilities and ρ_E and ρ_I are probability densities, the total mass is conserved:

$$\int_{-\infty}^{V_F} \rho_\alpha(v, t) \, dv + R_\alpha(t) = \int_{-\infty}^{V_F} \rho_\alpha^0(v) \, dv + R_\alpha^0 = 1 \quad \forall \, t \geq 0, \quad \alpha = E, I.$$

0.3 Other models

Once the full NNLIF model has been derived, it should be mentioned that there is a wide range of mathematical models that share with the NNLIF model the aim to describe the behavior of neural networks through PDEs. Below, we describe some of the models on which we have started to work with perspective of future investigations after finishing this thesis, since they maintain a close relationship with the NNLIF model. Among others, we aim to locate relations between them, following the ideas of, e.g., [42].

- **Age structured models or of Pakdaman, Perthame y Salort (PPS).** In this model the dynamics of a neural network at mesoscopic level is described by means of a PDE that remembers age structured models, applied usually in ecology and widely studied, e.g., in [77]. The unknown is a probability density $n(s, t)$ that determines the probability of finding a neuron of age s at the time instant t. In this case the "age" refers to the time elapsed since the last spike. The model,

widely analized in [74], [75] and [76], is:

$$\begin{cases} \frac{\partial}{\partial t} n(s,t) + \frac{\partial}{\partial s} n(s,t) + p\left(s, X(t)\right) n(s,t) = 0, \\\\ X(t) = J \int_0^t \alpha(s) N(t-s) \, ds \text{ with delay}, \\\\ X(t) = N(t) \text{ without delay}, \\\\ N(t) := n(0,t) = \int_0^\infty p\left(s, X(t)\right) n(s,t) \, ds, \end{cases}$$

where the non-negative functions $\alpha(s)$ y $p(s,x)$ have to satisfy the following modelling hypotheses

$$\int_0^\infty \alpha(s) \, ds, \qquad \alpha(.) \geq 0,$$

$$\frac{\partial}{\partial s} p(s,x) \geq 0, \quad p(s,x) = 0 \text{ para } s \in (0, s^*(x)), \quad p(s,x) > 0 \text{ para } s > s^*(x), \quad p(s,x) \xrightarrow[s \to \infty]{} 1,$$

$$\frac{\partial}{\partial x} p(s,x) \geq 0, \qquad p(s,x) \xrightarrow[x \to \infty]{} 1.$$

The biological meanings of the functions and parameters that appear in this model are:

- $N(t)$ is the density of neurons that spike at time t,
- $\alpha(s) \geq 0$ is the distributed delay function,
- $X(t)$ is the global activity at time t,
- $p(s, X)$ is the firing rate of neurons in state s and with global activity X,
- $J \geq 0$ represents the connectivity of the network.

Some relevant aspects that are studied in the cited works consist of the analysis of the behavior of the solutions depending on the parameters and variable functions of the model: steady states, existence of solution, convergence to a stationary state and spontaneous periodic oscillations. This theoretical results are illustrated and complemented with numerical simulations. Moreover, in [42] it is found an integral transform that allows to rewrite a solution of the PPS models as a solution of the NNLIF model for a drift term given by $h(v,N) = \mu - v$ where $\mu \in \mathbb{R}$ is constant and a constant difussion term $a(N) = \frac{\sigma^2}{2}$, that avoid the non-linearity of the model.

On the other hand, there are several works that link the PPS model with its microscopic version. This is interesting, since for some microscopic models it has been proved that they fit statistically well to the data of real spike trains [79, 86]. Specifically, in [34] it are linked several microscopic models (Poisson, Wold, Hawkes) to the PPS model and in [33] it is obtained that the PPS model is the mean fiel limit of n interacting age structured Hawkes mean field processes.

- **Population density models of IF neuron with jumps.** This models, which was initially presented in [73] in order to facilitate the numerical simulation of mesoscopic neural populations, appears from the same microscopic approximation as the NNLIF model, and thus, its unknown ρ refers to a similar probability density. Specifically, ρ is the probability density of finding a neuron of the network with membrane potencial v at time t. Nevertheless, the concrete expression of the

PDE that represents these models changes, since to obtain it, it are made less approximations:

$$
\begin{cases}
\frac{\partial}{\partial t}\rho(t,v) - \frac{\partial}{\partial v}\left(v\rho(t,v)\right) = \sigma(t)\left(\rho(t,v-h) - \rho(t,v)\right) + \delta(v - V_R)r(t), \\[2mm]
\sigma(t) := \sigma_0(t) + J\ r(t)\text{without synaptic delay, or,} \\[2mm]
\sigma(t) := \sigma_0(t) + J\int_0^t \alpha(u)r(t-u)\ du \text{ with synaptic delay,} \\[2mm]
r(t) = \sigma(t)\int_{1-h}^1 \rho(t,w)\ dw, \\[2mm]
\rho(t,1) = 0, \\[2mm]
\rho(0,.) = \rho_0 \in L^1_+(0,1),
\end{cases}
$$

where

- h is the size of the jump that makes the potential v when the neuron receives a spike at one of its synapses,
- $\alpha(u)$ is the delay's density function and, thus, $\int_0^\infty \alpha(u)\ du = 1$,
- V_R is the reset value,
- $\sigma(t)$ is the reception rate of each neuron,
- $r(t)$ is the firing rate of the population,
- $\sigma_0(t)$ is the excitatory external influence,
- J is the mean number of presynaptic neurons for each neuron.

From the theoretical point of view it has been studied, among others, in [41, 40, 39]. The most relevant result of [41] is that it is proved that the firing rate blows-up in finite time in some situations and the one of [40] consists of showing that this blow-up disappears if a synaptic delay is considered. In [39], among others, they study the well-posedness of the equation and the existence, uniqueness and stability of the steady states for certain values of the connectivity parameter.

- **NNLIF model with conductance.** This model is a more realistic version of the NNLIF model than (7), since it considers one more variable: the conductance. This variable is needed to take into account slow post-sypnatic receptors [84]. As a consequence, the unknown of the PDE that represents this model is a probability density $\rho(v,g,t)$ that describes the probability of finding a neuron at time t with a membrane potential $v \in [V_R, V_F]$ and with conductance $g > 0$. The equation, derived in [23, 22] and [83] is as follows:

$$
\frac{\partial \rho(v,g,t)}{\partial t} + \frac{\partial[(-g_L v + g(V_E - v))\rho(v,g,t)]}{\partial v} + \frac{\partial}{\partial g}\left[\frac{g_{in}(t) - g}{\sigma_E}\rho(v,g,t)\right] - \frac{a(t)}{\sigma_E}\frac{\partial^2 \rho(v,g,t)}{\partial g^2} = 0,
$$

which is completed with these initial data

$$
\rho^0(v,g) \geq 0, \quad \text{such that} \quad \int_0^{V_F}\int_0^\infty \rho^0(v,g)\ dv\ dg = 1.
$$

The non-linearity of this equation appears due to the terms $g_{in}(t)$ and $a(t)$, which depend on the total firing rate $\mathcal{N} > 0$, defined as follows

$$N(g,t) := [-g_L V_F + g(V_E - V_F)]\rho(V_F, g, t) \geq 0, \qquad \mathcal{N} := \int_0^\infty N(g,t)dg,$$

where $N(g,t)$ represents the firing rate that depends on g and

$$\begin{aligned} g_{in}(t) &= f_E \nu(t) + S_E \mathcal{N}(t), \\ a(t) &= \frac{1}{2\sigma_E}\left(f_E^2 \nu(t) + \frac{S_E^2}{N_E}\mathcal{N} \right). \end{aligned}$$

The parameters that appear in the equation are interpreted as follows

- V_E is the excitatory reversal potential,
- V_F is the threshold potential,
- the reset is at V_R and we consider that $0 = V_R < V_F < V_E$,
- $g_L > 0$ denotes the leaky conductance,
- $g_{in}(t) \geq 0$ is the conductance induced by input currents,
- $a(t) = a(\mathcal{N}, t) > 0$ represents the intensity of the synaptic noise,
- $\sigma_E > 0$ denotes the decay constant of the excitatory conductance,
- $S_E \geq 0$ represents the synaptic strength of the excitatory coupling of the network,
- $\nu(t)$ is the external input,
- $f_E > 0$ in the synaptic strength of $\nu(t)$,
- N_E provides the total normalization of the coupling strength.

This model has been studied from an analytical point of view, among others, in [78], where it has been analyzed, among others, if a blow-up of the firing rate appears for this model. It are obtained several a priori bounds over ρ and the firing rate, that allow to conclude that this phenomenon does not appear. On the other hand, in [16] it is presented a deterministic numerical solver for this model, it are done several simulations and the deterministic results are compared to Monte Carlo simulations.

0.4 Starting point

In this section we offer a review of the related literature in order to make clear the starting point of the investigation of this thesis. Initially, in [11] it was derived the full NNLIF model, considering all the biological properties described before. Nevertheless, the mathematical study of this model is quite complicated. Thus, to start the mathematical analysis, in [15] it was proposed a simplified toy model that considers a neural network composed by only one neural population, that can be on average excitatory or inhibitory. This fact is reflected in the sign of one of the model parameters, known as *connectivity parameter*. Moreover, it was supposed that neurons do to enter in the refractory and that there is no synaptic delay in the transmission of the nerve impulse. From the mathematical point of view, this model is represented by a Fokker-Planck like PDE that has been widely studied in [15], [29] and [26].

Some relevant results of [15] are the study of the number of steady states in terms of the parameter values and the proof of the existence of some parameter values and/or initial conditions for the excitatory case, for which the solutions do not exist for every time (blow-up). Moreover, the numerical simulations showed suggest that this is because of the blow-up of the firing rate in finite time.

In [29] it is provided a criterium to determine the maximal time of existence of solution for this simplified model. It ensures that solutions exist and are unique while the firing rate is finite. Thus, this underlines the numerical observations of the previous work. Moreover, using this criterium it is proved that there is a global-in-time existence of the solution for the inhibitory case. As a consequence, solutions cannot blow-up for on average inhibitory populations.

In [26] it is proved the exponential convergence of the solutions to the equilibrium in case the connectivity parameter is small in absolute value, using a Poincaré like inequality and the entropy dissipation method. Also it is recovered the global existence result for the inhibitory case, using the maximal time of existence criterium combined with an upper-solution concept. It allows, on the other hand, to obtain some a priori bounds for the firing rate.

Later, in [17] it was considered a more complete model, adding the refractory state to the initial simplified model of [15]. Among others, the models was studied following the ideas of [15] and it were analyzed the changes of the behavior of the solutions: e.g., for the previous model there were cases where there are no steady states, and for this more complete model there is always at least one. Moreover, it is proved that the blow-up appears again in the same situations as the ones given in [15].

On the other hand, it have been developed also some works that study IF neural networks at microscopic level, through stochastic equations. Among then, it can be found [37] y [38]. In [37] as in [15], it is considered that neurons do not enter in a refractory state and that there is no delay. Here, among others, the authors prove that the blow-up is reflected also at microscopic level. In [38] the delay is included in the model, but not the refractory state. The most relevant result is that it is proved that the blow-up disappears. Immediately, this makes us think that this fact probably will be also observed at the mesoscopic level.

There is a great deal of works that include the delay in neural models. Among others, we can find the works of Touboul [96, 98, 97] where it is taken into account also the spatial distribution of the populations.

This, together with the results for the Omurtag-Dumont model of [40], is the starting point of the work developed in this thesis. The aim now is to study simplified models more and more completed, until we reach the analysis of most realistic model (7), derived in [11].

0.5   Summary of results

The results obtained for the full NNLIF model and for some of its simplifications, are presented in three chapters. The chapters are arranged in an increasing manner, depending on the completeness of the model that is studied. Thus, in the first chapter it is considered the NNLIF model for only one population, with delay and without refractory state; in the second chapter we analyze the NNLIF model for two populations, but without refractory states and without delays; and in the third chapter we present the results for the full NNLIF model: two populations, with refractory states and with delays. Moreover, it has been implemented a numerical resolutor, used to illustrate many of the theoretical results and also to shed some light on the aspects which could not be addressed from an analytical point of view due to its complexity. The numerical schemes and implementation techniques used to get the resolutor are detailed in the appendix.

Before explaining in detail the results, we clarify the notation and acronyms used in this work.

For $1 \leq p < \infty$, $L^p(\Omega)$ is the space of functions such that f^p is integrable in Ω, $L^\infty(\Omega)$ is the space of essentially bounded functions in Ω, $L^\infty_+(\Omega)$ represents the space of non-negative essentially bounded functions in Ω, $C^p(\Omega)$ is the set of p times differentiable functions in Ω, $C^\infty(\Omega)$ is the set of infinitely differentiable functions in Ω, $L^1_{loc,+}(\Omega)$ denotes the set of non-negative functions that are locally integrable in Ω and the Sobolev space $H^p = W^{p,2}$ is the subset of functions f in $L^p(\mathbb{R})$ such that the function f and its weak derivatives up to order k have a finite L^p norm. The following table summarizes the meaning of the acronyms used.

Acronym	Meaning
NNLIF	Nonlinear Noisy Leaky Integrate and Fire
IF	Integrate and Fire
PDE	Partial differential Equation
ODE	Ordinary Differential Equation
WENO	Weighted Essentially Non-Oscillatory
CFL	Courant-Friedrich-Lewy
TVD	Total Variation Diminishing
MPI	Message Passing Interface
IVP	Initial Value Problem
RHS	Right Hand Side

0.5.1   Main results of chapter 1

The first chapter, which is based on the work [18], considers a simplified NNLIF model that describes a neural network composed of only one population with synaptic delay $D \geq 0$ and without refractory state. The associated system is simpler than (7), since it consist of only one PDE:

$$\frac{\partial \rho}{\partial t}(v,t) + \frac{\partial}{\partial v}[(v - \mu(t-D))\rho(v,t)] - a\frac{\partial^2 \rho}{\partial v^2}(v,t) = N(t)\delta(v - V_R), \qquad v \leq V_F = 0, \tag{13}$$

where $\rho(v,t)$ is the probability density of finding a neuron of the population with a voltage value v at time t. The drift term μ and the firing rate N are given by

$$\mu(t) = b_0 + bN(t) \quad \text{with} \quad N(t) = -a\frac{\partial \rho}{\partial v}(V_F, t) \geq 0, \tag{14}$$

where b is the connectivity parameter that determines the type of network considered: excitatory $(b > 0)$ or inhibitory $b < 0$, and b_0 is the parameter that controls the strength of the external stimuli. It can be either positive or negative. The PDE (13) has to be completed with initial and boundary conditions

$$N(t) = N^0(t) \geq 0, \quad \forall\, t \in [-D, 0), \quad \rho(v,0) = \rho^0(v) \geq 0, \quad \rho(V_F, t) = 0, \quad p(-\infty, t) = 0. \tag{15}$$

Moreover, as ρ is a probability densitiy the total mass is conserved

$$\int_{-\infty}^{V_F} \rho(v,t)\, dv = \int_{-\infty}^{V_F} \rho^0(v)\, dv = 1, \qquad \forall\, t \geq 0.$$

The main result of this chapter is the proof of the global-in-time existence and uniqueness of the solutions of (13)-(14)-(15) for the excitatory case if there is a nonzero delay. Remember that this had been already observed at microscopic level in [33]. As a consequence, the blow-up in finite time of the firing rate, that was observed in [15] for this model without delay for some parameter values and/or initial data, disappears. As a by-product, we obtain the global-in-time existence also for the inhibitory case with delay. This was an expected result, since in [29] it was shown that the solutions are global-in-time for the inhibitory case without delay. The result is this:

Theorem 0.5.1 (Global existence - delayed excitatory and inhibitory cases) *Let (ρ, N) be a local classical solution of (1.1)-(1.2)-(1.4) for $b_0 = 0$ and $D > 0$ for the non-negative initial condition (ρ^0, N^0) where $N^0 \in C^0([-D, 0))$ is bounded and $\rho^0 \in L^1((-\infty, V_F)) \cap C^1((-\infty, V_R) \cup (V_R, V_F]) \cap C^0((-\infty, V_F])$, is such that $\rho^0(V_F) = 0$. Suppose that ρ^0 admits finite left and right derivatives at V_R and that ρ^0 and $(\rho^0)_v$ decay to zero as $v \to -\infty$. Then, the maximal time existence for the solution (ρ, N) is $T^* = +\infty$.*

Obtaining this result is complicated, we have to combine aguments and techniques of [26] with the ones of [29] and find an appropiate strategy to treat the delay. We start rewriting (13)-(14)-(15) as a Stefan like problem with a nonstandard right hand side. With that purpose, we perfom two well known changes of variables (widely studied in [30]) and some computations in order to translate also properly the synaptic delay:

- The *first change of variables* is given by

$$y = e^t v, \qquad \tau = \frac{1}{2}(e^{2t} - 1).$$

As a consequence,

$$v = y\alpha(\tau), \qquad t = -\log(\alpha(\tau)),$$

where $\alpha(\tau) = (\sqrt{2\tau + 1})^{-1}$, and we define

$$w(y, \tau) = \alpha(\tau)\rho(y\alpha(\tau), -\log(\alpha(\tau))),$$

differentiating we obtain the equation

$$w_\tau(y, \tau) = w_{yy}(y, \tau) - \alpha(\tau)\mu(t - D)w_y(y, \tau) + M(\tau)\delta\left(y - \frac{V_R}{\alpha(\tau)}\right), \tag{16}$$

where $M(\tau) = -w_y(0, \tau) = \alpha^2(\tau)N(t)$.

- The *second change of variables*. In order to remove the term with w_y in (16) we introduce the change of variables

$$x = y - \int_0^\tau \mu(t - D)\alpha(s)\, ds = y - b_0(\sqrt{2\tau + 1} - 1) - b\int_0^\tau N(t - D)\alpha(s)\, ds,$$

and we define

$$u(x, \tau) = w(x + \int_0^\tau \mu(t - D)\alpha(s)\, ds, \tau).$$

34

Differentiating again we obtain this system for u_τ

$$\begin{cases} u_\tau(x,\tau) = u_{xx}(x,\tau) + M(\tau)\delta(x - s_1(\tau)), & x < s(\tau), \tau > 0, \\ s_1(\tau) = s(\tau) + \frac{V_R}{\alpha(\tau)}, & \tau > 0, \\ s(\tau) = -b_0(\sqrt{2\tau + 1} - 1) - b\int_0^\tau N(t - D)\alpha(s)\, ds, & \tau > 0, \\ M(\tau) = -u_x(s(\tau), \tau), & \tau > 0, \\ N(t) = N(0), & t \in (-D, 0], \\ u(-\infty, \tau) = u(s(\tau), \tau) = 0, & \tau > 0, \\ u(x, 0) = u_I(x), & x < 0. \end{cases} \tag{17}$$

- *Translating the delay.* We have to remove the explicit t dependance in (17) in the term $N(t-D)$. With that purpose we remember that t and τ are related through the change of variables $\tau = \frac{1}{2}(e^{2t} - 1)$, $t = \frac{1}{2}\log(2\tau + 1)$. As a consequence if we consider the time $t - D$, there is a related τ_D: $\tau_D = \frac{1}{2}(e^{2(t-D)} - 1)$, which makes complicated the handling of D. In order to work with the delay in an easier way, we propose the following strategy. As $D \geq 0$, $\tau_D \leq \tau$, and thus, there is a $\bar{D} > 0$ such that $\tau_D = \tau - \bar{D}$. By direct computations we obtain that $\bar{D} = \frac{1}{2}e^{2t}(1 - e^{-2D}) > 0$. Replacing now t by the related τ and defining $\hat{D} = (1 - e^{-2D})$, finally we conlude that $\bar{D} = \hat{D}(\tau + \frac{1}{2})$.

This results allows us to write properly the following relation

$$\begin{aligned} N(t - D) &= \alpha^{-2}(\tau_D)M(\tau_D) = \alpha^{-2}(\tau - \bar{D})M(\tau - \bar{D}) \\ &= \alpha^{-2}\left((1 - \hat{D})\tau - \frac{1}{2}\hat{D}\right)M\left((1 - \hat{D})\tau - \frac{1}{2}\hat{D}\right). \end{aligned} \tag{18}$$

In this way, the initial synaptic delay D is translated into the delay $\hat{D}$, which is scaled between 0 and 1, being $\hat{D} = 0$ if $D = 0$ and $\hat{D} = 1$ if $D = \infty$.

- The *equivalent Stefan like equation.* Using (18) we can rewrite $s(\tau)$ of (17) in terms of $M(\tau)$, avoiding its t dependance through $N(t)$

$$\begin{aligned} s(\tau) &= -b_0(\sqrt{2\tau + 1} - 1) - b\int_0^\tau N(t - D)\alpha(s)\, ds \\ &= -b_0(\sqrt{2\tau + 1} - 1) - b\int_0^\tau \alpha^{-2}((1 - \hat{D})s - \frac{1}{2}\hat{D})M((1 - \hat{D})s - \frac{1}{2}\hat{D})\alpha(s)\, ds. \end{aligned}$$

A simple change of variables yields

$$s(\tau) = -b_0(\sqrt{2\tau + 1} - 1) - \frac{b}{\sqrt{1 - \hat{D}}}\int_{-\frac{1}{2}\hat{D}}^{(1-\hat{D})\tau - \frac{1}{2}\hat{D}} M(s)\alpha^{-1}(s)\, ds.$$

Denoting $t = \tau$ and $D = \hat{D}$ finally we reach the following Stefan like equation

$$
\begin{cases}
u_t(x,t) = u_{xx}(x,t) + M(t)\delta(x - s_1(t)), & x < s(t), t > 0, \\
s_1(t) = s(t) + \frac{V_R}{\alpha(t)}, & t > 0, \\
s(t) = -b_0(\sqrt{2t+1} - 1) - \frac{b}{\sqrt{1-D}} \int_{-\frac{1}{2}D}^{(1-D)t - \frac{1}{2}D} M(s)\alpha^{-1}(s) \; ds, & t > 0, \\
M(t) = -u_x(s(t), t), & t > 0, \\
M(t) = M(0), & t \in (-D, 0], \\
u(-\infty, t) = u(s(t), t) = 0, & t > 0, \\
u(x, 0) = u_I(x), & x < 0,
\end{cases}
\tag{19}
$$

where $D \in [0, 1)$ and $\alpha(t) = \frac{1}{\sqrt{2t+1}}$. Notice that this problem is well defined since $\alpha(t) \in \mathbb{R}^+ \; \forall \, t > -\frac{1}{2}$.

Once we have obtained the equivalent Stefan like system, we perform some tedious computations in order to obtain an implicit integral formulation for M:

$$
\begin{aligned}
M(t) &= -2\int_{-\infty}^{V_R} G(s(t), t, \xi, 0)u_I'(\xi)d\xi - 2\int_{V_R}^{0} G(s(t), t, \xi, 0)u_I'(\xi)d\xi \\
&\quad + 2\int_0^t M(\tau)G_x(s(t), t, s(\tau), \tau)d\tau - 2\int_0^t M(\tau)G_x(s(t), t, s_1(\tau), \tau)d\tau,
\end{aligned}
\tag{20}
$$

where G is Green's function for the heat equation on the real line

$$
G(x, t, \xi, \tau) = \frac{1}{[4\pi(t - \tau)]^{\frac{1}{2}}} e^{-\frac{|x-\xi|^2}{4(t-\tau)}}.
$$

This integral formulation will be crucial for the development of many of the computations done in this chapter. First, by means of a fixed point argument, it will allow to get a local existence of solution result for problem (19). Moreover, this result provides an estimate of the time of existence of the local solution:

Theorem 0.5.2 *Let $u_I(x)$ be a non-negative $\mathcal{C}^0((-\infty, 0]) \cap \mathcal{C}^1((-\infty, V_R) \cup (V_R, 0]) \cap L^1(-\infty, 0))$ function such that $u_I(0) = 0$. Suppose that u_I and $(u_I)_x$ decay to zero as $x \to -\infty$ and that the left and right derivatives at V_R are finite. Then there exists a time $T > 0$ such that $M(t)$ defined by the integral formulation (20) exists for $t \in [0, T]$ and is unique in $\mathcal{C}([0, T])$. The existence time T satisfies*

$$
T \leq \left(\sup_{x \in (-\infty, V_R) \cup (V_R, 0]} |u_I'(x)| \right)^{-1}.
$$

For the sake of completeness we have to show how Theorem 0.5.2 is translated into our initial equation. First, as in [49], once M is known, the equation for u uncouples, and can be solved by a Duhamel's formula. As a consequence, the local existence is reflected also for the system (19). Afterwards, ρ is recovered from u undoing the changes of variables. Thus finally we obtain local existence for (13).

The result of local existence is the main tool used to prove a criterium that determines the maximal time of existence of the solution in terms of the growth of the firing rate. This result will be the key to derive the main result of this chapter (Theorem 0.5.1).

Theorem 0.5.3 (Maximal time of existence) *Suppose that the hypotheses of Theorem 0.5.2 hold. Then the solution u can be extended up to a maximal time $0 < \bar{T} \leq \infty$ given by*

$$\bar{T} = \sup\{t > 0 : M(t) < \infty\}.$$

Translating again this result to (13) using the same procedure as described for the local existence, we can ensure that the solutions existe whenever the firing rate N is finite. In order to proof the global existence using this criterium we need the notion of upper-solution:

Definition 0.5.4 *Let $T \in \mathbb{R}_+$, $(\bar{\rho}, \bar{N})$ is said to be a (classical) upper-solution for (13)-(14)-(15) for $D \geq 0$ and $b_0 = 0$ on $(-\infty, V_F] \times [0, T]$ if for all $t \in [0, T]$ we have $\bar{\rho}(V_F, t) = 0$ and*

$$\partial_t \bar{\rho} + \partial_v[(-v + b\bar{N}(t - D))\bar{\rho}] - a\partial_{vv}\bar{\rho} \geq \delta_{v=V_R}\bar{N}(t), \quad \bar{N}(t) = -a\partial_v\bar{\rho}(V_F, t).$$

on $(-\infty, V_F] \times [0, T]$ in the distributional sense and on $((-\infty, V_F] \setminus V_R) \times [0, T]$ in the classical sense, with arbitrary values for $\bar{N}$ on $[-D, 0)$.

It will allow us to compute a family of upper-solutions, that will provide the needed control over the firing rate, so that the criterium for the maximal time of existence of the solution can be applied, by means of this theorem:

Theorem 0.5.5 *Let $T < D$. Let (ρ, N) be a classical solution of (13)-(14)-(15) for $b_0 = 0$ and $D > 0$ on $(-\infty, V_F] \times [0, T]$ for the initial condition (ρ^0, N^0) and let $(\bar{\rho}, \bar{N})$ be a classical upper-solution of (13)-(14)-(15) for $b_0 = 0$ and $D > 0$ for $b_0 = 0$ and $D > 0$ on $(-\infty, V_F] \times [0, T]$. Assume that*

$$\forall v \in (-\infty, V_F], \quad \bar{\rho}(v, 0) \geq \rho^0(v) \qquad and \qquad \forall t \in [-D, 0), \quad \bar{N}(t) = N^0(t).$$

Then,

$$\forall (v, t) \in (-\infty, V_F] \times [0, T], \quad \bar{\rho}(v, t) \geq p(v, t) \qquad and \qquad \forall t \in [0, T], \quad \bar{N}(t) \geq N(t).$$

Notice that for this model it is not necessary to analyze the number of steady states, since the result presented in [15] that, e.g., ensures uniqueness of the steady state for small values of b in absolute value, holds also for the model (13).

0.5.2 Main results of chapter 2

The contents of the second chapter corresponds to the publication [19], addressing a more complete version of the model, since it considers a neural network composed of two populations, which leads to two coupled Fokker Planck like PDEs. In order to reduce complexity, we assume that there are no delays and no refractory states. The resulting model is given by this system:

$$\begin{cases} \frac{\partial \rho_I}{\partial t}(v, t) + \frac{\partial}{\partial v}[h^I(v, N_E(t), N_I(t))\rho_I(v, t)] - a_I(N_E(t), N_I(t))\frac{\partial^2 \rho_I}{\partial v^2}(v, t) = N_I(t)\delta(v - V_R), \\ \\ \frac{\partial \rho_E}{\partial t}(v, t) + \frac{\partial}{\partial v}[h^E(v, N_E(t), N_I(t))\rho_E(v, t)] - a_E(N_E(t), N_I(t))\frac{\partial^2 \rho_E}{\partial v^2}(v, t) = N_E(t)\delta(v - V_R). \end{cases} \quad (21)$$

which is completed with Dirichlet boundary conditions and initial data

$$\rho_\alpha(-\infty, t) = 0, \ \rho_\alpha(V_F, t) = 0, \ \rho_\alpha(v, 0) = \rho_\alpha^0(v) \geq 0, \quad \alpha = E, I. \tag{22}$$

The drift and diffusion coefficients are given by

$$h^\alpha(v, N_E(t), N_I(t)) = -v + b_E^\alpha N_E(t) - b_I^\alpha N_I(t) + (b_E^\alpha - b_E^E)\nu_{E,ext}, \tag{23}$$
$$a_\alpha(N_E(t), N_I(t)) = d_E^\alpha + d_E^\alpha N_E(t) + d_I^\alpha N_I(t), \quad \alpha = E, I. \tag{24}$$

where $d_\alpha > 0$, $d_i^\alpha \geq 0$, $b_i^\alpha > 0$, $D_i^\alpha \geq 0$ for $\alpha, i = E, I$. The mean firing rates N_α obey to

$$N_\alpha(t) = -a_\alpha(N_E(t), N_I(t))\frac{\partial \rho_\alpha}{\partial v}(V_F, t) \geq 0, \quad \alpha = E, I. \tag{25}$$

On the other hand, since ρ_E and ρ_I represent probability densities, the total mass is conserved:

$$\int_{-\infty}^{V_F} \rho_\alpha(v, t) \ dv = \int_{-\infty}^{V_F} \rho_\alpha^0(v) \ dv = 1 \quad \forall \, t \geq 0, \quad \alpha = E, \, I.$$

The concept of weak solutions we consider is the following:

Definition 0.5.6 *A weak solution of* (21)*-*(25) *is a quadruple of nonnegative functions* $(\rho_E, \rho_I, N_E, N_I)$ *with* $\rho_\alpha \in L^\infty(\mathbb{R}^+; L_+^1((-\infty, V_F)))$ *and* $N_\alpha \in L_{loc,+}^1(\mathbb{R}^+) \ \forall \ \alpha = E, I$, *satisfying*

$$\int_0^T \int_{-\infty}^{V_F} \rho_\alpha(v, t) \left[-\frac{\partial \phi}{\partial t} - \frac{\partial \phi}{\partial v} h^\alpha(v, N_E(t), N_I(t)) - a_\alpha(N_E(t), N_I(t))\frac{\partial^2 \phi}{\partial v^2} \right] dv \ dt$$

$$= \int_0^T N_\alpha(t)[\phi(V_R, t) - \phi(V_F, t)]dt + \int_{-\infty}^{V_F} \rho_\alpha^0(v)\phi(v, 0)dv - \int_{-\infty}^{V_F} \rho_\alpha(v, T)\phi(v, T)dv, \qquad \alpha = E, I,$$

for any test function $\phi(v, t) \in C^\infty((-\infty, V_F] \times [0, T])$ *such that* $\frac{\partial^2 \phi}{\partial v^2}$, $v\frac{\partial \phi}{\partial v} \in L^\infty((-\infty, V_F) \times (0, T))$.

We start the analysis of this model studying the blow-up phenomenon. It appears under some constraints, despite of the presence of an inhibitory population. Remember that, in [29], it was proved that the on average inhibitory delayed NNLIF model has global-in-time existence of solution. Initially this made us think that, perhaps, the presence of an inhibitory population could help to avoid the blow-up for two populations models. Nevertheless, this it not the case, as stated in the theorem:

Theorem 0.5.7 *Assume that*

$$h^E(v, N_E, N_I) + v \geq b_E^E N_E - b_I^E N_I,$$

$$a_E(N_E, N_I) \geq a_m > 0,$$

$\forall v \in (-\infty, V_F]$ *and* $\forall \ N_I, N_E \geq 0$. *Assume also that there exist* $M \geq 0$ *such that*

$$\int_0^t N_I(s) \ ds \leq M \, t, \qquad \forall \, t \geq 0,$$

Then, a weak solution to the system (21)*-*(25) *cannot be global in time in the following cases:*

1. $b_E^E > 0$ *is large enough, for ρ_E^0 fixed.*

2. ρ_E^0 *is 'concentrated enough' around V_F:*

$$\int_{-\infty}^{V_F} e^{\mu v} \rho_E^0(v) \; dv \geq \frac{e^{\mu V_F}}{b_E^E \mu}, \qquad \textit{for a certain } \mu > 0$$

for $b_E^E > 0$ fixed.

Afterwards we analyze the number of steady states in terms of the parameter values. This analysis for this model is more complex than the one done in [15] (where this study was done for a one population model). Moreover, we obtain a large variety of behaviors: cases of uniqueness of the equilibrium, cases of an odd or even number of steady states and, even, situations without steady states. In fact, from a numerical point of view it have been detected cases of three stationary states. For one population models this kind of situations have not been located. Moreover, on the other hand, the numerical results suggest that for the cases without steady states the firing rates always blow-up. This theorem summarizes the analytical results that have been obtained in this direction:

Theorem 0.5.8 *Assume that the connectivity parameters b_I^E and b_E^I do not vanish (b_I^E, $b_E^I > 0$), a_α is independent of N_E and N_I, $a_\alpha(N_E, N_I) = a_\alpha$, and $h^\alpha(v, N_E, N_I) = V_0^\alpha(N_E, N_I) - v$ with $V_0^\alpha(N_E, N_I) = b_E^\alpha N_E - b_I^\alpha N_I + (b_E^\alpha - b_E^E) v_{E,ext}$ for all $\alpha = E, I$. Then:*

1. *There is an even number of steady states or no steady state for (21)-(25) if:*

$$(V_F - V_R)^2 < (V_F - V_R)(b_E^E - b_I^I) + b_E^E b_I^I - b_I^E b_E^I.$$

If b_E^E is large enough in comparison with the rest of connectivity parameters, there are no steady states.

2. *There is an odd number of steady states for (21)-(25) if:*

$$(V_F - V_R)^2 > (V_F - V_R)(b_E^E - b_I^I) + b_E^E b_I^I - b_I^E b_E^I.$$

If b_E^E is small enough in comparison with the rest of connectivity parameters, there is a unique steady state.

Once the question of the number of steady states has been cleared, we analyze the long time behavior of the solutions for small connectivity parameters in absolute value. We observe that the solutions converge exponentially fast to the unique steady state if the initial datum is close enough to it. In order to obtain this result, we use the entropy dissipation method, considering the total entropy of the system:

$$E[t] = \int_{-\infty}^{V_F} \left[\rho_E^\infty(v) \left(\frac{\rho_E(v,t)}{\rho_E^\infty(v)} - 1 \right)^2 + \rho_I^\infty(v) \left(\frac{\rho_I(v,t)}{\rho_I^\infty(v)} - 1 \right)^2 \right] dv. \tag{26}$$

In order to control the entropy production, we apply a Poincaré like inequality, that yields finally the results:

Theorem 0.5.9 *Assume a_α constant for $\alpha = E, I$, the connectivity parameters b_E^E, b_E^I, b_I^E and b_I^I small enough and an initial data (ρ_E^0, ρ_I^0) such that*

$$E[0] < \frac{1}{2 \max\left(b_E^E + b_I^E, b_E^I + b_I^I\right)}.$$

Then, for fast decaying solutions to (21)-(25) there is a constant $\mu > 0$, such that, for all $t \geq 0$

$$E[t] \leq e^{-\mu t} E[0].$$

Consequently, for $\alpha = E, I$

$$\int_{-\infty}^{V_F} \rho_\alpha^\infty \left(\frac{\rho_\alpha(v,t)}{\rho_\alpha^\infty(v)} - 1\right)^2 dv \leq e^{-\mu t} E[0].$$

At the end of the chapter we illustrate all the theoretical results with numerical results. We also provide the numerical study of the stability of the steady states in case there are more than one. All this numerical results have been obtained using a numerical scheme (detailed in the appendix) that uses a Weighted Essentially Non-Oscillatory (WENO) scheme for the drift term, standard second order finite differences for the difussion and an explicit Total Variation Diminishing (TVD) Runge Kutta method combined with a Courant-Friedrich-Lewy (CFL) condition for the time evolution. The code that runs this numerical scheme has been programmed for two cores using parallel computation techniques, due to the complexity of the simulations.

0.5.3 Main results of chapter 3

The third chapter, which is based on the work [20], considers the full NNLIF model (7): two populations, refractory states and synaptic delays (see Section 0.2). We start defining the concept of weak solution for this model, following the idea of the previous chapter:

Definition 0.5.10 *Let $\rho_\alpha \in L^\infty(\mathbb{R}^+; L^1_+((-\infty, V_F)))$, $N_\alpha \in L^1_{loc,+}(\mathbb{R}^+)$ and $R_\alpha \in L^\infty_+(\mathbb{R}^+)$ for $\alpha = E, I$. Then $(\rho_E, \rho_I, R_E, R_I, N_E, N_I)$ is a weak solution of (7)-(12) if for any test function $\phi(v,t) \in C^\infty((-\infty, V_F] \times [0, T])$ and such that $\frac{\partial^2 \phi}{\partial v^2}$, $v\frac{\partial \phi}{\partial v} \in L^\infty((-\infty, V_F) \times (0, T))$ the following relation*

$$\int_0^T \int_{-\infty}^{V_F} \rho_\alpha(v,t) \left[-\frac{\partial \phi}{\partial t} - \frac{\partial \phi}{\partial v} h^\alpha(v, N_E(t - D_E^\alpha), N_I(t - D_I^\alpha)) - a_\alpha(N_E(t - D_E^\alpha), N_I(t - D_I^\alpha))\frac{\partial^2 \phi}{\partial v^2}\right] dv dt$$

$$= \int_0^T [M_\alpha(t)\phi(V_R, t) - N_\alpha(t)\phi(V_F, t)]dt + \int_{-\infty}^{V_F} \rho_\alpha^0(v)\phi(v,0)dv - \int_{-\infty}^{V_F} \rho_\alpha(v,T)\phi(v,T)\, dv$$

is satisfied $\forall\ \alpha = E, I$, and R_α, for $\alpha = E, I$, are solutions of the ODEs

$$\frac{dR_\alpha(t)}{dt} = N_\alpha(t) - M_\alpha(t).$$

Once the concept of weak solution has been defined, we study if the blow-up phenomenon appears for this model. We conclude that if there are refractory states and delays for all the synapses except the excitatory to excitatory ones, the solutions are not global-in-time in some cases. That is to say, the blow-up appears also if there are delays and refractory states, provided that there is no delay for

the excitatory to excitatory connections. Probably, if this delay is nonzero, the blow-up is avoided, as it has been shown in the first chapter for the case of only one excitatory population. The blow-up result for this model is this:

Theorem 0.5.11 *Assume that*

$$h^E(v, N_E, N_I) + v \geq b_E^E N_E - b_I^E N_I,$$

$$a_E(N_E, N_I) \geq a_m > 0,$$

$\forall\, v \in (-\infty, V_F]$, *and* $\forall\, N_I, N_E \geq 0$. *Assume also that* $D_E^E = 0$ *and that there exists some* $C > 0$ *such that*

$$\int_0^t N_I(s - D_I^E)\, ds \leq C\, t, \qquad \forall\, t \geq 0.$$

Then, a weak solution to the system (7)–(12) *cannot be global in time because one of the following reasons:*

- $b_E^E > 0$ *is large enough, for* ρ_E^0 *fixed.*

- ρ_E^0 *is 'concentrated enough' around* V_F:

$$\int_{-\infty}^{V_F} e^{\mu v} \rho_E^0(v)\, dv \geq \frac{e^{\mu V_F}}{b_E^E \mu}, \qquad \text{for a certain } \mu > 0$$

and for $b_E^E > 0$ *fixed.*

We also study the stationary states for this model, observing that there is always an odd number of them. Thus, there is always at least one steady state, which is unique in some cases. Let us remember that for the case without refractory states analyzed in the previous chapter, there were some parameter values for which there are no steady states. The analysis of the number of steady states is summarized in the following theorem:

Theorem 0.5.12 *Assume that* $b_I^E > 0$, $b_E^I > 0$, $\tau_E > 0$, $\tau_I > 0$, $a_\alpha(N_E, N_I) = a_\alpha$ *constant, and* $h^\alpha(v, N_E, N_I) = V_0^\alpha(N_E, N_I) - v$ *with* $V_0^\alpha(N_E, N_I) = b_E^\alpha N_E - b_I^\alpha N_I + (b_E^\alpha - b_E^E)v_{E,ext}$ *for all* $\alpha = E, I$. *Then there is always an odd number of steady states for* (7)-(12).

Moreover, if b_E^E *is small enough or* τ_E *is large enough (in comparison with the rest of parameters), then there is a unique steady state for* (7)-(12).

Afterwards, we analyze the long time behavior of the solutions in case of small connectivity parameters in absolute value and without delays. We obtain that the solutions converge exponentially fast to the unique steady state if the initial data are close enough to the steady state. The proof of this result uses the entropy dissipation method and a Poincaré like inequality that is adapted to the presence of the refractory states, in order to control the entropy production. To apply the entropy dissipation method we have to identify the total entropy function. For two population it is given by:

$$\mathcal{E}[t] := \int_{-\infty}^{V_F} \rho_E^\infty(v) \left(\frac{\rho_E(v) - \rho_E^\infty(v)}{\rho_E^\infty(v)} \right)^2 dv + \int_{-\infty}^{V_F} \rho_I^\infty(v) \left(\frac{\rho_I(v) - \rho_I^\infty(v)}{\rho_I^\infty(v)} \right)^2 dv$$
$$+ \frac{(R_E(t) - R_E^\infty)^2}{R_E^\infty} + \frac{(R_I(t) - R_I^\infty)^2}{R_I^\infty}.$$

Finally, the theorem that describes the long time behavior of the solutions is this:

Theorem 0.5.13 *Consider system (7)-(12). Assume that the connectivity parameters b_i^α are small enough, the diffusion terms $a_\alpha > 0$ are constant, the transmission delays D_i^α vanish ($\alpha = I, E$, $i = I, E$), and that the initial data (ρ_E^0, ρ_I^0) are close enough to the unique steady state $(\rho_E^\infty, \rho_I^\infty)$:*

$$\mathcal{E}[0] < \frac{1}{2 \max \left(b_E^E + b_I^E, b_E^I + b_I^I \right)}.$$

Then, for fast decaying solutions to (7), there is a constant $\mu > 0$ such that for all $t \geq 0$

$$\mathcal{E}[t] \leq e^{-\mu t} \mathcal{E}[0].$$

Consequently, for $\alpha = E, I$

$$\int_{-\infty}^{V_F} \rho_\alpha^\infty(v) \left(\frac{\rho_\alpha(v) - \rho_\alpha^\infty(v)}{\rho_\alpha^\infty(v)} \right)^2 dv + \frac{(R_\alpha(t) - R_\alpha^\infty)^2}{R_\alpha^\infty} \leq e^{-\mu t} \mathcal{E}[0].$$

The proof of this long time behavior theorem, can be extended to cases with small delays, that is to say for small values of $D_i^\alpha \geq 0$. With that purpose we have to use some a priori L^2 estimates over the firing rates. They can be obtained following the ideas of [26] [Section 3]. Moreover, Theorem 0.5.13 also holds for the one population NNLIF model with refractory states and without delay or with a small delay.

We complete the study presenting an improved numerical resolutor with respect to the one showed in the previous chapter and in [15, 17]: it considers a flux splitting WENO scheme and allows to simulate the full NNLIF model both for one and two populations, with refractory states and delays. To our knowledge, this resolutor is the first deterministic solver that describes the behavior of the full NNLIF model taking into account all the charateristic phenomena of real networks. Developing efficient numerical resolutors that consider all relevant phenoma is essential to work out strategies that, on the one hand, give answer to the open questions; and, on the other hand, help to implement resolutors for other large-scaled models, which are becoming more common in computational neuroscience [56, 63, 81, 92, 93, 100]. Moreover, it are shown some strategies used for the save and recovery of values, needed to include a nonzero delay in the simulations. Finally, we present some new numerical results, that are an interesting line for future investigations: For both models (one and two populations) with refractory states and delays, it seems that there is never a blow-up of the firing rate, and the solutions tend to a steady state or become periodic.

Summarizing, the problems studied in this work are: existence problems, analysis of the number of steady states, long time behavior of the solutions and numerical study. The numerical analysis has been used, on the one hand, to study certain behaviors of the solutions, that have been proved analytically and, on the other hand, to shed some light on some aspects that, due to its complexity, have not yet been treated from a theoretical point of view: the stability of the steady states in case there is more than one, the fact that the blow-up is avoided when there is a delay in excitatory to excitatory synapses, the appearance of periodic solutions,...

The main tools used in thesis from an analytical point of view are: an appropiate transformation of the one population NNLIF model with delay into a Stefan like problem with a nonstandard right

hand side, fixed point arguments and the notion of universal upper-solution, which allowed to proof the global existence for this model; for the asymptotic behavior, the entropy dissipation method and different inequalities, being the most relevant a Poincaré like inequality in order to control the entropy production; and different strategies applied to determine the number of steady states.

From a numerical point of view, the main techniques that have been learned are the fifth order (flux splitting) WENO approximation used to approximate the drifts, and the third order TVD Runge-Kutta method combined with a CFL condition for the evolution in time of the solutions. Moreover, all the codes are programmed using C++ and, sometimes, MPI. Thus, this techniques and programming languages are part of the training obtained during the development of this work.

Our analytical and numerical results contribute to support the NNLIF system as an appropiate model to describe well known neoruphysiological phenomena, as e.g., synchronization/asynchronization of the network (As in [11] we will call *asynchronous* the states in which the firing rate tends to be constant in time and *synchronous* every other state), since the blow-up might depict a synchronization of a part of the network, while the presence of an unique asymptotically stationary solution represents an asynchronization of the network. In addition, the abundance in the number of steady states, in terms of the connectivity parameter values, that can be observed for this simplified models (Theorem 0.5.8 and Theorem 0.5.12), probably will help us to characterize situations of multi-stability for more complete NNLIF models and also other models including conductance variables as in [16]. In [17] it was shown that if a refractory period is included in the model, there are situations of multi-stability, with two stable and one unstable steady state. In [16] bi-stability phenomena were numerically described. Multi-stable networks are related, for instance, to the visual perception and the decision making [50, 3], the short term working memory [104] and oculomotor integrators [59]. On the other hand, periodic or oscillatory solutions are used to model synchronous states and oscillations, observed, e.g., during cortical processing [50, 53].

Chapter 1

One population NNLIF model with delay

The NNLIF equation is widely used to approximate the behavior of a neural network; which depends strongly on the type of network considered: excitatory or inhibitory. If we neglect the synaptic delay, for the excitatory case there are some situations where the solutions are not global-in-time [17] since a divergence of the firing rate occurs [29][Theorem 1.1]. On the other hand, the numerical results of [20] and the analytical study at microscopic level of [38] suggest that the presence of the delay avoids the blow-up of the solutions. The main result of this chapter is the analytical proof of the global-in-time existence and unicity of classical solutions for excitatory networks when a non-zero delay is included in the model. As a by-product we also obtain the global-in-time existence for the inhibitory case with delay. The main tools used are: an appropiate change of variables to rewrite the NNLIF equation as a non standard Stefan like free boundary problem, a fixed point argument and the notion of universal upper-solution.

1.1 The model

In the present chapter we deal with the delayed NNLIF equation. This equation is a slight modification of the NNLIF model presented in [15, 29] at the level of the drift term, which includes the synaptic delay. Precisely, the evolution in time of the probability density $\rho(v, t)$ is governed by

$$\frac{\partial \rho}{\partial t}(v, t) + \frac{\partial}{\partial v}[(-v + \mu(t - D)\rho(v, t)] - a(N(t - D))\frac{\partial^2 \rho}{\partial v^2}(v, t) = N(t)\delta(v - V_R), \qquad v \leq V_F, \quad (1.1)$$

where $D \geq 0$ and $V_F \in \mathbb{R}$. The diffusion term $a(N)$, the drift term μ and the firing rate N are given by

$$a(N) = a_0 + a_1 N \quad \text{and} \quad \mu(t) = b_0 + bN(t) \quad \text{with} \quad N(t) = -a\frac{\partial p}{\partial v}(V_F, t) \geq 0, \qquad (1.2)$$

where $a_0 > 0$, $a_1 \geq 0$ and b is the *connectivity parameter* which is positive for excitatory networks and negative for inhibitory ones. The parameter b_0 controls the strength of the external stimuli and can be either positive or negative. In what follows we will consider that the diffusion term is constant: $a(N) = a > 0$. Furthermore, for simplicity, sometimes we will suppose that $a = 1$ and $V_F = 0$. Nevertheless, this hypotheses really are not a constraint, since we can transform the general equation

into one satisfying the restriction, by a new density $\bar{\rho}$ as follows:

$$\bar{\rho}(\bar{v}, t) = \sqrt{a}\rho(\sqrt{a}v + V_F, t). \tag{1.3}$$

Also for simplicity, sometimes we will assume that $b_0 = 0$, but again this does not imply a loss of generality, since we can pass from the general equation for $b_0 \neq 0$ to an equation with $b_0 = 0$ by translating the voltage variable v by the factor b_0.

The PDE (1.1) is completed with initial and boundary conditions

$$N(t) = N^0(t) \geq 0, \quad \forall\, t \in [-D, 0), \quad \rho(v, 0) = \rho^0(v) \geq 0, \quad \text{and} \quad \rho(V_F, t) = 0, \quad p(-\infty, t) = 0. \tag{1.4}$$

Besides, as ρ is a probability density, the total mass is conserved

$$\int_{-\infty}^{V_F} \rho(v, t)\; dv = \int_{-\infty}^{V_F} \rho^0(v)\; dv = 1, \qquad \forall\, t \geq 0.$$

1.2 The equivalent free boundary Stefan problem

The target of this section is to rewrite equation (1.1) for $a = 1$ and $V_F = 0$, as a freee boundary Stefan problem with a nonstandard right hand side as in [29]. With that purpose we perform the two changes of variables presented below, which are more complicated than the ones of [29] due to the presence of the delay. Indeed, once the changes have been completed, we have to do some more calculations in order to set the synaptic delay properly for the new variables. Afterwards, we write the final expression of the equivalent equation, we introduce the notion of classical solution for it and remember some basic a priori properties for this kind of solutions.

1. **The first change of variables.** We introduce the following change of variables, which has been widely studied in [30]:

$$y = e^t v, \quad \tau = \frac{1}{2}(e^{2t} - 1). \tag{1.5}$$

Therefore,

$$t = -\log(\alpha(\tau)), \quad v = y\alpha(\tau), \tag{1.6}$$

where $\alpha(\tau) = (\sqrt{2\tau + 1})^{-1}$, and we define

$$w(y, \tau) = \alpha(\tau)\rho(y\alpha(\tau), -\log(\alpha(\tau))). \tag{1.7}$$

Differentiating w with respect to τ, and using that ρ is a solution of (1.1), yields

$$
\begin{aligned}
w_\tau(y, \tau) &= \alpha'(\tau)\rho(y\alpha(\tau), -\log(\alpha(\tau)))\\
&\quad + y\alpha'(\tau)\alpha(\tau)\rho_v(y\alpha(\tau), -\log(\alpha(\tau))) - \alpha'(\tau)\rho_t(y\alpha(\tau), -\log(\alpha(\tau)))\\
&= -\alpha'(\tau)\rho_{vv}(y\alpha(\tau), -\log(\alpha(\tau)))\\
&\quad \alpha'(\tau)\mu(-\log(\alpha(\tau)) - D)\rho_v(y\alpha(\tau), -\log(\alpha(\tau))) - \alpha'(\tau)N(-log(\alpha(\tau)))\delta(y\alpha(\tau) - V_R).
\end{aligned}
\tag{1.8}
$$

Finally, taking into account that

$$
\begin{aligned}
-\alpha'(\tau) &= \alpha^3(\tau), \\
w_y(y,\tau) &= \alpha^2(\tau)\rho_v(y\alpha(\tau), -\log(\alpha(\tau))), \\
w_{yy}(y,\tau) &= \alpha^3(\tau)\rho_{vv}(y\alpha(\tau), -\log(\alpha(\tau))),
\end{aligned}
$$

we obtain

$$
w_\tau(y,\tau) = w_{yy}(y,\tau) - \alpha(\tau)\mu(t-D)w_y(y,\tau) + M(\tau)\delta\left(y - \frac{V_R}{\alpha(\tau)}\right), \tag{1.9}
$$

where $M(\tau) = -w_y(0,\tau) = \alpha^2(\tau)N(t)$, and we use that $\mu(t-D) = \mu(-\log(\alpha(\tau)) - D)$ due to (1.6). We keep this term with t because it is useful in the next change.

2. **The second change of variables.** In order to remove the term with w_y in (1.9) we introduce the change of variables

$$
x = y - \int_0^\tau \mu(t-D)\alpha(s)\,ds \tag{1.10}
$$

and define

$$
u(x,\tau) = w\left(x + \int_0^\tau \mu(t-D)\alpha(s)\,ds, \tau\right).
$$

Differentiating u with respect to τ produces

$$
u_\tau(x,\tau) = w_y\left(x + \int_0^\tau \mu(t-D)\alpha(s)\,ds, \tau\right)\mu(t-D)\alpha(\tau) + w_\tau\left(x + \int_0^\tau \mu(t-D)\alpha(s)\,ds, \tau\right).
$$

Using equation (1.9) to substitute w_τ yields

$$
u_\tau(x,\tau) = w_{yy}\left(x + \int_0^\tau \mu(t-D)\alpha(s)\,ds, \tau\right) + M(\tau)\delta\left(x + \int_0^\tau \mu(t-D)\alpha(s)\,ds - \frac{V_R}{\alpha(\tau)}\right).
$$

Taking into account now that

$$
\begin{aligned}
u_x(x,\tau) &= w_y\left(x + \int_0^\tau \mu(t-D)\alpha(s)\,ds, \tau\right), \\
u_{xx}(x,\tau) &= w_{yy}\left(x + \int_0^\tau \mu(t-D)\alpha(s)\,ds, \tau\right),
\end{aligned}
$$

defining

$$
s(\tau) := -\int_0^\tau \mu(t-D)\alpha(s)\,ds = -b_0(\sqrt{2\tau+1} - 1) - b\int_0^\tau N(t-D)\alpha(s)\,ds,
$$

47

remembering the definition of $M(\tau)$, finally we obtain:

$$
\begin{cases}
u_\tau(x, \tau) = u_{xx}(x, \tau) + M(\tau)\delta(x - s_1(\tau)), & x < s(\tau), \tau > 0, \\
s_1(\tau) = s(\tau) + \frac{V_R}{\alpha(\tau)}, & \tau > 0, \\
s(\tau) = -b_0(\sqrt{2\tau + 1} - 1) - b\int_0^\tau N(t - D)\alpha(s)\, ds, & \tau > 0, \\
M(\tau) = -u_x(s(\tau), \tau), & \tau > 0, \\
N(t) = N(0), & t \in (-D, 0], \\
u(-\infty, \tau) = u(s(\tau), \tau) = 0, & \tau > 0, \\
u(x, 0) = u_I(x), & x < 0.
\end{cases}
\tag{1.11}
$$

3. **Handling the delay.** The two previous changes were introduced in [29] for the model without delay, $D = 0$. In that case $N(t) = M(\tau)\alpha^{-2}(\tau)$. Nevertheless, when $D > 0$ the firing rate is evaluated in $t - D$, and we also have to take into account that $N(t - D) \neq M(\tau - D)\alpha^{-2}(\tau - D)$ due to the nonlinearity of the first change of variables. To overcome the problem we proceed as follows.

Recall that $\tau = \frac{1}{2}(e^{2t} - 1)$ and $t = \frac{1}{2}\log(2\tau + 1)$. In consequence, if we consider the time $t - D$, there is a related $\tau_D = \frac{1}{2}(e^{2(t-D)} - 1)$. Observe that, since $D \geq 0$, $\tau_D \leq \tau$, and therefore there exists some $\bar{D} > 0$ such that $\tau_D = \tau - \bar{D}$. Let us compute the expression of $\bar{D}$ using the relation (1.6):

$$
\tau_D = \frac{1}{2}(e^{2(t-D)} - 1) = \tau - \bar{D} = \frac{1}{2}(e^{2t} - 1) - \bar{D},
$$

thus, we get that $\bar{D} = \frac{1}{2}e^{2t}(1 - e^{-2D}) > 0$. Substituting now in the expression of $\bar{D}$, t by the related τ and defining $\hat{D} = (1 - e^{-2D})$, we finally conclude that $\bar{D} = \hat{D}(\tau + \frac{1}{2})$. Notice that $0 < \hat{D} < 1$ and thus, $0 < \bar{D} < \tau + \frac{1}{2} = \frac{1}{2}\alpha^{-2}(\tau)$.

This result allows us to write properly the following relation

$$
\begin{aligned}
N(t - D) &= \alpha^{-2}(\tau_D)M(\tau_D) = \alpha^{-2}(\tau - \bar{D})M(\tau - \bar{D}) \\
&= \alpha^{-2}\left((1 - \hat{D})\tau - \frac{1}{2}\hat{D}\right)M\left((1 - \hat{D})\tau - \frac{1}{2}\hat{D}\right).
\end{aligned}
\tag{1.12}
$$

4. **The equivalent equation.** Using (1.12) we can rewrite $s(\tau)$ from (1.11) in terms of $M(\tau)$, avoiding its t dependance via $N(t)$

$$
\begin{aligned}
s(\tau) &= -b_0(\sqrt{2\tau + 1} - 1) - b\int_0^\tau N(t - D)\alpha(s)\, ds \tag{1.13} \\
&= -b_0(\sqrt{2\tau + 1} - 1) - b\int_0^\tau \alpha^{-2}\left((1 - \hat{D})s - \frac{1}{2}\hat{D}\right)M\left((1 - \hat{D})s - \frac{1}{2}\hat{D}\right)\alpha(s)\, ds.
\end{aligned}
$$

The change of variable $z = (1 - \hat{D})s - \frac{1}{2}\hat{D}$ yields

$$
s(\tau) = -b_0(\sqrt{2\tau + 1} - 1) - \frac{b}{\sqrt{1 - \hat{D}}}\int_{-\frac{1}{2}\hat{D}}^{(1-\hat{D})\tau - \frac{1}{2}\hat{D}} M(z)\alpha^{-1}(z)\, dz.
\tag{1.14}
$$

48

Denoting $s = z$, $t = \tau$ and $D = \hat{D}$ finally leads to the following equivalent Stefan-like equation

$$
\begin{cases}
u_t(x,t) = u_{xx}(x,t) + M(t)\delta(x - s_1(t)), & x < s(t), t > 0, \\
s_1(t) = s(t) + \frac{V_R}{\alpha(t)}, & t > 0, \\
s(t) = -b_0(\sqrt{2t+1} - 1) - \frac{b}{\sqrt{1-D}} \int_{-\frac{1}{2}D}^{(1-D)t - \frac{1}{2}D} M(s)\alpha^{-1}(s) \; ds, & t > 0, \\
M(t) = -u_x(s(t),t), & t > 0, \\
M(t) = M(0), & t \in (-D, 0], \\
u(-\infty, t) = u(s(t), t) = 0, & t > 0, \\
u(x, 0) = u_I(x), & x < 0.
\end{cases}
\tag{1.15}
$$

where $D \in [0,1)$ and $\alpha(t) = \frac{1}{\sqrt{2t+1}}$. Let us remark that this problem is well defined since $\alpha(t) \in \mathbb{R}^+ \; \forall \; t > -\frac{1}{2}$.

Once we have derived the equivalent Stefan-like problem with a free boundary, we are in the conditions to introduce the notion of classical solution for this kind of equations, which is quite similar to that defined in [29]. After that, we present some a priori properties, that will be useful for the rest of computations of the present work.

Definition 1.2.1 *Let $u_I(x)$ be a non-negative $C^0((-\infty, V_F]) \cap C^1((-\infty, V_R) \cup (V_R, 0]) \cap L^1((-\infty, 0))$ function such that $u_I(0) = 0$. Suppose that u_I, $(u_I)_x$ vanish at $-\infty$ and that the left and right derivatives at V_R are finite. We say that $(u(x,t), s(t))$ is a classical solution of (1.15) with initial data $u_I(x)$ on the interval $J = [0, T)$ or $J = [0, T]$, for a given $0 < T \leq \infty$ if:*

1. *$M(t)$ is a continuous function for all $t \in J$,*

2. *u is continuous in the region $\{(x,t) : -\infty < x \leq s(t), t \in J\}$,*

3. *u_{xx} and u_t are continuous in the region $\{(x,t) : -\infty < x < s_1(t), t \in J - \{0\}\} \cup \{(x,t) : s_1(t) < x < s(t), t \in J - \{0\}\}$,*

4. *$u_x(s_1(t)^-, t)$, $u_x(s_1(t)^+, t)$, $u_x(s(t)^-, t)$ are well defined,*

5. *u_x vanishes at $-\infty$,*

6. *Equations (1.15) are satisfied.*

Lemma 1.2.2 (A priori properties) *Let $u(x,t)$ be a solution to (1.15) in the sense of the previous definition. Then:*

1. *The mass is conserved*

$$
\int_{-\infty}^{s(t)} u(x,t)dx = \int_{-\infty}^{0} u_I(x)dx, \qquad \forall \; t > 0.
$$

2. *The flux across the free boundary s_1 is exactly the strength of the source term:*

$$
M(t) := -u_x(s(t),t) = u_x(s_1(t)^-, t) - u_x(s_1(t)^+, t).
$$

3. If $b_0 \leq 0$ and $b < 0$ (respectively, $b_0 \geq 0$ and $b > 0$), the free boundary $s(t)$ is a monotone increasing (respectively, decreasing) function of time.

Proof. The proof of properties 1. and 2. is exactly the same as in [29] [Lemma 2.3], because it does not take into account the expression of $s(t)$. The proof of property 3. is as follows.

For $b_0 \leq 0$ and $b < 0$ the free boundary is a monotone increasing function of t, since $\sqrt{2t+1} > 0$ for $t > -\frac{1}{2}D$ and

$$s(t) = -b_0(\sqrt{2t+1} - 1) - \frac{b}{\sqrt{1-D}} \int_{-\frac{1}{2}D}^{(1-D)t-\frac{1}{2}D} M(s)\sqrt{2s+1}\, ds \qquad \forall t > 0,$$

where $M(t) = M(0) > 0\ \forall\ t \in (-D, 0]$ and $M(t) > 0\ \forall\ t > 0$ thanks to the classical Hopf's lemma, as in [29] [Lemma 2.3]. $\quad\square$

1.3 Local existence and uniqueness

In this section we introduce an implicit integral equation for M. Then, thanks to the form of that equation, it will be possible to solve it for local time using an fixed point argument. Besides, since we will be able to proof that the fixed point function is a contraction, we will also get the local unicity of M. This is useful, since once M is known, (1.15) decouples, and u can be calculated easily by a Duhamel's formula.

Our first goal is achieved performing exactly the same steps as in [29] [Section 3.1], which is reasonable since they do not take into account the concrete expression of $s(t)$. The implicit integral equation for M is given by:

$$
\begin{aligned}
M(t) \;=\; & -2 \int_{-\infty}^{V_R} G(s(t), t, \xi, 0) u_I'(\xi) d\xi - 2 \int_{V_R}^{0} G(s(t), t, \xi, 0) u_I'(\xi) d\xi \\
& + 2 \int_{0}^{t} M(\tau) G_x(s(t), t, s(\tau), \tau) d\tau - 2 \int_{0}^{t} M(\tau) G_x(s(t), t, s_1(\tau), \tau) d\tau,
\end{aligned}
\qquad (1.16)
$$

where G is the Green's function for the heat equation on the real line

$$G(x, t, \xi, \tau) = \frac{1}{[4\pi(t-\tau)]^{\frac{1}{2}}} e^{-\frac{|x-\xi|^2}{4(t-\tau)}}. \qquad (1.17)$$

The second part of this section, which deals with the local existence and unicity of classical solutions to (1.15), can be summed up in this theorem:

Theorem 1.3.1 *Let $u_I(x)$ be a non-negative $C^0((-\infty, 0]) \cap C^1((-\infty, V_R) \cup (V_R, 0]) \cap L^1((-\infty, 0))$ function such that $u_I(0) = 0$. Suppose u_I, $(u_I)_x$ decay to zero as $x \to -\infty$ and that the left and right derivatives at V_R are finite. Then there exists a time $T > 0$ such that $M(t)$ defined by the integral formulation (1.16) exists for $t \in [0, T]$ and is unique in $C^0([0, T])$. The existence time T satisfies*

$$T \leq \left(\sup_{x \in (-\infty, V_R) \cup (V_R, 0]} |u_I'(x)| \right)^{-1}.$$

50

Proof. The proof is similar to the one done in [29], so we are going to omit here the detailed calculations that can be performed in exactly the same way. Below, we only develop the parts of the proof that are different. Specifically, the calculations that change are the ones which take into account the concrete expression of $s(t)$, since this is the term where appears the delay D.

The expected local in time existence and unicity of $M(t)$ is obtained via a fixed point argument. With that purpose we start introducing some definitions. Consider

$$m := 1 + 2 \sup_{x \in (-\infty, V_R) \cup (V_R, 0]} |u_I'(x)|. \tag{1.18}$$

and then let us define for $\sigma, m > 0$ the following norm and space

$$\|M\| := \sup_{0 \le t \le \sigma} |M(t)|, \qquad C_{\sigma,m} := \{M \in C^0([0,\sigma]) : \|M\| \le m\},$$

and the functional

$$\begin{aligned}
T(M)(t) &:= -2 \left(\int_{-\infty}^{V_R} G(s(t), t, \xi, 0) u_I'(\xi) d\xi + \int_{V_R}^{0} G(s(t), t, \xi, 0) u_I'(\xi) d\xi \right) \\
&\quad + 2 \int_0^t M(\tau) G_x(s(t), t, s(\tau), \tau) d\tau - 2 \int_0^t M(\tau) G_x(s(t), t, s_1(\tau), \tau) d\tau, \tag{1.19} \\
&:= J_1 + J_2 + J_3.
\end{aligned}$$

Thus, in order to apply a fixed point argument to this functional we have to show that for $\sigma > 0$ small enough the following conditions are satisfied:

1. $T : C_{\sigma,m} \to C_{\sigma,m}$,

2. T is a contraction.

Step 1. In this step we show that the first condition is satisfied. We will show the argumentation for $b < 0$, including how to proceed for excitatory case at the end.
We consider $\sigma > 0$ small enough such that

(a) $\alpha^{-1}(t) \le 2, \ \forall \ t \le \sigma$,

(b) $\frac{m(|b_0| + 2m|b|)}{\sqrt{\pi}} \sigma^{\frac{1}{2}} \le \frac{1}{2}$,

(c) $|V_R| - |b_0|\sigma > 0$,

(d) $\frac{2m}{\sqrt{\pi}} \int_{\frac{|V_R| - |b_0|\sigma}{\sqrt{8\sigma}}}^{\infty} z^{-1} e^{-z^2} dz \le \frac{1}{2}$.

If $0 \le \tau < t \le \sigma$ and $M \in C_{\sigma,m}$, we can prove that $s(t)$ is a Lipschitz continuous function of time for

both $b < 0$ and $b > 0$:

$$
\begin{aligned}
|s(t) - s(\tau)| &= \left| -b_0(\sqrt{2t+1} - \sqrt{2\tau+1}) - \frac{b}{\sqrt{1-D}} \int_{(1-D)\tau - \frac{1}{2}D}^{(1-D)t - \frac{1}{2}D} M(s)\alpha^{-1}(s)\, ds \right| \\
&\leq |b_0||t - \tau| + 2m\frac{|b|}{\sqrt{1-D}} \int_{(1-D)\tau - \frac{1}{2}D}^{(1-D)t - \frac{1}{2}D} 1\, ds \\
&= \left(|b_0| + 2|b|m\sqrt{1-D} \right)|t - \tau| \leq (|b_0| + 2|b|m)|t - \tau|, \quad (1.20)
\end{aligned}
$$

where (a) and that α^{-1} is a 1-Lipschitz function are used.

Using this information, we bound each addend J_i for $i = 1, 2, 3$. These bounds are calculated as in [29], so they are shown here in a simplified manner.

- J_1 can be estimated exactly as in [29] since the concrete expression of $s(t)$ is not relevant for the computations. Thus, using that $\int_{-\infty}^{0} G(x, t, \xi, 0)\, d\xi \leq 1$, we obtain

$$
\begin{aligned}
|J_1| &\leq 2\left\{ \sup_{x \in (-\infty, V_R) \cup (V_R, 0]} |u_I'(x)| \right\} \left(\int_{-\infty}^{V_R} G(x, t, \xi, 0)\, d\xi + \int_{V_R}^{0} G(x, t, \xi, 0)\, d\xi \right) \\
&\leq 2 \sup_{-\infty < x \leq 0} |u_I'(x)|. \quad (1.21)
\end{aligned}
$$

- Using (b), (1.20) and operating as in [29] (which is possible due to the fact that (b) and inequality (1.20) are the same as $ii.$ and inequality (3.9) of [29], respectively) we obtain the bound

$$
\begin{aligned}
|J_2| &\leq 2m \int_0^t |G_x(s(t), t, s(\tau), \tau)|\, d\tau \\
&= \frac{m}{\sqrt{4\pi}} \int_0^t \frac{|s(t) - s(\tau)|}{(t - \tau)^{3/2}} e^{-\frac{|s(t) - s(\tau)|^2}{4(t - \tau)}}\, d\xi \\
&\leq \frac{m(|b_0| + 2m|b|)}{\sqrt{4\pi}} \int_0^t \frac{1}{(t - \tau)^{1/2}}\, d\tau \\
&\leq \frac{2m(|b_0| + 2m|b|)}{\sqrt{4\pi}} \sigma^{1/2} \\
&\leq \frac{1}{2}. \quad (1.22)
\end{aligned}
$$

- In order to derive the estimate of J_3 we need a lower bound of $|s(t) - s_1(\tau)|$. Using $b_0 < 0$, $V_R < 0$, $\alpha^{-1}(\tau) \leq 1$, $\alpha^{-1}(\tau)$ is 1-Lipschitz and condition (c) we write

$$
\begin{aligned}
|s(t) - s_1(\tau)| &= \left| -b_0(\sqrt{2t+1} - \sqrt{2\tau+1}) - b \int_{(1-D)\tau - \frac{1}{2}D}^{(1-D)t - \frac{1}{2}D} \frac{M(s)\alpha^{-1}}{\sqrt{1-D}}\, ds - V_R\alpha^{-1}(\tau) \right| \\
&\geq | -b_0(\sqrt{2t+1} - \sqrt{2\tau+1}) - V_R\alpha^{-1}(\tau)| \geq \left| -|b_0||\sqrt{2t+1} - \sqrt{2\tau+1}| + |V_R|\alpha^{-1}(\tau) \right| \\
&\geq \left| |V_R| - |b_0||\sqrt{2t+1} - \sqrt{2\tau+1}| \right| \geq ||V_R|| - |b_0||t - \tau|| \geq |V_R| - |b_0|\sigma > 0. \quad (1.23)
\end{aligned}
$$

Then, using (1.23) and proceding as in [29] (which works since the bound (1.23) is the same as

bound (3.12) of [29]), we estimate J_3 as follows. We start writing the auxiliary bound

$$|G_x(x, t, \xi, \tau)| \leq \frac{1}{\sqrt{4\pi(t-\tau)}} e^{-\frac{|x-\xi|^2}{8(t-\tau)}}, \tag{1.24}$$

which is a consequence of the inequality $y e^{-y^2} \leq e^{-\frac{y^2}{2}}$. Integrating (1.24) yields

$$
\begin{aligned}
\int_0^t |G_x(s(t), t, s_1(\tau), \tau)| \, d\tau &\leq \frac{1}{\sqrt{4\pi}} \int_0^t \frac{1}{t-\tau} e^{-\frac{|s(t)-s_1(\tau)|^2}{8(t-\tau)}} \\
&\leq \frac{1}{\sqrt{4\pi}} \int_0^t \frac{1}{t-\tau} e^{-\frac{(|V_R|-|b_0|\sigma)^2}{8(t-\tau)}} \\
&\leq \frac{1}{\sqrt{\pi}} \int_{\frac{|V_R|-|b_0|\sigma}{\sqrt{8\sigma}}} \frac{1}{z} e^{-z^2} \, dz,
\end{aligned} \tag{1.25}
$$

where we used (1.23) and the change of variables $z = \frac{|V_R|-|b_0|\sigma}{\sqrt{8t}}$. By the bound (1.25) and condition (d) we get

$$|J_3| \leq \frac{2m}{\sqrt{\pi}} \int_{\frac{|V_R|-|b_0|\sigma}{\sqrt{8\sigma}}}^{\infty} \frac{1}{z} e^{-z^2} \leq \frac{1}{2}. \tag{1.26}$$

Joining all the estimates for J_i we finally obtain that $\|T(M)\| \leq J_1 + J_2 + J_3 \leq m$, $\forall M \in C_{\sigma,m}$ using the choice of m of (1.18). So our first aim is achieved. It only remains to show how this proof can be extended to the excitatory case. The most relevant modification needed for $b > 0$ is estimate (1.23). We obtain an analogous bound, using inequality (1.20), $0 < \tau < t < \sigma$, and $\alpha^{-1}(\tau) \leq 1$

$$
\begin{aligned}
|s(t) - s_1(\tau)| &= |s(t) - s(\tau) - V_R \alpha^{-1}(\tau)| = |V_R \alpha^{-1}(\tau) - (s(t) - s(\tau))| \\
&\geq \left| |V_R| \alpha^{-1}(\tau) - |s(t) - s(\tau)| \right| \geq \left| |V_R| \alpha^{-1}(\tau) - (|b_0| + 2|b|m\sqrt{1-D})|t-\tau| \right| \\
&\geq \left| |V_R| - (|b_0| + 2|b|m\sqrt{1-D})|t-\tau| \right| \geq \left| |V_R| - (|b_0| + 2|b|m\sqrt{1-D})\sigma \right| \\
&\geq |V_R| - (|b_0| + 2|b|m)\sigma.
\end{aligned} \tag{1.27}
$$

For $\sigma > 0$ small enough, this lower bound is the same as (3.15) of [29], and thus, it can be estimated by some positive constant, as in [29]. Then, assuming analogous conditions (a)-(d) and proceeding in a similar way as for the inhibitory case, we get the result also for $b > 0$.

Step 2. We want to prove that for $\sigma > 0$ small enough T is a contraction. With that purpose we start deriving some auxiliary estimates. Let $M, \hat{M} \in C_{\sigma,m}$ and, using expression (1.13) instead of (1.14) for $s(t)$, define

$$
\begin{aligned}
s(t) &= -b_0(\sqrt{2t+1}-1) - b(1-D)\int_0^t M((1-D)s - \frac{1}{2}D)\alpha^{-1}(s) \, ds, \\
\hat{s}(t) &= -b_0(\sqrt{2t+1}-1) - b(1-D)\int_0^t \hat{M}((1-D)s - \frac{1}{2}D)\alpha^{-1}(s) \, ds.
\end{aligned} \tag{1.28}
$$

Then:

$$
\begin{aligned}
|s(t) - \hat{s}(t)| &\leq |b|(1-D) \int_0^t |M((1-D)s - \tfrac{1}{2}D) - \hat{M}((1-D)s - \tfrac{1}{2}D)|\alpha^{-1}(s)\, ds \\
&\leq |b|(1-D)\|M - \hat{M}\| \int_0^t \sqrt{2s+1}\, ds \\
&= \frac{|b|}{3}(1-D)\|M - \hat{M}\| \left((2t+1)^{\frac{3}{2}} - \right) \leq \frac{|b|}{3}\|M - \hat{M}\| \left((2t+1)^{\frac{3}{2}} - 1 \right). \quad (1.29)
\end{aligned}
$$

And also, directly from (1.28) we get that

$$
|s'(t) - \hat{s}'(t)| \leq 2|b|\|M - \hat{M}\|, \qquad \forall 0 < t \leq \sigma < 1. \quad (1.30)
$$

Finally, from condition (a) on σ and (1.20) we obtain

$$
\max\{|s(t) - s(\tau)|, |\hat{s}(t) - \hat{s}(\tau)|\} \leq (|b_0| + 2m|b|)|t - \tau|. \quad (1.31)
$$

Now we are ready to bound T as follows

$$
\begin{aligned}
|T(M) - T(\hat{M})| &\leq 2\left[\int_{-\infty}^{V_R} |u_I'(\xi)||G(s(t),t,\xi,0) - G(\hat{s}(t),t,\xi,0)|\, d\xi \right.\\
&\quad \left. + \int_{V_R}^0 |u_I'(\xi)||G(s(t),t,\xi,0) - G(\hat{s}(t),t,\xi,0)|\, d\xi \right] \\
&\quad + 2\left| \int_0^t M(\tau)G_x(s(t),t,s(\tau),\tau) - \hat{M}(\tau)G_x(\hat{s}(t),t,\hat{s}(\tau),\tau)\, d\tau \right| \\
&\quad + 2\left| \int_0^t M(\tau)G_x(s(t),t,s_1(\tau),\tau) - \hat{M}(\tau)G_x(\hat{s}(t),t,\hat{s}_1(\tau),\tau)\, d\tau \right| \\
&=: A_1 + A_2 + A_3.
\end{aligned}
$$

Then, assuming without loss of generality that $\hat{s}(t) > s(t)$, using (1.20), (1.29), (1.30) and following exactly the same calculations as in [29] (which is possible since (1.20), (1.29) and (1.30) are the same as (3.9), (3.17) and (3.18) of [29], respectively) each of the addends A_1, A_2 and A_3 is bounded separately. To estimate A_1 we start applying the mean value theorem to G, and thus, for some $\bar{s} \in [s(t), \hat{s}(t)]$ we have that

$$
|G(s(t),t,\xi,0) - G(\hat{s}(t),t,\xi,0)| \leq |G_x(\bar{s},t,\xi,0)||s(t) - \hat{s}(t)|.
$$

Then, using (1.17) and the relation $ye^{-y^2} \leq e^{-y^2/2}$, integrating in ξ and applying (1.29), yields, for σ sufficiently small

$$
A_1 \leq \frac{1}{6}\|M - \hat{M}\|.
$$

A_2 is bounded as follows

$$
\begin{aligned}
|A_2| &\leq 2\left| \int_0^t M(\tau)G_x(s(t),t,s(\tau),\tau) - \hat{M}(\tau)G_x(s(t),t,s(\tau),\tau)\, d\tau \right| \\
&\quad 2\left| \int_0^t \hat{M}(\tau)G_x(s(t),t,s(\tau),\tau) - \hat{M}(\tau)G_x(\hat{s}(t),t,\hat{s}(\tau),\tau)\, d\tau \right| \\
&=: A_{21} + A_{22}.
\end{aligned}
$$

Then, proceeding in a similar manner as in (1.22) we get for σ small enough

$$|A_{21}| \leq \frac{(|b_0| + 2m|b|)}{\sqrt{4\pi}}\sigma^{1/2}||M - \hat{M}|| \leq \frac{1}{12}||M - \hat{M}||.$$

The estimate of A_{22} is quite more involved and omitted here for the sake of simplicity, since the computations are exactly the same as is [29]. Mainly they consist of splitting A_{22} in two terms, bounding each of them separately, using the mean value theorem and the auxiliary estimates (1.30) and (1.31). Finally, it is obtained that

$$A_{22} \leq \frac{1}{12}||M - \hat{M}||.$$

The last step is to get a bound for A_3

$$
\begin{aligned}
|A_3| \quad \leq \quad & 2\left|\int_0^t M(\tau)G_x(s(t), t, s_1(\tau), \tau) - \hat{M}(\tau)G_x(s(t), t, s_1(\tau), \tau)\ d\tau\right| \\
& 2\left|\int_0^t \hat{M}(\tau)G_x(s(t), t, s_1(\tau), \tau) - \hat{M}(\tau)G_x(\hat{s}(t), t, \hat{s}_1(\tau), \tau)\ d\tau\right| \\
=: \quad & A_{31} + A_{32}.
\end{aligned}
$$

The first addend is estimated as J_3 in (1.26),

$$|A_{31}| \leq C||M - \hat{M}|| \int_{\frac{\omega}{\sqrt{8\sigma}}}^\infty \frac{1}{z}e^{-z^2}\ dz < \frac{1}{12}||M - \hat{M}||,$$

where we used that $\hat{s}(t) - \hat{s}_1(\tau) \geq \omega > 0$ for σ sufficiently small, with

$$\omega := \begin{cases} |V_R| & - & |b_0|\sigma & b < 0, \\ |V_R| & - & (|b_0| + m)\sigma & b > 0. \end{cases}$$

Bounding A_{32} again involves some tedious computations, that are omitted, and can be found in [29]. They consist of splitting A_{32} in two terms, and then estimating each of them on its own using the mean value theorem, (1.30), (1.31), inequality $ye^{y^2} \leq e^{-y^2/2}$ and that $\hat{s}(t) - \hat{s}_1(\tau) \geq \omega > 0$. It is concluded then that for some σ small enough

$$|A_{32}| \leq \frac{1}{12}||M - \hat{M}||.$$

Joining all the previous estimates, we finally obtain that T is a contraction, that for some σ small enough inversely proportional to m satisfies

$$||TM - T\hat{M}|| \leq \frac{1}{2}||M - \hat{M}||.$$

$\square$

We have to show how Theorem 1.3.1, that ensures that we have short time existence and uniqueness of solution in the integral sense for problem (1.15), is translated into our initial equation (1.1)-(1.2)-(1.4). With that purpose we start showing that:

55

Corollary 1.3.2 *There exists a unique solution of problem* (1.15) *in the sense of Definition* 1.2.1 *for* $t \in [0, T]$.

Proof. The proof is ommited, since it is performed as in [29] [Corollary 3.3]. Let us only point out that, once M is known the equation for u decouples, and u can be calculated via the Duhamel's formula

$$
\begin{aligned}
u(x,t) \;=\; & \int_{-\infty}^{V_R} G(x,t,\xi,0) u_I(\xi) \; d\xi + \int_{V_R}^0 G(x,t,\xi,0) u_I(\xi) \; d\xi \\
& - \int_0^t M(\tau) G(x,t,s(\tau)\tau) \; d\tau + \int_0^t M(\tau) G(x,t,s_1(\tau)\tau) \; d\tau,
\end{aligned}
$$

where G is defined by (1.17). $\square$

Then, after computing u with the Duhamel's formula, ρ and N are recovered undoing the changes of variables (1.5) and (1.10).

1.4 Global existence of solutions for the delayed model

In this section we derive the main result of the chapter: Classical solutions for (1.1) are global-in-time for both the inhibitory and the excitatory cases, when we include a synaptic delay in the model. The result is obtained directly for the inhibitory case, while for the excitatory case, it has to be derived through some of the properties of upper-solutions.

1.4.1 A criterion for the maximal time of existence

Here we obtain a criterion for the maximal time of existence of solution, summarized in Theorem 1.4.2, which is the key result to obtain the main results of the chapter. Indeed, it ensures that solutions exists and are unique, while the firing rate is finite. With that purpose we start presenting an auxiliary proposition, Proposition 1.4.1, which provides the tool to prove Theorem 1.4.2. Then using Theorem 1.4.2 we derive Proposition 1.4.4 which will allow to derive the global existence of solution for the inhibitory case. Notice that the proofs of the following results are all omitted or sketched since they are the same as in [29] [Proposition 4.1, Theorem 4.2., Proposition 4.3]. They are all consequences of the local existence result of Theorem 1.3.1, whose proof is different from the one of Theorem 3.2 of [29] due to the presence of the delay, $D > 0$, as showed in the previous section.

Proposition 1.4.1 *Suppose that the hypotheses of Theorem* 1.3.1 *hold and that* $(u(t), s(t))$ *is a solution to* (1.15) *in the time interval* $[0, T]$. *Assume in addition, that*

$$
U_0 := \sup_{x \in (-\infty, s(t_0 - \varepsilon)]} |u_x(x, t_0 - \varepsilon)| < \infty \qquad \text{and that} \qquad M^* = \sup_{t \in (t_0 - \varepsilon, t_0)} M(t) < \infty,
$$

for some $0 < \varepsilon < t_0 \leq T$. *Then*

$$
\sup\{|u_x(x,t)| \; with \; x \in (-\infty, s(t)], \; t \in [t_0 - \varepsilon, t_0)\} < \infty,
$$

with a bound depending only on the quantities M^* *and* U_0.

Using this proposition we obtain the key result:

Theorem 1.4.2 *Suppose that the hypotheses of Theorem 1.3.1 hold. Then the solution u can be extended up to a maximal time $0 < \bar{T} \leq \infty$ given by*

$$\bar{T} = \sup\{t > 0 : M(t) < \infty\}.$$

This result, translated to our initial equation (1.1)-(1.2)-(1.4) reads:

Theorem 1.4.3 (Maximal time of existence) *Let $\rho^0(v)$ be a non-negative $C^0((-\infty, V_F]) \cap C^1((-\infty, V_R) \cup (V_R, 0]) \cap L^1((-\infty, 0))$ function such that $\rho^0(V_F) = 0$. Suppose that ρ^0 and $(\rho^0)_v$ decay to zero as $v \to -\infty$ and that the left and right derivatives at V_R are finite. Then there exist a unique classical solution to the problem (1.1)-(1.2)-(1.4) with $D \geq 0$ on the time interval $[0, T^*)$ where $T^* > 0$ can be characterized by*

$$T^* = \sup\{t > 0 : N(t) < \infty\}.$$

Using Theorem 1.4.2 we derive the key result for the global existence for the inhibitory case. As in the case for $D = 0$, this result is derived showing that every solution defined until a certain time t_0 can be extended up to a short (but unifom) time ε, because the firing rate up to this additional time $t_0 + \varepsilon$ is uniformly bounded.

Proposition 1.4.4 *Suppose that the hypotheses of Theorem 1.3.1 hold and that $(u(t), s(t))$ is a solution to (1.15) in the time interval $[0, t_0)$ for $b < 0$. Then there exists $\varepsilon > 0$ small enough such that, if*

$$\bar{U} := \sup_{x \in (-\infty, s(t_0 - \varepsilon)]} |u_x(x, t_0 - \varepsilon)| < \infty, \tag{1.32}$$

then for $0 < \varepsilon < t_0$

$$\sup_{t_0 - \varepsilon < t < t_0} M(t) < \infty.$$

Although the estimate depends on the bound (1.32), ε does not depend on t_0.

Finally, combining Theorem 1.4.2 with the previous result we obtain the global existence and unicity of classical solutions for the inhibitory case with synaptic delay for system (1.15):

Proposition 1.4.5 *Suppose that the hypotheses of Theorem 1.3.1 hold and that $b < 0$. Then there exists a unique global-in-time classical solution $(u(x, t), s(t))$ for sytem (1.15) in the sense of Definition 1.2.1 with initial data u_I. Besides, if both b and b_0 are negative, $s(t)$ is a monotone increasing function.*

This proposition, translated to the initial delayed Fokker-Planck equation (1.1) provides the global existence for the inhibitory case, as follows:

Theorem 1.4.6 (Global existence - inhibitory case) *Let $\rho^0(v)$ be a non-negative $C^0((-\infty, V_F]) \cap C^1((-\infty, V_R) \cup (V_R, 0]) \cap L^1((-\infty, 0))$ function such that $\rho^0(V_F) = 0$. Suppose that ρ^0 and $(\rho^0)_v$ decay to zero as $v \to -\infty$ and that the left and right derivatives at V_R are finite. Then there exist a unique classical solution to the problem (1.1)-(1.2)-(1.4) with $b < 0$ and $D \geq 0$ on the time interval $[0, T^*)$ with $T^* = \infty$.*

1.4.2 Upper-solutions and control over the firing rate

We are not able to obtain the global existence of solution for the excitatory case as it is done for the inhibitory case in Proposition 1.4.4. One key step of its demonstration is to obtain

$$|s(t) - s_1(\tau)| \geq |V_R| - |b_0|\varepsilon, \quad \text{for} \quad t > \tau \quad \text{and} \quad t, \tau \in (t_0 - \varepsilon, t_0),$$

which is a direct consequence of inequality (1.23). Moreover, $\varepsilon > 0$ is chosen small enough so that $|V_R| - |b_0|\varepsilon > 0$ and thus, independent of the initial time t_0. Nevertheless, if we write this proposition for $b > 0$ with the additional hypothesis $\bar{M} := \sup_{t \in [0, t_0 - \varepsilon]} M(t) < \infty$ (taking advantage of the presence of the delay) we obtain the bound

$$
\begin{aligned}
|s(t) - s(\tau)| &= \left| -b_0(\alpha^{-1}(t) - \alpha^{-1}(\tau)) - \frac{b}{\sqrt{1-D}} \int_{(1-D)\tau - \frac{1}{2}D}^{(1-D)t - \frac{1}{2}D} M(s)\alpha^{-1}(s)ds \right| \\
&\leq |b_0||\alpha^{-1}(t) - \alpha^{-1}(\tau)| + \frac{|b|}{\sqrt{1-D}} \int_{(1-D)\tau - \frac{1}{2}D}^{(1-D)t - \frac{1}{2}D} M(s)\alpha^{-1}(s)ds \\
&\leq |b_0||t - \tau| + \frac{|b|}{\sqrt{1-D}}\bar{M} \int_{(1-D)\tau - \frac{1}{2}D}^{(1-D)t - \frac{1}{2}D} \alpha^{-1}(s)\ ds \\
&= |b_0||t - \tau| + |b|(1-D)\bar{M} \int_{\tau}^{t} \sqrt{2s+1}\ ds \\
&\leq \left(|b_0| + 2|b|\bar{M}\sqrt{2t_0+1} \right)\varepsilon, \qquad \forall\ t, \tau \in (t_0 - \epsilon, t_0),
\end{aligned}
\tag{1.33}
$$

which leads to estimate

$$|s(t) - s_1(\tau)| \geq |V_R| - \left(|b_0| + 2|b|\bar{M}\sqrt{2t_0+1} \right)\varepsilon.$$

To follow the same argumentation as for the inhibitory case, now $\varepsilon > 0$ has to be chosen small enough so that $|V_R| - \left(|b_0| + 2|b|\bar{M}\sqrt{2t_0+1} \right)\varepsilon > 0$, and thus, the election of ε clearly depends on t_0. In fact, it is inversely proportional to t_0.

Thus we have to proceed with a different strategy, by means of an upper-solution, to prove that the firing rate of any local solution cannot diverge in finite time. Then, applying the criterium of Theorem 1.4.3 the result is reached. We start introducing the notion of upper-solution.

Definition 1.4.7 *Let $T \in \mathbb{R}_+$, $(\bar{\rho}, \bar{N})$ is said to be a (classical) upper-solution to (1.1)-(1.2)-(1.4) for $D \geq 0$ and $b_0 = 0$ on $(-\infty, V_F] \times [0, T]$ if for all $t \in [0, T]$ we have $\bar{\rho}(V_F, t) = 0$ and*

$$\partial_t \bar{\rho} + \partial_v[(-v + b\bar{N}(t-D))\bar{\rho}] - a\partial_{vv}\bar{\rho} \geq \delta_{v=V_R}\bar{N}(t), \quad \bar{N}(t) = -a\partial_v\bar{\rho}(V_F, t).$$

on $(-\infty, V_F] \times [0, T]$ in the distributional sense and on $((-\infty, V_F] \setminus V_R) \times [0, T]$ in the classical sense, with arbitrary values for $\bar{N}$ on $[-D, 0)$.

Notice that for a solution in $C^{2,1}((-\infty, V_R) \cup (V_R, V_F] \times [0, T]) \cap C^0((-\infty, V_R] \times [0, T])$, the condition reduces to satisfy the property in the classical sense in $(-\infty, V_R) \cup (V_R, V_F] \times [0, T]$ and having a decreasing jump discontinuity for the derivative on V_R of size at least $\bar{N}/a$. Notice also that if we find such a function $\bar{\rho}$, then for every constant $\alpha > 0$, the function $\alpha\bar{\rho}$ is also an upper-solution.

Theorem 1.4.8 *Let $T < D$. Let (ρ, N) be a classical solution of (1.1)-(1.2)-(1.4) for $b_0 = 0$ and $D > 0$ on $(-\infty, V_F] \times [0, T]$ for the initial condition (ρ^0, N^0) and let $(\bar{\rho}, \bar{N})$ be a classical upper-solution of (1.1)-(1.2)-(1.4) for $b_0 = 0$ and $D > 0$ on $(-\infty, V_F] \times [0, T]$. Assume that*

$$\forall v \in (-\infty, V_F], \quad \bar{\rho}(v, 0) \geq \rho^0(v) \qquad and \qquad \forall t \in [-D, 0), \quad \bar{N}(t) = N^0(t).$$

Then,

$$\forall (v, t) \in (-\infty, V_F] \times [0, T], \quad \bar{\rho}(v, t) \geq p(v, t) \qquad and \qquad \forall t \in [0, T], \quad \bar{N}(t) \geq N(t).$$

Proof. First, notice that due to the Dirichlet boundary condition for ρ and the definition of upper-solution we chose, we have $\rho(V_F, t) = \bar{\rho}(V_F, t) = 0$ on $[0, T]$. Thus, as long as $\bar{\rho}(v, t) \geq \rho(v, t)$ holds, we have

$$-a \frac{\bar{\rho}(V_F, t) - \bar{\rho}(v, t)}{V_F - v} \geq -a \frac{\rho(V_F, t) - \rho(v, t)}{V_F - v}.$$

Passing to the limit, we get

$$\bar{N}(t) \geqslant N(t).$$

Then, denoting $w = \bar{\rho} - \rho$, we have for all $(v, t) \in (-\infty, V_F] \times [0, T]$,

$$\partial_t w + \partial_v(-vw) + b\bar{N}(t - D)\partial_v\bar{\rho} - bN(t - D)\partial_v\rho - a\partial_{vv}w \geq \delta_{v=V_R}(\bar{N}(t) - N(t)).$$

As we assume $T < D$ we have by hypothesis $\bar{N}(t - D) = N^0(t - D)$ for all $t \in [0, T]$. Thus, as long as $w \geq 0$ holds,

$$\partial_t w + \partial_v[(-v + bN^0(t))w] - a\partial_{vv}w \geq 0.$$

As $w(\cdot, 0) \geq 0$, by a standard maximum principle theorem, we have

$$\forall t \in [0, T], \quad w(\cdot, t) \geq 0,$$

and then the results hold. $\quad\square$

Now, for fixed and bounded $N^0(t)$ and the choice $\bar{N}(t) = N^0(t)$ in $[-D, 0)$, we shall look for upper-solution $\bar{\rho}$ of the form

$$\bar{\rho}(v, t) = e^{\xi t} f(v),$$

where ξ is large enough and f is a carefully selected function. Replacing the function $\bar{\rho}$ in the condition, the problem reduces to find a function f such that

$$(\xi - 1)f + (-v + bN^0(t))f' - af'' \geq \delta_{v=V_R}V(t), \quad V(t) = -af'(V_F). \tag{1.34}$$

We construct a suitable function f :

1. Let $\varepsilon > 0$ be small enough to have $\frac{V_F + V_R}{2} + \varepsilon < V_F$ and let $\psi \in C_b^\infty(\mathbb{R})$ satisfying $0 \leq \psi \leq 1$ and

$$\psi \equiv 1 \text{ on } (-\infty, \frac{V_F + V_R}{2}) \text{ and } \psi \equiv 0 \text{ on } (\frac{V_F + V_R}{2} + \varepsilon, +\infty).$$

2. Then let $B > 0$ such that

$$\forall t \in [-D, 0), \forall v \in (V_R, V_F), \quad |-v + bN^0(t)| \leq B$$

and $\delta > 0$ such that $a\delta - B \geq 0$.

3. Let define

$$
f: \quad (-\infty, V_F] \quad \rightarrow \quad \mathbb{R}_+
$$
$$
v \quad \mapsto \quad \begin{cases} 1 & \text{on } (-\infty, V_R] \\ e^{V_R - v}\psi(v) + \frac{1}{\delta}(1 - \psi(v))(1 - e^{\delta(v - V_F)}) & \text{on } (V_R, V_F] \end{cases}
$$

With these choices, $\bar{\rho}(v, t)$ is an upper-solution on $[0, D]$ for ξ large enough. Indeed,

- On $(-\infty, V_R)$, $\bar{\rho}$ is independent of v, thus the definition is satisfied if and only if $\xi > 1$.

- Around the V_R point the inequality has to hold in the sense of distribution, that is in our case

$$
f'(V_R^+) - f'(V_R^-) \leqslant f'(V_F)
$$

This inequality is satisfied as $f'(V_R^-) = 0$, $f'(V_R^+) = -1$ and $f'(V_F) = -1$.

- On $\left(V_R, \frac{V_F + V_R}{2} + \varepsilon\right)$, we choose ξ such that

$$
(\xi - 1) \inf_{v \in \left(V_R, \frac{V_F + V_R}{2} + \varepsilon\right)} f(v) \geq \sup_{v \in \left(V_R, \frac{V_F + V_R}{2} + \varepsilon\right)} \left(B|\partial_v f(v)| + a|\partial_{vv} f(v)|\right),
$$

which is possible because $\inf_{v \in \left(V_R, \frac{V_F + V_R}{2} + \varepsilon\right)} f(v) > 0$. Then the upper-solution inequality holds.

- On $\left(\frac{V_F + V_R}{2} + \varepsilon, V_F\right)$, the desired inequality holds because

$$
(-v + b\bar{N}(t - D))\partial_v f - a\partial_{vv} f = e^{\delta(V_F - v)}\left[a\delta - (-v + b\bar{N}(t - D))\right] \geq e^{\delta(V_F - v)}\left[a\delta - B\right] \geq 0.
$$

Given this upper-solution on $[0, D]$ for any fixed bounded $N^0(t)$, we can prove global existence for local solutions.

Theorem 1.4.9 (Global existence - delayed excitatory and inhibitory cases) *Let (ρ, N) be a local classical solution of (1.1)-(1.2)-(1.4) for $b_0 = 0$ and $D > 0$ for the non-negative initial condition (ρ^0, N^0) where $N^0 \in C^0([-D, 0))$ is bounded and $\rho^0 \in L^1((-\infty, V_F)) \cap C^1((-\infty, V_R) \cup (V_R, V_F]) \cap C^0((-\infty, V_F])$, with $\rho^0(V_F) = 0$. Suppose that ρ^0 and $(\rho^0)_v$ decay to zero as $v \to -\infty$ and that the right and left derivatives at V_R are finite. Then, the maximal time existence for the solution (ρ, N) is $T^* = +\infty$.*

Proof. Assume the maximal time of existence T^* is finite. As the maximal solution was showed previously to be unique, we assume without loss of generality that $T^* = \frac{D}{2} < D$ by using the new initial conditions

$$
\tilde{\rho}^0(v) = \rho(v, T^* - \frac{D}{2}) \quad \forall v \in (-\infty, V_F] \quad \text{and} \quad \tilde{N}^0(\tilde{t}) = N\left(T^* - \frac{D}{2} + \tilde{t}\right), \quad \tilde{t} \in [-D, 0).
$$

By Corollary 1.3.2 the new initial conditions satisfy all the hypotheses of the result we are proving. As $\tilde{\rho}^0$ is continuous and vanish at V_F and $-\infty$, it belongs to $L^\infty((-\infty, V_F])$ and therefore there exists $\alpha \in \mathbb{R}^*_+$ such that the upper-solution $\bar{\rho}$ we constructed satisfy

$$\forall v \in (-\infty, V_F], \quad \alpha \bar{\rho}(v, 0) \geq \tilde{\rho}^0(v),$$

where we use the fact that $\bar{\rho}$ never vanish on $(-\infty, V_F)$. Then, by Theorem 1.4.8, we have

$$N\left(T^* - \frac{D}{2} + \tilde{t}\right) = \tilde{N}(\tilde{t}) \leq \bar{N}(\tilde{t}) = ae^{\xi \tilde{t}} \quad \forall \tilde{t} \in [0, D/2].$$

Thus

$$N(t) \leq ae^{\xi(t - T^* + D/2)} \quad \forall t \in [T^* - D/2, T^*).$$

Therefore, by continuity, there is no divergence of the firing rate N when $t \to T^*$, and thus, and by Theorem 1.4.3 we reach a contradiction. Notice that we have used that, due to Theorem 1.4.3, the only way to obtain that $T^* < \infty$ is that $N(t)$ diverges as $t \to T^*$. $\square$

1.5 Numerical results

The numerical results showed have been obtained using the numerical solver explained in Section 3.4.2 [Chapter 3]. Moreover, some of them have been presented in [20]. On one hand, we observe how the blow-up (Fig. 1.1 top left) is avoided (Fig. 1.1 top right) if we include a synaptic delay. For this case, we have a small value of b combined with a concentrated initial condition, which produces the blow-up of the solution without delay [15]. For this value of b there is a unique steady state [15], and the solution seem to tend to it, after avoiding the blow due to the delay.

On the other hand, we show a blow-up situation (Fig. 1.1 bottom left), which happens due to a large value of b [15]. If we include the delay, the solutions avoid the blow-up (Fig. 1.1 bottom right), but they do not tend to an equilibrium, since for large values of b there is no steady state [15]. Numerically, the firing rate seems to grow slowly all the time with limit $+\infty$, but without blowing-up in finite. Initially, we expected solutions to present a somehow periodic behavior, but we did not find it.

1.6 Conclusions

This chapter is devoted to the NNLIF equation with a synaptic delay, which is a more realistic version than the one considered in [15]. For the model without delay, there are some situations for the excitatory case where the solutions are not global-in-time [15] due to the divergence of the firing rate [29]. Nevertheless, at microscopic level, it has been proved that if the synaptic delay is taken into account, solutions are always global-in-time [38].

Starting from this observations, we included the delay in the equation, in order to prove global-in-time existence also for the delayed mesoscopic NNLIF model. With that purpose, we have followed the ideas of [29] combined with the ones of [26] and adapted them to our equation. First, we performed an appropiate change of variables in order to rewrite the delayed NNLIF equation as a free boundary Stefan problem with a nonstandard right hand side. Then, using an integral formulation of this new equation we were able to proof a criterium for maximal time of existence of the solutions, in terms of
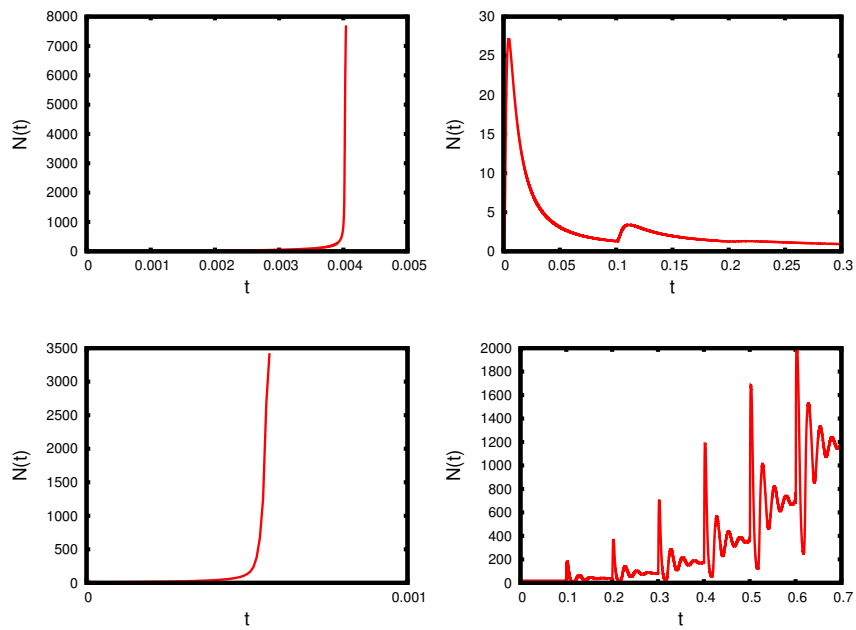
Figure 1.1: Top: We consider the initial data (3.40) with $v_0 = 1.83$, and $\sigma_0 = 0.0003$, and the connectivity parameter $b = 0.5$. Left: N blows-up in finite time, if there is no delay, $D = 0$. Right: N tends to the equilibrium if there is delay, $D = 0.1$. Bottom: We consider the initial data (3.40) with $v_0 = 1.83$, and $\sigma_0 = 0.003$, and the connectivity parameter $b = 2.2$. Left: N blows-up in finite time, if there is no delay, $D = 0$. Right: N does not blow-up if there is delay, $D = 0.1$.

the size of the firing rate. Using this result, we obtained the global-in-time existence and unicity for the inhibitory case in a straightforward computation.

However, to show the global-in-time existence of the excitatory case, we had to add a different strategy. We need to consider an upper-solution in order to obtain some control on the firing rate. Finally, this control, joined to the maximal time of existence criterium, allowed us to get the global-in-time existence and unicity, for the delayed equation for both the excitatory and inhibitory cases.

In conclusion, we were able to show the global in time existence for the delayed NNLIF model for both the excitatory and the inhibitory cases, which implies that the blow-up observed in previous models that neglected this delay, appears due to the simplifications made. Moreover, this validates the NNLIF model once more as a competent model to reproduce biological fact.

Chapter 2

Two populations NNLIF model

In this chapter we extend the results obtained for one population NNLIF models [15, 17, 26, 29] to the excitatory-inhibitory coupled NNLIF model. This model was also studied in [11], where time delay and refractory period were included. Here we focus on other aspects: We prove that, although in a purely inhibitor network the solutions are global in time (see [29]), in the presence of excitatory neurons the system can blow-up in finite time. We also analyze the set of stationary states, which is more complicated than in the case of purely excitatory or inhibitory networks, and prove exponential convergence to the unique steady state when all the connectivity parameters are small. This exponential convergence can be demonstrated, in terms of the entropy method, since for this case the system is a "small" perturbation of the linear one. Finally, the complexity of the coupled excitatory-inhibitory network is numerically described.

2.1 The model and the definition of solution

The mathematical model that we are going to analyze in this chapter has already been derived in the Introduction [Section 0.2], in the case with delas y and refractory states. If we neglect this two properties, the model consists of a system of two coupled PDEs for the evolution of the probability densities $\rho_\alpha(v, t)$, where $\rho_\alpha(v, t)$ denotes the probability of finding a neuron in the population α, with a voltage $v \in (-\infty, V_F]$ at a time $t \geq 0$, and is given by

$$
\begin{cases}
\frac{\partial \rho_I}{\partial t}(v, t) + \frac{\partial}{\partial v}[h^I(v, N_E(t), N_I(t))\rho_I(v, t)] - a_I(N_E(t), N_I(t))\frac{\partial^2 \rho_I}{\partial v^2}(v, t) = N_I(t)\delta(v - V_R), \\
\\
\frac{\partial \rho_E}{\partial t}(v, t) + \frac{\partial}{\partial v}[h^E(v, N_E(t), N_I(t))\rho_E(v, t)] - a_E(N_E(t), N_I(t))\frac{\partial^2 \rho_E}{\partial v^2}(v, t) = N_E(t)\delta(v - V_R).
\end{cases}
\tag{2.1}
$$

The right hand sides in (2.1) represent the fact that when neurons reach the threshold potential V_F, they emit a spike over the network and reset their membrane potential to the reset value V_R. The system (2.1) is completed with Dirichlet boundary conditions and an initial datum

$$
\rho_\alpha(-\infty, t) = 0, \ \rho_\alpha(V_F, t) = 0, \ \rho_\alpha(v, 0) = \rho_\alpha^0(v) \geq 0, \quad \alpha = E, I.
\tag{2.2}
$$

The drift and diffusion coefficients are given by

$$
\begin{aligned}
h^\alpha(v, N_E(t), N_I(t)) &= -v + b_E^\alpha N_E(t) - b_I^\alpha N_I(t) + (b_E^\alpha - b_E^E)\nu_{E,ext}, &\tag{2.3} \\
a_\alpha(N_E(t), N_I(t)) &= d_\alpha + d_E^\alpha N_E(t) + d_I^\alpha N_I(t), \quad \alpha = E, I, &\tag{2.4}
\end{aligned}
$$

where $b_i^\alpha > 0$, $d_i^\alpha \geq 0$ and $d_\alpha > 0$ $\forall \alpha, i = E, I$. The coupling of the system (2.1) is hidden in these two terms, since the mean firing rates N_α obey to

$$N_\alpha(t) = -a_\alpha(N_E(t), N_I(t))\frac{\partial \rho_\alpha}{\partial v}(V_F, t) \geq 0, \quad \alpha = E, I. \tag{2.5}$$

Moreover, (2.5) gives rise to the nonlinearity of the system (2.1), since firing rates are defined in terms of boundary conditions on distribution functions ρ_α. On the other hand, since ρ_E and ρ_I represent probability densities, the total mass should be conserved:

$$\int_{-\infty}^{V_F} \rho_\alpha(v, t) \, dv = \int_{-\infty}^{V_F} \rho_\alpha^0(v) \, dv = 1 \quad \forall \, t \geq 0, \quad \alpha = E, \, I.$$

Let us now introduce the definition of solution considered in this chapter.

Definition 2.1.1 *A weak solution of* (2.1)-(2.5) *is a quadruple of nonnegative functions* $(\rho_E, \rho_I, N_E, N_I)$ *with* $\rho_\alpha \in L^\infty(\mathbb{R}^+; L^1_+((-\infty, V_F)))$ *and* $N_\alpha \in L^1_{loc,+}(\mathbb{R}^+)$ $\forall \, \alpha = E, I$, *satisfying*

$$\int_0^T \int_{-\infty}^{V_F} \rho_\alpha(v, t) \left[-\frac{\partial \phi}{\partial t} - \frac{\partial \phi}{\partial v} h^\alpha(v, N_E(t), N_I(t)) - a_\alpha(N_E(t), N_I(t))\frac{\partial^2 \phi}{\partial v^2} \right] dv \, dt \tag{2.6}$$

$$= \int_0^T N_\alpha(t)[\phi(V_R, t) - \phi(V_F, t)]dt + \int_{-\infty}^{V_F} \rho_\alpha^0(v)\phi(v, 0)dv - \int_{-\infty}^{V_F} \rho_\alpha(v, T)\phi(v, T)dv, \qquad \alpha = E, I,$$

for any test function $\phi(v, t) \in C^\infty((-\infty, V_F] \times [0, T])$ *such that* $\frac{\partial^2 \phi}{\partial v^2}$, $v\frac{\partial \phi}{\partial v} \in L^\infty((-\infty, V_F) \times (0, T))$.

Additionally, if test functions of the form $\psi(t)\phi(v)$ are considered, the formulation (2.6) is equivalent to say that for all $\phi(v) \in C^\infty((-\infty, V_F])$ such that $v\frac{\partial \phi}{\partial v} \in L^\infty((-\infty, V_F))$

$$\frac{d}{dt}\int_{-\infty}^{V_F} \phi(v)\rho_\alpha(v, t) \, dv = \int_{-\infty}^{V_F} \left[\frac{\partial \phi}{\partial v} h^\alpha(v, N_E(t), N_I(t)) + a_\alpha(N_E(t), N_I(t))\frac{\partial^2 \phi}{\partial v^2} \right] \rho_\alpha(v, t) \, dv$$
$$+ N_\alpha(t) \left[\phi(V_R) - \phi(V_F) \right] \tag{2.7}$$

holds in the distributional sense for $\alpha = E, I$. Checking that weak solutions conserve the mass of the initial data is a straightforward computation after choosing $\phi = 1$ in (2.7),

$$\int_{-\infty}^{V_F} \rho_\alpha(v, t) \, dv = \int_{-\infty}^{V_F} \rho_\alpha^0(v) \, dv = 1 \quad \forall \, t \geq 0.$$

2.2 Finite time blow-up

In [15] and [17] it was proved that weak solutions can blow-up in finite time for a purely excitatory network, when neurons are considered or not to remain a time at refractory state. However, for a purely inhibitory network it was shown in [49] that weak solutions are global in time. The following theorem claims that a network with excitatory and inhibitory neurons can blow up in finite time. We remark that the theorem is formulated in a more general setting of drift terms h^E than that considered in (2.3). The diffusion term (2.4) of the excitatory equation is assumed to not vanish at any time. For the inhibitory firing rate we assume (2.10), which is satisfied, for instance, if $N_I(t)$ is bounded for every time. This hypothesis should not be a strong constraint, because in [29] it was proved, in the

case of only one population (in average excitatory or inhibitory), that if the firing rate is bounded for every time, then there exists a global solution in time. It could be natural to think that an analogous criterion should hold in a coupled network, although its proof seems much more complicated and remains as an open problem.

Theorem 2.2.1 *Assume that*

$$h^E(v, N_E, N_I) + v \geq b_E^E N_E - b_I^E N_I, \tag{2.8}$$

$$a_E(N_E, N_I) \geq a_m > 0, \tag{2.9}$$

$\forall v \in (-\infty, V_F]$ *and* $\forall N_I, N_E \geq 0$. *Assume also that there exist* $M \geq 0$ *such that*

$$\int_0^t N_I(s) \, ds \leq M \, t, \qquad \forall \, t \geq 0. \tag{2.10}$$

Then, a weak solution to the system (2.1)*-*(2.5) *cannot be global in time in the following cases:*

1. $b_E^E > 0$ *is large enough, for* ρ_E^0 *fixed.*

2. ρ_E^0 *is 'concentrated enough' around* V_F*:*

$$\int_{-\infty}^{V_F} e^{\mu v} \rho_E^0(v) \, dv \geq \frac{e^{\mu V_F}}{b_E^E \mu}, \qquad \text{for a certain } \mu > 0 \tag{2.11}$$

for $b_E^E > 0$ *fixed.*

Proof. Using (2.7), considering $\mu = \max\left(\frac{b_I^E M + 2V_F}{a_m}, \frac{1}{b_E^E}\right)$ and the multiplier $\phi(v) = e^{\mu v}$, a weak solution $(\rho_E(v, t), \rho_I(v, t), N_E(t), N_I(t))$ satisfies the following inequality

$$
\begin{aligned}
\frac{d}{dt} \int_{-\infty}^{V_F} \phi(v) \rho_E(v, t) \, dv \;\geq\;& \mu \int_{-\infty}^{V_F} \phi(v) \left[b_E^E N_E(t) - b_I^E N_I(t) - v \right] \rho_E(v, t) \, dv \\
& + \mu^2 a_m \int_{-\infty}^{V_F} \phi(v) \rho_E(v, t) \, dv + N_E(t) \left[\phi(V_R) - \phi(V_F) \right] \\
\;\geq\;& \mu \left[b_E^E N_E(t) - b_I^E N_I(t) - V_F + \mu a_m \right] \int_{-\infty}^{V_F} \phi(v) \rho_E(v, t) \, dv \\
& - N_E(t) \phi(V_F),
\end{aligned}
$$

where assumptions (2.8)-(2.9) and the fact that $v \in (-\infty, V_F)$ and $N_E(t)\phi(V_R) > 0$ were used. This inequality and Grönwall's lemma[1] provide the following inequality for the exponential moment

---

[1] **Grönwall's inequality.** Let $[0, b]$ be an interval in $\mathbb{R}_+$, $u \in C([0, b])$ and β, ψ nonnegative, summable functions on $[0, b]$ so that $u'(t) \leq \beta(t)u(t) + \psi(t) \; \forall t \in (0, b)$ then

$$u(t) \leq e^{\int_0^t \beta(s) \, ds} \left[u(0) + \int_0^t \psi(s) \, ds \right] \qquad \forall t \in [0, b]$$

For details of the proof or the integral form of this inequality look at [43].

$M_\mu(t) := \int_{-\infty}^{V_F} \phi(v)\rho_E(v,t)\, dv$:

$$M_\mu(t) \;\geq\; e^{\mu \int_0^t f(s)\, ds}\left[M_\mu(0) - \phi(V_F)\int_0^t N_E(s)\, e^{-\mu \int_0^s f(z)\, dz}\, ds\right],$$

where $f(s) = b_E^E N_E(s) - b_I^E N_I(s) + \mu\, a_m - V_F$. Using (2.10), we notice that

$$-\phi(V_F)\int_0^t N_E(s)\, e^{-\mu \int_0^s f(z)\, dz}\, ds \geq -\phi(V_F)\int_0^t N_E(s)\, e^{-\mu \int_0^s \left[b_E^E N_E(z) + \mu a_m - V_F\right]\, dz + \mu b_I^E M s}\, ds.$$

After some more computations that include integrating by parts and using the definition of μ the right hand side of the previous inequality can be bounded by $-\frac{\phi(V_F)}{\mu b_E^E}$:

$$
\begin{aligned}
&-\phi(V_F)\int_0^t N_E(s)\, e^{-\mu \int_0^s \left[b_E^E N_E(z) + \mu a_m - V_F\right]\, dz + \mu b_I^E M s}\, ds \\[4pt]
=\;& \int_0^t \frac{\phi(V_F)}{\mu b_E^E}\frac{d}{ds}\left[e^{-\mu b_E^E \int_0^s N_E(z)\, dz}\right] e^{-\mu(\mu a_m - V_F - b_I^E M)s}\, ds \\[4pt]
=\;& \frac{\phi(V_F)}{\mu b_E^E}\left[e^{-\mu b_E^E \int_0^s N_E(z)\, dz}\, e^{-\mu(\mu a_m - V_F - b_I^E M)s}\right]_0^t \\[4pt]
&+ \mu(\mu a_m - V_F - b_I^E M)\frac{\phi(V_F)}{\mu b_E^E}\int_0^t e^{-\mu b_E^E \int_0^s N_E(z)\, dz}\, e^{-\mu(\mu a_m - V_F - b_I^E M)s}\, ds \\[4pt]
=\;& \frac{\phi(V_F)}{\mu b_E^E} e^{-\mu b_E^E \int_0^t N_E(z)\, dz}\, e^{-\mu(\mu a_m - V_F - b_I^E M)t} - \frac{\phi(V_F)}{\mu b_E^E} \\[4pt]
&+ \mu(\mu a_m - V_F - b_I^E M)\frac{\phi(V_F)}{\mu b_E^E}\int_0^t e^{-\mu b_E^E \int_0^s N_E(z)\, dz}\, e^{-\mu(\mu a_m - V_F - b_I^E M)s}\, ds \\[4pt]
\geq\;& -\frac{\phi(V_F)}{\mu b_E^E}.
\end{aligned}
\tag{2.12}
$$

Inequality (2.12) was achieved thanks to that the first and last addend of the third equality are positive (the last addend is positive because of the choice of μ). Finally, the following inequality holds

$$M_\mu(t) \;\geq\; e^{\mu \int_0^t f(s)\, ds}\left[M_\mu(0) - \frac{\phi(V_F)}{\mu b_E^E}\right].$$

We observe that if the initial state satisfies

$$b_E^E \mu\, M_\mu(0) > \phi(V_F), \tag{2.13}$$

then, denoting $K = M_\mu(0) - \frac{\phi(V_F)}{\mu b_E^E} > 0$,

$$\int_{-\infty}^{V_F} \phi(v)\rho_E(v,t)\, dv = M_\mu(t) \geq K e^{\mu \int_0^t f(s)\, ds}, \quad \forall t \geq 0. \tag{2.14}$$

On the other hand, using again the definition of μ and (2.10), we observe that

$$\mu \int_0^t f(s)\, ds \geq \mu \left[b_E^E \int_0^t N_E(s)\, ds + \left(\mu a_m - V_F - b_I^E M \right) t \right] \geq \mu\, V_F t. \qquad (2.15)$$

Thus, $e^{\mu \int_0^t f(s)\, ds} \geq e^{\mu V_F t}$ and consequently, considering (2.14), we obtain

$$\int_{-\infty}^{V_F} \phi(v)\rho_E(v,t)\, dv = M_\mu(t) \quad \geq \quad K\, e^{\mu V_F t}.$$

On the other hand, since $\rho_E(v,t)$ is a probability density and $\mu > 0$, for all $t \geq 0$: $\int_{-\infty}^{V_F} \phi(v)\rho_E(v,t)\, dv \leq e^{\mu V_F}$, which leads to a contradiction if the weak solution is assumed to be global in time. Therefore, to conclude the proof there only remains to show inequality (2.13) in the two cases of the theorem.

1. For a fixed initial datum and b_E^E large enough, μ, $M_\mu(0)$ and $\phi(V_F)$ are fixed, thus (2.13) holds.

2. For $b_E^E > 0$ fixed, if the initial data satisfy (2.11) then condition (2.13) holds immediately. Now, there only remains to show that such initial data exist.

   For that purpose we can approximate an initial Dirac mass at V_F by smooth probability densities, so that $\rho_E^0 \simeq \delta(v - V_F)$. This gives the following condition

   $$e^{\mu V_F} \geq \frac{e^{\mu V_F}}{b_E^E \mu},$$

   which is satisfied if $\mu > \frac{1}{b_E^E}$. So, with our initial choice of μ we can ensure that the set of initial data we are looking for is not empty. $\square$

Remark 2.2.2 *1. Hypothesis (2.10) could be relaxed by*

$$\int_0^t N_I(s)\, ds \leq M\, t + C \int_0^t N_E(s)\, ds \quad \text{for some} \quad M \geq 0,\ 0 < C < \frac{b_E^E}{b_I^E}. \qquad (2.16)$$

2. Using a priori estimates (as done in Lemma 2.3 in [15]) it could be proved that

$$\int_0^t N_I(s)\, ds \leq M\,(1 + t) + C \int_0^t N_E(s)\, ds, \qquad (2.17)$$

for some $M > 0$, $\frac{b_E^E}{b_I^E} > C$, (where $\frac{b_E^E}{b_I^E} > C > 0$ for b_E^E large enough) which seems not to be enough to reach the whole result. Precisely, it yields the blow-up for fixed initial data and large b_E^E in the case where the drift term is given by (2.3) and the excitatory diffusion term is taken constant, $a_E(N_E, N_I) = a_E$, but does not provide any blow-up result for fixed b_E^E and concentrated initial data.

Proof.

1. In the proof of Theorem 2.2.1 hypothesis (2.10) was used to obtain the bounds (2.12) and (2.15).

Operating in the same way, but using the relaxed hypothesis (2.16) and considering

$$\mu = \max\left(\frac{b_I^E M + 2V_F}{a_m}, \frac{1}{b_E^E - b_I^E C}\right), \tag{2.18}$$

bound (2.12) is transformed into $\frac{-\phi(V_F)}{\mu(b_E^E - b_I^E C)}$, while bound (2.15) remains hardly the same

$$\mu \int_0^t f(s)\ ds \geq \mu\left[(b_E^E - b_I^E C)\int_0^t N_E(s)\ ds + \left(\mu a_m - V_F - b_I^E M\right) t\right] \geq \mu V_F t.$$

As a consequence of the new value for bound (2.12), now the initial state has to satisfy

$$\mu(b_E^E - b_I^E C)M_\mu(0) > \phi(V_F), \tag{2.19}$$

instead of (2.13). The existence of initial data that fullfil (2.19) for the two cases pointed out in Theorem 2.2.1 can be proved in a similar manner. We just have to take into account that for the case of fixed b_E^E, hypothesis (2.11) has to be changed slightly. Specifically, instead of (2.11) we consider

$$\int_{-\infty}^{V_F} e^{\mu v}\rho_E^0(v)\ dv \geq \frac{e^{\mu V_F}}{\mu(b_E^E - b_I^E C)}, \tag{2.20}$$

for $\mu > 0$ defined by (2.18).

2. *Step 1. Computation of bound (2.17).*

Following similar ideas as in Lemma 2.3 in [15], let us choose as test function, $\phi_\epsilon(v)$, a uniform C^2 approximation of the truncation $\frac{(v-V_R)_+}{b_E^E(V_F-V_R)}$. It can be obtained by integrating twice a smooth suitable approximation of $\frac{\delta(v-V_R)}{b_E^E(V_F-V_R)}$. As a consequence, $\phi_\epsilon(v)$ is a smooth C^2 truncation function, for $\epsilon \in (0, \frac{V_F-V_R}{2})$, whose properties are

$$\phi_\epsilon(V_F) = \frac{1}{b_E^E}, \quad \phi_\epsilon(v) = 0\ \text{ for }\ v \leq V_R, \quad \phi_\epsilon' \geq 0, \quad \phi_\epsilon'' \geq 0$$

with $\phi_\epsilon'' = 0$ outside the interval $(V_R, V_R + \epsilon)$ so that

$$\phi_\epsilon'(v) \to \frac{1}{b_E^E(V_F - V_R)}\ \ \forall\ v \in (V_R, V_F]\ \text{ as }\ \epsilon \to 0,$$

and thus $\phi_\epsilon'' \in L^\infty(-\infty, V_F)$.

Then, if we use definition (2.3) for the drift term and take the difussion term constant, (2.7)

gives

$$\frac{d}{dt} \int_{V_R}^{V_F} \phi_\epsilon(v)\rho(v,t) \ dv + N_E(t)\phi_\epsilon(V_F)$$

$$= -\int_{V_R}^{V_F} v\phi'_\epsilon(v)\rho_\epsilon(v,t) \ dv + b_E^E N_E(t) \int_{V_R}^{V_F} \phi'_\epsilon(v)\rho_\epsilon(v,t) \ dv - b_I^E N_I(t) \int_{V_R}^{V_F} \phi'_\epsilon(v)\rho_\epsilon(v,t) \ dv$$

$$+ a_E \int_{V_R}^{V_F} \phi''_\epsilon(v)\rho_E(v,t) \ dv$$

$$\leq \int_{V_R}^{V_F} |v|\phi'_\epsilon(v)\rho_\epsilon(v,t) \ dv + \phi'_\epsilon(V_F)b_E^E N_E(t) - \phi'_\epsilon(V_R)b_I^E N_I(t) + |a_E| \ ||\phi''_\epsilon||$$

$$\leq V_F\phi'_\epsilon(V_F) + \phi'_\epsilon(V_F)b_E^E N_E(t) - \phi'_\epsilon(V_R)b_I^E N_I(t) + |a_E| \ ||\phi''_\epsilon||_{L^\infty(V_R,V_F)}. \quad (2.21)$$

Integrating in time inequality (2.21), yields

$$\phi'_\epsilon(V_R) \ b_I^E \int_0^t N_I(s) \ ds$$

$$\leq \left(\phi'_\epsilon(V_F)b_E^E - \frac{1}{b_E^E}\right) \int_0^t N_E(s) \ ds + \left[V_F\phi'_\epsilon(V_F) + |a_E| \ ||\phi''_\epsilon||_{L^\infty(V_R,V_F)}\right] t$$

$$- \int_{V_R}^{V_F} \phi_\epsilon(v)\rho_E(v,t) \ dv + \int_{V_R}^{V_F} \phi_\epsilon(v)\rho_E(0,t) \ dv$$

$$\leq \left(\phi'_\epsilon(V_F)b_E^E - \frac{1}{b_E^E}\right) \int_0^t N_E(s) \ ds + \left[V_F\phi'_\epsilon(V_F) + |a_E| \ ||\phi''_\epsilon||_{L^\infty(V_R,V_F)}\right] t + \phi_\epsilon(V_F).$$

Which can be rewritten as

$$\int_0^t N_I(s) \ ds$$

$$\leq \left(\frac{\phi'_\epsilon(V_F)b_E^E}{\phi'_\epsilon(V_R)b_I^E} - \frac{1}{\phi'_\epsilon(V_R)b_I^E b_E^E}\right) \int_0^t N_E(s) \ ds + \left[\frac{V_F\phi'_\epsilon(V_F) + |a_E| \ ||\phi''_\epsilon||_{L^\infty(V_R,V_F)}}{\phi'_\epsilon(V_R)b_I^E}\right] t + \frac{\phi_\epsilon(V_F)}{\phi'_\epsilon(V_R)b_I^E}$$

$$\leq \left(\frac{\phi'_\epsilon(V_F)b_E^E}{\phi'_\epsilon(V_R)b_I^E} - \frac{1}{\phi'_\epsilon(V_R)b_I^E b_E^E}\right) \int_0^t N_E(s) \ ds$$

$$+ \max\left\{\frac{V_F\phi'_\epsilon(V_F) + |a_E| \ ||\phi''_\epsilon||_{L^\infty(V_R,V_F)}}{\phi'_\epsilon(V_R)b_I^E}, \frac{\phi_\epsilon(V_F)}{\phi'_\epsilon(V_R)b_I^E}\right\} (1+t).$$

Calling $C := \frac{\phi'_\epsilon(V_F)b_E^E}{\phi'_\epsilon(V_R)b_I^E} - \frac{1}{\phi'_\epsilon(V_R)b_I^E b_E^E}$ and $M := \max\left\{\frac{V_F\phi'_\epsilon(V_F) + |a_E| \ ||\phi''_\epsilon||_{L^\infty(V_R,V_F)}}{\phi'_\epsilon(V_R)b_I^E}, \frac{\phi_\epsilon(V_F)}{\phi'_\epsilon(V_R)b_I^E}\right\}$, and using that due to the definition of $\phi_\epsilon(v)$

$$C \to \frac{b_E^E}{b_I^E} - \frac{V_F - V_R}{b_I^E} \quad \text{as} \quad \epsilon \to 0, \quad (2.22)$$

which implies that for ϵ small enough $C < \frac{b_E^E}{b_I^E}$, and thus we obtain (2.17). Let us remark, that due to (2.22) we have that $0 < C < \frac{b_E^E}{b_I^E}$ for b_E^E large enough.

Step 2. Blow -up result. Considering

$$\mu = \max\left(\frac{b_I^E M + 2V_F}{a_E}, \frac{1}{b_E^E - b_I^E C}\right),$$

the new bound (2.17), which was obtained without using hypothesis (2.10), as shown in *Step 1*, has to be used to obtain bounds (2.12) and (2.15). The first one, operating as in Theorem 2.2.1, is transformed into $\frac{-\phi(V_F)}{\mu(b_E^E - b_I^E C)}$, while bound (2.15), for b_E^E large enough, which is necessary to control the term $-b_I^E M$, now reads

$$\mu \int_0^t f(s) \, ds \geq \mu \left[(b_E^E - b_I^E C) \int_0^t N_E(s) \, ds - b_I^E M + \left(\mu a_m - V_F - b_I^E M\right) t \right] \geq \mu V_F t. \quad (2.23)$$

Again, as a consequence of the new value for bound (2.12), the initial state has to satisfy (2.19). Notice that in the case considered the initial state is fixed, and thus, for b_E^E large enough it is fullfilled.

Finally let us remark that for the case of fixed value for b_E^E and concentrated initial datum this argument does not work, because we are not able to control the negative term $-b_I^E M$ of (2.23). As a consequence it is not possible to obtain the right hand side bound of (2.23), which is necessary to conclude the proof. □

Theorem 2.2.1 shows that blow-up occurs when the connectivity parameter of the excitatory to excitatory synapses, b_E^E, is large enough or if initially there are many excitatory neurons with a voltage value of their membrane potential very close to the threshold value, V_F. From a biological perspective, and in view of the numerical results in Section 2.4.1 (Figs. 2.3, 2.4 and 2.5), in the first case, blow-up appears due to the strong influence of the excitatory population on the behavior of the network, poducing the incontrolled growth of the firing rate at finite time. In the second case, even with small connectivity parameter b_E^E, the abundance of excitatory neurons with membrane potential voltage values sufficiently close to V_F causes the firing rate to diverge in finite time. Notice that, although the numerical results and the criterium for the maximal time of existence presented in [29] (for a one population NNLIF model), suggest that the blow-up is reflected in the system by the divergence of the firing rate, Theorem 2.2.1 only ensures that there are solutions that do not exist for all time. This result is usual for this kind of blow-up theorems, that follow the spirit of the classical Keller-Segel model for chemotaxis [9, 35, 25, 24]. For a microscopic description, at the level of individual neurons, we refer to [38] and [37] where the blow-up phenomenon is also analysed.

As mentioned above it was proved in [17] that fully excitatory networks can blow-up in finite time, when one includes the refractory state. This result can be extended to the case of excitatory-inhibitory networks by following the same ideas of Theorem 2.2.1.

2.3 Steady states and long time behavior

2.3.1 Steady states

For excitatory and inhibitory networks, the study of their steady states follows a similar strategy as the full excitatory or inhibitory cases. However, for coupled networks the system to obtain the

stationary solutions is much more complicated, as we will see in this section.

As in [15], let us search for continuous stationary solutions (ρ_E, ρ_I) of (2.1) such that ρ_E, ρ_I are C^1 regular, except possibly at $V = V_R$ where they are *Lipschitz*, and satisfy the following identity:

$$\frac{\partial}{\partial v}[h^\alpha(v)\rho_\alpha(v) - a_\alpha(N_E, N_I)\frac{\partial \rho_\alpha}{\partial v}(v) - N_\alpha H(v - V_R)] = 0, \quad \alpha = E, I, \qquad (2.24)$$

in the sense of distributions, where H denotes the Heaviside function. Considering $h^\alpha(v, N_E, N_I) = V_0^\alpha(N_E, N_I) - v$, with $V_0^\alpha(N_E, N_I) = b_E^\alpha N_E - b_I^\alpha N_I + (b_E^\alpha - b_E^E)\nu_{E,ext}$, the definition of N_α in (2.5) and the Dirichlet boundary conditions in (2.2), we find the following Initial Value Problem (IVP) for every $\alpha = E, I$

$$\begin{cases} \frac{\partial \rho_\alpha}{\partial v}(v) = \frac{V_0^\alpha(N_E, N_I) - v}{a_\alpha(N_E, N_I)}\rho_\alpha(v) - \frac{N_\alpha H(v - V_R)}{a_\alpha(N_E, N_I)}, \\ \rho_\alpha(V_F) = 0, \end{cases}$$

which can be solved using the variation of constants technique for ODEs, giving rise to solutions of the form

$$\rho_\alpha(v) = \frac{N_\alpha}{a_\alpha(N_E, N_I)}e^{-\frac{(v - V_0^\alpha(N_E, N_I))^2}{2a_\alpha(N_E, N_I)}}\int_{\max(v, V_R)}^{V_F} e^{\frac{(w - V_0^\alpha(N_E, N_I))^2}{2a_\alpha(N_E, N_I)}}dw, \quad \alpha = E, I. \qquad (2.25)$$

Expression (2.25) is not an explicit formula for ρ_α, since the right hand side depends on N_α, but it provides a system of implicit equations for N_α

$$\frac{a_\alpha(N_E, N_I)}{N_\alpha} = \int_{-\infty}^{V_F} e^{-\frac{(v - V_0^\alpha(N_E, N_I))^2}{2a_\alpha(N_E, N_I)}}\left[\int_{\max(v, V_R)}^{V_F} e^{\frac{(w - V_0^\alpha(N_E, N_I))^2}{2a_\alpha(N_E, N_I)}}dw\right]dv, \qquad \alpha = E, I. \qquad (2.26)$$

for which the conservation of mass ($\int_{-\infty}^{V_F} \rho_\alpha(v, t)dv = 1$) has been used. Therefore, the stationary solutions (ρ_E, ρ_I) have the profile (2.75), where (N_E, N_I) are positive solutions of the implicit system (2.26). And there are as many as solutions of the system (2.26). Of course, in the particular case of a linear system, that is $V_0^\alpha(N_E, N_I)) = 0$ and $a_\alpha(N_E, N_I)$ independent of the firing rates, there is a unique steady state.

Determining the number of solutions of the implicit system (2.26) is a difficult task. In this section we find some conditions on the parameters of the model in order to reach this goal. Firstly, we consider the following change of variables and notation:

$$z = \frac{v - V_0^E(N_E, N_I)}{\sqrt{a_E(N_E, N_I)}}, \ u = \frac{w - V_0^E(N_E, N_I)}{\sqrt{a_E(N_E, N_I)}}, \ w_F := \frac{V_F - V_0^E(N_E, N_I)}{\sqrt{a_E(N_E, N_I)}}, \ w_R := \frac{V_R - V_0^E(N_E, N_I)}{\sqrt{a_E(N_E, N_I)}},$$

$$\tilde{z} = \frac{v - V_0^I(N_E, N_I)}{\sqrt{a_I(N_E, N_I)}}, \ \tilde{u} = \frac{w - V_0^I(N_E, N_I)}{\sqrt{a_I(N_E, N_I)}}, \ \tilde{w}_F := \frac{V_F - V_0^I(N_E, N_I)}{\sqrt{a_I(N_E, N_I)}}, \ \tilde{w}_R := \frac{V_R - V_0^I(N_E, N_I)}{\sqrt{a_I(N_E, N_I)}}.$$

With these new variables, the system (2.26) is rewritten as

$$\begin{aligned} \frac{1}{N_E} &= I_1(N_E, N_I), \ \text{where } I_1(N_E, N_I) = \int_{-\infty}^{w_F} e^{-\frac{z^2}{2}}\int_{\max(z, w_R)}^{w_F} e^{\frac{u^2}{2}}du \ dz, \\ \frac{1}{N_I} &= I_2(N_E, N_I), \ \text{where } I_2(N_E, N_I) = \int_{-\infty}^{\tilde{w}_F} e^{-\frac{\tilde{z}^2}{2}}\int_{\max(\tilde{z}, \tilde{w}_R)}^{\tilde{w}_F} e^{\frac{\tilde{u}^2}{2}}d\tilde{u} \ d\tilde{z}. \end{aligned} \qquad (2.27)$$

Now, using $s = \frac{z-u}{2}$ and $\tilde{s} = \frac{z+u}{2}$, the functions I_1 and I_2 can be formulated as

$$
\begin{aligned}
I_1(N_E, N_I) &= \int_0^\infty \frac{e^{-\frac{s^2}{2}}}{s}(e^{s\,w_F} - e^{s\,w_R})\,ds, \\
I_2(N_E, N_I) &= \int_0^\infty \frac{e^{-\frac{s^2}{2}}}{s}(e^{s\,\tilde{w}_F} - e^{s\,\tilde{w}_R})\,ds.
\end{aligned}
$$

When $b_I^E = b_E^I = 0$ the equations are uncoupled and the number of steady states can be determined in the same way as in [15], depending on the values of b_E^E, since for the inhibitory equation there is always a unique steady state. The following theorem establishes a classification of the number of steady states in terms of the model parameters, in the case that the connectivity parameters b_I^E and b_E^I do not vanish, and in comparison with the values of the purely connectivity parameters b_E^E and b_I^I.

Theorem 2.3.1 *Assume that the connectivity parameters b_I^E and b_E^I do not vanish (b_I^E, $b_E^I > 0$), a_α is independent of N_E and N_I, $a_\alpha(N_E, N_I) = a_\alpha$, and $h^\alpha(v, N_E, N_I) = V_0^\alpha(N_E, N_I) - v$ with $V_0^\alpha(N_E, N_I) = b_E^\alpha N_E - b_I^\alpha N_I + (b_E^\alpha - b_E^E)v_{E,ext}$ for all $\alpha = E, I$. Then:*

1. *There is an even number of steady states or no steady state for (2.1)-(2.5) if:*

$$
(V_F - V_R)^2 < (V_F - V_R)(b_E^E - b_I^I) + b_E^E b_I^I - b_I^E b_E^I. \tag{2.28}
$$

   If b_E^E is large enough in comparison with the rest of connectivity parameters, there are no steady states. Specifically, there are no steady states if both (2.28) and

$$
max\left\{ I_1(0)2(V_F + b_I^E N_I(\bar{N}_E)), \frac{b_E^I b_I^E}{b_I^I}, 2(V_F - V_R) \right\} < b_E^E \tag{2.29}
$$

   are fulfilled, where

$$
\bar{N}_E = max\left\{ N_E^* \geq 0 : N_E^* = \frac{2(b_E^I N_I(N_E^*) + V_F)}{b_E^E} \right\}. \tag{2.30}
$$

2. *There is an odd number of steady states for (2.1)-(2.5) if:*

$$
(V_F - V_R)^2 > (V_F - V_R)(b_E^E - b_I^I) + b_E^E b_I^I - b_I^E b_E^I. \tag{2.31}
$$

   If b_E^E is small enough in comparison with the rest of connectivity parameters, there is a unique steady state.

Proof. The proof reduces to study the existence of solutions to (2.27) and it is organized in several steps.

Step 1. To prove that $\frac{1}{N_I} = I_2(N_E, N_I)$ admits a unique solution $N_I(N_E)$ for N_E fixed.

Given $N_E \in [0, \infty)$ and following analogous ideas as in [15], it is easy to observe that there is a unique solution N_I to

$$
\frac{1}{N_I} = I_2(N_E, N_I). \tag{2.32}
$$

This fact is a consequence of the following properties of I_2:

1. $I_2(N_E, N_I)$ is C^∞ on both variables.

2. For every N_E fixed, $I_2(N_E, N_I)$ is an increasing strictly convex function on N_I, since for all integers $k \geq 1$

$$\frac{\partial^k I_2}{\partial N_I^k} = \left(\frac{b_I^I}{\sqrt{a_I}}\right)^k \int_0^\infty e^{-\frac{s^2}{2}} s^{k-1} (e^{s\tilde{w}_F} - e^{s\tilde{w}_R}) \, ds. \tag{2.33}$$

Thus, $\lim\limits_{N_I \to \infty} I_2(N_E, N_I) = \infty$ for every N_E fixed.

3. If we consider $N_I \in [0, \infty)$, $I_2(N_E, N_I)$ is a decreasing convex function on N_E, since for all integers $k \geq 1$

$$\frac{\partial^k I_2}{\partial N_E^k} = (-1)^k \left(\frac{b_E^I}{\sqrt{a_I}}\right)^k \int_0^\infty e^{-\frac{s^2}{2}} s^{k-1} (e^{s\tilde{w}_F} - e^{s\tilde{w}_R}) \, ds. \tag{2.34}$$

Thus, $\lim\limits_{N_E \to \infty} I_2(N_E, N_I) = 0$, for every N_I fixed.

4. Using expression (2.27) for I_2, for every N_E fixed, $I_2(N_E, 0) < \infty$, since

$$I_2(N_E, 0) = \int_{-\infty}^{\tilde{w}_F(0)} e^{-\frac{\tilde{z}^2}{2}} \int_{\max(\tilde{z}, \tilde{w}_R(0))}^{\tilde{w}_F(0)} e^{\frac{\tilde{u}^2}{2}} \, d\tilde{u} \, d\tilde{z} \leq \sqrt{2\pi} \left(\frac{V_F - V_R}{\sqrt{a_I}}\right) e^{\frac{m}{2a_I}},$$

where $m = \max\{(V_F - b_E^I N_E - (b_E^I - b_E^E)v_{E,ext})^2, (V_R - b_E^I N_E - (b_E^I - b_E^E)v_{E,ext})^2\}$.

Figure 2.1 depicts the function I_2 in terms of N_I, for different values of N_E fixed. In this figure, the properties of I_2 enumerated above can be observed.
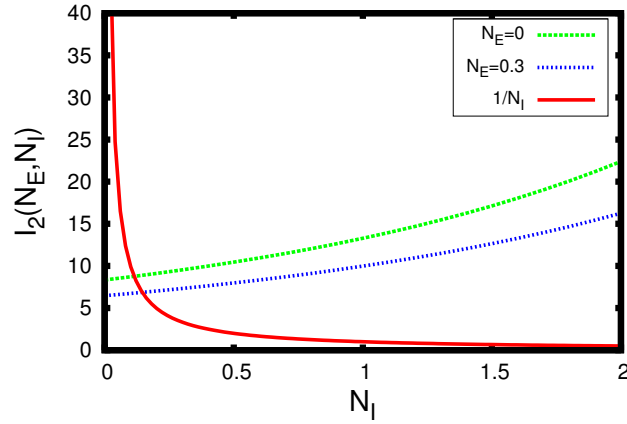
Figure 2.1: The function I_2 in terms of N_I, for different values of N_E fixed. I_2 is an increasing function on N_I and decreasing on N_E.

Step 2. Properties of $N_I(N_E)$.

Obtaining an analytical expression of $N_I(N_E)$ is not easy, however some properties of $N_I(N_E)$ are enough to prove the theorem:

1. $N_I(N_E) > 0$, $\forall N_E \in [0, \infty)$.

2. $N_I(N_E)$ is an increasing function, $\forall\ N_E \in [0, \infty)$, since

$$N_I'(N_E) = \frac{-N_I^2(N_E)\frac{\partial I_2}{\partial N_E}(N_E, N_I(N_E))}{1 + N_I^2(N_E)\frac{\partial I_2}{\partial N_I}(N_E, N_I(N_E))} \tag{2.35}$$

is nonnegative. Expression (2.35) is obtained by differentiating $N_I(N_E)I_2(N_E, N_I(N_E)) = 1$ with respect to N_E.

3. $\lim\limits_{N_E \to \infty} N_I(N_E) = \infty$, because $N_I(N_E)$ is a positive increasing function, thus its limit could be infinite or a constant $C > 0$. The finite limit leads to a contradiction since $\frac{1}{N_I(N_E)} = I_2(N_E, N_I(N_E))$ and then, $\lim\limits_{N_E \to \infty} \frac{1}{N_I(N_E)} = \frac{1}{C}$, while $\lim\limits_{N_E \to \infty} I_2(N_E, N_I(N_E)) = 0$ because $\lim\limits_{N_E \to \infty} I_2(N_E, C) = 0$.

4. $0 < N_I'(N_E) < \frac{b_E^I}{b_I^I}$. It is a consequence of the fact that

$$N_I'(N_E) = \frac{b_E^I N_I^2(N_E)I(N_E)}{\sqrt{a_I} + b_I^I N_I^2(N_E)I(N_E)}, \tag{2.36}$$

where $I(N_E) = \int_0^\infty e^{-s^2/2} e^{\frac{-(b_E^I N_E - b_I^I N_I(N_E) + (b_E^I - b_E^E)\nu_{E,ext})s}{\sqrt{a_I}}} \left(e^{sV_F/\sqrt{a_I}} - e^{sV_R/\sqrt{a_I}} \right)\ ds$.

Expression (2.36) is obtained using (2.33), (2.34), (2.35) and the definition of $\tilde{w}_F$ and $\tilde{w}_R$.

5. $\lim\limits_{N_E \to \infty} N_I'(N_E) = \frac{b_E^I L}{\sqrt{a_I} + b_I^I L}$, where $\lim\limits_{N_E \to \infty} N_I^2(N_E)I(N_E) = L$.

6. $L = \frac{\sqrt{a_I}}{V_F - V_R}$. The computation of this limit consists of some easy but tedious calculation. For the sake of simplicity, the proof is divided in several steps.

   Step 1. Limit of $N_I'(N_E)$.

   Applying L'Hôpital's rule
   $$\lim\limits_{N_E \to \infty} \frac{N_I(N_E)}{N_E} = \lim\limits_{N_E \to \infty} N_I'(N_E). \tag{2.37}$$

   Let us denote
   $$\bar{N}_I' := \lim\limits_{N_E \to \infty} N_I'(N_E). \tag{2.38}$$

   Step 2. Rewritting the limit of $N_I^2(N_E)I(N_E)$.

   Combining (2.37) and (2.38) it can be derived that
   $$\lim\limits_{N_E \to \infty} \frac{N_I(N_E)}{N_E} = \bar{N}_I'.$$

   In particular, we are allowed to write
   $$\lim\limits_{N_E \to \infty} N_I^2(N_E)I(N_E) = \bar{N}_I'^2 \lim\limits_{N_E \to \infty} N_E^2 I(N_E). \tag{2.39}$$

76

Step 3. Rewritting the limit of $I(N_E)$.

In this step the limit $I(N_E)$ is rewritten in order to simplify the calculation of the limit (2.39). Let us remember that $I(N_E)$ is defined as

$$I(N_E) = \int_0^\infty e^{-\frac{s^2}{2}} e^{-\frac{b_E^I N_E - b_I^I N_I(N_E) + (b_E^I - b_E^E)v_{E,ext}}{\sqrt{a_I}} s} \left(e^{\frac{sV_F}{\sqrt{a_I}}} - e^{\frac{sV_R}{\sqrt{a_I}}} \right) ds.$$

Denoting $\bar{v} = (b_E^I - b_E^E)v_{E,ext}$ we get that

$$I(N_E) = \int_0^\infty e^{-\frac{s^2}{2}} e^{-\frac{b_E^I N_E - b_I^I N_I(N_E) + \bar{v}}{\sqrt{a_I}} s} \left(e^{\frac{sV_F}{\sqrt{a_I}}} - e^{\frac{sV_R}{\sqrt{a_I}}} \right) ds.$$

Using that $\lim_{N_E \to \infty} N_I(N_E) = \lim_{N_E \to \infty} \bar{N}_I' N_E$, and defining $b = \frac{b_E^I - b_I^I \bar{N}_I'}{\sqrt{a_I}} \geq 0$ (the positivity of b is due to the fact that $0 < N_I'(N_E) < \frac{b_E^I}{b_I^I}$, obtained in point 4 of *Step 2* of the proof of Theorem 2.3.1) and $K = -\frac{\bar{v}}{\sqrt{a_I}}$ yields

$$\lim_{N_E \to \infty} \frac{b_E^I N_E - b_I^I N_I(N_E) + \bar{v}}{\sqrt{a_I}} = \lim_{N_E \to \infty} \frac{N_E(b_E^I - b_I^I \bar{N}_I') + \bar{v}}{\sqrt{a_I}} = \lim_{N_E \to \infty} bN_E - K.$$

Thus

$$\lim_{N_E \to \infty} I(N_E) = \lim_{N_E \to \infty} \int_0^\infty e^{-\frac{s^2}{2}} e^{-(bN_E - K)s} \left(e^{\frac{sV_F}{\sqrt{a_I}}} - e^{\frac{sV_R}{\sqrt{a_I}}} \right) ds.$$

Making a Taylor expansion centered on 0 over the function $f(s) := e^{\frac{sV_F}{\sqrt{a_I}}} - e^{\frac{sV_R}{\sqrt{a_I}}}$ produces

$$\lim_{N_E \to \infty} I(N_E)$$
$$= \frac{V_F - V_R}{\sqrt{a_I}} \lim_{N_E \to \infty} \int_0^\infty e^{-\frac{s^2}{2}} e^{-(bN_E - K)s} s \, ds + \sum_{i=2}^\infty \frac{V_F^i - V_R^i}{\sqrt{a_I}^i i!} \lim_{N_E \to \infty} \int_0^\infty e^{-\frac{s^2}{2}} e^{-(bN_E - K)s} s^i \, ds,$$
$$=: A + B.$$

The change of variables $y = \frac{s}{\sqrt{2}} + \frac{bN_E - K}{\sqrt{2}}$ and i-times L'Hôpital's rule yields

$$\lim_{N_E \to \infty} N_E^2 \lim_{N_E \to \infty} \int_0^\infty e^{-\frac{s^2}{2}} e^{-(bN_E - K)s} s^i \, ds$$
$$= \lim_{N_E \to \infty} N_E^2 e^{\frac{(bN_E - K)^2}{2}} \int_0^\infty e^{-(\frac{s}{\sqrt{2}} + \frac{bN_E - K}{\sqrt{2}})^2} s^i \, ds$$
$$= \sqrt{2} \lim_{N_E \to \infty} \frac{\int_{\frac{bN_E - K}{\sqrt{2}}}^\infty e^{-y^2} (\sqrt{2}y - (bN_E - K))^i \, dy}{\frac{1}{N_E^2} e^{-\frac{(bN_E - K)^2}{2}}}$$
$$= b^i i! \sqrt{2} \lim_{N_E \to \infty} \frac{\frac{b}{\sqrt{2}} e^{-\frac{(bN_E - K)^2}{2}}}{e^{-\frac{(bN_E - K)^2}{2}} b^{i+3} (bN_E - K)^{i-1}} = 0.$$

Thus, $\lim\limits_{N_E \to \infty} B = 0$ and we finally get that

$$\lim_{N_E \to \infty} I(N_E) = \frac{V_F - V_R}{\sqrt{a_I}} \lim_{N_E \to \infty} \int_0^\infty e^{-\frac{s^2}{2}} e^{-(bN_E - K)s} s \; ds. \tag{2.40}$$

Step 4. Computation of the limit of $N_I^2(N_E)I(N_E)$.

In this step the limit $\lim\limits_{N_E \to \infty} N_I^2(N_E)I(N_E)$ is calculated. Thanks to (2.39) and (2.40)

$$\lim_{N_E \to \infty} N_I^2(N_E)I(N_E) = \frac{\bar{N}_I'(V_F - V_r)}{\sqrt{a_I}} \lim_{N_E \to \infty} N_E^2 \int_0^\infty e^{-\frac{s^2}{2} + (bN_E - K)s} s \; ds. \tag{2.41}$$

Now, the computation of the limit is reduced to determine the value of

$$
\begin{aligned}
&\lim_{N_E \to \infty} N_E^2 \int_0^\infty e^{-\frac{s^2}{2} + (bN_E - K)s} s \; ds \\
&= \lim_{N_E \to \infty} N_E^2 e^{\frac{(bN_E - K)^2}{2}} \int_0^\infty e^{-\left(\frac{s}{\sqrt{2}} + \frac{bN_E - K}{\sqrt{2}}\right)^2} s \; ds \\
&= \sqrt{2} \lim_{N_E \to \infty} \frac{\int_{\frac{bN_E - K}{\sqrt{2}}}^\infty e^{-y^2}(\sqrt{2}y - (bN_E - K)) \; dy}{\frac{1}{N_E^2} e^{-\frac{(bN_E - K)^2}{2}}} \\
&= \sqrt{2}b \lim_{N_E \to \infty} \frac{\int_{\frac{bN_E - K}{\sqrt{2}}}^\infty e^{-y^2} \; dy}{e^{-\frac{(bN_E - K)^2}{2}} \left(\frac{b^2}{N_E} - \frac{Kb}{N_E^2} + \frac{2}{N_E^3}\right)} \\
&= \sqrt{2}b \lim_{N_E \to \infty} \frac{\frac{b}{\sqrt{2}} e^{-\frac{(bN_E - K)^2}{2}}}{e^{-\frac{(bN_E - K)^2}{2}} \left[b(bN_E - K)\left(\frac{b^2}{N_E} - \frac{Kb}{N_E^2} - \frac{2}{N_E^3}\right) - \left(-\frac{b^2}{N_E^2} + \frac{2Kb}{N_E^3} - \frac{6}{N_E^4}\right)\right]} \\
&= \frac{1}{b^2}
\end{aligned}
\tag{2.42}
$$

where a change of variables, differentiation of integrals with respect to parameters and L'Hôpital's rule were used. Joining (2.41) with (2.42) we get

$$\lim_{N_E \to \infty} N_I^2(N_E)I(N_E) = \frac{\sqrt{a_I}(V_F - V_R)\bar{N}_I'}{(b_E^I - b_I^I \bar{N}_I')^2} =: L. \tag{2.43}$$

Step 5. Calculation of the exact values of $\bar{N}_I'$ and L.

Once the value of $\bar{N}_I'$ is obtained, the proof is concluded. Let us remind that

$$N_I'(N_E) = \frac{b_E^I N_I^2(N_E)I(N_E)}{\sqrt{a_I} + b_I^I N_I^2(N_E)I(N_E)},$$

thus

$$\bar{N}_I' = \lim_{N_E \to \infty} N_I'(N_E) = \lim_{N_E \to \infty} \frac{b_E^I N_I^2(N_E)I(N_E)}{\sqrt{a_I} + b_I^I N_I^2(N_E)I(N_E)} = \frac{b_E^I L}{\sqrt{a_I} + b_I^I L}.$$

In consequence

$$L = \frac{\bar{N}_I' \sqrt{a_I}}{b_E^I - \bar{N}_I' b_I^I}. \tag{2.44}$$

So, L is defined by (2.43) and (2.44). If we equate both expressions and suppose that $\bar{N}_I' \neq 0$ we get that

$$\bar{N}_I' = \frac{b_E^I}{V_F - V_R + b_I^I},$$

and thus

$$\lim_{N_E \to \infty} N_I^2(N_E) I(N_E) = \frac{\sqrt{a_I}}{V_F - V_R}.$$

7. As a consequence of the two previous properties, $\displaystyle\lim_{N_E \to \infty} N_I'(N_E) = \frac{b_E^I}{V_F - V_R + b_I^I}$.

The limit of $N_I'(N_E)$ ensures that the rate of increase for $N_I(N_E)$ (in point 3 of Step 2 it was proved that $N_I(N_E)$ tends to infinity) is constant at infinity, and can be controlled in terms of the parameters b_E^I, b_I^I, V_R and V_F.

Step 3. Properties of the function $\mathcal{F}(N_E) = N_E I_1(N_E, N_I(N_E))$.

For every fixed $N_E \in [0, \infty)$, it is obtained $N_I(N_E)$, the unique solution to (2.32) (cf. *Step 1*). To conclude the proof of the theorem there remains to determine the number of solutions to

$$N_E I_1(N_E, N_I(N_E)) = 1. \tag{2.45}$$

With this aim we define $\mathcal{F}(N_E) = N_E I_1(N_E, N_I(N_E))$. Depending on the properties of $\mathcal{F}$ we can find a different number of solutions to (2.45). First, following analogous ideas as in [15], let us show some properties of I_1:

1. $I_1(N_E, N_I)$ is C^∞ in both variables.

2. For every $N_E \in [0, \infty)$ fixed, $I_1(N_E, N_I)$ is an increasing strictly convex function on N_I, since for all integers $k \geq 1$

$$\frac{\partial^k I_1}{\partial N_I^k} = \left(\frac{b_E^I}{\sqrt{a_E}} \right)^k \int_0^\infty e^{-\frac{s^2}{2}} s^{k-1} (e^{s w_F} - e^{s w_R}) \, ds.$$

Thus, $\displaystyle\lim_{N_I \to \infty} I_1(N_E, N_I) = \infty$, for every $N_E \in [0, \infty)$ fixed.

3. For every $N_I \in [0, \infty)$ fixed, $I_1(N_E, N_I)$ is a decreasing convex function on N_E, since for all integers $k \geq 1$

$$\frac{\partial^k I_1}{\partial N_E^k} = (-1)^k \left(\frac{b_E^E}{\sqrt{a_E}} \right)^k \int_0^\infty e^{-\frac{s^2}{2}} s^{k-1} (e^{s w_F} - e^{s w_R}) \, ds.$$

Thus, $\displaystyle\lim_{N_E \to \infty} I_1(N_E, N_I) = 0$, for every $N_I \in [0, \infty)$ fixed.

4. $I_1(N_E) := I_1(N_E, N_I(N_E))$, has the following properties of monotonicity:

   4.1. If $b_E^I b_I^E < b_E^E b_I^I$ then $I_1(N_E)$ is a decreasing function with $\displaystyle\lim_{N_E \to \infty} I_1(N_E) = 0$.

4.2. If $b_E^I b_I^E > b_E^E b_I^I$

    4.2.1. and $\frac{b_E^I}{V_F - V_R + b_I^I} < \frac{b_E^E}{b_I^E}$, then $I_1(N_E)$ decreases for N_E large enough and $\lim\limits_{N_E \to \infty} I_1(N_E) = 0$.

    4.2.2. and $\frac{b_E^I}{V_F - V_R + b_I^I} > \frac{b_E^E}{b_I^E}$ then $I_1(N_E)$ increases for N_E large enough and $\lim\limits_{N_E \to \infty} I_1(N_E) = \infty$.

        If b_E^E is small enough, such that $b_E^E < b_I^E N_I'(N_E)$ for all $N_E \geq 0$, $I_1(N_E)$ is an increasing function and $\lim\limits_{N_E \to \infty} I_1(N_E) = \infty$.

These properties are proved using that

$$\frac{d}{dN_E} I_1(N_E, N_I(N_E)) = \left(\frac{-b_E^E}{\sqrt{a_E}} + \frac{b_I^E}{\sqrt{a_E}} N_I'(N_E) \right) \int_0^\infty e^{\frac{-s^2}{2}} (e^{sw_F} - e^{sw_R}) ds.$$

Therefore, we have that $I_1(N_E)$ decreases iff $N_I'(N_E) < \frac{b_E^E}{b_I^E}$. Consequently it increases iff $N_I'(N_E) > \frac{b_E^E}{b_I^E}$. Now, using properties 4. and 7. of $N_I(N_E)$ and properties 2. and 3. of I_1 the monotonicity properties of $I_1(N_E)$ are immediate.

Taking into account the previous points, the following properties of $\mathcal{F}$ are obtained:

1. $\mathcal{F}(0) = 0$.

2. Monotonicity.

    2.1. If $b_E^I b_I^E < b_E^E b_I^I$ or if $b_E^I b_I^E > b_E^E b_I^I$ and $\frac{b_E^I}{V_F - V_R + b_I^I} < \frac{b_E^E}{b_I^E}$ then, for N_E large enough, $\mathcal{F}$ is a decreasing function until the limit.

    2.2. If $b_E^I b_I^E > b_E^E b_I^I$ and $\frac{b_E^I}{V_F - V_R + b_I^I} > \frac{b_E^E}{b_I^E}$ then, for N_E large enough, $\mathcal{F}$ is an increasing function. Note that if b_E^E is small enough so that $b_E^E < b_I^E N_I'(N_E)$ for all $N_E \geq 0$, then $\mathcal{F}$ is an increasing function for all $N_E \geq 0$.

    2.3. Close to $N_E = 0$, $\mathcal{F}$ is an increasing function.

The monotonicity of $\mathcal{F}$ is given by the sign of its derivative

$$\mathcal{F}'(N_E) = I_1(N_E) + N_E \left[-\frac{b_E^E}{\sqrt{a_E}} + \frac{b_I^E}{\sqrt{a_E}} N_I'(N_E) \right] \int_0^\infty e^{\frac{-s^2}{2}} (e^{sw_F} - e^{sw_R}) \, ds.$$

If we define

$$A(N_E) := \frac{I_1(N_E)}{\int_0^\infty e^{\frac{-s^2}{2}} (e^{sw_F} - e^{sw_R}) \, ds}$$

and

$$B(N_E) := -N_E \left[\frac{-b_E^E}{\sqrt{a_E}} + N_I'(N_E) \frac{b_I^E}{\sqrt{a_E}} \right],$$

it is easy to conclude that

$$\mathcal{F}'(N_E) < 0 \quad \text{iif} \quad A(N_E) < B(N_E)$$

and

$$\mathcal{F}'(N_E) > 0 \quad \text{iif} \quad A(N_E) > B(N_E).$$

We observe that

$$\lim_{N_E \to \infty} \mathcal{F}'(N_E) = \lim_{N_E \to \infty} \left(I_1(N_E) + k\, N_E \int_0^\infty e^{\frac{-s^2}{2}} (e^{sw_F} - e^{sw_R}) ds \right),$$

where $k = \frac{(b_E^I b_I^E - b_E^E b_I^I) - b_E^E (V_F - V_R)}{\sqrt{a_E}(b_I^I + V_F - V_R)}$. So the monotonicity properties of $\mathcal{F}$ can be proven as follows.

2.1. If $b_E^I b_I^E < b_E^E b_I^I$ or if $b_E^I b_I^E > b_E^E b_I^I$ and $\frac{b_E^I}{V_F - V_R + b_I^I} < \frac{b_E^E}{b_I^E}$ then $\lim_{N_E \to \infty} \mathcal{F}'(N_E) = 0_-$.

2.2. If $b_E^I b_I^E > b_E^E b_I^I$ and $\frac{b_E^I}{V_F - V_R + b_I^I} > \frac{b_E^E}{b_I^E}$ then $\lim_{N_E \to \infty} \mathcal{F}'(N_E) = \infty$. Note that for this case $\mathcal{F}'(N_E) > 0$ for all $N_E \geq 0$. Thus $\mathcal{F}$ increases for all $N_E \geq 0$ for small enough values of b_E^E.

2.3. Since $\mathcal{F}(0) = 0$ and $\mathcal{F}(N_E) > 0$, $\mathcal{F}$ increases close to 0.

3. Limit of $\mathcal{F}$.

3.1. If $b_E^I b_I^E < b_E^E b_I^I$ or if $b_E^I b_I^E > b_E^E b_I^I$ and $\frac{b_E^I}{V_F - V_R + b_I^I} < \frac{b_E^E}{b_I^E}$ then

$$\lim_{N_E \to \infty} \mathcal{F}(N_E) = \frac{(V_F - V_R)(V_F - V_R + b_I^I)}{b_E^E(V_F - V_R) + b_E^E b_I^I - b_I^E b_E^I}.$$

This limit is calculated using the limit of $N_I'(N_E)$ and proceeding in a similar way than in [15]. Using Taylor series, there it was proved that

$$\left| \frac{e^{\frac{sV_F}{\sqrt{a_E}}} - e^{\frac{sV_F}{\sqrt{a_E}}}}{s} - \frac{V_F - V_R}{\sqrt{a_E}} \right| \leq \frac{\max(V_F^2, V_R^2)}{2a_E} se^{\frac{s\max(|V_F|, |V_R|)}{\sqrt{a_E}}} := C_0 se^{\frac{s\max(|V_F|, |V_R|)}{\sqrt{a_E}}}. \quad (2.46)$$

Applying (2.46) we obtain

$$\left| \mathcal{F}(N_E) - N_E \frac{V_F - V_R}{\sqrt{a_E}} \int_0^\infty e^{-\frac{s^2}{2}} e^{-\frac{sV_0^E(N_E, N_I(N_E))}{\sqrt{a_E}}} ds \right|$$

$$= \left| N_E \int_0^\infty \left(\frac{e^{\frac{sV_F}{\sqrt{a_E}}} - e^{\frac{sV_R}{\sqrt{a_E}}}}{s} - \frac{V_F - V_R}{\sqrt{a_E}} \right) e^{-\frac{s^2}{2}} e^{-\frac{sV_0^E(N_E, N_I(N_E))}{\sqrt{a_E}}} ds \right| \quad (2.47)$$

$$\leq C_0 N_E \int_0^\infty se^{-\frac{s^2}{2}} e^{-\frac{sV_0^E(N_E, N_I(N_E))}{\sqrt{a_E}}} e^{\frac{s\max(|V_F|, |V_R|)}{\sqrt{a_E}}} ds.$$

Using the dominated convergence theorem, the last expression of (2.47) converges to 0 as N_E tends to ∞ if

$$\lim_{N_E \to \infty} V_0^E(N_E, N_I(N_E)) = \lim_{N_E \to \infty} b_E^E N_E - b_I^E N_I(N_E) = +\infty. \quad (2.48)$$

As the limit of $N'_I(N_E)$ is known (see point 7 of *Step 2*),

$$\lim_{N_E \to \infty} \frac{b_I^E N_I(N_E)}{b_E^E N_E} = \lim_{N_E \to \infty} \frac{b_I^E N'_I(N_E)}{b_E^E} = \frac{b_I^E b_E^I}{b_E^E(V_F - V_R) + b_I^I b_E^E}.$$

Thus, (2.48) is satisfied if $b_I^E b_E^I < b_I^I b_E^E + b_E^E(V_F - V_R)$. In particular, this implies that the limit of $\mathcal{F}$ can be obtained via (2.47) if $b_E^I b_I^E < b_E^E b_I^I$ or if $b_E^I b_I^E > b_E^E b_I^I$ and $\frac{b_E^I}{V_F - V_R b + b_I^I} < \frac{b_E^E}{b_I^E}$. It only remains to compute the value of the limit

$$\frac{V_F - V_R}{\sqrt{a_E}} \lim_{N_E \to \infty} N_E \int_0^\infty e^{-\frac{s^2}{2}} e^{-\frac{s V_0^E(N_E, N_I(N_E))}{\sqrt{a_E}}} \, ds.$$

Using the complementary error function defined by

$$\mathrm{erfc}(x) := \frac{2}{\sqrt{\pi}} \int_x^\infty e^{-t^2} \, dt,$$

L'Hôpital's rule and the limit of $N'_I(N_E)$, finally yield

$$\frac{V_F - V_R}{\sqrt{a_E}} \lim_{N_E \to \infty} N_E \int_0^\infty e^{-\frac{s^2}{2}} e^{-\frac{s V_0^E(N_E, N_I(N_E))}{\sqrt{a_E}}} \, ds$$

$$= \frac{V_F - V_R}{\sqrt{a_E}} \frac{\sqrt{\pi}}{\sqrt{2}} \lim_{N_E \to \infty} \frac{\mathrm{erfc}\left(\frac{V_0^E(N_E, N_I(N_E))}{\sqrt{2a_E}}\right)}{\frac{e^{-\frac{V_0^E(N_E, N_I(N_E))}{\sqrt{2a_E}}}}{N_E}}$$

$$= \frac{V_F - V_R}{\sqrt{a_E}} \lim_{N_E \to \infty} \frac{\frac{1}{\sqrt{a_E}}(b_E^E - b_I^E N'_I(N_E))}{\frac{1}{a_E}(b_E^E - b_I^E N'_I(N_E))(b_E^E - b_I^E \frac{N_I(N_E)}{N_E}) - \frac{1}{N_E^2}}$$

$$= \frac{V_F - V_R}{\sqrt{a_E}} \frac{\sqrt{a_E}(\sqrt{a_I} + b_I^I)}{b_E^E(\sqrt{a_I} + b_I^I) - b_I^E b_E^I}.$$

3.2. If $b_E^I b_I^E > b_E^E b_I^I$ and $\frac{b_E^I}{V_F - V_R + b_I^I} > \frac{b_E^E}{b_I^E}$ then, $\lim_{N_E \to \infty} \mathcal{F}(N_E) = \infty$.

For this case $\mathcal{F}$ on its limit is a product of increasing functions with limit ∞.

Step 4. The proof of the theorem is a consequence of the previous steps.

The monotonicity of $\mathcal{F}$ and its limit, calculated in step 3, provide the number of steady states in terms of (2.28) and (2.31), since these conditions give the range of the parameter values for which the limit of $\mathcal{F}$ can be compared to 1.

Under assumptions (2.28) and (2.29), there are no steady states. The reason is that for these values of b_E^E the function $I_1(N_E)$ decreases, as $b_E^I b_I^E < b_E^E b_I^I$ (see property 4.1 of $I_1(N_E)$). Thus,

$$I_1(N_E) < I_1(0) < \frac{b_E^E}{2(V_F + b_I^E N_I(\bar{N}_E))} = \frac{1}{\bar{N}_E} < \frac{1}{N_E} \quad \forall \, N_E < \bar{N}_E.$$

On the other hand, in an analogous way as in [15][Therem 3.1(iv)], we can prove

$$I_1(N_E) < \frac{V_F - V_R}{b_E^E N_E - V_F - b_I^E N_I(N_E)} < \frac{1}{N_E} \qquad \forall \ N_E \geq \bar{N}_E,$$

if

$$w_F < 0 \quad \text{and} \quad \frac{V_F - V_R}{b_E^E N_E - V_F - b_I^E N_I(N_E)} < \frac{1}{N_E} \quad \text{for all} \quad N_E \geq \bar{N}_E. \qquad (2.49)$$

Therefore, to conclude this part of the proof we show (2.49). Defining $g(N_E) := \frac{2[V_F + b_I^E N_I(N_E)]}{N_E}$, since $b_E^E > \lim_{N_E \to \infty} g(N_E) = \frac{2 b_I^E b_E^I}{V_F - V_R + b_I^I}$ and $g(0) = \infty$, there is $N_E^* \geq 0$ so that $g(N_E^*) = b_E^E$. As the monotonicity of g is not known, there might be several values of N_E^* that solve the equation $g(N_E^*) = b_E^E$. However, the largest value $\bar{N}_E$ (see (2.30)) ensures that $g(N_E) < b_E^E$ for all $N_E > \bar{N}_E$. Thus, $b_E^E > g(N_E) > \frac{V_F + b_I^E N_I(N_E)}{N_E}$ for $N_E \geq \bar{N}_E$ and we obtain that $w_F < 0$ for $N_E \geq \bar{N}_E$. The inequality $\frac{V_F - V_R}{b_E^E N_E - V_F - b_I^E N_I(N_E)} < \frac{1}{N_E}$, for all $N_E \geq \bar{N}_E$, is proved using that $b_E^E > 2(V_F - V_R)$ and $N_E > \frac{2[V_F + b_I^E(N_I(N_E)]}{b_E^E}$ due to (2.29) and (2.30).

To conclude the proof we note that there is a unique steady state for parameters where $\lim_{N_E \to \infty} \mathcal{F}(N_E) = \infty$. Indeed, if b_E^E is small enough, $\mathcal{F}$ is an increasing function. And, for b_E^E small but such that the limit of $\mathcal{F}$ is finite, we deduce that there is a unique stationary solution in an analogous way as in [15][Theorem 3.1(i)] for a purely excitatory network: Denoting by $I_1^*(N_E)$ the function asociated to the parameter $b_E^E *$ and choosing

$$0 < b_E^E < b_E^E * < \frac{b_I^E b_E^I + \frac{1}{2}(V_F - V_R)(V_F - V_R + b_I^I)}{V_F - V_R + b_I^I},$$

then $I_1(N_E) > I_1^*(N_E) \ \forall N_E \geq 0$, as $I_1(N_E)$ is a decreasing function on b_E^E. Using now the value of the limit of $\mathcal{F}$, there is a $N_E^* > 0$ such that for the choice of $b_E^E *$

$$N_E I_1(N_E) > N_E I_1^*(N_E) > \frac{1}{2} \frac{(V_F - V_R)(V_F - V_R + b_I^I)}{b_E^E * (V_F - V_R) + b_E^E b_I^I - b_I^E b_E^I} > 1 \quad \forall N_E \geq N_E^*.$$

So, the solutions to $\mathcal{F}(N_E) = 1$ are on the interval $[0, N_E^*]$. Thanks to property 2.2 of $\mathcal{F}$, there is a unique solution, i.e., a unique steady state, if b_E^E is chosen small enough so that $b_E^E < b_I^E N_I'(N_E)$ $\forall N_E \in [0, N_E^*]$. $\square$

As proved in [15] we can find conditions for the connectivity parameters in order to have at least two steady states. We explain it in the following remark.

Remark 2.3.2 *If the parameters of the model satisfy (2.28) and*

$$2 a_E b_E^E < \left[V_R + b_I^E N_I \left(\frac{2 a_E}{(V_F - V_R)^2} \right) \right] (V_F - V_R)^2, \qquad (2.50)$$

there are at least two stationary solutions to (2.1)-(2.5).

Proof. . As $\mathcal{F}(0) = 0$ and $\lim_{N_E \to \infty} \mathcal{F}(N_E) < 1$ (due to (2.28)), we have to prove that $\mathcal{F}(N_E) > 1$ for

$N_E \in D := \left(\frac{2a_E}{(V_F - V_R)^2}, \frac{V_R + b_I^E N_I \left(\frac{2a_E}{(V_F - V_R)^2} \right)}{b_E^E} \right)$. This interval is not empty since (2.50) holds, and for

all $N_E \in D$ we have $N_E \leq \frac{V_R + b_I^E N_I(N_E)}{b_E^E}$ because $N_I(N_E)$ is an increasing function. Thus, $w_R > 0$ for $N_E \in D$. Finally, in an analogous way as in case (ii) of Theorem 3.1 in [15], using (2.27) we obtain

$$
\begin{aligned}
I_1(N_E) &\geq \int_{w_R}^{w_F} \left[e^{-\frac{z^2}{2}} \int_{\max(z, w_R)}^{w_F} e^{\frac{u^2}{2}} \, du \right] \, dz \\
&= \int_{w_R}^{w_F} \left[e^{-\frac{z^2}{2}} \int_z^{w_F} e^{\frac{u^2}{2}} \, du \right] \, dz \geq \int_{w_R}^{w_F} \left[\int_z^{w_F} du \right] \, dz = \frac{(V_F - V_R)^2}{2a_E} > \frac{1}{N_E}
\end{aligned}
$$

for $N_E \in D$. $\square$

From a biological point of view, the previous analysis of the number of steady states shows the complexity of the set of stationary solutions in terms of the model parameters: the reset and threshold potentials, V_R and V_F, and the connectivity parameters, b_E^E, b_E^I, b_I^E and b_I^I, which describe the strengths of the synapses between excitatory and inhibitory neurons. For example, in function of the connectivity parameter b_E^E, considering the rest of parameters fixed, we observe that if it is small (there are weak connections between excitatory neurons) there is a unique steady state. Whereas, if it is large (strong connections between excitatory neurons) there are no steady states. For intermediate values of b_E^E different situations can occur: one, two or three steady states. In Section 2.4.1 we illustrate this complexity with numerical experiments (see Figs. 2.6, 2.7, 2.8, 2.9).

2.3.2 Long time behavior

In [15] it was proved exponential convergence to the steady state for the linear case. Later, these results were extended in [26] to the nonlinear case, for a purely excitatory or inhibitory network with small connectivity parameters. In both papers the main tools used were the relative entropy and Poincaré inequalities. These techniques can be adapted for a coupled excitatory-inhibitory network, where the diffusion terms are considered constant, a_α, where $\alpha = E, I$. This is the goal of this subsection.

In Theorem 2.3.1 it was proved that for small connectivity parameters and constant diffusion terms there is only one stationary solution of the system (2.1)-(2.5). Let us denote that unique solution by $(\rho_E^\infty, \rho_I^\infty, N_E^\infty, N_I^\infty)$. Therefore for any smooth convex function $G : \mathbb{R}^+ \to \mathbb{R}$ following the idea of (2.63) (as the NNLIF equation is Fokker-Planck like) we can define the *relative entropy* for $\alpha = E, I$ as

$$
E[\rho_\alpha | \rho_\alpha^\infty] := \int_{-\infty}^{V_F} \rho_\alpha^\infty(v) G\left(\frac{\rho_\alpha(v, t)}{\rho_\alpha^\infty(v)} \right) \, dv.
$$

Remark 2.3.3 *In what follows we will say that a weak solution is* fast-decaying *(at $-\infty$) if it is a weak solution in the sense of Definition 2.1.1 and the weak formulation (2.7) holds for all test functions growing algebraically in v.*

We start proving an equation for the entropy production of the relative entropy (its time derivative) of each population.

Proposition 2.3.4 *Fast-decaying solutions to system* (2.1)-(2.5), *satisfy for* $\alpha = E, I$:

$$
\begin{aligned}
\frac{d}{dt} & E[\rho_\alpha | \rho_\alpha^\infty] \\
= & \frac{d}{dt} \int_{-\infty}^{V_F} \rho_\alpha^\infty(v) G\left(\frac{\rho_\alpha(v,t)}{\rho_\alpha^\infty(v)} \right) dv \\
= & - a_\alpha \int_{-\infty}^{V_F} \rho_\alpha^\infty(v) G''\left(\frac{\rho_\alpha(v,t)}{\rho_\alpha^\infty(v)} \right) \left(\frac{\partial}{\partial v} \frac{\rho_\alpha(v,t)}{\rho_\alpha^\infty(v)} \right)^2 dv \\
& - N_\alpha^\infty \left[G\left(\frac{N_\alpha(t)}{N_\alpha^\infty} \right) - G\left(\frac{\rho_\alpha(V_R,t)}{\rho_\alpha^\infty(V_R)} \right) - \left(\frac{N_\alpha(t)}{N_\alpha^\infty} - \frac{\rho_\alpha(V_R,t)}{\rho_\alpha^\infty(V_R)} \right) G'\left(\frac{\rho_\alpha(V_R,t)}{\rho_\alpha^\infty(V_R)} \right) \right] \\
& + \left(b_E^\alpha \bar{N}_E(t) - b_I^\alpha \bar{N}_I(t) \right) \int_{-\infty}^{V_F} \frac{\partial \rho_\alpha^\infty(t)}{\partial v} \left[G\left(\frac{\rho_\alpha(v,t)}{\rho_\alpha^\infty(v)} \right) - \left(\frac{\rho_\alpha(v,t)}{\rho_\alpha^\infty(v)} \right) G'\left(\frac{\rho_\alpha(v,t)}{\rho_\alpha^\infty(v)} \right) \right],
\end{aligned}
\tag{2.51}
$$

where $\bar{N}_\alpha(t) = N_\alpha(t) - N_\alpha^\infty$.

Proof. The proof follows similar computations to those developed in [15] and [17]. For the sake of simplicity it is divided in several steps. Each step contains the calculation of one of the auxiliary relations that will be necessary to derive equation (2.51). Furthermore, it will always be considered that $\alpha = E, I$ and that ρ_α and ρ_α^∞ depend both on (v,t) omitting in the expressions below this explicit dependency.

Step 1. Equation for $\frac{\partial}{\partial t} \frac{\rho_\alpha}{\rho_\alpha^\infty}$.

We start computing two auxiliary equations. The first one

$$
\frac{\partial \rho_\alpha}{\partial v} = \rho_\alpha^\infty \frac{\partial}{\partial v} \left(\frac{\rho_\alpha}{\rho_\alpha^\infty} \right) + \frac{\rho_\alpha}{\rho_\alpha^\infty} \frac{\partial \rho_\alpha^\infty}{\partial v},
\tag{2.52}
$$

is obtained using that

$$
\frac{\partial}{\partial v} \left(\frac{\rho_\alpha}{\rho_\alpha^\infty} \right) = \frac{1}{\rho_\alpha^\infty} \frac{\partial \rho_\alpha}{\partial v} - \frac{\rho_\alpha}{(\rho_\alpha^\infty)^2} \frac{\partial \rho_\alpha^\infty}{\partial v}.
$$

The second one is calculated differentiating (2.52). It reads

$$
\frac{\partial^2 \rho_\alpha}{\partial v^2} = \rho_\alpha^\infty \frac{\partial^2}{\partial v^2} \left(\frac{\rho_\alpha}{\rho_\alpha^\infty} \right) + 2 \frac{\partial}{\partial v} \left(\frac{\rho_\alpha}{\rho_\alpha^\infty} \right) \frac{\partial \rho_\alpha^\infty}{\partial v} + \frac{\rho_\alpha}{\rho_\alpha^\infty} \frac{\partial^2 \rho_\alpha^\infty}{\partial v^2}.
\tag{2.53}
$$

Applying (2.1), (2.52), (2.53) and (2.24), it can be obtained that

$$
\begin{aligned}
\frac{\partial}{\partial t} \left(\frac{\rho_\alpha}{\rho_\alpha^\infty} \right) = & \frac{1}{\rho_\alpha^\infty} \frac{\partial \rho_\alpha}{\partial t} \\
= & \frac{1}{\rho_\alpha^\infty} \left[-\frac{\partial}{\partial v} \left[h^\alpha(v, N_E, N_I) \rho_\alpha \right] + a_\alpha \frac{\partial^2 \rho_\alpha}{\partial v^2} + N_\alpha \delta(v - V_R) \right] \\
= & -\frac{\rho_\alpha}{\rho_\alpha^\infty} \frac{\partial}{\partial v} h^\alpha(v, N_E, N_I) - \frac{h^\alpha(v, N_E, N_I)}{\rho_\alpha^\infty} \frac{\partial \rho_\alpha}{\partial v} + \frac{a_\alpha}{\rho_\alpha^\infty} \frac{\partial^2 \rho_\alpha}{\partial v^2} + \frac{N_\alpha}{\rho_\alpha^\infty} \delta(v - V_R),
\end{aligned}
$$

and with some more computations, that

$$
\begin{aligned}
\frac{\partial}{\partial t}\left(\frac{\rho_\alpha}{\rho_\alpha^\infty}\right) &= \left[-h^\alpha(v, N_E, N_I) + \frac{2a_\alpha}{\rho_\alpha^\infty}\frac{\partial \rho_\alpha^\infty}{\partial v}\right]\frac{\partial}{\partial v}\left(\frac{\rho_\alpha}{\rho_\alpha^\infty}\right) + a_\alpha \frac{\partial^2}{\partial v^2}\left(\frac{\rho_\alpha}{\rho_\alpha^\infty}\right) + \frac{N_\alpha}{\rho_\alpha^\infty}\delta(v - V_R) \\
&\quad + a_\alpha \frac{\rho_\alpha}{(\rho_\alpha^\infty)^2}\frac{\partial^2 \rho_\alpha^\infty}{\partial v^2} - \frac{\rho_\alpha}{(\rho_\alpha^\infty)^2}[h^\alpha(v, N_E, N_I)\rho_\alpha^\infty] \\
&= \left[-h^\alpha(v, N_E, N_I) + \frac{2a_\alpha}{\rho_\alpha^\infty}\frac{\partial \rho_\alpha^\infty}{\partial v}\right]\frac{\partial}{\partial v}\left(\frac{\rho_\alpha}{\rho_\alpha^\infty}\right) + a_\alpha \frac{\partial^2}{\partial v^2}\left(\frac{\rho_\alpha}{\rho_\alpha^\infty}\right) + \frac{N_\alpha}{\rho_\alpha^\infty}\delta(v - V_R) \\
&\quad + a_\alpha \frac{\rho_\alpha}{(\rho_\alpha^\infty)^2}\frac{\partial^2 \rho_\alpha^\infty}{\partial v^2} - \frac{\rho_\alpha}{(\rho_\alpha^\infty)^2}[h^\alpha(v, N_E^\infty, N_I^\infty)\rho_\alpha^\infty] - \frac{\rho_\alpha}{(\rho_\alpha^\infty)^2}[b_E^\alpha \bar{N}_E - b_I^\alpha \bar{N}_I]\frac{\partial \rho_\alpha^\infty}{\partial v} \\
&= \left[-h^\alpha(v, N_E, N_I) + \frac{2a_\alpha}{\rho_\alpha^\infty}\frac{\partial \rho_\alpha^\infty}{\partial v}\right]\frac{\partial}{\partial v}\left(\frac{\rho_\alpha}{\rho_\alpha^\infty}\right) + a_\alpha \frac{\partial^2}{\partial v^2}\left(\frac{\rho_\alpha}{\rho_\alpha^\infty}\right) \\
&\quad + \frac{N_\alpha^\infty}{\rho_\alpha^\infty}\delta(v - V_R)\left[\frac{N_\alpha}{N_\alpha^\infty} - \frac{\rho_\alpha}{\rho_\alpha^\infty}\right] - \frac{\rho_\alpha}{(\rho_\alpha^\infty)^2}[b_E^\alpha \bar{N}_E - b_I^\alpha \bar{N}_I]\frac{\partial \rho_\alpha^\infty}{\partial v}.
\end{aligned}
\tag{2.54}
$$

Step 2. Equation for $\frac{\partial}{\partial t}G\left(\frac{\rho_\alpha}{\rho_\alpha^\infty}\right)$.

Differentiating G yields

$$
\frac{\partial}{\partial t}G\left(\frac{\rho_\alpha}{\rho_\alpha^\infty}\right) = G'\left(\frac{\rho_\alpha}{\rho_\alpha^\infty}\right)\frac{\partial}{\partial t}\left(\frac{\rho_\alpha}{\rho_\alpha^\infty}\right)
\tag{2.55}
$$

$$
\frac{\partial}{\partial v}G\left(\frac{\rho_\alpha}{\rho_\alpha^\infty}\right) = G'\left(\frac{\rho_\alpha}{\rho_\alpha^\infty}\right)\frac{\partial}{\partial v}\left(\frac{\rho_\alpha}{\rho_\alpha^\infty}\right)
\tag{2.56}
$$

$$
\frac{\partial^2}{\partial v^2}G\left(\frac{\rho_\alpha}{\rho_\alpha^\infty}\right) = G''\left(\frac{\rho_\alpha}{\rho_\alpha^\infty}\right)\left(\frac{\partial}{\partial v}\left(\frac{\rho_\alpha}{\rho_\alpha^\infty}\right)\right)^2 + G'\left(\frac{\rho_\alpha}{\rho_\alpha^\infty}\right)\frac{\partial^2}{\partial v^2}\left(\frac{\rho_\alpha}{\rho_\alpha^\infty}\right).
\tag{2.57}
$$

Using (2.54) and (2.55)-(2.57) this relation holds

$$
\begin{aligned}
\frac{\partial}{\partial t}G\left(\frac{\rho_\alpha}{\rho_\alpha^\infty}\right) &= G'\left(\frac{\rho_\alpha}{\rho_\alpha^\infty}\right)\frac{\partial}{\partial t}\left(\frac{\rho_\alpha}{\rho_\alpha^\infty}\right) \\
&= G'\left(\frac{\rho_\alpha}{\rho_\alpha^\infty}\right)\left[-h^\alpha(v, N_E, N_I) + \frac{2a_\alpha}{\rho_\alpha^\infty}\frac{\partial \rho_\alpha^\infty}{\partial v}\right]\frac{\partial}{\partial v}\left(\frac{\rho_\alpha}{\rho_\alpha^\infty}\right) + G'\left(\frac{\rho_\alpha}{\rho_\alpha^\infty}\right)a_\alpha \frac{\partial^2}{\partial v^2}\left(\frac{\rho_\alpha}{\rho_\alpha^\infty}\right) \\
&\quad + G'\left(\frac{\rho_\alpha}{\rho_\alpha^\infty}\right)\frac{N_\alpha^\infty}{\rho_\alpha^\infty}\delta(v - V_R)\left[\frac{N_\alpha}{N_\alpha^\infty} - \frac{\rho_\alpha}{\rho_\alpha^\infty}\right] - G'\left(\frac{\rho_\alpha}{\rho_\alpha^\infty}\right)\frac{\rho_\alpha}{(\rho_\alpha^\infty)^2}[b_E^\alpha \bar{N}_E - b_I^\alpha \bar{N}_I]\frac{\partial \rho_\alpha^\infty}{\partial v} \\
&= \left[-h^\alpha(v, N_E, N_I) + \frac{2a_\alpha}{\rho_\alpha^\infty}\frac{\partial \rho_\alpha^\infty}{\partial v}\right]\frac{\partial}{\partial v}G\left(\frac{\rho_\alpha}{\rho_\alpha^\infty}\right) - a_\alpha \frac{\partial^2}{\partial v^2}G\left(\frac{\rho_\alpha}{\rho_\alpha^\infty}\right) \\
&\quad - a_\alpha G''\left(\frac{\rho_\alpha}{\rho_\alpha^\infty}\right)\left(\frac{\partial}{\partial v}\left(\frac{\rho_\alpha}{\rho_\alpha^\infty}\right)\right)^2 + G'\left(\frac{\rho_\alpha}{\rho_\alpha^\infty}\right)\frac{N_\alpha^\infty}{\rho_\alpha^\infty}\delta(v - V_R)\left[\frac{N_\alpha}{N_\alpha^\infty} - \frac{\rho_\alpha}{\rho_\alpha^\infty}\right] \\
&\quad - G'\left(\frac{\rho_\alpha}{\rho_\alpha^\infty}\right)\frac{\rho_\alpha}{(\rho_\alpha^\infty)^2}[b_E^\alpha \bar{N}_E - b_I^\alpha \bar{N}_I]\frac{\partial \rho_\alpha^\infty}{\partial v}.
\end{aligned}
\tag{2.58}
$$

Step 3. Equation for $\frac{\partial}{\partial t}\rho_\alpha^\infty G\left(\frac{\rho_\alpha}{\rho_\alpha^\infty}\right)$.

This equation can be derived directly using (2.58) and (2.24). Thus,

$$
\begin{aligned}
\frac{\partial}{\partial t}\left[\rho_\alpha^\infty G\left(\frac{\rho_\alpha}{\rho_\alpha^\infty}\right)\right] =& \rho_\alpha^\infty \frac{\partial}{\partial t} G\left(\frac{\rho_\alpha}{\rho_\alpha^\infty}\right) \\
=& N_\alpha^\infty\left(\frac{N_\alpha}{N_\alpha^\infty} - \frac{\rho_\alpha}{\rho_\alpha^\infty}\right)\delta(v - V_R)G'\left(\frac{\rho_\alpha}{\rho_\alpha^\infty}\right) - \rho_\alpha^\infty a_\alpha G''\left(\frac{\rho_\alpha}{\rho_\alpha^\infty}\right)\left(\frac{\partial}{\partial v}\left(\frac{\rho_\alpha}{\rho_\alpha^\infty}\right)\right)^2 \\
& - \rho_\alpha^\infty h^\alpha(v, N_E, N_I)\frac{\partial}{\partial v}G\left(\frac{\rho_\alpha}{\rho_\alpha^\infty}\right) + 2a_\alpha\frac{\partial\rho_\alpha^\infty}{\partial v}\frac{\partial}{\partial v}G\left(\frac{\rho_\alpha}{\rho_\alpha^\infty}\right) \\
& + a_\alpha\rho_\alpha^\infty\frac{\partial^2}{\partial v^2}G\left(\frac{\rho_\alpha}{\rho_\alpha^\infty}\right) - G'\left(\frac{\rho_\alpha}{\rho_\alpha^\infty}\right)\frac{\rho_\alpha}{\rho_\alpha^\infty}[b_E^\alpha\bar{N}_E - b_I^\alpha\bar{N}_I]\frac{\partial\rho_\alpha^\infty}{\rho_\alpha} \\
=& N_\alpha^\infty\left(\frac{N_\alpha}{N_\alpha^\infty} - \frac{\rho_\alpha}{\rho_\alpha^\infty}\right)\delta(v - V_R)G'\left(\frac{\rho_\alpha}{\rho_\alpha^\infty}\right) - \rho_\alpha^\infty a_\alpha G''\left(\frac{\rho_\alpha}{\rho_\alpha^\infty}\right)\left(\frac{\partial}{\partial v}\left(\frac{\rho_\alpha}{\rho_\alpha^\infty}\right)\right)^2 \\
& - \frac{\partial}{\partial v}\left[h^\alpha(v, N_E, N_I)\rho_\alpha^\infty G\left(\frac{\rho_\alpha}{\rho_\alpha^\infty}\right)\right] + a_\alpha\frac{\partial^2}{\partial v^2}\left[\rho_\alpha G\left(\frac{\rho_\alpha}{\rho_\alpha^\infty}\right)\right] \\
& + N_\alpha^\infty G\left(\frac{\rho_\alpha}{\rho_\alpha^\infty}\right)\delta(v - V_R) + G\left(\frac{\rho_\alpha}{\rho_\alpha^\infty}\right)[b_E^\alpha\bar{N}_E - b_I^\alpha\bar{N}_I]\frac{\partial\rho_\alpha^\infty}{\partial v} \\
& - G'\left(\frac{\rho_\alpha}{\rho_\alpha^\infty}\right)\frac{\rho_\alpha}{\rho_\alpha^\infty}[b_E^\alpha\bar{N}_E - b_I^\alpha\bar{N}_I]\frac{\partial\rho_\alpha^\infty}{\partial v} \\
=& -\frac{\partial}{\partial v}\left[h^\alpha(v, N_E, N_I)\rho_\alpha^\infty G\left(\frac{\rho_\alpha}{\rho_\alpha^\infty}\right)\right] + a_\alpha\frac{\partial^2}{\partial v^2}\left[\rho_\alpha G\left(\frac{\rho_\alpha}{\rho_\alpha^\infty}\right)\right] \\
& - a_\alpha\rho_\alpha^\infty G''\left(\frac{\rho_\alpha}{\rho_\alpha^\infty}\right)\left(\frac{\partial}{\partial v}\left(\frac{\rho_\alpha}{\rho_\alpha^\infty}\right)\right)^2 \\
& + N_\alpha^\infty\delta(v - V_R)\left[\left(\frac{N_\alpha}{N_\alpha^\infty} - \frac{\rho_\alpha}{\rho_\alpha^\infty}\right)G'\left(\frac{\rho_\alpha}{\rho_\alpha^\infty}\right) + G\left(\frac{\rho_\alpha}{\rho_\alpha^\infty}\right)\right] \\
& + [b_E^\alpha\bar{N}_E - b_I^\alpha\bar{N}_I]\frac{\partial\rho_\alpha^\infty}{\partial v}\left[G\left(\frac{\rho_\alpha}{\rho_\alpha^\infty}\right) - \frac{\rho_\alpha}{\rho_\alpha^\infty}G'\left(\frac{\rho_\alpha}{\rho_\alpha^\infty}\right)\right].
\end{aligned}
\tag{2.59}
$$

Step 4. Equation (2.51).
Thanks to L'Hôpital's rule it holds that

$$
\lim_{v \to V_F}\frac{\rho_\alpha}{\rho_\alpha^\infty} = \frac{N_\alpha}{N_\alpha^\infty}.
\tag{2.60}
$$

Integrating equation (2.59) from $-\infty$ to $V_F - \epsilon$, taking the limit as $\epsilon \to 0^+$, using the definition of fast-decaying solutions, the boundary conditions of (2.2) and relation (2.60) finally equation (2.51) is obtained.

$\square$

Identifying the relative entropy is crucial in order to apply the entropy dissipation method[2]. This method provides a useful tool for the study of the convergence to the steady state of the solutions of

---

[2] The entropy dissipation method comes from the idea of looking for a convergence in time of a solution of an equation, f, to the steady state solution f_∞, in terms of the entropy. In other words, if we denote by E the entropy functional associated to the solution of the equation, the goal is to show that $E(f) \to E(f_\infty)$ in time [5, 102]. In order to quantify that convergence we define the *relative entropy* as the "distance/discrepancy" between f and f_∞. In this way, if f converges to f_∞ in terms of relative entropy, the "distance" on larger times will always be smaller than the initial one,

some equations (Boltzmann, Fokker-Planck, etc). In our case we consider as relative entropy of the system the sum of the relative entropies of each population

$$E[t] := E[\rho_E | \rho_E^\infty] + E[\rho_I | \rho_I^\infty], \tag{2.64}$$

since the entropy production of the relative entropy for the excitatory (resp. inhibitory) population depends on the firing rate of the inhibitory (resp. excitatory) population. In other words, both entropy productions are linked by means of the firing rates. This will allow us to calculate an exponential rate of convergence to the equilibrium thanks to an *entropy-entropy production inequality* like this

$$\frac{d}{dt} E[t] \leq -\mu E[t],$$

for some constant $\mu > 0$. In concrete, for the quadratic entropy generating function, $G(x) = (x-1)^2$, a control of the sum (2.64) can be obtained for small connectivity parameters, proving an analogous result as Theorem 2.1 in [26]. Note that considering the quadratic entropy generating function, the relative entropy of our system takes the form

$$E[t] = \int_{-\infty}^{V_F} \left[\rho_E^\infty(v) \left(\frac{\rho_E(v,t)}{\rho_E^\infty(v)} - 1 \right)^2 + \rho_I^\infty(v) \left(\frac{\rho_I(v,t)}{\rho_I^\infty(v)} - 1 \right)^2 \right] dv. \tag{2.65}$$

Thus, we are now ready to state the main theorem about long time convergence of the solutions to the unique steady state.

Theorem 2.3.5 *Assume a_α constant for $\alpha = E, I$, the connectivity parameters b_E^E, b_E^I, b_I^E and b_I^I*

---

and thus, the relative entropy has to be a positive decreasing function, presenting a minimum at f_∞:

$$E[f | f_\infty] := E(f) - E(f_\infty). \tag{2.61}$$

Bounding the expression of the derivative of the relative entropy, i. e. of the *entropy dissipation*, in terms of an entropy functional, in general allows the computation of an inequality like this

$$\frac{d}{dt} E[f | f_\infty] \leq -\mathcal{H}(E[f | f_\infty]), \tag{2.62}$$

where $\mathcal{H}(x)$ is a continuous strictly positive function for $x > 0$. As a consequence, depending on the function $\mathcal{H}$ it will be possible to get a more or less strong convergence to the steady state. In (2.62) we appreciate that the relative entropy controls the entropy dissipation, from where comes the name of entropy dissipation method.

The entropy dissipation method was initially developed for the Boltzmann equation [102, 103]. Nevertheless, we can use this method for other kind of kinetic equations, for which the relative entropy considered not necessarily has to coincide with a physical relative entropy of the form (2.61). It is enough to find a Lyapunov functional that presents the required properties (f_∞ is a minimum, being positive). For example, for the Fokker-Planck equation there is a whole family of admitted relative entropies [6, 64]

$$E[f | f_\infty] = \int f G \left(\frac{f}{f_\infty} \right) dv, \tag{2.63}$$

where G is called *entropy generating function*. To be an appropiate generating function, G has to satisfy that $G(1) = 0$ and that it is strictly convex and positive. Futhermore, in [6], it is proved that for all admitted relative entropies the convergence in terms of relative entropy implies the L^1 norm convergence and that, under some constraints, there is an exponencial convergence of the solutions to the equilibrium in terms of relative entropy. Moreover, there is a nice overview of more general entropy inequalities in [66, 77].

small enough and initial data (ρ_E^0, ρ_I^0) such that

$$E[0] < \frac{1}{2\max\left(b_E^E + b_I^E, b_E^I + b_I^I\right)}. \tag{2.66}$$

Then, for fast decaying solutions to (2.1)-(2.5) there is a constant $\mu > 0$, such that, for all $t \geq 0$

$$E[t] \leq e^{-\mu t} E[0].$$

Consequently, for $\alpha = E, I$

$$\int_{-\infty}^{V_F} \rho_\alpha^\infty \left(\frac{\rho_\alpha(v,t)}{\rho_\alpha^\infty(v)} - 1\right)^2 dv \leq e^{-\mu t} E[0].$$

Proof. The proof follows analogous steps as in [26][Theorem 2.1], with the main difficulty that, in this case, the entropy productions for excitatory and inhibitory populations are linked. This is the reason why the total relative entropy, given by the functional (2.65), has to be considered. Thus, the entropy production is the sum of the entropy productions of each population. In this way, the terms of $\bar{N}_\alpha$ can be gathered and bound properly, as it is shown below.

Using equality (2.51) with $G(x) = (x-1)^2$ for each term of the entropy (2.65), its time derivative can be written as

$$\begin{aligned}
\frac{d}{dt} E[t] = \; & 2a_E \int_{-\infty}^{V_F} \rho_E^\infty(v) \left(\frac{\partial}{\partial v} \frac{\rho_E(v,t)}{\rho_E^\infty(v)}\right)^2 dv - 2a_I \int_{-\infty}^{V_F} \rho_I^\infty(v) \left(\frac{\partial}{\partial v} \frac{\rho_I(v,t)}{\rho_I^\infty(v)}\right)^2 dv \\
& - N_E^\infty \left(\frac{N_E(t)}{N_E^\infty} - \frac{\rho_E(V_R,t)}{\rho_E^\infty(V_R)}\right)^2 - N_I^\infty \left(\frac{N_I(t)}{N_I^\infty} - \frac{\rho_I(V_R,t)}{\rho_I^\infty(V_R)}\right)^2 \\
& + 2\left(b_E^E \bar{N}_E(t) - b_I^E \bar{N}_I(t)\right) \int_{-\infty}^{V_F} \rho_E^\infty(v) \left[\frac{\partial}{\partial v} \frac{\rho_E(v,t)}{\rho_E^\infty(v)} \left(\frac{\rho_E(v,t)}{\rho_E^\infty(v)} - 1\right) + \frac{\partial}{\partial v} \frac{\rho_E(v,t)}{\rho_E^\infty(v)}\right] dv \\
& + 2\left(b_E^I \bar{N}_E(t) - b_I^I \bar{N}_I(t)\right) \int_{-\infty}^{V_F} \rho_I^\infty(v) \left[\frac{\partial}{\partial v} \frac{\rho_I(v,t)}{\rho_I^\infty(v)} \left(\frac{\rho_I(v,t)}{\rho_I^\infty(v)} - 1\right) + \frac{\partial}{\partial v} \frac{\rho_I(v,t)}{\rho_I^\infty(v)}\right] dv,
\end{aligned} \tag{2.67}$$

where last two terms where obtained using that $G(x) - xG'(x) = 1 - x^2$, and integrating by parts taking into account the boundary conditions (2.2).

Considering the inequality[3] $(a + b)^2 \geq \epsilon\left(a^2 - 2b^2\right)$ for $a, b \in \mathbb{R}$ and $0 < \epsilon < 1/2$, the Sobolev injection of $L^\infty(I)$ in $H^1(I)$ for a small neighborhood I of V_R where ρ_α^∞ is bounded below and the Poincaré inequality[4] (for more details of this inequality see [15] [Appendix] and [26]), the third and

---

[3] Inequality $(a+b)^2 \geq \epsilon(a^2 - 2b^2)$ for $a, b \in \mathbb{R}$ and $0 < \epsilon < \frac{1}{2}$. This inequality is a consecuence of the fact that $a^2 - 2b^2 \leq 2(a+b)^2$, which can be proved by simple algebraic computations.

[4] In [15] a more general Hardy-Poincaré's like inequality was proved. Let us remember that result.

Proposition 2.3.6 *Given $m, n > 0$ such that $\int_0^\infty m(y)\, dy = 1$ for all functions f on $(0, \infty)$ such that $\int_0^\infty m(y)f(y)\, dy = 0$ the following inequality holds:*

$$\int_0^\infty m(x)|f(x)|^2 \, dx \leq A \int_0^\infty n(x)|f'(x)|^2 \, dx, \tag{2.68}$$

for some $A > 0$ not necessary finite, provided all integrals make sense.

In addition, it was stated that, if we choose $n(x) = m(x) = K\min(x, e^{-\frac{x^2}{2}})$, with K a constant taken so that

fourth terms in (2.67) satisfy:

$$-N_\alpha^\infty \left(\frac{N_\alpha(t)}{N_\alpha^\infty} - \frac{\rho_\alpha(V_R,t)}{\rho_\alpha^\infty(V_R)} \right)^2 \leq -C_0^\alpha \left(\frac{N_\alpha(t)}{N_\alpha^\infty} - 1 \right)^2 + \frac{a_\alpha}{2} \int_{-\infty}^{V_F} \rho_\alpha^\infty(v) \left(\frac{\partial}{\partial v} \frac{\rho_\alpha(v,t)}{\rho_\alpha^\infty}(v,t) \right)^2 dv,$$

for some positive constant C_0^α.

The estimate of the last two terms of (2.67) is quite more involved. First, each term is split in its four addends, obtaining for $\alpha = E, I$

$$2 \left(b_E^\alpha \bar{N}_E(t) - b_I^\alpha \bar{N}_I(t) \right) \int_{-\infty}^{V_F} \rho_\alpha^\infty(v) \left[\frac{\partial}{\partial v} \frac{\rho_\alpha(v,t)}{\rho_\alpha^\infty(v)} \left(\frac{\rho_\alpha(v,t)}{\rho_\alpha^\infty(v)} - 1 \right) + \frac{\partial}{\partial v} \frac{\rho_\alpha(v,t)}{\rho_\alpha^\infty(v)} \right] dv$$

$$= 2b_E^\alpha \bar{N}_E(t) \int_{-\infty}^{V_F} \rho_\alpha^\infty(v) \frac{\partial}{\partial v} \frac{\rho_\alpha(v,t)}{\rho_\alpha^\infty(v)} \left(\frac{\rho_\alpha(v,t)}{\rho_\alpha^\infty(v)} - 1 \right) dv + 2b_E^\alpha \bar{N}_E(t) \int_{-\infty}^{V_F} \rho_\alpha^\infty(v) \frac{\partial}{\partial v} \frac{\rho_\alpha(v,t)}{\rho_\alpha^\infty(v)} dv$$

$$- 2b_I^\alpha \bar{N}_I(t) \int_{-\infty}^{V_F} \rho_\alpha^\infty(v) \frac{\partial}{\partial v} \frac{\rho_\alpha(v,t)}{\rho_\alpha^\infty(v)} \left(\frac{\rho_\alpha(v,t)}{\rho_\alpha^\infty(v)} - 1 \right) dv - 2b_I^\alpha \bar{N}_I(t) \int_{-\infty}^{V_F} \rho_\alpha^\infty(v) \frac{\partial}{\partial v} \frac{\rho_\alpha(v,t)}{\rho_\alpha^\infty(v)} dv.$$

$$(2.70)$$

$\int_0^\infty m(y) \, dy = 1$, then $0 < A < \infty$. In particular, although for this choose of m and n the Muckenhoupt's criterion for Poincaré's inequality or their variants [61, 8] cannot be used since $1/n(x)$ is not integrable at zero, inequality (2.68) holds. The proof has to be performed as in [15] and [29]. Thus, we can state the following result.

Proposition 2.3.7 (Poincaré's inequality) *Let $\rho_\alpha^\infty(v)$ for $\alpha = E, I$, be the unique solution to (2.1)-(2.5) for small enough connectivity parameter values, and constant diffusion terms. Then there exist $\gamma > 0$ depending just on the connectivity parameters, so that for any function $h(v)$ that satisfies $\int_{-\infty}^{V_F} \rho_\alpha^\infty(v) h(v) \, dv = 1$, for $\alpha = E, I$, it holds that*

$$\gamma \int_{-\infty}^{V_F} \rho_\alpha^\infty(v)(h(v) - 1)^2 \, dv \leq \int_{-\infty}^{V_F} \rho_\alpha^\infty(v) \left[\frac{\partial h}{\partial v} \right]^2 (v) \, dv \quad \text{for } \alpha = E, I. \tag{2.69}$$

Proof. Let us remind the expression of ρ_α^∞ for $\alpha = E, I$ in (2.25)

$$\rho_\alpha^\infty(v) = \frac{N_\alpha^\infty}{a_\alpha} e^{-\frac{(v - b_E^\alpha N_E^\infty + b_I^\alpha N_I^\infty - (b_E^\alpha - b_E^E)v_{E,ext})^2}{2a_\alpha}} \int_{\max(v,V_R)}^{V_F} e^{\frac{(w - b_E^\alpha N_E^\infty + b_I^\alpha N_I^\infty - (b_E^\alpha - b_E^E)v_{E,ext})^2}{2a_\alpha}} dw.$$

Parametrizing the interval $(-\infty, V_F]$ instead of $[0, \infty)$ in (2.68), it can be observed that if the connectivity parameter values are small enough, the asymptotic behavior at the interval ends of ρ_α^∞ for $\alpha = E, I$ is equivalent to that of the the the function $K\min(V_F - v, e^{-\frac{(V_F-v)^2}{2}})$. Thus, as for the proof of inequality (2.68) just the behavior at the interval ends was used, (2.69) holds. $\square$

Remark 2.3.8 *Note that in the proof of Theorem 2.3.5, in order to apply (2.69), $h(v)$ was chosen for $\alpha = E, I$ as*

$$h^\alpha(v) := \frac{\rho_\alpha(v,t)}{\rho_\alpha^\infty(v)}.$$

Then, Cauchy-Schwarz's[5] and Young's inequalities[6], provide

$$2b_E^\alpha|\bar{N}_E(t)| \int_{-\infty}^{V_F} \rho_\alpha^\infty(v) \left| \frac{\partial}{\partial v} \frac{\rho_\alpha(v,t)}{\rho_\alpha^\infty(v)} \left(\frac{\rho_\alpha(v,t)}{\rho_\alpha^\infty(v)} - 1 \right) \right| \, dv$$

$$\leq \frac{b_E^\alpha}{a_E}(N_E^\infty)^2 \left(\frac{N_E(t)}{N_E^\infty} - 1 \right)^2 + a_E b_E^\alpha \int_{-\infty}^{V_F} \rho_\alpha^\infty(v) \left(\frac{\partial}{\partial v} \frac{\rho_\alpha(v,t)}{\rho_\alpha^\infty(v)} \right)^2 \, dv \int_{-\infty}^{V_F} \rho_\alpha^\infty(v) \left(\frac{\rho_\alpha(v,t)}{\rho_\alpha^\infty(v)} - 1 \right)^2 \, dv$$

and

$$2b_E^\alpha|\bar{N}_E(t)| \int_{-\infty}^{V_F} \rho_\alpha^\infty(v) \left| \frac{\partial}{\partial v} \frac{\rho_\alpha(v,t)}{\rho_\alpha^\infty(v)} \right| \, dv$$

$$\leq 4\frac{(b_E^\alpha)^2}{a_E} N_E^{\infty 2} \left(\frac{N_E(t)}{N_E^\infty} - 1 \right)^2 + \frac{a_E}{4} \int_{-\infty}^{V_F} \rho_\alpha^\infty(v) \left(\frac{\partial}{\partial v} \frac{\rho_\alpha(v,t)}{\rho_\alpha^\infty(v)} \right)^2 \, dv.$$

Getting together all these bounds

$$\frac{d}{dt} E[t] \leq \left(\frac{b_E^E}{a_E} + \frac{b_E^I}{a_I} + 4\frac{(b_E^E)^2}{a_E} + 4\frac{(b_E^I)^2}{a_I} - \frac{C_0^E}{N_E^{\infty 2}} \right) (N_E^\infty)^2 \left(\frac{N_E(t)}{N_E^\infty} - 1 \right)^2$$

$$+ \left(\frac{b_I^E}{a_E} + \frac{b_I^I}{a_I} + 4\frac{(b_I^E)^2}{a_E} + 4\frac{(b_I^I)^2}{a_I} - \frac{C_0^I}{N_I^{\infty 2}} \right) (N_I^\infty)^2 \left(\frac{N_I(t)}{N_I^\infty} - 1 \right)^2$$

$$- a_E \int_{-\infty}^{V_F} \rho_E^\infty(v) \left(\frac{\partial}{\partial v} \frac{\rho_E(v,t)}{\rho_E^\infty}(v,t) \right)^2 \, dv \left[1 - (b_E^E + b_E^I) \int_{-\infty}^{V_F} \rho_E^\infty(v) \left(\frac{\rho_E(v,t)}{\rho_E^\infty}(v,t) - 1 \right)^2 \, dv \right]$$

$$- a_I \int_{-\infty}^{V_F} \rho_I^\infty(v) \left(\frac{\partial}{\partial v} \frac{\rho_I(v,t)}{\rho_I^\infty}(v,t) \right)^2 \, dv \left[1 - (b_I^E + b_I^I) \int_{-\infty}^{V_F} \rho_I^\infty(v) \left(\frac{\rho_I(v,t)}{\rho_I^\infty}(v,t) - 1 \right)^2 \, dv \right].$$

$$(2.71)$$

In this way, for b_k^α, with $k, \alpha = E, I$, small enough such that $\left(\frac{b_\alpha^E}{a_E} + \frac{b_\alpha^I}{a_I} + 4\frac{(b_\alpha^E)^2}{a_E} + \frac{(b_\alpha^I)^2}{a_I} - \frac{C_0^\alpha}{(N_\alpha^\infty)^2} \right) < 0,$

---

[5]**Cauchy-Schwarz's inequality.** Given two vectors a and b of an inner product (denoted by $<,>$) space it is satisfied that

$$| < a, b > |^2 \leq ||a||^2 ||b||^2,$$

where $||.|| = \sqrt{<,>}$ refers to the norm associated to the inner product.

[6]**Young's inequality.** Let $a, b \in \mathbb{R}^+$ and $p, q \in \mathbb{R}^+ - 0$ so that $\frac{1}{p} + \frac{1}{q} = 1$ then

$$ab \leq \frac{1}{p}a^p + \frac{1}{q}b^q.$$

A particular case of this inequality appears when $p = q = 2$, then it reads

$$ab \leq \frac{1}{2}a^2 + \frac{1}{2}b^2.$$

the first and second terms of the right hand side (2.71) are negative, thus

$$
\begin{aligned}
\frac{d}{dt}&E[t] \\
\leq &- a_E \int_{-\infty}^{V_F} \rho_E^\infty(v) \left(\frac{\partial}{\partial v} \frac{\rho_E(v,t)}{\rho_E^\infty}(v,t) \right)^2 dv \left[1 - (b_E^E + b_E^I) \int_{-\infty}^{V_F} \rho_E^\infty(v) \left(\frac{\rho_E(v,t)}{\rho_E^\infty}(v,t) - 1 \right)^2 dv \right] \\
&- a_I \int_{-\infty}^{V_F} \rho_I^\infty(v) \left(\frac{\partial}{\partial v} \frac{\rho_I(v,t)}{\rho_I^\infty}(v,t) \right)^2 dv \left[1 - (b_I^E + b_I^I) \int_{-\infty}^{V_F} \rho_I^\infty(v) \left(\frac{\rho_I(v,t)}{\rho_I^\infty}(v,t) - 1 \right)^2 dv \right].
\end{aligned} \tag{2.72}
$$

Denoting $C = \max \left(b_E^E + b_I^E, b_E^I + b_I^I \right)$ the entropy production can be bound as follows

$$
\frac{d}{dt} E[t] \leq - \int_{-\infty}^{V_F} \left[a_E \rho_E^\infty(v) \left(\frac{\partial}{\partial v} \frac{\rho_E(v,t)}{\rho_E^\infty}(v,t) \right)^2 + a_I \rho_I^\infty(v) \left(\frac{\partial}{\partial v} \frac{\rho_I(v,t)}{\rho_I^\infty}(v,t) \right)^2 \right] dv \left(1 - CE[t] \right). \tag{2.73}
$$

Now using (2.66) and Grönwall's inequality for the function $f(t) := CE[t] - 1$ taking into account inequality (2.73), it can be proved that $CE[t] < 1$ for all times. Thanks to (2.73) it can be concluded that $E[t]$ decreases for all times, implying that $E[t] < \frac{1}{2C}$ $\forall t \geq 0$. Thus, estimate (2.73) now can be improved by

$$
\frac{d}{dt} E[t] \leq - \frac{a_E}{2} \int_{-\infty}^{V_F} \rho_E^\infty(v) \left(\frac{\partial}{\partial v} \frac{\rho_E(v,t)}{\rho_E^\infty}(v,t) \right)^2 dv - \frac{a_I}{2} \int_{-\infty}^{V_F} \rho_I^\infty(v) \left(\frac{\partial}{\partial v} \frac{\rho_I(v,t)}{\rho_I^\infty}(v,t) \right)^2 dv.
$$

Applying the Poincaré inequality on each term, there exist $\gamma, \gamma' > 0$, such that

$$
\frac{d}{dt} E[t] \leq - \frac{a_E \gamma}{2} \int_{-\infty}^{V_F} \rho_E^\infty(v) \left(\frac{\rho_E(v,t)}{\rho_E^\infty(v)} - 1 \right)^2 dv - \frac{a_I \gamma'}{2} \int_{-\infty}^{V_F} \rho_I^\infty(v) \left(\frac{\rho_I(v,t)}{\rho_I^\infty(v)} - 1 \right)^2 dv.
$$

Considering $\mu = \min \left(\frac{a_E \gamma}{2}, \frac{a_I \gamma'}{2} \right)$ we obtain $\frac{d}{dt} E[t] \leq -\mu E[t]$. Finally, Grönwall's inequality concludes the proof. $\square$

2.4 Numerical results

2.4.1 Numerical scheme

The analytical results proved in previous sections are shown numerically in the present section. The numerical scheme considered for this purpose is based on a fifth order conservative finite difference WENO scheme for the advection term, see Appendix A [Section A.1], standard second order centered finite differences for the diffusion term, detailed in Appendix A [Section A.3], and an explicit third order TVD Runge-Kutta scheme for the time evolution, explained in Appendix A [Section A.4]. To reduce the computation time, parallel computation techniques for a two cores code is developed. Thus, the time evolution for both equations of the system is calculated simultaneously. Each core handles one of the equations. MPI communication between the cores has been included in the code, since the system is coupled by the firing rates. Therefore, at the end of each Runge-Kutta step, each core needs to know the value of the firing rate of the other core.

For the simulations, an uniform mesh for $v \in [-V_{left}, V_F]$ is considered. The value of $-V_{left}$ is chosen such that $\rho_\alpha(-V_{left}, t) \sim 0$ (since $\rho_\alpha(-\infty, t) = 0$). The time step size is adapted dynamically during the simulations via a CFL time step condition, for more details have a look at Appendix A [Section A.4]. Some parameter values are common to most simulations, $V_F = 2$, $V_R = 1$ and $\nu_{E,ext} = 0$ and the diffusion terms $a_\alpha(N_E, N_I)$ have been taken constant as $a_\alpha = 1$. In the simulations where these values are different, the considered values are indicated in their figures and explanations. In most cases, the initial condition is

$$\rho_\alpha^0(v) = \frac{k}{\sqrt{2\pi}} e^{-\frac{(v - v_0^\alpha)^2}{2\sigma_0^{\alpha 2}}}, \tag{2.74}$$

where k is a constant such that $\int_{-V_{left}}^{V_F} \rho_\alpha^0(v) \, dv \approx 1$ numerically. However, in order to analyze the stability of steady states, stationary profiles are taken as initial conditions

$$\rho_\alpha^0(v) = \frac{N_\alpha}{a_\alpha(N_E, N_I)} e^{-\frac{(v - V_0^\alpha(N_E, N_I))^2}{2a_\alpha(N_E, N_I)}} \int_{\max(v, V_R)}^{V_F} e^{\frac{(w - V_0^\alpha(N_E, N_I))^2}{2a_\alpha(N_E, N_I)}} \, dw, \quad \alpha = E, I, \tag{2.75}$$

with $V_0^\alpha(N_E, N_I) = b_E^\alpha N_E - b_I^\alpha N_I + (b_E^\alpha - b_E^E)\nu_{E,ext}$ and where N_α is an approximated value of the stationary firing rate.

To get an idea about the number of steady states, the system (2.27) is solved numerically. For every N_E fixed, $N_I(N_E)$ is calculated as the root of $N_I(N_E)I_2(N_E, N_I(N_E)) - 1 = 0$ using the bisection method with tolerance 10^{-8}, and then a numerical approximation of $\mathcal{F}(N_E)$ is developed by quadrature formulas to find the number of intersections with the function 1. Fig. 2.2 shows the graphics of $N_I^2(N_E)I(N_E)$ (see (2.36)) and $\mathcal{F}(N_E)$ for parameter values for which the limit of $\mathcal{F}(N_E)$ is finite. The numerical approximation of the limits is in agreement with their analytical limits.

2.4.2 Numerical results

Blow-up. Numerical results for three situations in which the solutions are not global-in-time are described. In Fig. 2.3 we depict a blow-up situation produced by a big value of b_E^E, where the initial datum is far from V_F. However, for a value of the connectivity parameter b_E^E small, we show a blow-up situation originated by an initial condition quite concentrated around V_F in Fig. 2.4. In both cases we observe that an extremely fast increase of the firing rate of the excitatory population causes the blow-up of the system. Furthermore, we notice that the firing rate of the inhibitory population also starts to grow sharply. Nevertheless, the values it takes are quite small in comparison with those from the excitatory population.

For a purely inhibitory network the global existence of its solutions was proved in [29]. Therefore, one could think that high values of b_I^I could prevent the blow-up of the excitatory-inhibitory system. However, Theorem 2.2.1 shows that this is not the case and Fig. 2.5 describes this situation; although the value of b_I^I is big, a high value of b_E^E causes the divergence of $N_E(t)$ and the blow-up of the system.

Steady states. The proof of Theorem 2.3.1 provides a strategy to find numerically the stationary firing rates, which consists of finding the intersection points between the functions $\mathcal{F}(N_E)$ and constant 1 (see (2.45)). With this idea, we have plotted both functions for different parameter values.

The first case of Theorem 2.3.1 (there is an even number of steady states or there are no steady

states) is shown in Fig. 2.6. In this situation, the relation between the parameters implies

$$\lim_{N_E \to \infty} \mathcal{F}(N_E) < 1.$$

In the left plot, the pure connectivity parameters (b_E^E and b_I^I) are high in comparison with the connectivity parameters b_E^I and b_I^E, in such a way that there are no steady states. In the right plot, there are two steady states because the pure connectivity parameters are small, since in this case the maximum value of $\mathcal{F}$ is bigger than one.

The second case of Theorem 2.3.1 (there is an odd number of steady states), which implies

$$\lim_{N_E \to \infty} \mathcal{F}(N_E) > 1,$$

is depicted in Fig. 2.7. In the left plot, b_E^E is small enough such that $\mathcal{F}$ is an increasing function, and therefore there is a unique steady state. Also, in the center plot there is only one stationary solution, but in this case the values of connectivity parameters do not guarantee the monotonicity of $\mathcal{F}$. Finally, the right plot shows values of connectivity parameters for which there are three steady states.

To conclude the analysis of the number of steady states, in Fig. 2.8 it is depicted a comparison between an uncoupled excitatory-inhibitory network ($b_E^I = b_I^E = 0$) and a coupled network with small b_E^I and b_I^E. In Fig. 2.8 (left) the number of steady states for the uncoupled system ($b_E^I = b_I^E = 0$) is analyzed, while Fig. 2.8 (right) investigates the number of steady states when the parameters b_E^I and b_I^E are small ($b_E^I = b_I^E = 0.1$). As expected, it can be observed that the number of steady states does not change if we choose small values for b_E^I and b_I^E. It depends only on the value of b_E^E in the same way as described in [15]. For small values of b_E^E there is a unique steady state. As b_E^E increases, it appears another steady state, that merges with the first one and then disappears, apparently yielding a saddle node bifurcation. In Fig. 2.10 we show the time evolution of the firing rates, for the case described in Fig. 2.6 (right), with two steady states. We use as initial condition profiles like the one presented in (2.75). The numerical results show that the larger steady state is unstable, while the lower one seems to be stable. Therefore, numerical stability analysis indicates that the unique steady state is stable, while, when there are two steady states the highest seems to be unstable.

In this direction, another interesting bifurcation analysis that can be obtained in terms of the parameter b_I^E is depicted in Fig. 2.9. For large values of b_E^I there is a unique stable steady. Then, as it decreases it appears another steady state that bifurcates and gives rise to two equilibria. The largest disappears, and the lower one approaches the smallest steady state. Afterwards, both disappear, probably through a saddle node bifurcation. Numerical stability analysis determines that the lowest steady state is always stable, while the other ones are all unstable.

The Fig. 2.7 (right) depicts three steady states. The stability analysis of this situation is more complicated than the previous one (the case of two stationary solutions). Fig. 2.11 shows the time evolution of the solutions for different initial data; the steady state with less firing rate seems to be stable, while the other two steady states are unstable.
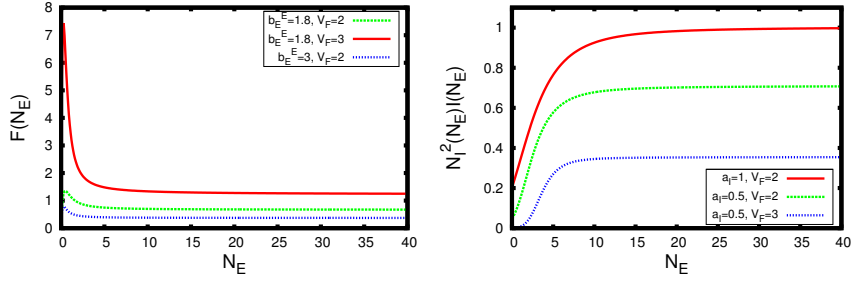
94

Figure 2.2: Study of the limits of $\mathcal{F}(N_E)$ and $N_I^2(N_E)I(N_E)$ (see (2.36)) when it is finite.
Left figure: $b_I^E = 0.75$, $b_E^I = 0.5$, $b_I^I = 0.25$, $a_E = 1$, $a_I = 1$ for different values of b_E^E and V_F.
Right figure: $b_E^E = 1.8$, $b_I^E = 0.75$, $b_E^I = 0.5$, $b_I^I = 0.25$ $a_E = 1$ for different values of a_I and V_F.
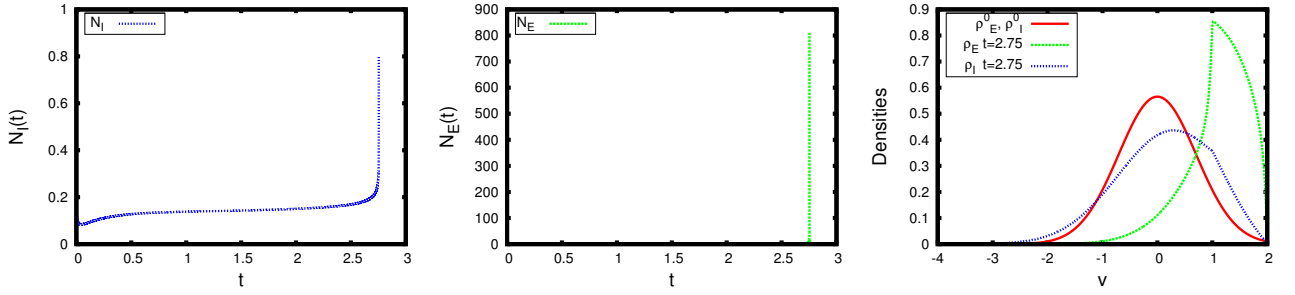

Figure 2.3: Firing rates and probability densities for $b_E^E = 3$, $b_I^E = 0.75$, $b_E^I = 0.5$, $b_I^I = 0.25$, in case of a normalized Maxwellian initial condition with mean 0 and variance 0.5 (see (2.74)). N_E blows-up because of the large value of b_E^E.
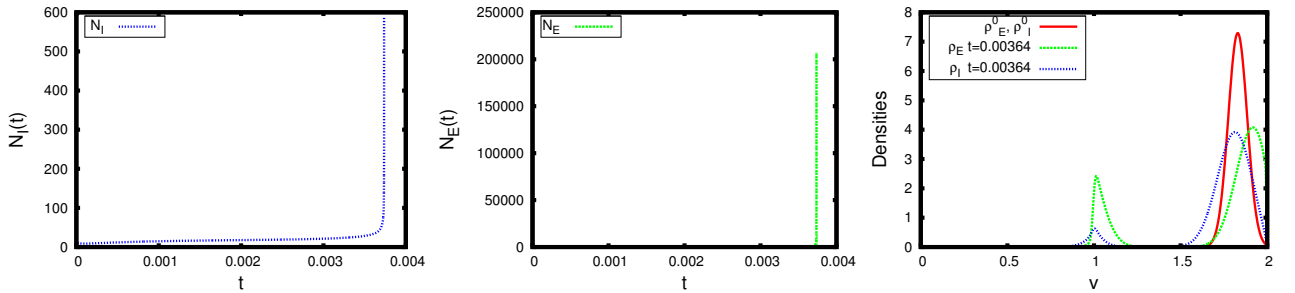
Figure 2.4: Firing rates and probability densities for $b_E^E = 0.5$, $b_I^E = 0.25$, $b_E^I = 0.25$, $b_I^I = 1$, in case of a normalized concentrated Maxwellian initial condition with mean 1.83 and variance 0.003 (see (2.74)).The initial condition concentrated close to V_F provokes the blow-up of N_E.
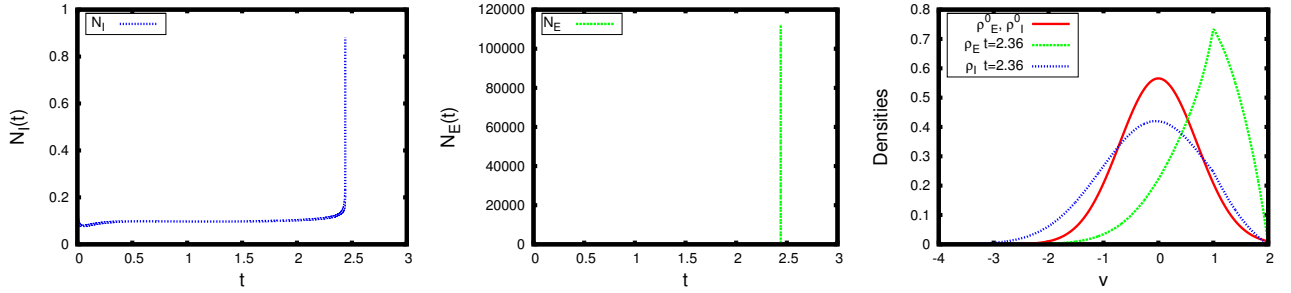
Figure 2.5: Firing rates and probability densities for $b_E^E = 3$, $b_I^E = 0.75$, $b_E^I = 0.5$, $b_I^I = 3$, in case of a normalized Maxwellian initial condition with mean 0 and variance 0.5 (see (2.74)).The blow-up of N_E cannot be avoided by a large value of b_I^I.
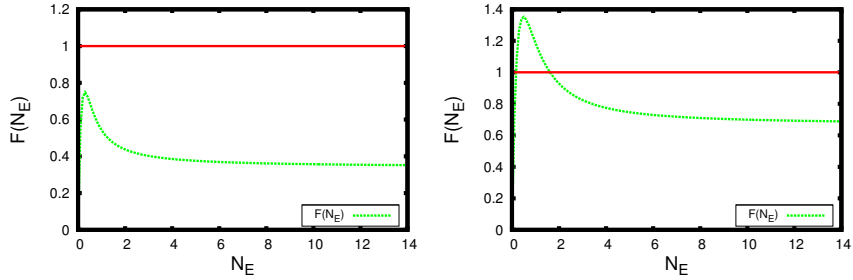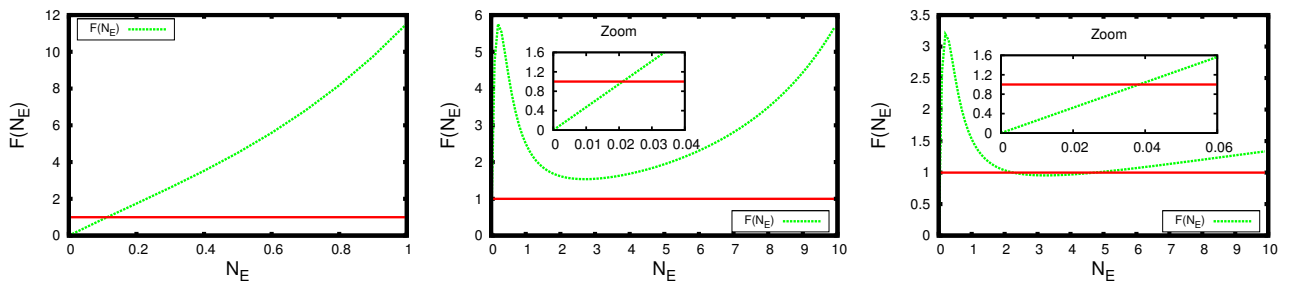

Figure 2.6: $\mathcal{F}(N_E)$ for different parameter values corresponding to the first case of Theorem 2.3.1: there are no steady states (left) or there is an even number of steady states (right).
Left figure: $b_E^E = 3$, $b_I^E = 0.75$, $b_E^I = 0.5$ and $b_I^I = 5$. Right figure: $b_E^E = 1.8$, $b_I^E = 0.75$, $b_E^I = 0.5$ and $b_I^I = 0.25$.

Figure 2.7: $\mathcal{F}(N_E)$ for different parameter values corresponding to the second case of Theorem 2.3.1: there is an odd number of steady states.
Left figure: $b_E^E = 0.5$, $b_I^E = 0.5$, $b_E^I = 3$ and $b_I^I = 0.5$ (one steady state). Center figure: $b_E^E = 3$, $b_I^E = 9$, $b_E^I = 0.5$, $b_I^I = 0.25$ (one steady state). Right figure: $b_E^E = 3$, $b_I^E = 7$, $b_E^I = 0.5$ and $b_I^I = 0.25$ (three steady states).
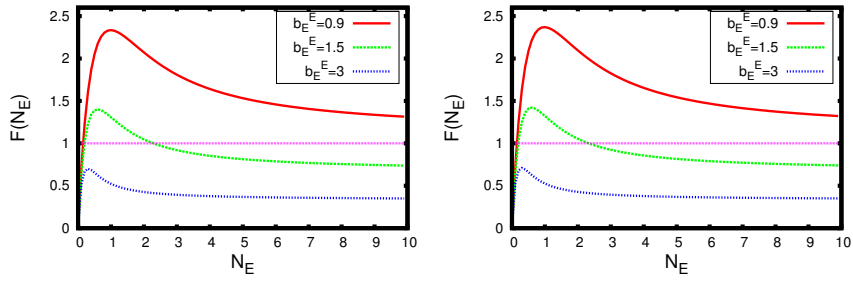
Figure 2.8: Comparison between an uncoupled excitatory-inhibitory network ($b_E^I = b_I^E = 0$) and a coupled network with small b_E^I and b_I^E. The qualitative behavior is the same in both cases.
Left figure: $b_I^E = b_E^I = 0$, $b_I^I = 0.25$, and different values for b_E^E. Right figure: $b_I^E = b_E^I = 0.1$, $b_I^I = 0.25$ and different values for b_E^E.
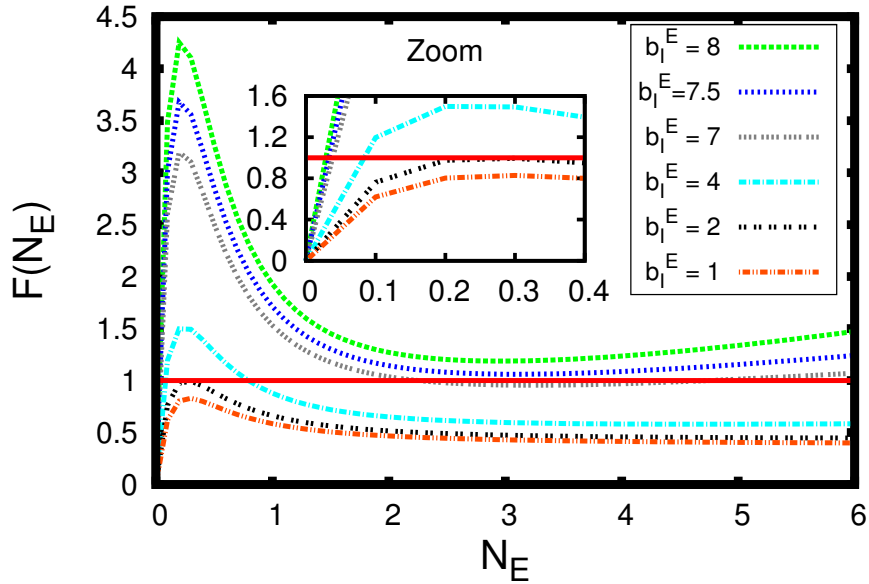

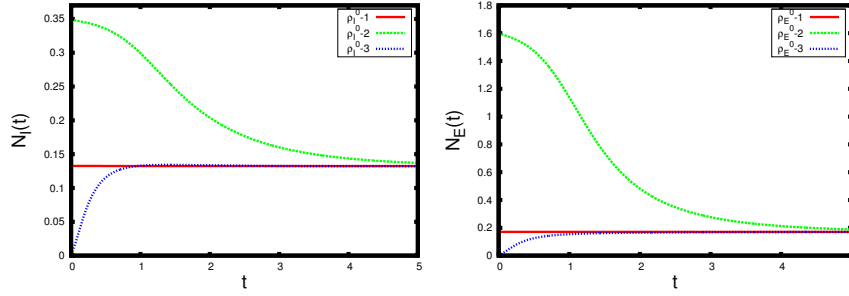Figure 2.9: Analysis of the number of steady states for $b_E^E = 3$, $b_E^I = 0.5$, $b_I^I = 0.25$ and different values for b_I^E.

97

Figure 2.10: Firing rates for the case of two steady states (right in Fig. 2.6), for different initial conditions: $\rho_\alpha^0 - 1, 2$ are given by the profile (2.75) with (N_E, N_I) stationary values and $\rho_\alpha^0 - 3$ is a normalized Maxwellian with mean 0 and variance 0.25 (see (2.74)). For both firing rates, the lower steady state seems to be asymptotically stable whereas the higher one seems to be unstable.
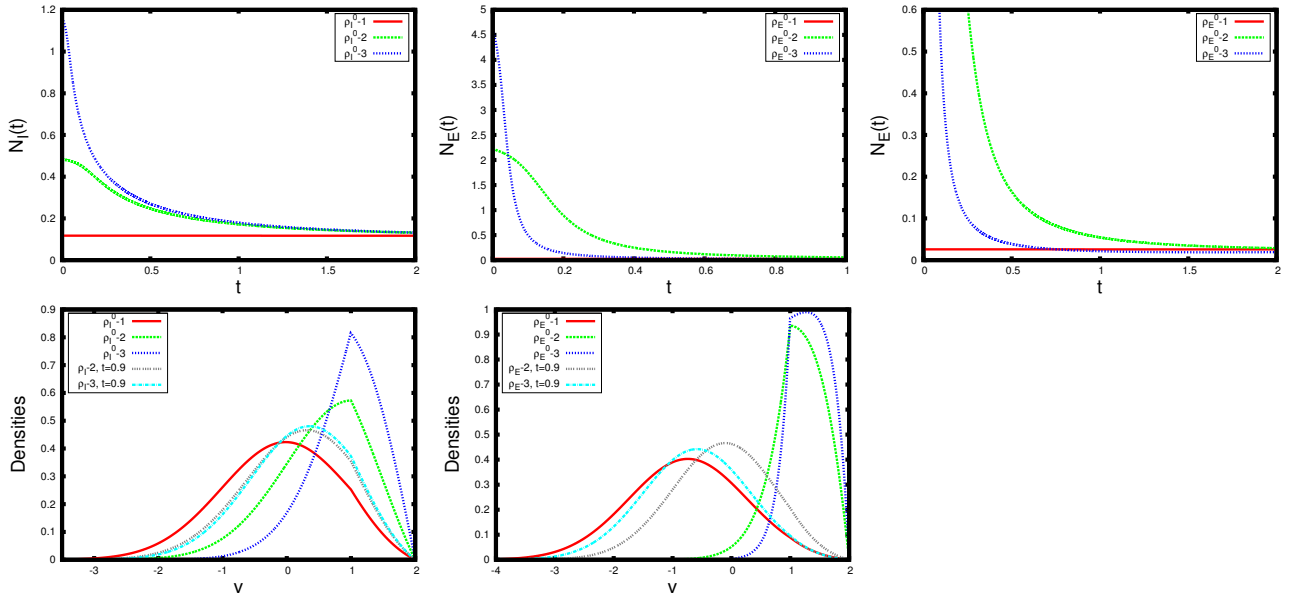

Figure 2.11: Stability analysis for the case of three steady states (right in Fig. 2.7).
Top figures: firing rates for different initial conditions: $\rho_\alpha^0 - 1, 2, 3$ which are given by the profile (2.75) with (N_E, N_I) stationary values. Only the lowest steady state seems to be asymptotically stable. The top right figure is a zoomed version of the top center figure. Bottom figures: evolution of the probability densities.
(Simulations were developed considering $v \in [-6, 2]$).

2.5   Conclusions

In conclusion, in this chapter we have extended the known results for purely excitatory or inhibitory networks [15] to excitatory-inhibitory coupled networks. We have proved that the presence of an inhibitory population in a coupled network does not avoid the blow-up phenomenon, as happens in a purely inhibitory network. Besides, we have analysed the number of steady states of the system, which is a more complicated issue than in the case of uncoupled systems. For small connectivity parameter values, we have shown that solutions converge exponentially fast to the unique steady state.

Our analytical and numerical results contribute to support the two-populations NNLIF system as an appropriate model to describe well known neurophysiological phenomena, as for example synchronization/asynchronization of the network, since the blow-up in finite time might depict a synchronization of a part of the network, while the presence of a unique asymptotically stable stationary solution represents an asynchronization of the network.

In addition, the abundance in the number of steady states, in terms of the connectivity parameter values, that can be observed for this simplified model, probably will help us to characterize situations of multi-stability for more complete NNLIF models and also other models including conductance variables as in [16]. In [17] it was shown that if a refractory period is included in the model, there are situations of multi-stability, with two stable and one unstable steady state. In [16] bi-stability phenomena were numerically described. Multi-stable networks are related, for instance, to the visual perception and the decision making [50, 3].

Chapter 3

Full NNLIF model: one and two populations

In the current chapter we aim to study the most realistic NNLIF model consisting of two populations with refractory states and transmission delays, completing the results of [11]. We demonstrate that neural networks with part of their neurons in a refractory state always have steady states—which has been proved for the simpler case of only one population [17]. This shows that in the complete model with refractory states there is always at least one steady state, while in the absence of refractory states, as shown in Chapter 2 [Theorem 2.3.1], there are some values of the parameters for which the model has no steady states. We are also able to give conditions for the values of the model parameters which ensure the uniqueness of the steady state. This result is completed with a proof of exponential convergence of the solution to the steady state for networks with small connectivity parameters and without transmission delay. The entropy method will be used to achieve this goal, with the additional difficulty that we deal with a complex system involving four equations, for which the entropy functional is composed of excitatory and inhibitory densities and their corresponding refractory probabilities. Moreover, we extend to this case the analysis of blow-up phenomena started in [17] and in Chapter 2 [Theorem 2.2.1]. We will observe that the network can blow-up in finite time if the transmission delay between excitatory neurons vanishes, even if there are transmission delays between inhibitory neurons or between inhibitory and excitatory neurons. Consequently, we show that the only way to avoid the blow-up is to consider a nonzero transmission delay between excitatory neurons. Indeed, in Chapter 1 this fact was proved for the one-population NNLIF model without refractory state. Moreover, at the microscopic level, it is known that global-in-time solutions exist if there is transmission delay in the case of only one average-excitatory population (see [37] and [38]).

On the other hand, in order to better understand some of the analytical open problems related to this model and show visually the behaviour of the network, we develop a numerical solver for the full model. Our solver is based on high order flux-splitting WENO schemes, TVD Runge-Kutta methods, and an efficient numerical strategy to deal with the saving and recovering of data needed to take the delays into account. This new numerical solver improves previous ones [15, 17], including the one presented in Chapter 2 [Section 2.4.1] not only because it describes the complete NNLIF model, but also due to it being optimized. It allows us to describe the wide range of phenomena displayed by the network: blow-up, asynchronous/synchronous solutions, instability/stability of the steady states, as well as the time evolution of the firing rates, the proportion of refractory states, and the probability distributions of the excitatory and inhibitory populations. Besides, we explore numerically the importance of the

transmission delay between excitatory neurons to avoid the blow-up phenomenon; situations which present blow-up without delay are prevented it if a nonzero transmission delay is considered. Instead of blowing-up, solutions converge to a stationary or periodic solution. Notice that the appearance of oscillatory solutions for neural networks is a known fact, that has been widely studied in, e.g., [1, 11, 12, 13].

3.1 The model and the definition of solution

Let us consider a neural network composed of an excitatory population and an inhibitory population. Furthermore, suppose that the neurons of the network enter in a refractory state just after spiking and that the transmission of the nerve impulse presents synaptic delay. We denote by $\rho_\alpha(v, t)$ the probability density of finding a neuron in the population α, with a voltage $v \in (-\infty, V_F]$ at a time $t \geq 0$, where $\alpha = E$, if the population is excitatory, and $\alpha = I$, if it is inhibitory. Again we consider the NNLIF model to describe the network, taking into account the transmission delay and the refractory state. As already derived in the Introduction [Section 0.2] we then obtain a complicated system of two PDEs for the evolution of these probability densities $\rho_\alpha(v, t)$, coupled with another two ODEs for the refractory states, $R_\alpha(t)$, for $\alpha = E, I$:

$$
\begin{cases}
\dfrac{\partial \rho_\alpha(v, t)}{\partial t} + \dfrac{\partial}{\partial v}[h^\alpha(v, N_\alpha(t - D_E^\alpha), N_I(t - D_I^\alpha))\rho_\alpha(v, t)] - a_\alpha(N_E(t - D_E^\alpha), N_I(t - D_I^\alpha))\dfrac{\partial^2 \rho_\alpha(v, t)}{\partial v^2} = \\
\qquad\qquad\qquad M_\alpha(t)\delta(v - V_R), \\[2mm]
\dfrac{dR_\alpha(t)}{dt} = N_\alpha(t) - M_\alpha(t), \\[2mm]
N_\alpha(t) = -a_\alpha(N_E(t - D_E^\alpha), N_I(t - D_I^\alpha))\frac{\partial \rho_\alpha}{\partial v}(V_F, t) \geq 0, \\[2mm]
\rho_\alpha(-\infty, t) = 0, \quad \rho_\alpha(V_F, t) = 0, \quad \rho_\alpha(v, 0) = \rho_\alpha^0(v) \geq 0, \quad R_\alpha(0) = R_\alpha^0.
\end{cases}
\tag{3.1}
$$

For each population α, $R_\alpha(t)$ denotes the probability to find a neuron in the refractory state and $D_i^\alpha \geq 0$, for $i = E, I$, is the transmission delay of a spike arriving at a neuron of population α, coming from a neuron of population i. The drift and diffusion coefficients are defined by

$$
\begin{aligned}
h^\alpha(v, N_E(t), N_I(t)) &= -v + b_E^\alpha N_E(t) - b_I^\alpha N_I(t) + (b_E^\alpha - b_E^E)\nu_{E,ext}, &(3.2) \\
a_\alpha(N_E(t), N_I(t)) &= d_\alpha + d_E^\alpha N_E(t) + d_I^\alpha N_I(t), \quad \alpha = E, I, &(3.3)
\end{aligned}
$$

where, for $i, \alpha = E, I$, $b_i^\alpha > 0$, $d_\alpha > 0$ and $d_i^\alpha \geq 0$, and b_i^α are the connectivity parameters for a spike emitted by a neuron of population i and arriving at a neuron of population α, and $\nu_{E,ext} \geq 0$ describes frequency of the external input. Both populations (excitatory and inhibitory) are coupled by means of the drift and diffusion coefficients. Moreover, the system (3.1) is nonlinear because the firing rates, N_α, are defined in terms of the boundary conditions for ρ_α.

Denoting the refractory period τ_α, different choices of $M_\alpha(t)$ can be considered: $M_\alpha(t) = N_\alpha(t - \tau_\alpha)$ (studied in [11]), and $M_\alpha(t) = \frac{R_\alpha(t)}{\tau_\alpha}$ (analyzed in [17]). Depending on the refractory state used, slightly different behaviors of the solutions will appear.

On the other hand, since the number of neurons is assumed to be preserved, we have the conservation

law:

$$\int_{-\infty}^{V_F} \rho_\alpha(v,t) \, dv + R_\alpha(t) = \int_{-\infty}^{V_F} \rho_\alpha^0(v) \, dv + R_\alpha^0 = 1 \quad \forall \, t \geq 0, \quad \alpha = E, I. \tag{3.4}$$

To finish the description of the model, we remark that system (3.1) also includes the case of only one population (in average excitatory or inhibitory), with refractory state and transmission delay. Specifically, we can remove α in (3.1) considering only one PDE for the probability density, $\rho(v,t)$, which is coupled to an ODE for the probability that a neuron is in a refractory state, $R(t)$:

$$\begin{cases} \dfrac{\partial \rho}{\partial t}(v,t) + \dfrac{\partial}{\partial v}[h(v, N(t-D))\rho(v,t)] - a(N(t-D))\dfrac{\partial^2 \rho}{\partial v^2}(v,t) = M(t)\delta(v - V_R), \\[2mm] \dfrac{dR(t)}{dt} = N(t) - M(t), \\[2mm] N(t) = -a(N(t-D))\dfrac{\partial \rho}{\partial v}(V_F, t) \geq 0, \\[2mm] \rho(-\infty, t) = 0, \quad \rho(V_F, t) = 0, \quad \rho(v,0) = \rho^0(v) \geq 0, \quad R(0) = R^0, \end{cases} \tag{3.5}$$

with drift and diffusion terms

$$\begin{aligned} h(v, N(t)) &= -v + bN(t) + \nu_{ext}, \tag{3.6} \\ a(N(t)) &= d_0 + d_1 N_E(t), \tag{3.7} \end{aligned}$$

where the connectivity parameter b is positive for an average-excitatory population and negative for an average-inhibitory population, and where $d_0 > 0$, $d_1 \geq 0$, and $\nu_{ext} \geq 0$ describes the external input (note that this parameter and $\nu_{E,ext}$ have different units, since ν_{ext} includes other model constants).

As in [15, 17] and Chapter 2, the notion of solution that we consider is the following:

Definition 3.1.1 *Let $\rho_\alpha \in L^\infty(\mathbb{R}^+; L^1_+((-\infty, V_F)))$, $N_\alpha \in L^1_{loc,+}(\mathbb{R}^+)$ and $R_\alpha \in L^\infty_+(\mathbb{R}^+)$ for $\alpha = E, I$. Then $(\rho_E, \rho_I, R_E, R_I, N_E, N_I)$ is a weak solution of (3.1)-(3.3) if for any test function $\phi(v,t) \in C^\infty((-\infty, V_F] \times [0,T])$ and such that $\frac{\partial^2 \phi}{\partial v^2}$, $v\frac{\partial \phi}{\partial v} \in L^\infty((-\infty, V_F) \times (0,T))$ the following relation*

$$\int_0^T \int_{-\infty}^{V_F} \rho_\alpha(v,t) \left[-\frac{\partial \phi}{\partial t} - \frac{\partial \phi}{\partial v} h^\alpha(v, N_E(t - D_E^\alpha), N_I(t - D_I^\alpha)) - a_\alpha(N_E(t - D_E^\alpha), N_I(t - D_I^\alpha))\frac{\partial^2 \phi}{\partial v^2} \right] dv dt$$

$$= \int_0^T [M_\alpha(t)\phi(V_R, t) - N_\alpha(t)\phi(V_F, t)] dt + \int_{-\infty}^{V_F} \rho_\alpha^0(v)\phi(v,0) dv - \int_{-\infty}^{V_F} \rho_\alpha(v,T)\phi(v,T) \, dv \tag{3.8}$$

is satisfied $\forall \, \alpha = E, I$, and R_α, for $\alpha = E, I$, are solutions of the ODEs

$$\frac{dR_\alpha(t)}{dt} = N_\alpha(t) - M_\alpha(t).$$

3.2   Finite time blow-up

To conclude the study about the long time behavior we have to remember that solutions to (3.1) may blow-up in finite time if there are no delays. Specifically, following similar steps as those developed in

[17] [Theorem 3.1] and Chapter 2 [Theorem 2.2.1], we can prove an analogous result for the general system (3.1) without delay between excitatory neurons, this is $D_E^E = 0$:

Theorem 3.2.1 *Assume that*

$$h^E(v, N_E, N_I) + v \geq b_E^E N_E - b_I^E N_I, \tag{3.9}$$

$$a_E(N_E, N_I) \geq a_m > 0, \tag{3.10}$$

$\forall\, v \in (-\infty, V_F]$, *and* $\forall\, N_I, N_E \geq 0$. *Assume also that* $D_E^E = 0$ *and that there exists some* $C > 0$ *such that*

$$\int_0^t N_I(s - D_I^E)\, ds \leq C\, t, \qquad \forall\, t \geq 0. \tag{3.11}$$

Then, a weak solution to the system (3.1) *cannot be global in time because one of the following reasons:*

- $b_E^E > 0$ *is large enough, for* ρ_E^0 *fixed.*

- ρ_E^0 *is 'concentrated enough' around* V_F:

$$\int_{-\infty}^{V_F} e^{\mu v}\rho_E^0(v)\, dv \geq \frac{e^{\mu V_F}}{b_E^E \mu}, \qquad \text{for a certain } \mu > 0 \tag{3.12}$$

and for $b_E^E > 0$ *fixed.*

Proof. Using (3.8), considering $\mu = \max\left(\frac{b_I^E C + 2V_F}{a_m}, \frac{1}{b_E^E}\right)$ and the multiplier $\phi(v) = e^{\mu v}$, a weak solution $(\rho_E(v, t), \rho_I(v, t), N_E(t), N_I(t))$ satisfies the following inequality

$$\begin{aligned}
\frac{d}{dt} \int_{-\infty}^{V_F} \phi(v)\rho_E(v, t)\, dv \;\geq\;& \mu \int_{-\infty}^{V_F} \phi(v)\left[b_E^E N_E(t) - b_I^E N_I(t - D_I^E) - v\right]\rho_E(v, t)\, dv \\
&+ \mu^2 a_m \int_{-\infty}^{V_F} \phi(v)\rho_E(v, t)\, dv + N_E(t)\left[\phi(V_R) - \phi(V_F)\right] \\
\;\geq\;& \mu\left[b_E^E N_E(t) - b_I^E N_I(t - D_I^E) - V_F + \mu a_m\right]\int_{-\infty}^{V_F}\phi(v)\rho_E(v, t)\, dv \\
&- N_E(t)\phi(V_F),
\end{aligned}$$

where assumptions (3.9)-(3.10) and the fact that $v \in (-\infty, V_F)$ and $N_E(t)\phi(V_R) > 0$ were used. This inequality, Grönwall's lemma (for details see Chapter 2 [Footnote 1]) and the definition of μ provide the following inequality for the exponential moment $M_\mu(t) := \int_{-\infty}^{V_F}\phi(v)\rho_E(v, t)\, dv$:

$$M_\mu(t) \;\geq\; e^{\mu \int_0^t f(s)\, ds}\left[M_\mu(0) - \phi(V_F)\int_0^t N_E(s)\, e^{-\mu \int_0^s f(z)\, dz}\, ds\right],$$

where $f(s) = b_E^E N_E(s) - b_I^E N_I(s - D_I^E) + \mu\, a_m - V_F$. Using the definition of μ and (3.11), we notice that

$$-\phi(V_F)\int_0^t N_E(s)\, e^{-\mu \int_0^s f(z)\, dz}\, ds \geq -\phi(V_F)\int_0^t N_E(s)\, e^{-\mu \int_0^s \left[b_E^E N_E(z) + \mu a_m - V_F\right]\, dz + \mu b_I^E C s}\, ds.$$

After some more computations that include integrating by parts and using the definition of μ the right hand side of the previous inequality can be bounded by $-\frac{\phi(V_F)}{\mu b_E^E}$:

$$-\phi(V_F) \int_0^t N_E(s) \, e^{-\mu \int_0^s \left[b_E^E N_E(z) + \mu a_m - V_F \right] \, dz + \mu b_I^E C s} \, ds$$

$$= \int_0^t \frac{\phi(V_F)}{\mu b_E^E} \frac{d}{ds} \left[e^{-\mu b_E^E \int_0^s N_E(z) \, dz} \right] e^{-\mu(\mu a_m - V_F - b_I^E C)s} \, ds$$

$$= \frac{\phi(V_F)}{\mu b_E^E} \left[e^{-\mu b_E^E \int_0^s N_E(z) \, dz} \, e^{-\mu(\mu a_m - V_F - b_I^E C)s} \right]_0^t$$

$$+ \mu(\mu a_m - V_F - b_I^E C) \frac{\phi(V_F)}{\mu b_E^E} \int_0^t e^{-\mu b_E^E \int_0^s N_E(z) \, dz} \, e^{-\mu(\mu a_m - V_F - b_I^E C)s} \, ds$$

$$= \frac{\phi(V_F)}{\mu b_E^E} e^{-\mu b_E^E \int_0^t N_E(z) \, dz} \, e^{-\mu(\mu a_m - V_F - b_I^E C)t} - \frac{\phi(V_F)}{\mu b_E^E}$$

$$+ \mu(\mu a_m - V_F - b_I^E C) \frac{\phi(V_F)}{\mu b_E^E} \int_0^t e^{-\mu b_E^E \int_0^s N_E(z) \, dz} \, e^{-\mu(\mu a_m - V_F - b_I^E C)s} \, ds$$

$$\geq -\frac{\phi(V_F)}{\mu b_E^E}. \tag{3.13}$$

Inequality (3.13) was achieved thanks to that the first and last addend of the third equality are positive (the last addend is positive because of the choice of μ). Finally, the following inequality holds

$$M_\mu(t) \geq e^{\mu \int_0^t f(s) \, ds} \left[M_\mu(0) - \frac{\phi(V_F)}{\mu b_E^E} \right].$$

We observe that if the initial state satisfies

$$b_E^E \mu \, M_\mu(0) > \phi(V_F), \tag{3.14}$$

then, denoting $K = M_\mu(0) - \frac{\phi(V_F)}{\mu b_E^E} > 0$,

$$\int_{-\infty}^{V_F} \phi(v)\rho_E(v,t) \, dv = M_\mu(t) \geq K e^{\mu \int_0^t f(s) \, ds}, \quad \forall \, t \geq 0. \tag{3.15}$$

On the other hand, using the again definition of μ and (3.11), we observe that

$$\mu \int_0^t f(s) \, ds \geq \mu \left[b_E^E \int_0^t N_E(s) \, ds + \left(\mu a_m - V_F - b_I^E C \right) t \right] \geq \mu V_F t. \tag{3.16}$$

Thus, $e^{\mu \int_0^t f(s) \, ds} \geq e^{\mu V_F t}$ and consequently, considering (3.15), we obtain

$$\int_{-\infty}^{V_F} \phi(v)\rho_E(v,t) \, dv = M_\mu(t) \geq K e^{\mu V_F t}.$$

On the other hand, since $\rho_E(v,t)$ is a probability density and $\mu > 0$, for all $t \geq 0$: $\int_{-\infty}^{V_F} \phi(v)\rho_E(v,t) \, dv \leq e^{\mu V_F}$, which leads to a contradiction if the weak solution is assumed to be global in time. Therefore,

to conclude the proof there only remains to show inequality (3.14) in the two cases of the theorem.

1. For a fixed initial datum and b_E^E large enough, μ, $M_\mu(0)$ and $\phi(V_F)$ are fixed, thus (3.14) holds.

2. For $b_E^E > 0$ fixed, if the initial data satisfy (3.12) then condition (3.14) holds immediately. Now, there only remains to show that such initial data exist.

   For that purpose we can approximate an initial Dirac mass at V_F by smooth probability densities, so that $\rho_E^0 \simeq \delta(v - V_F)$. This gives the following condition

   $$e^{\mu V_F} \geq \frac{e^{\mu V_F}}{b_E^E \mu},$$

   which is satisfied if $\mu > \frac{1}{b_E^E}$. So, with our initial choice of μ we can ensure that the set of initial data we are looking for is not empty. $\qquad\square$

Therefore, thanks to Theorem 3.2.1 we may conclude that, if system (3.1) has immediate spike transmissions between excitatory neurons, (that is $D_E^E = 0$) then solutions can blow-up, whether initially they are close enough to the threshold potential or whether the excitatory neurons are highly connected (that is b_E^E is large enough). In the numerical experiments of Section 3.4.2 we will show that the transmission delay between excitatory neurons prevent the blow-up phenomenon, but the remaining transmission delays cannot avoid it.

3.3 Steady states and long time behavior

3.3.1 Steady states

The study of the number of steady states for excitatory and inhibitory NNLIF neural networks, with refractory periods and transmission delays of the spikes (3.1) (considering R_α either as defined in [17] or in [11]), can be done combining the ideas of [15, 17] and Chapter 2 [Section 2.3.1], with the additional difficulty that the system to be dealt with is now more complicated. The steady states $(\rho_E, \rho_I, N_E, N_I, R_E, R_I)$ of (3.1) satisfy

$$\frac{\partial}{\partial v}[h^\alpha(v)\rho_\alpha(v) - a_\alpha(N_E, N_I)\frac{\partial \rho_\alpha}{\partial v}(v) + \frac{R_\alpha}{\tau_\alpha}H(v - V_R)] = 0, \quad R_\alpha = \tau_\alpha N_\alpha, \qquad \alpha = E, I,$$

in the sense of distributions, with H denoting the Heaviside function and $h^\alpha(v, N_E, N_I) = V_0^\alpha(N_E, N_I) - v$, where $V_0^\alpha(N_E, N_I) = b_E^\alpha N_E - b_I^\alpha N_I + (b_E^\alpha - b_E^E)\nu_{E,ext}$. We remark that this equation is the same as the equation for stationary solutions in a network without transmission delays. Using the definition of N_α and the Dirichlet bounday conditions of (3.1) we obtain an initial value problem for every $\alpha = E, I$, whose solutions are

$$\rho_\alpha(v) = \frac{N_\alpha}{a_\alpha(N_E, N_I)}e^{-\frac{(v - V_0^\alpha(N_E, N_I))^2}{2a_\alpha(N_E, N_I)}}\int_{\max(v, V_R)}^{V_F} e^{\frac{(w - V_0^\alpha(N_E, N_I))^2}{2a_\alpha(N_E, N_I)}}\,dw \qquad \alpha = E, I. \qquad (3.17)$$

Moreover, the conservation of mass (3.4), which takes into account the refractory states, yields a system of implicit equations for N_α

$$1 - \tau_\alpha N_\alpha = \frac{N_\alpha}{a_\alpha(N_E, N_I)} \int_{-\infty}^{V_F} e^{-\frac{(v - V_0^\alpha(N_E, N_I))^2}{2a_\alpha(N_E, N_I)}} \int_{\max(v, V_R)}^{V_F} e^{\frac{(w - V_0^\alpha(N_E, N_I))^2}{2a_\alpha(N_E, N_I)}} \, dw \, dv. \tag{3.18}$$

If this system could be solved, the profile (3.17) would provide an exact expression for ρ_α. In order to handle the previous system more easily, we use two changes of variables as in Chapter 2 [Section 2.3.1]. First:

$$z = \frac{v - V_0^E(N_E, N_I)}{\sqrt{a_E(N_E, N_I)}}, \ u = \frac{w - V_0^E(N_E, N_I)}{\sqrt{a_E(N_E, N_I)}}, \ w_F := \frac{V_F - V_0^E(N_E, N_I)}{\sqrt{a_E(N_E, N_I)}}, \ w_R := \frac{V_R - V_0^E(N_E, N_I)}{\sqrt{a_E(N_E, N_I)}},$$

$$\tilde{z} = \frac{v - V_0^I(N_E, N_I)}{\sqrt{a_I(N_E, N_I)}}, \ \tilde{u} = \frac{w - V_0^I(N_E, N_I)}{\sqrt{a_I(N_E, N_I)}}, \ \tilde{w}_F := \frac{V_F - V_0^I(N_E, N_I)}{\sqrt{a_I(N_E, N_I)}}, \ \tilde{w}_R := \frac{V_R - V_0^I(N_E, N_I)}{\sqrt{a_I(N_E, N_I)}},$$

and (3.18) is then written as

$$\frac{1}{N_E} - \tau_E = I_1(N_E, N_I), \ \text{where } I_1(N_E, N_I) = \int_{-\infty}^{w_F} e^{-\frac{z^2}{2}} \int_{\max(z, w_R)}^{w_F} e^{\frac{u^2}{2}} \, du \, dz,$$

$$\frac{1}{N_I} - \tau_I = I_2(N_E, N_I), \ \text{where } I_2(N_E, N_I) = \int_{-\infty}^{\tilde{w}_F} e^{-\frac{z^2}{2}} \int_{\max(z, \tilde{w}_R)}^{\tilde{w}_F} e^{\frac{u^2}{2}} \, du \, dz, \tag{3.19}$$

with gives leads to the natural restrictions

$$N_\alpha < \frac{1}{\tau_\alpha} \quad \alpha = E, I, \tag{3.20}$$

since $R_\alpha = \tau_\alpha N_\alpha$ and $R_\alpha \le 1$ (we also observe these restrictions by the positivity of I_α, see (3.19)). Next, the change of variables $s = \frac{z-u}{2}$ and $\tilde{s} = \frac{z+u}{2}$ allows to formulate the functions I_1 and I_2 as

$$I_1(N_E, N_I) = \int_0^\infty \frac{e^{-\frac{s^2}{2}}}{s} (e^{s \, w_F} - e^{s \, w_R}) \, ds, \tag{3.21}$$

$$I_2(N_E, N_I) = \int_0^\infty \frac{e^{-\frac{s^2}{2}}}{s} (e^{s \, \tilde{w}_F} - e^{s \, \tilde{w}_R}) \, ds. \tag{3.22}$$

If $b_I^E = b_E^I = 0$ the equations are uncoupled, we are then reduced to the case of article [17]. The following theorem analyses the coupled case.

Theorem 3.3.1 *Assume that $b_I^E > 0$, $b_E^I > 0$, $\tau_E > 0$, $\tau_I > 0$, $a_\alpha(N_E, N_I) = a_\alpha$ constant, and $h^\alpha(v, N_E, N_I) = V_0^\alpha(N_E, N_I) - v$ with $V_0^\alpha(N_E, N_I) = b_E^\alpha N_E - b_I^\alpha N_I + (b_E^\alpha - b_E^E)v_{E,ext}$ for $\alpha = E, I$. Then there is always an odd number of steady states for (3.1).*

Moreover, if b_E^E is small enough or τ_E is large enough (in comparison with the rest of parameters), then there is a unique steady state for (3.1).

Proof. The proof is based on determining the number of solutions of the system

$$1 = N_E\left(\tau_E + I_1(N_E, N_I)\right), \quad 0 < N_E < \frac{1}{\tau_E}, \tag{3.23}$$

$$1 = N_I\left(\tau_I + I_2(N_E, N_I)\right), \quad 0 < N_I < \frac{1}{\tau_I}. \tag{3.24}$$

With this aim, we adapt some ideas of [17] and Chapter 2 [Section 2.3.1] to the system (3.23)-(3.24). We refer to Chapter 2 [Section 2.3.1] for details about the properties of the functions I_1 and I_2 (see (3.21) and (3.22)) and their proofs.

First, we observe that for every $N_E > 0$ fixed, there is a unique solution $N_I(N_E)$ that solves (3.24), because for $N_E > 0$ fixed, the function $f(N_I) = N_I\left(\tau_I + I_2(N_E, N_I)\right)$ satisfies: $f(0) = 0$, $f(\frac{1}{\tau_I}) = 1 + \frac{I_2(N_E, \frac{1}{\tau_I})}{\tau_I} > 1$ and is increasing, since $I_2(N_E, N_I)$ is an increasing, strictly convex function on N_I.

Then, taking into account that the function $\mathcal{F}(N_E) := N_E[I_1(N_E, N_I(N_E)) + \tau_E]$ satisfies that $\mathcal{F}(0) = 0$ and $\mathcal{F}(\frac{1}{\tau_E}) = 1 + \frac{I_1\left(\frac{1}{\tau_E}, N_I(\frac{1}{\tau_E})\right)}{\tau_E} > 1$, it can be concluded that there is always an odd number of steady states.

Finally, to derive the sufficient condition to have a unique steady state, we analyze the derivative of $\mathcal{F}$:

$$\mathcal{F}'(N_E) = I_1(N_E, N_I(N_E)) + \tau_E + N_E\left[-\frac{b_E^E}{\sqrt{a_E}} + \frac{b_I^E}{\sqrt{a_E}}N_I'(N_E)\right]\int_0^\infty e^{\frac{-s^2}{2}}(e^{sw_F} - e^{sw_R})\, ds.$$

It is non-negative for $0 < N_E < \frac{1}{\tau_E}$, for certain parameter values, and therefore there is a unique steady state in these cases. For b_E^E small, $\mathcal{F}'(N_E)$ is positive since all the terms are positive, because $N_I'(N_E)$ is positive (see the proof of Theorem 2.3.1 in Chapter 2). For τ_E large, the proof of the positivity of $\mathcal{F}'(N_E)$ is more complicated. It is necessary to use

$$N_I'(N_E) = \frac{b_E^I N_I^2(N_E) I(N_E)}{\sqrt{a_I} + b_I^I N_I^2(N_E) I(N_E)}, \tag{3.25}$$

where

$$I(N_E) = \int_0^\infty e^{-s^2/2} e^{\frac{-(b_E^I N_E - b_I^I N_I(N_E) + (b_E^I - b_E^E)\nu_{E,ext})s}{\sqrt{a_I}}}\left(e^{sV_F/\sqrt{a_I}} - e^{sV_R/\sqrt{a_I}}\right)\, ds.$$

The function $N_I(N_E)$ is increasing and $I(N_E)$ is decreasing, since $0 < N_I'(N_E) < \frac{b_E^I}{b_I^I}$ (see the proof of Theorem 2.3.1 [Chapter 2]). Therefore, for $0 < N_E < \frac{1}{\tau_E}$,

$$A < -\frac{b_E^E}{\sqrt{a_E}} + \frac{b_I^E}{\sqrt{a_E}}N_I'(N_E) < B,$$

where $A := -\frac{b_E^E}{\sqrt{a_E}} + \frac{b_I^E}{\sqrt{a_E}}\frac{b_E^I N_I^2(0)I(\frac{1}{\tau_E})}{\sqrt{a_I}+b_I^I N_I^2(\frac{1}{\tau_E})I(0)}$ and $B := -\frac{b_E^E}{\sqrt{a_E}} + \frac{b_I^E}{\sqrt{a_E}}\frac{b_E^I N_I^2(\frac{1}{\tau_E})I(0)}{\sqrt{a_I}+b_I^I N_I^2(0)I(\frac{1}{\tau_E})}$. Thus, if $0 \leq A$ it is obvious that $\mathcal{F}(N_E)$ is increasing. For the case $A < 0$, some additional computations are needed.

First, we consider $I_m := \min_{0 \leq N_E \leq \frac{1}{\tau_E}} I_1(N_E, N_I(N_E))$. Next, since $A < 0$,

$$I_m + \tau_E + \frac{A}{\tau_E}\tilde{I}(\tau_E) \leq \mathcal{F}'(N_E),$$

where $\tilde{I}(\tau_E) := \int_0^\infty e^{-\frac{s^2}{2}} e^{\frac{sb_I^E N_I(\frac{1}{\tau_E})}{\sqrt{a_E}}} \left(e^{\frac{sV_F}{\sqrt{a_E}}} - e^{\frac{sV_R}{\sqrt{a_E}}} \right) ds$. Finally, if $0 < I_m + \tau_E + \frac{A}{\tau_E}\tilde{I}(\tau_E)$, or equivalently $-A\tilde{I}(\tau_E) < \tau_E(I_m + \tau_E)$, then $\mathcal{F}(N_E)$ is increasing. We observe that it happens for τ_E large enough. $\quad\square$

Remark 3.3.2 *Analyzing in more detail the expression of A in the previous proof ($A = -\frac{b_E^E}{\sqrt{a_E}} + \frac{b_I^E}{\sqrt{a_E}} \frac{b_E^I N_I^2(0)I(\frac{1}{\tau_E})}{\sqrt{a_I}+b_I^I N_I^2(\frac{1}{\tau_E})I(0)}$), we observe that for $b_E^I b_I^E$ large or b_I^I small enough, in comparison with the rest of parameters, there is also a unique stationary solution, since $A > 0$.*

In other words, what we obtain is the uniqueness of the steady state in terms of the size of the parameters. More precisely: If one of the two pure connectivity parameters, b_E^E or b_I^I, is small, or one of the two cross connectivity parameters, b_E^I or b_E^I, is large, or the excitatory refractory period, τ_E, is large, then there exists a unique steady state.

3.3.2 Long time behavior

As proved in [26] and Chapter 2 [Section 2.3.2], where no refractory states were considered, the solutions converge exponentialy fast to the unique steady state when the connectivity parameters are small enough. We extend these results to the case where there are refractory states but no delays. We prove the result for the case of only one population in the following theorem, and then show the general case of two populations.

Theorem 3.3.3 *Consider system (3.5) and $M(t) = \frac{R(t)}{\tau}$. Assume that the connectivity parameter b is small enough, $|b| << 1$, the diffusion term is constant, $a(N) = a$ for some $a > 0$, there is no transmission delay, $D = 0$, and that the initial datum is close enough to the unique steady state $(\rho_\infty, R_\infty, N_\infty)$,*

$$\int_{-\infty}^{V_F} \rho_\infty(v) \left(\frac{\rho^0(v) - \rho_\infty(v)}{\rho_\infty(v)} \right)^2 dv + R_\infty \left(\frac{R(0)}{R_\infty} - 1 \right)^2 \leq \frac{1}{2|b|}. \tag{3.26}$$

Then, for fast decaying solutions to (3.5) there is a constant $\mu > 0$ such that for all $t \geq 0$

$$\int_{-\infty}^{V_F} \rho_\infty(v) \left(\frac{\rho(v) - \rho_\infty(v)}{\rho_\infty(v)} \right)^2 dv + \frac{(R(t) - R_\infty)^2}{R_\infty} \leq e^{-\mu t} \left[\int_{-\infty}^{V_F} \rho_\infty \left(\frac{\rho^0(v) - \rho_\infty(v)}{\rho_\infty(v)} \right)^2 dv + \frac{(R^0 - R_\infty)^2}{R_\infty} \right].$$

Proof. The proof combines a relative entropy (see Chapter 2 [Footnote 2]) argument with the Poincaré's inequality that is presented in [17] [Proposition 5.3] extended to small connectivity parameters as done in Chapter 2 [Footnote 4]. Additionally, to deal with the nonlinearity (the connectivity parameter does not vanish) we follow some ideas of [26] [Theorem 2.1]. Notice that along the proof

we will use the simplified notation

$$p(v,t) = \frac{\rho(v,t)}{\rho_\infty(v)}, \qquad r(t) = \frac{R(t)}{R_\infty}, \qquad \eta(t) = \frac{N(t)}{N_\infty}.$$

First, for any smooth convex function $G : \mathbb{R}^+ \to \mathbb{R}$, we recall that a natural relative entropy for equation (3.5) is defined as

$$E(t) := \int_{-\infty}^{V_F} \rho_\infty G(p(v,t)) \ dv + R_\infty G(r(t)). \tag{3.27}$$

The time derivative of the relative entropy (3.27) can be written as

$$\frac{d}{dt}E(t) = -a\int_{-\infty}^{V_F} \rho_\infty(v)G''(p(v,t))\left[\frac{\partial p}{\partial v}\right]^2(v,t) \ dv$$
$$- N_\infty \left[G(\eta(t)) - G(p(V_R,t)) - (r(t)-p(V_R,t))G'(p(V_R,t)) - (\eta(t)-r(t))G'(r(t)\right] \tag{3.28}$$
$$+ b(N(t)-N_\infty)\int_{-\infty}^{V_F} \frac{\partial\rho_\infty}{\partial v}(v)\left[G(p(v,t)) - p(v,t)G'(p(v,t))\right] \ dv.$$

Expression (3.28) is achieved after some simple computations, taking into account that (ρ, R, N) is a solution of equation (3.5) and that $(\rho_\infty, R_\infty, N_\infty)$ is the unique steady state of the same equation, thus given by

$$\begin{cases} \dfrac{\partial}{\partial v}[h(v,N_\infty)\rho_\infty(v)] - a\dfrac{\partial^2\rho_\infty}{\partial v^2}(v) = \dfrac{R_\infty}{\tau}\delta(v-V_R), \\[2mm] R_\infty = \tau N_\infty, \quad N_\infty = -a\dfrac{\partial\rho_\infty}{\partial v}(V_F) \geq 0, \\[2mm] \rho_\infty(-\infty) = 0, \quad \rho_\infty(V_F) = 0. \end{cases}$$

Specifically, following a similar procedure to the one showed in the proof of Theorem 2.3.5 [Chapter 2], we can obtain sucessively the relations:

$$\frac{\partial p}{\partial t} - \left(v - bN + \frac{2a}{\rho_\infty}\frac{\partial\rho_\infty}{\partial v}\right)\frac{\partial p}{\partial v} - a\frac{\partial^2 p}{\partial v^2} = \frac{R_\infty}{\tau\rho_\infty}\delta(v-V_R)(r-p) - \frac{p}{\rho_\infty}b(N-N_\infty)\frac{\partial\rho_\infty}{\partial v}, \tag{3.29}$$

$$\frac{\partial G(p)}{\partial t} - \left(v - bN + \frac{2a}{\rho_\infty}\frac{\partial\rho_\infty}{\partial v}\right)\frac{\partial G(p)}{\partial v} - a\frac{\partial^2 G(p)}{\partial v^2}$$
$$= -G'(p)\frac{p}{\rho_\infty}b(N-N_\infty)\frac{\partial\rho_\infty}{\partial v} - aG''(p)\left(\frac{\partial p}{\partial v}\right)^2 + G'(p)\frac{R_\infty}{\tau\rho_\infty}\delta(v-V_R)(r-p), \tag{3.30}$$

and

$$\frac{\partial}{\partial t}\rho_\infty G(p) - \frac{\partial}{\partial v}\left[(v-bN)\rho_\infty G(p)\right] - a\frac{\partial^2}{\partial v^2}\left[\rho_\infty G(p)\right] \tag{3.31}$$
$$= b(N-N_\infty)\frac{\partial\rho_\infty}{\partial v}\left[G(p) - pG'(p)\right] - a\rho_\infty G''(p)\left(\frac{\partial p}{\partial v}\right)^2 + \frac{R_\infty}{\tau}\delta(v-V_R)\left[(r-p)G'(p) + G(p)\right].$$

Finally, (3.28) is obtained after integrating (3.31) with respect to v, between $-\infty$ and V_F, taking into

account that

$$a\frac{\partial}{\partial v}\left[\rho_\infty G\left(p\right)\right]_{v=V_F} = -N_\infty G\left(\eta\right),$$

due to the boundary condition at V_F and the l'Hopital rule, and adding

$$\frac{d}{dt}R_\infty G\left(r\right) = \frac{R_\infty}{\tau}R_\infty G'\left(r\right)\left(\eta - r\right). \tag{3.32}$$

To obtain the exponential rate of convergence stated in the theorem, we consider $G(x) = (x-1)^2$ in (3.28). Its first term is negative and will provide the strongest control when combined with the Poincaré's inequality. After some algebraical computations, the second term can be written as

$$-N_\infty[G(\eta(t)) - G(p(V_R, t)) - (r(t) - p(V_R, t))G'(p(V_R, t)) - (\eta(t) - r(t))G'(r(t))]$$
$$= -N_\infty[(r(t) - \eta(t))^2 + (r(t) - p(V_R, t))^2].$$

Applying the inequality $(a+b)^2 \geq \epsilon(a^2 - 2b^2)$ for $a, b \in \mathbb{R}$ and $0 < \epsilon < \frac{1}{2}$ (see Chapter 2 [Footnote 3]), we obtain

$$-N_\infty(r(t) - \eta(t))^2 \leq -\epsilon N_\infty(\eta(t) - 1)^2 + 2\epsilon N_\infty(r(t) - 1)^2. \tag{3.33}$$

Recalling the Poincaré's inequality of [17][Proposition 5.3], and in a similar way as in [26] and in Chapter 2 [Footnote 4], for small connectivity parameters, there exists $\gamma > 0$ such that:

$$\int_{-\infty}^{V_F}\frac{(\rho - \rho_\infty)^2}{\rho_\infty}dv + \frac{(R - R_\infty)^2}{R_\infty} \leq \frac{1}{\gamma}\left[\int_{-\infty}^{V_F}\rho_\infty(v)\left[\frac{\partial p}{\partial v}\right]^2(v,t)\,dv + N_\infty(r(t) - p(V_R, t))^2\right], \quad (3.34)$$

thus

$$(r(t) - 1)^2 \leq \frac{1}{\gamma R_\infty}\int_{-\infty}^{V_F}\rho_\infty(v)\left[\frac{\partial p}{\partial v}\right]^2(v,t)\,dv + \frac{N_\infty}{\gamma R_\infty}(r(t) - p(V_R, t))^2, \tag{3.35}$$

and therefore

$$2\epsilon N_\infty(r(t) - 1)^2 \leq \frac{2\epsilon N_\infty}{\gamma R_\infty}\int_{-\infty}^{V_F}\rho_\infty(v)\left[\frac{\partial p}{\partial v}\right]^2(v,t)\,dv + \frac{2\epsilon N_\infty}{\gamma R_\infty}N_\infty(r(t) - p(V_R, t))^2. \tag{3.36}$$

Joining now estimates (3.33) and (3.36), choosing $0 < \epsilon < \frac{1}{2}$ such that $\frac{2\epsilon N_\infty}{\gamma R_\infty} < \min(\frac{a}{2}, \frac{1}{2})$ and denoting $C_0 := \epsilon N_\infty$ yields

$$-N_\infty[G(\eta(t)) - G(p(V_R, t)) - (r(t) - p(V_R, t))G'(p(V_R, t)) - (\eta(t) - r(t))G'(r(t))]$$
$$\leq -C_0 G(\eta(t)) + \frac{a}{2}\int_{-\infty}^{V_F}\rho_\infty(v)\left[\frac{\partial p}{\partial v}\right]^2(v,t)\,dv - \frac{1}{2}N_\infty(r(t) - p(V_R, t))^2. \tag{3.37}$$

The third term can be bounded combining Young's and Cauchy-Schwarz's inequalities (see Chapter 2 [Footnotes 6 and 5, respectively]) as it has already been done for one of the last two addends of expression (2.51) [Chapter 2] during the proof of Theorem 2.3.5 [Chapter 2]. Thus, for some $C > 0$

we have

$$b(N(t) - N_\infty) \int_{-\infty}^{V_F} \frac{\partial \rho_\infty}{\partial v}(v)[G(p(v,t)) - p(v,t)G'(p(v,t))]\ dv \qquad (3.38)$$

$$\leq\ C(2b^2 + |b|)(\eta(t) - 1)^2 + a \int_{-\infty}^{V_F} \rho_\infty \left[\frac{\partial p}{\partial v}\right]^2 (v,t)\ dv \left(\frac{1}{2} + |b| \int_{-\infty}^{V_F} \rho_\infty(v)(p(v,t) - 1)^2\ dv \right).$$

Combining estimates (3.37) and (3.38) gives the bound

$$\frac{d}{dt} E(t) \leq - C_0(\eta(t) - 1)^2 + C(2b^2 + |b|)(\eta(t) - 1)^2 - \frac{1}{2} N_\infty (r(t) - p(V_R,t))^2$$

$$- a \int_{-\infty}^{V_F} \rho_\infty(v) \left[\frac{\partial p}{\partial v}\right]^2 (v,t)\ dv \left(1 - |b| \int_{-\infty}^{V_F} \rho_\infty(v)(p(v,t) - 1)^2\ dv \right).$$

Taking now b small enough such that $C(2b^2 + |b|) \leq C_0$ we obtain

$$\frac{d}{dt} E(t) \leq - \tilde{C} \left[\int_{-\infty}^{V_F} \rho_\infty(v) \left[\frac{\partial p}{\partial v}\right]^2 (v,t)\ dv + N_\infty (r(t) - p(V_R,t))^2 \right]$$

$$- \frac{a}{2} \int_{-\infty}^{V_F} \rho_\infty(v) \left[\frac{\partial p}{\partial v}\right]^2 (v,t)\ dv \left(1 - 2|b| \int_{-\infty}^{V_F} \rho_\infty(v)(p(v,t) - 1)^2\ dv \right)$$

$$\leq -\mu E(t) - \frac{a}{2} (1 - 2|b|E(t)) \int_{-\infty}^{V_F} \rho_\infty(v) \left[\frac{\partial p}{\partial v}\right]^2 (v,t)\ dv,$$

where Poincaré's inequality (3.34) was used, with $\tilde{C} = \min(\frac{a}{2}, \frac{1}{2})$, $\mu = \tilde{C}\gamma$. Finally, thanks to the choice of the initial datum (3.26) and Grönwall's inequality, the relative entropy decreases for all times so that, $E(t) \leq \frac{1}{2|b|}$, $\forall t \geq 0$, and the result is proved:

$$E(t) \leq e^{-\mu t} E(0) \leq e^{-\mu t} \frac{1}{2|b|}.$$

□
For two populations with refractory states (as given in model [17]), this exponential rate of convergence to the unique steady can also be proved. The proof is achieved by considering the full entropy for both populations:

$$\mathcal{E}[t] := \int_{-\infty}^{V_F} \rho_E^\infty(v) \left(\frac{\rho_E(v) - \rho_E^\infty(v)}{\rho_E^\infty(v)} \right)^2\ dv + \int_{-\infty}^{V_F} \rho_I^\infty(v) \left(\frac{\rho_I(v) - \rho_I^\infty(v)}{\rho_I^\infty(v)} \right)^2\ dv$$

$$+ \frac{(R_E(t) - R_E^\infty)^2}{R_E^\infty} + \frac{(R_I(t) - R_I^\infty)^2}{R_I^\infty},$$

and proceeding in the same way as in Chapter 2 [Theorem 2.3.4], taking into account that now there are some terms with refractory states which have to be handled, as in Theorem 3.3.3. This result can be summarized in the following theorem:

Theorem 3.3.4 *Consider system (3.1) for two populations, with $M_\alpha(t) = \frac{R_\alpha(t)}{\tau_\alpha}$, $\alpha = I, E$. Assume that the connectivity parameters b_i^α are small enough, the diffusion terms $a_\alpha > 0$ are constant, the transmission delays D_i^α vanish ($\alpha = I, E$, $i = I, E$), and that the initial data (ρ_E^0, ρ_I^0) are close enough*

to the unique steady state $(\rho_E^\infty, \rho_I^\infty)$:

$$\mathcal{E}[0] < \frac{1}{2\max\left(b_E^E + b_I^E, b_E^I + b_I^I\right)}.$$

Then, for fast decaying solutions to (3.1), there is a constant $\mu > 0$ such that for all $t \geq 0$

$$\mathcal{E}[t] \leq e^{-\mu t}\mathcal{E}[0].$$

Consequently, for $\alpha = E, I$

$$\int_{-\infty}^{V_F} \rho_\alpha^\infty(v)\left(\frac{\rho_\alpha(v) - \rho_\alpha^\infty(v)}{\rho_\alpha^\infty(v)}\right)^2 dv + \frac{(R_\alpha(t) - R_\alpha^\infty)^2}{R_\alpha^\infty} \leq e^{-\mu t}\mathcal{E}[0].$$

The solutions also converge exponentially fast to the steady state for small non-zero values of the delay(s) for both the one and the two population model. In order to proof this result we have to proceed as above, with the main difference that we have to use some a priori L^2 estimates, similar to the ones of [26] [Section 3], to control the firing rate(s).

3.4   Numerical experiments

3.4.1   Numerical scheme

The numerical scheme used to simulate equation (3.5) approximates the advection term by a fifth order finite difference flux-splitting WENO scheme, see Appendix A [Section A.2] for details. The flux-splitting considered is the Lax-Friedrich splitting [90]

$$f_{pos}(\rho) = \frac{1}{2}(f(\rho) + \alpha\rho), \quad f_{neg}(\rho) = \frac{1}{2}(f(\rho) - \alpha\rho) \quad \text{where} \quad \alpha = \max_\rho |f'(\rho)|. \tag{3.39}$$

In our case $f(\rho) = h(v, N)\rho$, and thus $\alpha = \max_{v \in (-\infty, V_F)} |h(v, N)|$. The diffusion term is estimated by standard second order finite differences, see Appendix A [Section A.3], and the time evolution is calculated by an explicit third order TVD Runge-Kutta method, explained in A [Section A.4].

Due to the delay, during the time evolution of the solution we have to recover the value of N at time $t - D$, for every time t. To implement this, we fix a time step $\overline{dt}$ and define an array of $M = \frac{D}{\overline{dt}}$ positions. Therefore, this array will save only M values of $N(t)$ for a time interval $[kD, (k+1)D)$, $k = 0, 1, 2, ...$ In the time interval $[(k+1)D, (k+2)D)$ these values of the array will be used to obtain the delayed values $N(t-D)$ by linear interpolation between the corresponding positions of the array. We assume that $N(t) = 0 \; \forall t < 0$, so initially all the values of the array are zero, and the recovered values for the first time interval $(k = 0)$ are all zero. Notice that we use linear interpolation since the time step dt for the time evolution is taken according to the CFL condition, for details see Appendix A [Section A.4]. Furthermore, once a position of the array is no longer necessary for the interpolation, it is overwritten.

The refractory state used in [11] is based on considering a delayed firing rate, $N(t - \tau)$, on the right hand side of the PDE for ρ. This value is recovered in the same manner as the delayed N that appears due to the transmission delay. The refractory period τ and the delay D do not usually

coincide, and thus the firing rates have to be saved in two different arrays. The refractory state for which $M(t) = \frac{R(t)}{\tau}$ was implemented using a finite difference approximation of its ODE.

The numerical approximation of the solution for the two-populations model was implemented using the same numerical scheme as that described above for one population. The main difference here is that the code runs over two cores using parallel computational techniques, following the ideas in Chapter 2 [Section 2.4.1]. Each core handles the equations of one of the populations. At the end of every time step the cores communicate via Message Passing Interface (MPI) to exchange the values of the firing rates. Also the transmission delays were handled as for one population, taking into account that now each processor has to save two arrays of firing rates, one for each population, since there are four different delays. The approximation of the different refractory states was done as for one population.

3.4.2 Numerical results

For the following simulations we will consider a uniform mesh for $v \in [-V_{left}, V_F]$, where $-V_{left}$ is chosen so that $\rho_\alpha(-V_{left}, t) \sim 0$. Moreover, unless otherwise specified, $V_F = 2$, $V_R = 1$, $\nu_{E,ext} = 0$ and $a_\alpha(N_E, N_I) = 1$. We will consider two different types of initial condition:

$$\rho_\alpha^0(v) = \frac{k}{\sqrt{2\pi}} e^{-\frac{(v - v_0^\alpha)^2}{2\sigma_0^{\alpha 2}}}, \tag{3.40}$$

where k is a constant such that $\int_{-V_{left}}^{V_F} \rho_\alpha^0(v) \, dv \approx 1$ numerically, and

$$\rho_\alpha^0(v) = \frac{N_\alpha}{a_\alpha(N_E, N_I)} e^{-\frac{(v - V_0^\alpha(N_E, N_I))^2}{2a_\alpha(N_E, N_I)}} \int_{\max(v, V_R)}^{V_F} e^{\frac{(w - V_0^\alpha(N_E, N_I))^2}{2a_\alpha(N_E, N_I)}} \, dw, \quad \alpha = E, I, \tag{3.41}$$

with $V_0^\alpha(N_E, N_I) = b_E^\alpha N_E - b_I^\alpha N_I + (b_E^\alpha - b_E^E)\nu_{E,ext}$ and where N_α is an approximated value of the stationary firing rate. The second kind of initial data is an approximation of the steady states of the system and allows us to study their local stability.

Notice that we will also refer to (3.40) as the initial condition for the one-population model by just considering $\rho_\alpha = \rho$, $v_0^\alpha = v_0$ and $\sigma_0^{\alpha 2} = \sigma_0^2$.

Analysis of the number of steady states

As a first step in our numerical analysis we illustrate numerically some of the results of Theorem 3.3.1. Fig. 3.1 shows the behaviour of $\mathcal{F}(N_E) := N_E[I_1(N_E, N_I(N_E) + \tau_E]$ for different parameter values, which produces bifurcation diagrams. In the figure on the left we observe the influence of the excitatory refractory period τ_E, considering fixed the rest of parameters; a large τ_E gives rise to the uniqueness of the steady state. In figure on the right one, the impact of the connectivity parameter b_E^E is described. In this case, a small b_E^E guarantees a unique stationary solution. Moreover, as noted in Remark 3.3.2, we observe the uniqueness of the steady state if the system is highly connected between excitatory and inhibitory neurons, or if the excitatory neurons have enough refractory period.

As happens in the case of only one population [17], for two populations (excitatory and inhibitory), neurons in a refractory state guarantee the existence of stationary states. (However, the refractory

state itself does not prevent the blow-up phenomenon, as shown in Theorem 3.2.1 and Figs. 3.3, 3.4 and 3.5).

Blow-up

In [17], the blow-up phenomenon for one population of neurons with refractory states was shown. Theorem 3.2.1 extends this result to two populations of neurons, one excitatory and the other one inhibitory. The refractory period is not enough to deter the blow-up of the network; if the membrane potentials of the excitatory population are close to the threshold potential, or if the connectivity parameter b_E^E is large enough, then the network blows-up in finite time. To achieve the global-in-time existence, it seems necessary some transmission delay between excitatory neurons, as we observe in our simulations and as it was proved at the microscopic level for one population [38].

We start the analysis of the blow-up phenomenon by considering only one average-excitatory population (we recall that there is global existence for one average-inhibitory population, see [29]). In [17] it was proved that some solutions blow-up. In Fig. 3.2, we show how the transmission delay of the spikes between neurons prevents the network from blowing-up in finite time.

In Chapter 2, the excitatory-inhibitory system without refractory states was studied. In the current chapter, we extend this analysis to the presence of refractory states. Figs. 3.3 and 3.4 illustrate the results of Theorem 3.2.1; if there is no transmission delay between excitatory neurons, the solution blows-up because most of the excitatory neurons have a membrane potential close to the threshold potential, or because excitatory neurons are highly connected, that is, b_E^E is large enough. We observe in Fig. 3.5 that the remaining delays do not avoid the blow-up phenomenon, since in this figure all the delays are 0.1, except $D_E^E = 0$. The importance of D_E^E is discerned in Fig. 3.6. We show the evolution in time of the solution of (3.1), with the same initial data as considered in Fig. 3.4 and with $D_E^E = 0.1$; in this case, the solution exists for every time, thus avoiding the blow-up.

Steady states and periodic solutions

In Fig. 3.1 we examined several choices of the model parameters, for which the system (3.1) presents three steady states. For one of these cases, the analysis of their stability is numerically investigated in Fig. 3.7. For $\alpha = E, I$, the initial conditions $\rho_\alpha^0 - 1, 2, 3$ are given by the profiles (3.41), where N_α are approximations of the stationary firing rates. The evolution in time of the probability densities, the firing rates and the refractory states show that the lower steady state seems to be stable, while the two others are unstable. Moreover, considering as initial data (3.41) with N_α approximations of the higher stationary firing rates the solution blows-up in finite time, while with the intermediate firing rate the solution tends to the lower steady state. Fig. 3.8 also describes the stability when there are three steady states. In this case the intermediate state is very close to the highest one. Here, the lower steady state also appears to be stable. The two others are unstable, but the higher one does not blow-up in finite time.

The transmission delay not only prevents the blow-up phenomenon, but also should produce periodic solutions. In Fig. 3.9, we analyze the influence of the transmission delay for one average-excitatory population; if the initial datum is concentrated around V_F, periodic solutions appear; on the contrary, if it is far from V_F, the solution reaches a steady state. In Figs. 3.10 and 3.11, for one average-inhibitory population with transmission delay, we show that periodic solutions emerge if the initial condition is concentrated around the threshold potential, and even if the initial datum is far from the threshold and v_{ext} is large. A comparison between $R(t)$ and $N(t)$ for $M(t) = \frac{R(t)}{\tau}$ and $M(t) = N(t-\tau)$ is presented in Fig. 3.12. In both cases the steady state is the same and the solutions tend to it. If the

system tends to a synchronous state, these states are also almost the same for both possible choices of M.

Synchronous states appear also in the case of two populations (excitatory and inhibitory), as it is described in Fig. 3.13. In this particular case, they seem to appear due to the inhibitory population, which tends to a periodic solution. What is more, the excitatory population presents a solution that oscillates close around the equilibrium.
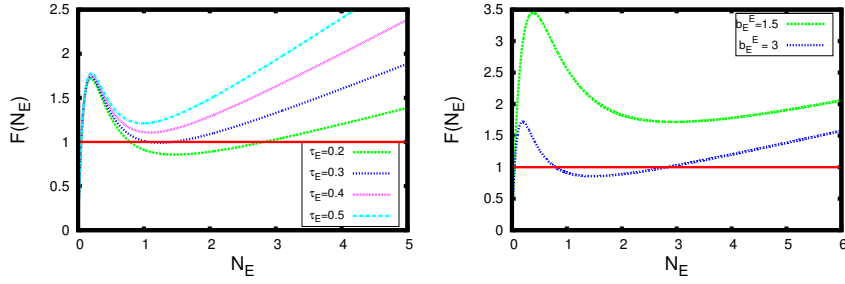
Figure 3.1: **Number of steady states for system (3.1) described by Theorem 3.3.1.-** Left: For fixed $b_I^E = 7$, $b_I^I = 2$, $b_E^E = 0.01$, $b_E^E = 3$ and $\tau_I = 0.2$, we observe the influence of the excitatory refractory period τ_E. Right: For fixed $b_I^E = 7$, $b_I^I = 2$, $b_E^I = 0.01$ and $\tau_E = \tau_I = 0.2$, we observe the influence of the connectivity parameter b_E^E.
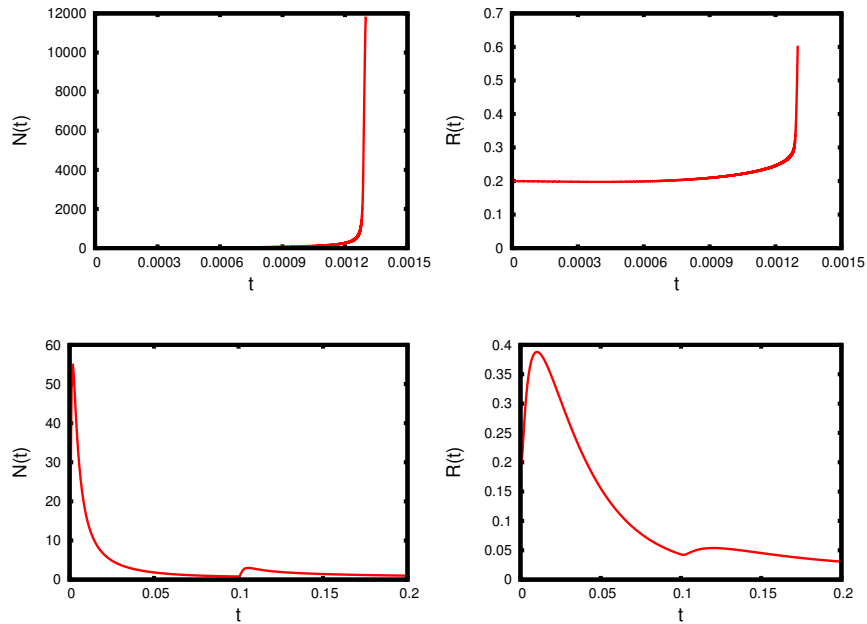
Figure 3.2: **System (3.5) (only one population) presents blow-up, if there is no transmission delay.-** We consider the initial data (3.40) with $v_0 = 1.83$, and $\sigma_0 = 0.0003$, and the connectivity parameter $b = 0.5$. Top: With refractory state $(M(t) = \frac{R(t)}{\tau})$, $R(0) = 0.2$, $\tau = 0.025$ and $D = 0$, since there is no transmission delay N and R blow-up in finite time.
Bottom: With refractory state $(M(t) = \frac{R(t)}{\tau})$, $R(0) = 0.2$, $\tau = 0.025$ and $D = 0.07$, the solution tends to the steady state, due to the transmission delay.
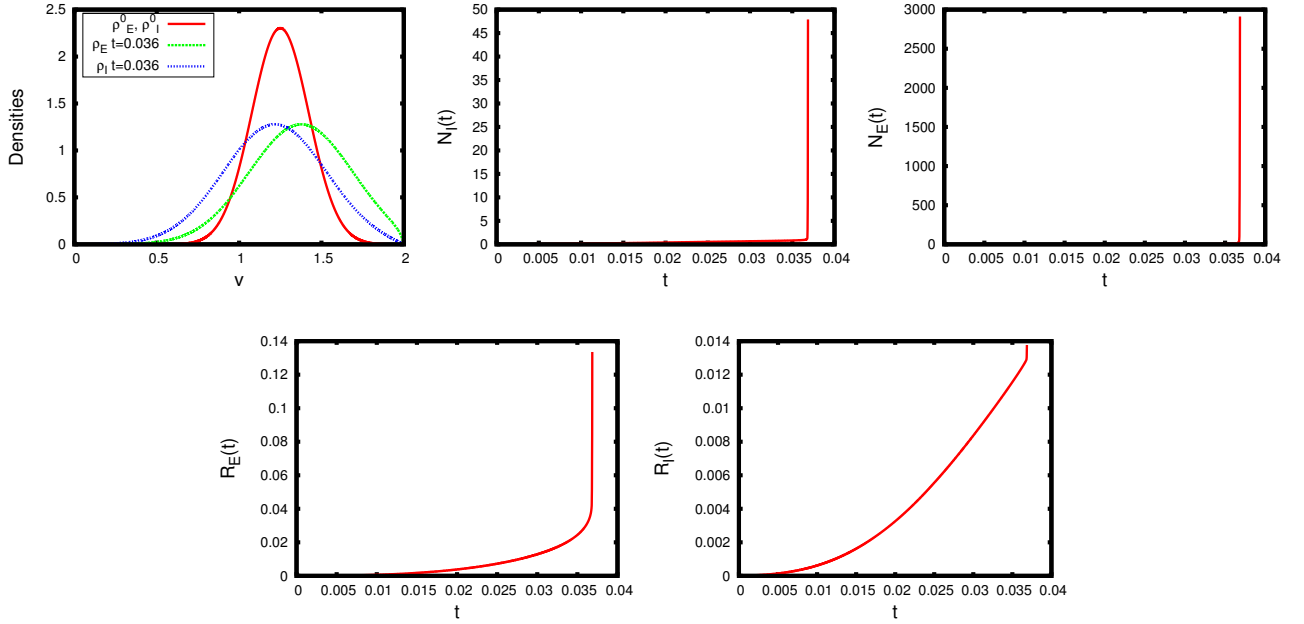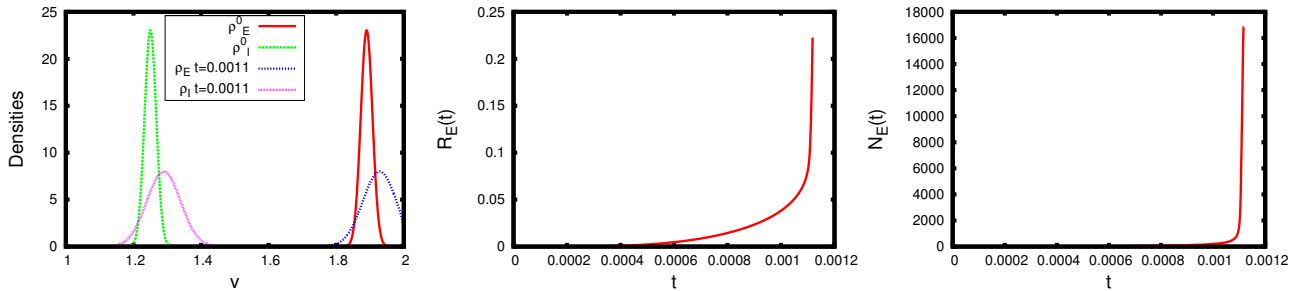
Figure 3.3: **System (3.1) (two populations: excitatory and inhibitory) presents blow-up, if there are no transmission delays.-** We consider initial data (3.40) with $v_0^E = v_0^I = 1.25$ and $\sigma_0^E = \sigma_0^I = 0.0003$, the connectivity parameters $b_E^E = 6$, $b_I^E = 0.75$, $b_I^I = 0.25$, $b_E^I = 0.5$, and with refractory states $(M_\alpha(t) = N_\alpha(t - \tau_\alpha))$ where $\tau_\alpha = 0.025$. We observe that the initial data are not concentrated around the threshold potential but the solution blows-up because $b_E^E = 6$ is large enough and there are no transmission delays (see Theorem 3.2.1).

Figure 3.4: **System (3.1) (two populations: excitatory and inhibitory) presents blow-up, if there are no transmission delays.-** We consider initial data (3.40) with $v_0^E = 1.89$, $v_0^I = 1.25$ and $\sigma_0^E = \sigma_0^I = 0.0003$, the connectivity parameters $b_E^E = 0.5$, $b_I^E = 0.75$, $b_I^I = 0.25$, $b_E^I = 0.5$, and with refractory states $(M_\alpha(t) = N_\alpha(t - \tau_\alpha))$ where $\tau = 0.025$. We observe that $b_E^E = 0.5$ is not large enough, but the solution blows-up because the initial condition for the excitatory population is concentrated around the threshold potential and there are no transmission delay (see Theorem 3.2.1).
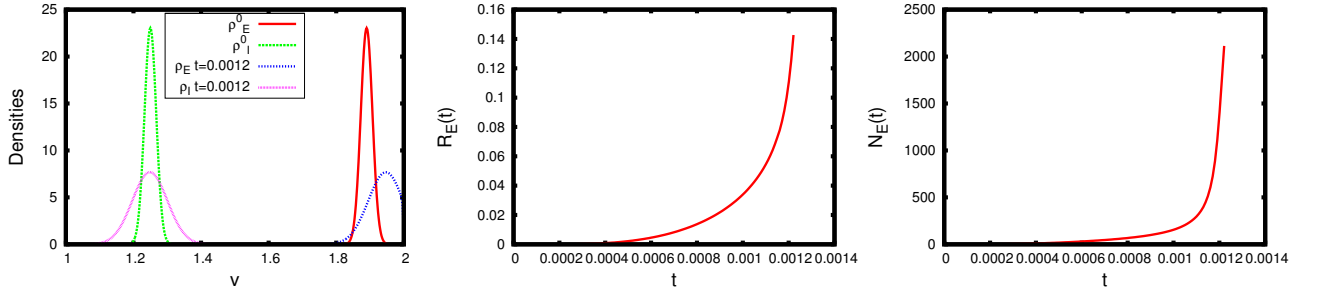
118

Figure 3.5: **System (3.1) (two populations: excitatory and inhibitory) presents blow-up, if there is no excitatory transmission delay.-** We consider initial data (3.40) with $v_0^E = 1.89$, $v_0^I = 1.25$ and $\sigma_0^E = \sigma_0^I = 0.0003$, the connectivity parameters $b_E^E = 0.5$, $b_I^E = 0.75$, $b_I^I = 0.25$, $b_E^I = 0.5$, and with refractory states $(M_\alpha(t) = N_\alpha(t - \tau_\alpha))$ where $\tau_\alpha = 0.025$. All the delays are 0.1, except $D_E^E = 0$. We observe that the other delays do not avoid the blow-up due to a concentrated initial condition for the excitatory population.
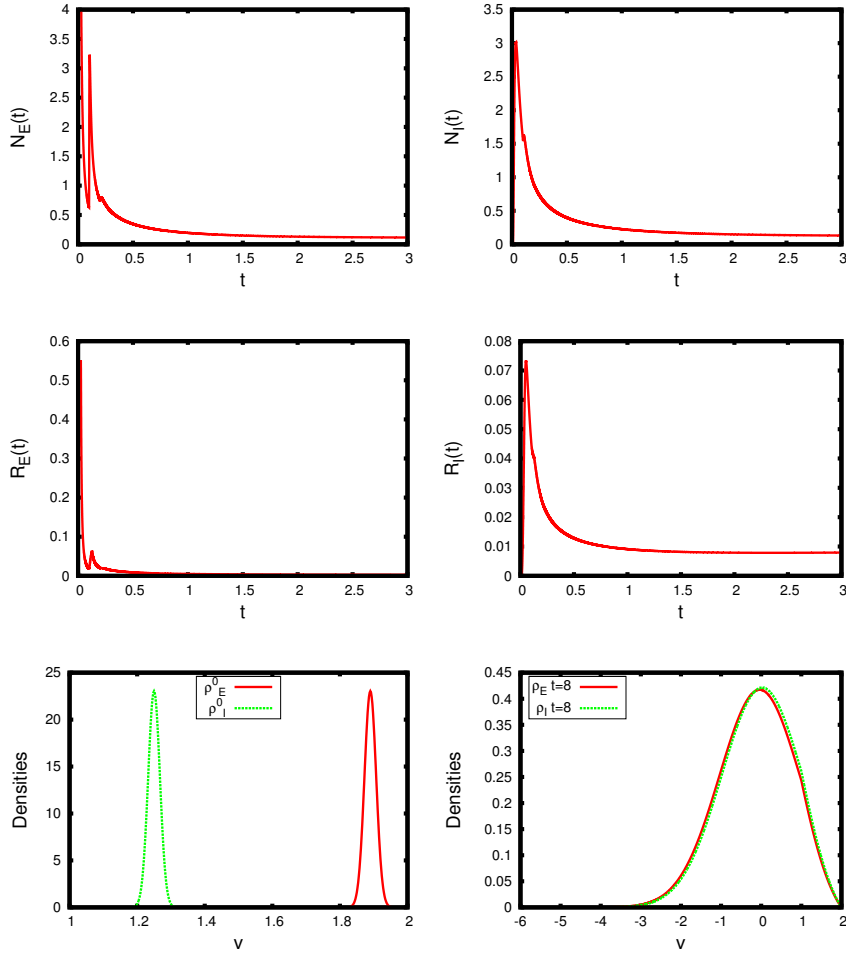
Figure 3.6: **System (3.1) (two populations: excitatory and inhibitory) avoids blow-up, if there is a transmission delay between excitatory neurons.-** We consider initial data (3.40) with $v_0^E = 1.89$, $v_0^I = 1.25$ and $\sigma_0^E = \sigma_0^I = 0.0003$, the connectivity parameters $b_E^E = 0.5$, $b_I^E = 0.75$, $b_I^I = 0.25$, $b_E^I = 0.5$, $D_E^I = D_I^E = D_I^I = 0$, and with refractory states $(M_\alpha(t) = N_\alpha(t - \tau_\alpha))$ where $\tau = 0.025$. We observe that if there is a transmission delay between excitatory neurons $D_E^E = 0.1$, the blow-up phenomenon is avoided. Top: Firing rates. Middle: Refractory states. Bottom: Probability densities.
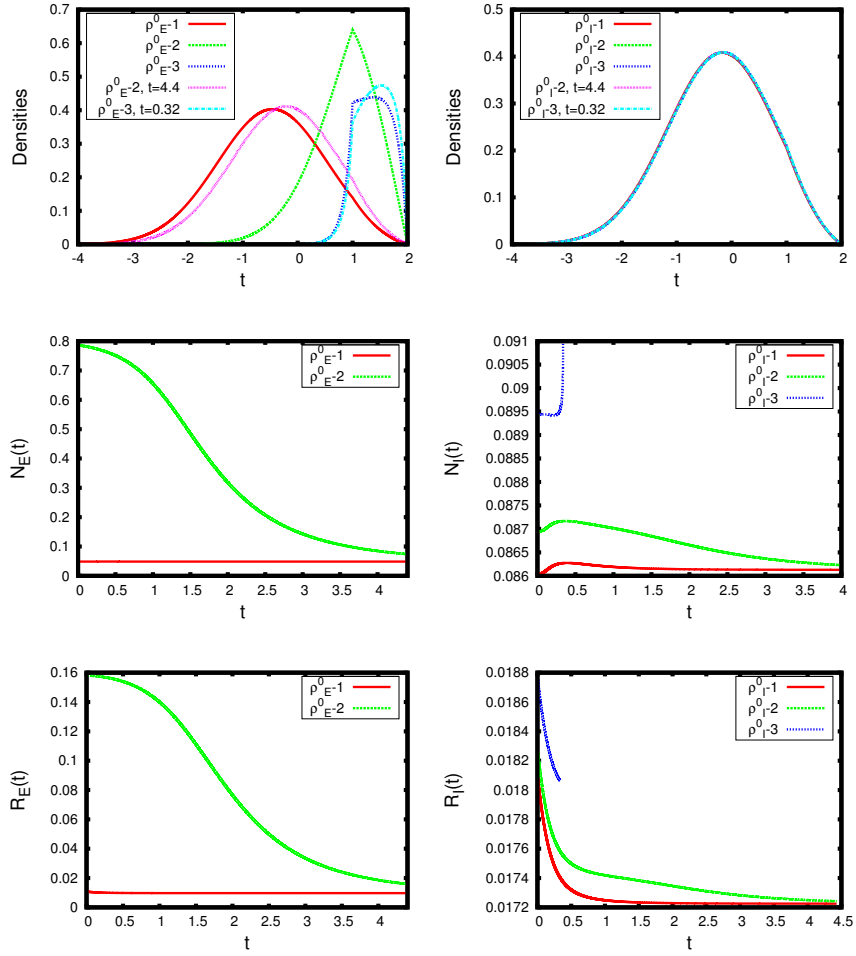
Figure 3.7: **Numerical analysis of the stability in the case of three steady states for the system** (3.1).**-** If $b_I^E = 7$, $b_I^I = 2$, $b_E^I = 0.01$, $\tau_E = \tau_I = 0.2$ and $b_E^E = 3$, there are three steady states (see Fig. 3.1). Top: Initial conditions $\rho_\alpha^0 - 1, 2, 3$ given by the profile (3.41), where N_α are approximations of the stationary firing rates, and evolution of densities 2 and 3 after some time. Middle: Evolution of the excitatory firing rates and the refractory states. Bottom: Evolution of the inhibitory firing rates and the refractory states.
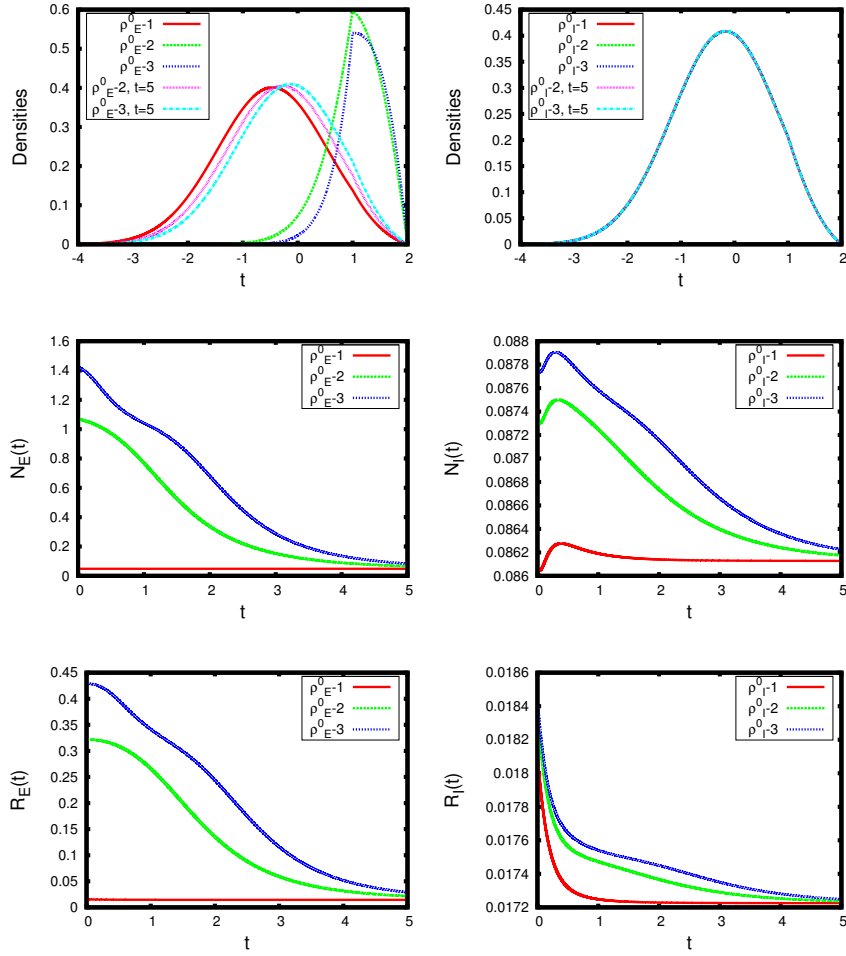We observe that the lowest steady state is stable and the other two are unstable.

Figure 3.8: **Numerical analysis of the stability in the case of three steady states for the system** (3.1).- If $b_I^E = 7$, $b_I^I = 2$, $b_E^E = 0.01$, $\tau_E = 0.3$, $\tau_I = 0.2$ and $b_E^E = 3$, there are three steady states (see Fig. 3.1). Top: Initial conditions $\rho_\alpha^0 - 1, 2, 3$ given by the profile (3.41), where N_α are approximations of the stationary firing rates, and evolution of densities 2 and 3 after some time. Middle: Evolution of the excitatory firing rates and the refractory states. Bottom: Evolution of the inhibitory firing rates and the refractory states.

We observe that the lowest steady state is stable and the other two are unstable.
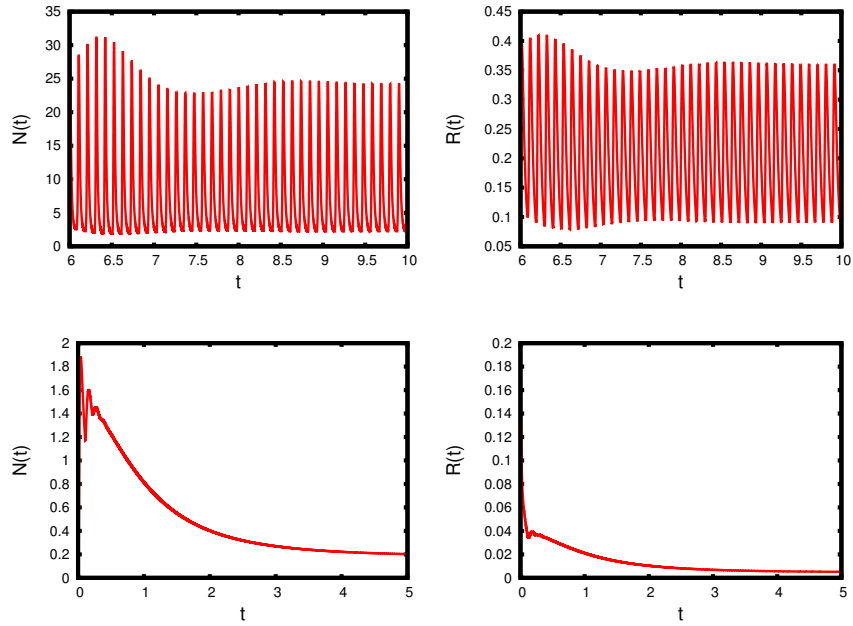
Figure 3.9: **System (3.5) (only one average-excitatory population) presents periodic solutions, if there is a transmission delay.-** We consider initial data (3.40) with $\sigma_0 = 0.0003$, the connectivity parameter $b = 1.5$, the transmission delay $D = 0.1$, $v_{ext} = 0$ and with refractory states $(M(t) = \frac{R(t)}{\tau})$, where $\tau = 0.025$ and $R(0) = 0.2$.
Periodic solutions appear if the initial condition is concentrated enough around the threshold potential
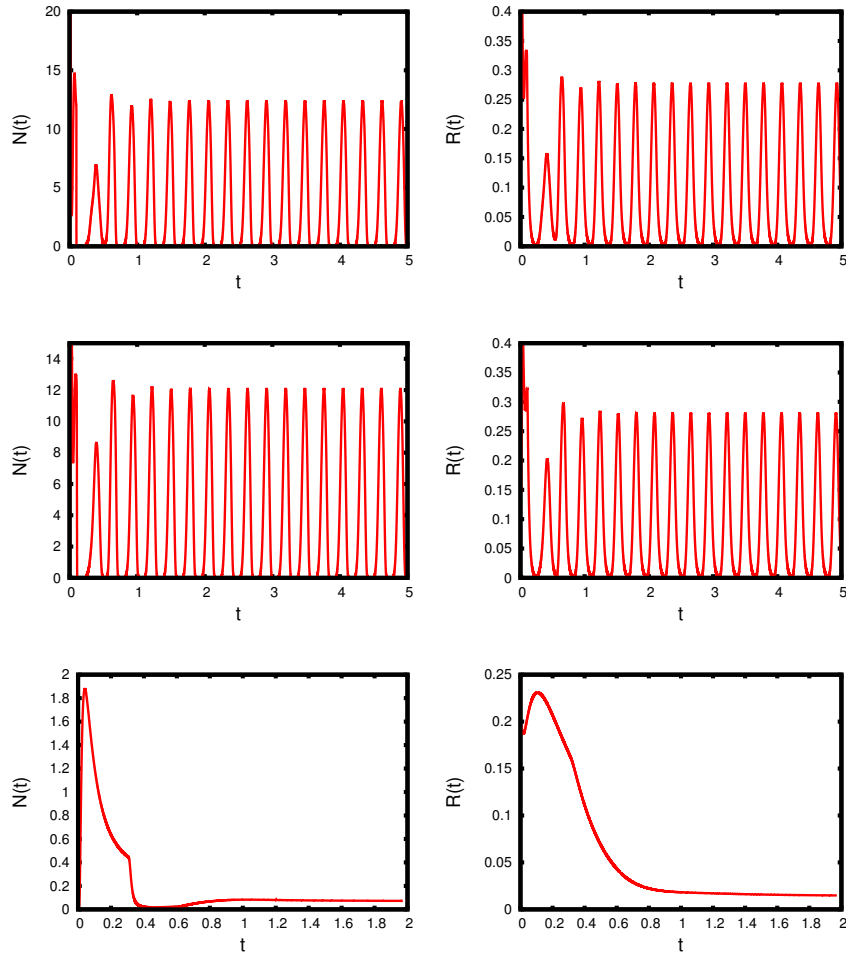Top: $v_0 = 1.83$. Botton: $v_0 = 1.5$.

Figure 3.10: **System (3.5) (only one average-inhibitory population) presents periodic solutions, if there is a transmission delay.-** We consider initial data (3.40) with $\sigma_0 = 0.0003$, the connectivity parameter $b = -4$, the transmission delay $D = 0.1$, and with refractory states $(M(t) = \frac{R(t)}{\tau})$, where $\tau = 0.025$ and $R(0) = 0.2$.

Periodic solutions appear if the initial condition is concentrated enough around the threshold potential, but even if the initial datum is far from the threshold and the v_{ext} is large. Top: $v_0 = 1.83$, $v_{ext} = 20$. Middle: $v_0 = 1.5$, $v_{ext} = 20$. Bottom: $v_0 = 1.5$, $v_{ext} = 0$.
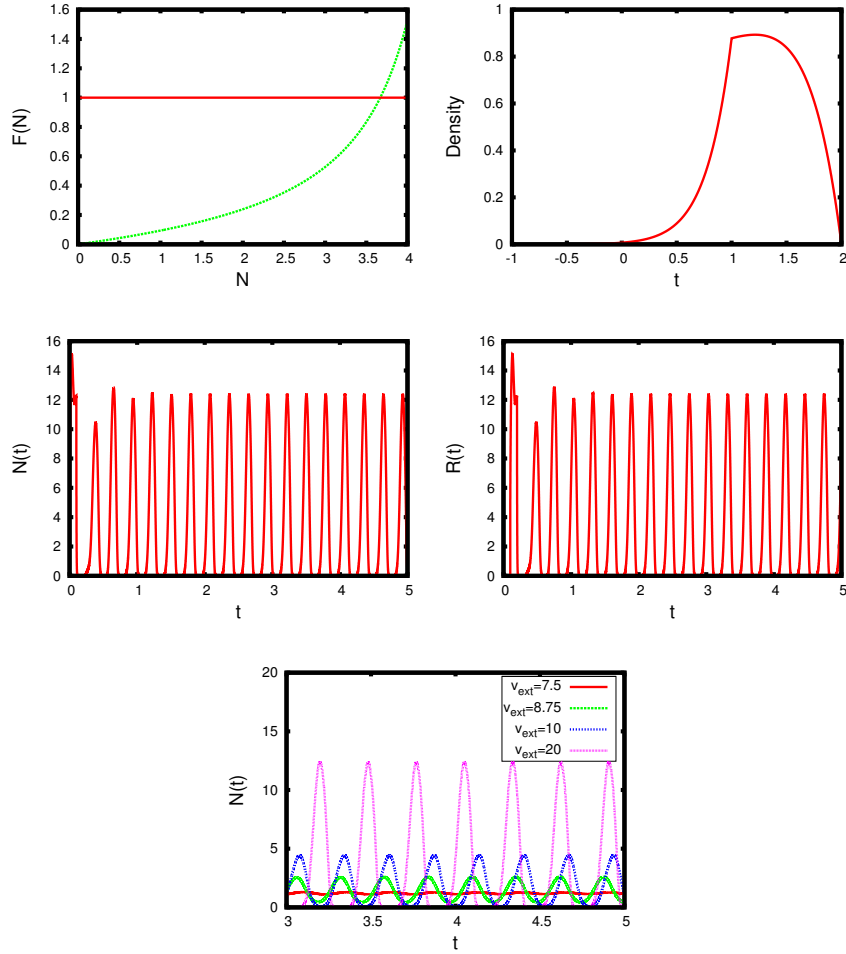
Figure 3.11: **System (3.5) (only one average-inhibitory population) presents periodic so-
lutions, if there is a transmission delay.-** We consider initial data (3.41) with $N = 3.669$, the
connectivity parameter $b = -4$, the transmission delay $D = 0.1$, $v_{ext} = 20$ and with refractory states
$(M(t) = \frac{R(t)}{\tau})$, where $\tau = 0.025$ and $R(0) = 0.091725$.
Periodic solutions also appear if the initial condition (top right) is very close to the unique equilibrium
when v_{ext} is large. Indeed, for this parameter space, solutions always converge to the same periodic
solution. Top: Description of the unique steady state. Left: $F(N) = N(I(N) + \tau)$ crosses with the
constant function 1 giving the unique N_∞. Right: Unique steady state given by the profile (3.41) with
firing rate $N = 3.669$. Middle: Evolution of the firing rate and the refractory state for the solution
with initial data given by (3.41) with firing rate $N = 3.669$. Bottom: Influence of v_{ext} in the behaviour
of the system.
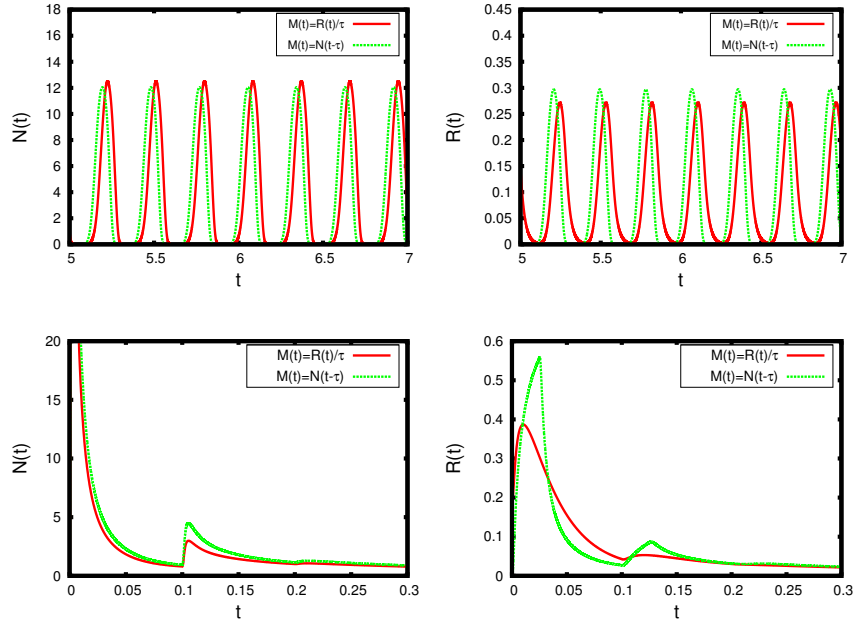
Figure 3.12: **Comparison between** $R(t)$ **and** $N(t)$ **for** $M(t) = \frac{R(t)}{\tau}$ **and** $M(t) = N(t - \tau)$. Top: initial data (3.40) with $v_0 = 1.83$ and $\sigma_0 = 0.0003$, the connectivity parameter $b = -4$, the transmission delay $D = 0.1$, $\tau = 0.025$, $R(0) = 0.2$ and $v_{ext} = 20$. Middle: parameter space of Fig. 3.2, bottom. The qualitative behavior is the same for both models, even the solutions seem to be hardly the same.
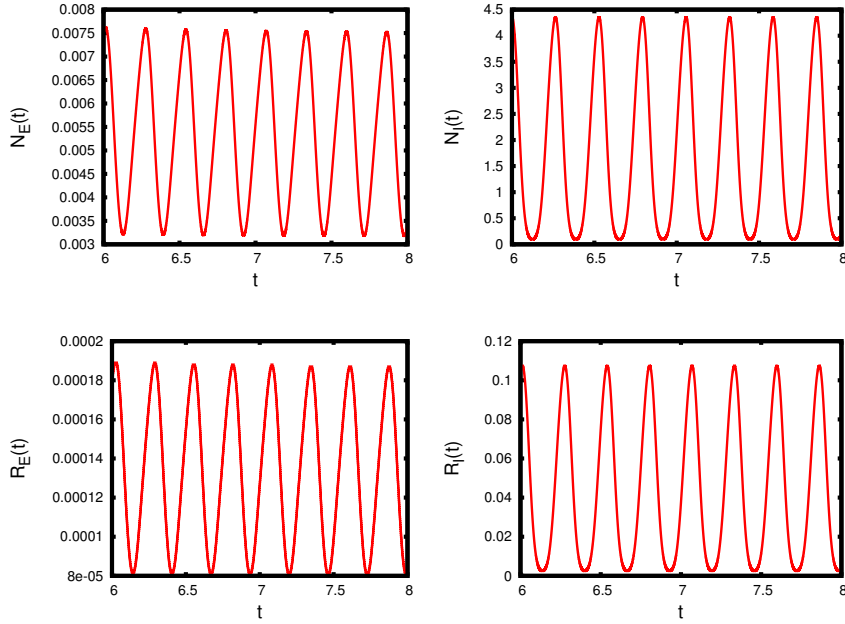
Figure 3.13: **System (3.1) (two populations: excitatory and inhibitory) presents periodic solutions if there is a delay.-** We consider initial data (3.40) with $v_0^E = v_0^I = 1.25$ and $\sigma_0^E = \sigma_0^I = 0.0003$, $v_{ext} = 20$ and the connectivity parameters $b_E^E = 0.5$, $b_I^E = 0.75$, $b_I^I = 4$, $b_E^I = 1$ and with refractory states $(M_\alpha(t) = N_\alpha(t - \tau_\alpha))$ where $\tau_\alpha = 0.025$. Top: Time evolution of the excitatory and inhibitory firing rates. Bottom: Time evolution of the excitatory and inhibitory refractory states.

3.5 Conclusions

In this chapter, we have extended the results presented in the second chapter and in [15, 17] to a general network with two populations (excitatory and inhibitory) with transmission delays between the neurons, and where the neurons remain in a refractory state for a certain time. From an analytical point of view we have explored the number of steady states in terms of the model parameters, the long time behaviour for small connectivity parameters, and blow-up phenomena if there is not a transmission delay between excitatory neurons.

Besides analytical results, we have presented a numerical resolutor for this model, based on high order flux-splitting WENO schemes and an explicit third order TVD Runge-Kutta method, in order to describe the wide range of phenomena displayed by the network: blow-up, asynchronous/synchronous solutions and instability/stability of the steady states. The solver also allows to observe the time evolution of not only the firing rates and refractory states, but also of the probability distributions of the excitatory and inhibitory populations.

The resolutor was used to illustrate the result of the blow-up theorem: as long as the transmission delay of the excitatory to excitatory synapses is zero ($D_E^E = 0$), blow-up phenomena appear in the full NNLIF model, even if there are nonzero transmission delays in the rest of the synapses.

We remark that the numerical results suggest that blow-up phenomena disappear when the excitatory to excitatory transmission delay is nonzero, and the solutions may tend to a steady state or to a synchronous state. In the case of only one average-inhibitory population the behavior of the solutions

after preventing a blow-up phenomenon seems to depend on the strength of the external synapses v_{ext}. Furthermore, we have also observed periodic solutions for small values of the excitatory connectivity parameter combined with an initial data far from the threshold potential. Thus, synchronous solutions are not a direct consequence of having avoided the blow-up phenomenon.

Our numerical study is completed with the stability analysis of the steady states, when the network presents three of them. In our simulations, we do not observe bistability phenomena since the two upper stationary firing rates are unstable, while the lowest one is stable.

Finally, to our knowledge, the numerical solver presented in this paper is the first deterministic solver to describe the behavior of the full NNLIF system involving all the characteristic phenomena of real networks.

Conclusions and open problems

In this thesis it have been analyzed the mathematical properties of a model widely used in neuroscience to describe the behavior of a neural network. Specifically, it has been focussed on the study of the full NNLIF model both from the analytical and numerical point of view. With this aim, it has been started from previous studies developed over simplified versions of this model and it has been analyzed models with increasing complexity until it was reached the full NNLIF model. The theoretical results of this thesis have been completed with an exhaustive numerical analysis. To achieve this goal, it has been implemented a numerical resolutor that allows to describe the time evolution of the probability distributions of the excitatory and inhibitory populations, the refractory states and the firing rates. The work presented in this memory gives answer to some of the question that remained open for the NNLIF model. Specifically, it has beem tackled the problem of the global existence of solution and the asymptotic behavior of the solutions, by means of the detailed study of the steady states of the system.

The starting point for the existence of solution for the NNLIF model were the results of [15, 29], at the level of the Fokker-Planck equation and the ones of [37, 38] for the microscopic description. In [15, 29] it was studied the most simplified version of the NNLIF model: only one on average excitatory or inhibitory neural population without synaptic delays nor refractory states. Specifically, in [15] it was proved that the solution can blow-up in finite time, if the population is on average excitatory and it was oberved numerically that the solution blows-up when the firing rate diverges in finite time. Later, in [29] it was proved this criterium: The solution exists as long as the firing rate is finite. Moreover, it was showed that for the inihibitory case there is always global existence of solution, since the firing rate does not blow-up in finite time. In parallel, at microscopic level, it was shown also that the system can blow-up in finite time if there is no synaptic delay and the network is excitatory [37], while if a delay is considered the solutions exist for every time [38].

In this thesis we have advanced the study of the existence of solution for the simplified NNLIF model that considers one neural population (on average excitatory or inhibitory) with delay, and, thus, is a more realistic version than the one considered in [15, 29], that does not take into account this delay. Specifically, we have proved that the presence of the delay allows to ensure the global existence of solution both for the excitatory and the inhibitory cases since the firing rate does not blow-up in finite time.

For the inhibitory case the proof of this result is based on the strategy presented in [29], which can be applied in a similar way handling the delay appropiately. Nevertheless, for the inhibitory case the strategy of [29] is not enough, since it does not allow to ensure that the firing rate does not blow-up in finite time. In order to get some control over the firing rate we constructed an upper-solution. This control, joined to a criterium for the maximal time of existence, finally has allowed us to obtain the searched global existence (Teorema 1.4.9).

Regarding the asymptotic behavior of the solutions of the NNLIF model it was known that for the

most simplified model of only one population, withot delays and with, or without, refractory states [15, 17, 26] the solution can blow-up in finite time [15] and, in case of a unique steady state, if the connectivity parameter if small in absolute value, this unique steady state is asymptotically stable [17, 26]. Thus, the solutions converge to it exponentially, if initially they are close enough. Also, it was known the analysis of the number of steady states [15, 17]. In this thesis we have extended this results to the full NNLIF model. As a previos step we have studied a simpler case: The NNLIF model for two populations, without delays and without refractory states. Our target was to analyze if the known results for purely excitatory or inihibitory networks could be extended to coupled excitatory-inihibitory networks. We have proved that the presence of an inhibitory population in a coupled network does not avoid the blow-up phenomenon (Theorem 2.2.1), as happens in a purely inhibitory network without delay [29]. Besides, we have analyzed the number of steady states of the system (Theorem 2.3.1), which is a more complicated issue than in the case of uncoupled systems. For small connectivity parameter values, we have shown that solutions converge exponentially fast to the unique steady state (Theorem 2.3.5).

Finally, getting support of the results presented for the two populations NNLIF model and the ones of [15, 17] we have analyzed the most realistic NNLIF model: two populations (excitatory and inhibitory) with transmission delays between the neurons, and where the neurons remain in a refractory state for a certain time. From an analytical point of view again we have explored the number of steady states in terms of the model parameters (Theorem 3.3.1), we have analyzed the long time behaviour for small connectivity parameters (Theorem 3.3.3), and we have proved that the blow-up phenomena appears, if there is not a transmission delay between excitatory neurons (Theorem 3.2.1). The key tools used to obtain this results have been the strategies developed previously for the simplified two populations model, that neglects the delays and refractory states.

We complete the theoretical study of this three models with a numerical analysis. With that purpose, we have developed a numerical resolutor based on high order (flux-splitting) WENO schemes, an explicit third order TVD Runge-Kutta method and some parallel computing techniques using MPI. The solver allows to observe the time evolution of the firing rates, the probability distributions of the excitatory and inhibitory populations and the probabilities of the refractory states.

We have been improving the resolutor during the development of this work. Initially, it was implemented a fifth order WENO scheme and the resolutor solved the two populations NNLIF model that neglects the delays and refractory states. Later, we improved the numerical scheme using a fifth order flux-splitting WENO scheme. We also extended the model that solves the resolutor. Specifically, we added the posibility of the presence of non-zero delays and refractory states. From a computational point of view the presence of non-zero delays requires the saving and recovery of the firing rates. On the other hand, it should be mentioned that we have also implemented a simplified version of the resolutor, that allows to analize from a numerical point of view the one population NNLIF model with (or without) delay and with (or without) refractory state.

Our resolutor allows to describe the wide range of phenomena displayed by the network: blow-up, or not, instability/stability of the steady states, periodic solutions,... The numerical experiments on the one hand illustrate the analytical results, but, on the other hand, probably the more interesting, they help to understand better some theoretical aspects that, until now, could not be solved. Among this problems we can find the study of the stability of the steady states, in case there is more than one, the analysis of the behavior of the solutions when there is a non-zero delay in the excitatory to excitatory synapses and the appearance of periodic solutions.

The numerical results suggest that blow-up phenomena disappear for the full NNLIF model when the excitatory to excitatory transmission delay is nonzero, and the solutions may tend to a steady

state or to a synchronous state. This results makes us think that the global existence result of the first chapter could be extended to the full NNLIF model, whenever there is a synaptic delay for the excitatory to excitatory synapses.

Furthermore, we have also observed periodic solutions for small values of the excitatory connectivity parameter combined with an initial data far from the threshold potential. Thus, synchronous solutions are not a direct consequence of having avoided the blow-up phenomenon. On the other hand, in the case of only one average-inhibitory population the behavior of the solutions (synchronous or asynchronous) seems to depend on the strength of the external synapses v_{ext}. Our numerical study is completed with the stability analysis of the steady states, when the network presents three of them. In our simulations, we do not observe bistability phenomena since the two upper-stationary firing rates are unstable, while the lowest one is stable.

Finally, to our knowledge, the numerical solver presented in this chapter is the first deterministic solver to describe the behavior of the full NNLIF system involving all the characteristic phenomena of real networks. Developing efficient numerical resolutors that consider all relevant phenoma is essential to work out strategies that, on the one hand, give answer to the open questions; and, on the other hand, help to implement resolutors for other large-scaled models, which are becoming more common in computational neuroscience [56, 63, 81, 92, 93, 100].

Our analytical and numerical results contribute to support the two-populations NNLIF system as an appropriate model to describe well known neurophysiological phenomena, as for example synchronization/asynchronization of the network, since the blow-up in finite time might depict a synchronization of a part of the network, while the presence of a unique asymptotically stable stationary solution represents an asynchronization of the network. In addition, the abundance in the number of steady states, in terms of the connectivity parameter values, that can be observed for this simplified model, probably will help us to characterize situations of multi-stability for more complete NNLIF models and also other models including conductance variables as in [16]. In [17] it was shown that if a refractory period is included in the model, there are situations of multi-stability, with two stable and one unstable steady state. In [16] bi-stability phenomena were numerically described. Multi-stable networks are related, for instance, to the visual perception and the decision making [50, 3], the short term working memory [104] and oculomotor integrators [59]. On the other hand, periodic or oscillatory solutions used to model synchronous states and oscillations observed, e.g., during cortical processing [50, 53].

Summarizing, the problems studied in this work are: existence problems, analysis of the number of steady states, long time behavior of the solutions and numerical study. The numerical analysis has been used, on the one hand, to study certain behaviors of the solutions, that have been proved analytically and, on the other hand, to shed some light on some aspects that, due to its complexity, have not yet been treated from a theoretical point of view: the stability of the steady states in case there is more than one, the fact that the blow-up is avoided when there is a delay in excitatory to excitatory synapses, the appearance of periodic solutions,...

The main tools used to deal with this problems from an analytical point of view are: an appropiate transformation of the one population NNLIF model with delay into a Stefan like problem with a nonstandard right hand side, fixed point arguments and the notion of universal upper-solution, which allowed to proof the global existence for this model; for the asymptotic behavior, the entropy dissipation method and different inequalities, being the most relevant a Poincaré like inequality in order to control the entropy production; and different strategies applied to determine the number of steady states.

From a numerical point of view, the main techniques that have been learned are the fifth order (flux

splitting) WENO approximation used to approximate the drifts, and the third order TVD Runge-Kutta method combined with a CFL condition for the evolution in time of the solutions. Moreover, all the codes are programmed using C++ and, sometimes, MPI. Thus, this techniques and programming languages are part of the training obtained during the development of this work.

Finally, we describe new directions for future work. Regarding the one population delayed NNLIF model from the analytical point of view some of the open questions are: What happens in the cases where there are no steady states and where the solutions of the non-delayed model used to blow-up? Do it appear periodic solutions? (Here we have to take into account that numerically, we have not observed them.) Also it would be interesting to determine the cases where solutions instead of blowing-up, with delay tend to the steady state. On the other hand, some of the numerical simulations suggest that, perhaps, the model has other kind of solutions, e.g., with an increasing firing rate, that does not blow-up in finite time. Analyzing its existence, or not, would complete the analysis of the type of solutions that presents this model.

For the one and two populations delayed NNLIF models with refractory state, it would be interesting to prove analytically the existence of the periodic solutions observed numerically. Moreover determining the parameter values and/or initial conditions which lead to a steady steady state and the ones which gives rise to a periodic solution would complete this proof. Another open question consists of studying if the result for the global-in-time existence can be extended to the full NNLIF model.

A task which remains open for all the NNLIF models analyzed in this thesis is the analytical study of the stability of the network when there is more than one steady state, and also when the connectivity parameters are not small.

Another possible direction of future work consists of searching strategies to compare the solutions of the different other neural models to the ones of the NNLIF model, as it was done, e.g., for the age structured model in [42] where it was found an integral transform that allows to rewrite its solutions as a solution of the linear NNLIF model. This direction is interesting, since understanding the relations between them, would help to explore different strategies to tackle the problems that still remain open for this models.

Conclusiones y problemas abiertos

En esta tesis se han analizado las propiedades matemáticas de un modelo muy aplicado en neurociencia para determinar el comportamiento de redes neuronales. En concreto, este estudio se ha centrado en el modelo NNLIF completo y se ha llevado a cabo tanto desde el punto de vista analítico como numérico. Con este objetivo, se ha partido de estudios previos sobre simplificaciones de este modelo y se han analizado modelos que incluyen cada vez más complejidades adicionales hasta llegar al modelo NNLIF completo. Los resultados teóricos de esta tesis se han completado con un exhaustivo análisis numérico. Para ello se ha implementado un potente resolutor numérico que permite conocer la evolución en el tiempo de las densidades de probabilidad de las neuronas excitadoras e inhibidoras, las probabilidades de que las neuronas estén en estado refractario y las tasas de disparo. El trabajo presentado en esta memoria da respuesta a preguntas que quedaban abiertas sobre el modelo NNLIF. Concretamente, se ha abordado el problema de la existencia global de la solución y el comportamiento asintótico de las soluciones, mediante el estudio detallado de los equilibrios del sistema.

Los resultados de existencia de solución para el modelo NNLIF de los que hemos partido son los dados en [15, 29], a nivel de la ecuación de Fokker-Planck y los de [37, 38] para la descripción microscópica. En [15, 29] se estudió la versión más simplificada del modelo NNLIF: una sola población de neuronas en media excitadora o inhibidora, sin considerar retrasos sinápticos ni estado refractarios. Concretamente, en [15] se probó que la solución puede explotar en tiempo finito, si la población es en media excitadora y se observó numéricamente que la solución explota cuando la tasa de disparo diverge en tiempo finito. Posteriormente, en [29] se probó ese criterio: la solución existe siempre que la tasa de disparo sea finita. Además se mostró que para el caso inhibidor hay existencia global de solución, ya que la tasa de disparo no explota en tiempo finito. Paralelamente, a nivel microscópico, se demostró también que el sistema puede explotar en tiempo finito si no hay retraso sináptico y la red es excitadora [37], mientras que si se incluye un retraso sináptico las soluciones existen para todo tiempo [38].

En esta tesis hemos avanzado en el estudio de la existencia de solución para el modelo NNLIF en el caso simplificado de una población de neuronas (en media excitadora o inhibidora) incluyendo el retraso sináptico, siendo, por lo tanto, una versión más realista que la considerada en [15, 29], que no tiene en cuenta este retraso. Concretamente, hemos probado que la presencia del retraso permite garantizar la existencia global de la solución para todo tiempo, tanto para el caso excitador como para el caso inhibidor, ya que la tasa de disparo no explota en tiempo finito.

Para el caso de neuronas en media inhibidoras la prueba de este resultado se basa en la estrategia de [29] que se puede replicar manejando de forma apropiada el retraso. Sin embargo, para el caso excitador la estrategia de [29] es insuficiente ya que no permite garantizar la no explosión en tiempo finito de la tasa de disparo. Para obtener un control sobre dicha tasa hemos construido una super-solución y este control, unido a un criterio del tiempo maximal de existencia, nos ha permitido obtener la existencia global de la solución (Teorema 1.4.9).

Sobre el comportamiento asintótico de las soluciones del modelo NNLIF se sabía que para el modelo

más simplificado de una sola población, sin retrasos y con, o sin, estados refractarios [15, 17, 26] la solución puede explotar en tiempo finito [15] y que en caso de haber un único estado estacionario, si el parámetro de conectividad es pequeño en valor absoluto, ese único estado estacionario es asintóticamente estable [17, 26]. Así, las soluciones convergen a él exponencialmente, si inicialmente están lo suficientemente cerca. También se conocía el análisis del número de estados estacionarios [15, 17]. En esta tesis hemos extendido estos resultados al modelo NNLIF completo. Como paso previo hemos estudiado un caso más sencillo: el modelo NNLIF para dos poblaciones, sin retrasos sinápticos ni estados refractarios. Nuestro propósito fue analizar si los resultados conocidos para redes puramente excitadoras o inihibidoras [15] se podían extender a redes acopladas excitadoras-inhibidoras. Así hemos probado que la presencia de una población inhibidora en una red acoplada no evita el fenómeno de la explosión en tiempo finito (Teorema 2.2.1), como ocurre en una red puramente inhibidora sin retraso [29]. Además, hemos analizado el número de estados estacionarios del sistema (Teorema 2.3.1), que es un asunto más complicado que para el caso de sistemas desacoplados. Para parámetros de conectividad pequeños, hemos mostrado que las soluciones convergen al único equilibrio con velocidad exponencial (Teorema 2.3.5).

Por último, apoyándonos en los resultados presentados para el modelo NNLIF para dos poblaciones hemos analizado al modelo NNLIF más realista: dos poblaciones (excitadora e inhibidora) con retrasos sinápticos y donde las neuronas permanecen en un estado refractario durante algún tiempo. Desde el punto de vista analítico, hemos clasificado el número de estados estacionarios en función de los parámetros del modelo (Teorema 3.3.1), hemos analizado el comportamiento a largo plazo para parámetros de conectividad pequeños (Teorema 3.3.3), y hemos probado que el fenómeno de la explosión en tiempo finito aparece si no hay retraso sináptico entre las neuronas excitadoras (Teorema 3.2.1). Para obtener estos resultados, han sido cruciales las estrategias desarrolladas anteriormente para la simplificación del modelo de dos poblaciones, que no tiene en cuenta los retrasos, ni los estados refractarios.

Completamos el estudio teórico de estos tres modelos con un análisis numérico. Para ello, hemos desarrollado un resolutor numérico, basado en esquemas WENO de alto orden (de tipo *flux-splitting*), un método de Runge-Kutta TVD explícito de tercer orden y algunas técnicas de computación en paralelo usando MPI. El resolutor permite observar la evolución en tiempo, tanto para la población excitadora como para la inhibidora, de las densidades de probabilidad, las tasas de disparo y las probabilidades de los estados refractarios.

Hemos ido mejorando este resolutor durante el desarrollo de este trabajo. Inicialmente se implementó un esquema WENO de quinto orden y se resolvía el modelo NNLIF de dos poblaciones, pero sin estados refractarios ni retrasos sinápticos. Después, mejoramos el esquema numérico usando un método WENO de quinto orden de tipo flux-splitting. También ampliamos el modelo que resuelve el resolutor. En concreto, añadimos la posibilidad de que hubiera retrasos no cero y estados refractarios. La presencia de retrasos no cero desde el punto de vista computacional requiere de un guardado y recuperación adecuado de las tasas de disparo. Por otro lado, cabe mencionar que también hemos implementado una versión simplificada del resolutor, que permite analizar desde el punto de vista numérico el modelo NNLIF para una población con (o sin) retraso y con (o sin) estado refractario.

Nuestro resolutor permite describir el amplio rango de fenómenos que aparecen en la red: explosión, o no, en tiempo finito, estabilidad/inestabilidad de los estados estacionarios, soluciones periódicas, etc. Los experimentos numéricos, por un lado, ilustran los resultados teóricos, pero por otro lado, quizás el más interesante, ayudan a entender mejor aspectos analíticos que, hasta el momento, no se han podido resolver. Entre estos podemos citar el estudio de la estabilidad de los equilibrios cuando hay más de uno, explorar el comportamiento de las soluciones cuando hay un retraso no cero entre las

neuronas excitadoras y la aparición de soluciones periódicas.

A la vista de los resultados numéricos obtenidos parece que la explosión en tiempo finito desaparece para el modelo NNLIF completo, si el retraso excitador-excitador es no cero, y las soluciones tienden a un equilibrio o a un estado síncrono. Estos resultados nos hacen pensar que el resultado de existencia global del primer capítulo se podría extender al modelo NNLIF completo, siempre que haya un retraso sináptico entre sinapsis excitadoras-excitadoras.

Además, también hemos observado soluciones periódicas para valores pequeños del parámetro de conectividad excitador combinados con un dato inicial lejos del potencial umbral. En consecuencia, las soluciones síncronas no son una consecuencia directa de haber evitado una explosión. Por otro lado, para el caso de una sola población en media inhibidora el comportamiento de las soluciones (síncrono o asíncrono) parece depender de la fuerza de las sinapsis externas v_{ext}. Nuestro estudio numérico se completa con el análisis de la estabilidad de los estados estacionarios, cuando hay más de uno. En concreto, no observamos fenómenos de biestabilidad, ya que cuando hay tres estados estacionarios, los dos equilibrios superiores de la tasa de disparo son inestables, mientras que el más bajo es estable.

Finalmente, desde lo que conocemos, el resolutor numérico presentado en esta tesis es el primer resolutor determinista que describe el comportamiento del modelo NNLIF completo, que involucra todos los fenómenos característicos de redes reales. Desarrollar resolutores numéricos eficientes que incluyen todos los fenómenos relevantes, es esencial para proponer estrategias que, por un lado, den respuestas a las preguntas que aún quedan abiertas; y, por otro lado, ayuden a implementar resolutores para otros modelos de gran escala, ya que estos son cada vez más frecuentes en neurociencia computacional [56, 63, 81, 92, 93, 100].

Nuestros resultados analíticos y numéricos contribuyen a respaldar que el modelo NNLIF es un modelo adecuado para describir fenómenos neurofisiológicos bien conocidos, como lo son la sincronización/asincronización de la red, ya que la explosión en tiempo finito quizás represente una sincronización de parte de la red, mientras que la presencia de un único estado estacionario asintóticamente estable describe un asincronización de la red. Asimismo, la abundancia del número de estados estacionarios, en función de los valores de los parámetros de conectividad, que puede ser observada para estos modelos simplificados (Teorema 2.3.1 y Teorema 3.3.1), probablemente nos ayude a caracterizar situaciones de multiestabilidad para otros modelos más completos, como p.e., los que incluyen variables de conductancia [16]. En [17] se mostró que si incluimos un estado refractario en el modelo, hay situaciones de multiestabilidad, con dos estados estables y uno inestable. En [16] se han descrito fenómenos de biestabilidad numéricamente. Redes multiestables están relacionadas, p.e., con la percepción visual y la toma de decisiones [50, 3], la memoria de trabajo a corto plazo [104] e integradores oculomotores [59]. Por otro lado, las soluciones periódicas u oscilantes se usan para modelar estados síncronos y oscilaciones observadas, p.e., durante el procesado cortical [50, 53].

En resumen, los problemas más relevantes estudiados en este trabajo son: problemas de existencia, análisis del número de estados estacionarios, comportamiento a largo plazo de las soluciones y estudio numérico. El análisis numérico se ha usado, por un lado, para estudiar ciertos comportamientos de las soluciones, probados analíticamente y, por otro lado, para aclarar algunos de los aspectos que, debido a su complejidad, no han podido ser abordados desde la perspectiva teórica: la estabilidad de los equilibrios cuando hay más de uno, la desaparición del *blow-up* cuando hay un retraso en las sinapsis excitadora-excitadora, la aparición de soluciones periódicas, etc.

Las principales herramientas usadas para trabajar en estos problemas desde el punto de vista analítico son: la transformación del modelo NNLIF de una población con retraso a un problema de Stefan con una parte derecha no estándar, argumentos de punto fijo y la noción de super-solución

global, que permitieron probar la existencia de solución para todo tiempo para este modelo; para el comportamiento asintótico el método de disipación de entropía y para controlar la producción de entropía varias desigualdades, siendo la más destacada una desigualdad de tipo Poincaré; y diferentes estrategias aplicadas para determinar el número de estados estacionarios.

Desde un punto de vista numérico, las principales técnicas aprendidas son el método WENO (flux splitting) de quinto orden usado para aproximar las términos de arrastre, y el método Runge-Kuttta TVD de tercer orden combinado con una condición CFL para simular la evolución en tiempo de las soluciones. Además, todos los códigos se han programado en C++, combinado, a veces, con técnicas de programación en paralelo usando MPI. Por lo tanto, el aprendizaje de estas técnicas y lenguajes de programación también es parte de la formación obtenida durante el desarrollo de este trabajo.

Finalmente, describimos posibles direcciones nuevas de trabajo. Para el modelo NNLIF retrasado de una sola población desde el punto de vista analítico las siguientes preguntas siguen sin respuesta: ¿Qué ocurre en los casos donde no hay estados estacionarios y donde las soluciones del modelo sin retraso solían explotar? ¿Aparecen soluciones periódicas? (Aquí tenemos que tener en cuenta que numéricamente no las hemos observado). También sería interesante determinar los casos donde las soluciones en vez de explotar, con retraso tienden a un estado estacionario. Por otro lado, algunas de las simulaciones nos hacen pensar que quizás el modelo presente otro tipo de soluciones, p.e., con una tasa de disparo creciente, pero que no explota en tiempo finito. Estudiar su existencia, o no, completaría el análisis del tipo de soluciones presentes en el modelo.

Para el modelo NNLIF retrasado y con estados refractarios de una y dos poblaciones, sería interesante probar de forma analítica la existencia de las soluciones periódicas observadas numéricamente. Además, determinar los valores de los parámetros y/o datos iniciales, que llevan al estado estacionario, y los que dan lugar a una solución periódica, complementaría de forma importante dicha prueba. Otra pregunta abierta consiste en analizar si se puede extender el resultado de existencia global al modelo NNLIF completo.

Una tarea que queda pendiente para todos los modelos NNLIF estudiados en esta tesis es el estudio analítico de la estabilidad de la red cuando hay más de un equlibrio, y también cuando los parámetros de conectividad no son pequeños.

Otra posible línea de trabajo consiste en buscar estrategias para comparar las soluciones de otros modelos neuronales con las del modelo NNLIF, como se ha hecho, p. e., para el modelo estructurado por edad en [42], donde se ha encontrada una transformada integral que permite reescribir sus soluciones como una solución del modelo NNLIF lineal. Esta dirección es interesante, ya que entender las relaciones entre ellos ayudaría a explorar distintas estrategias para abordar los problemas que aún quedan por resolver en estos modelos.

Appendices

Appendix A

Numerical Scheme

Here we describe the deterministic numerical scheme that has been used to get all the numerical results of this work. In fact, we will concentrate on a one population case, and only show how to extend it for two populations in the most difficult parts. Moreover, we recommend [62] for a great review of numerical methods for conservation laws and [4, 16, 31] for other deterministic methods developed for related kinetic methods.

Let us consider a one population NNLIF model that neglects the delay and the refractory state, and that considers a constant diffusion term, as an example to describe the different versions of the numerical solver that have been used through this thesis to obtain the numerical results. Its equations are given by:

$$\begin{cases} \dfrac{\partial \rho}{\partial t}(v,t) + \dfrac{\partial}{\partial v}[h(v,N(t))\rho(v,t)] - a\dfrac{\partial^2 \rho}{\partial v^2}(v,t) = N(t)\delta(v - V_R), \\[2mm] N(t) = -a\dfrac{\partial \rho}{\partial v}(V_F,t) \geq 0, \qquad h(v,N(t)) = -v + bN(t), \\[2mm] \rho(-\infty,t) = 0, \quad \rho(V_F,t) = 0, \quad \rho(v,0) = \rho^0(v) \geq 0, \end{cases} \tag{A.1}$$

We first rewrite the equation as:

$$\frac{\partial \rho}{\partial t}(v,t) = -\frac{\partial}{\partial v}[h(v,N(t))\rho(v,t)] - +a\frac{\partial^2 \rho}{\partial v^2}(v,t) + N(t)\delta(v - V_R).$$

Then we consider a uniform the space mesh for $v \in I := [-V_{left}, V_F]$ given by $v_i = v_0 + i dv \; \forall i = 1, ..., n$ and where $-V_{left}$ is chosen such that $\rho(-V_{left}, t) \sim 0$, since $\rho(-\infty, t) = 0$. After that, we aproximate the two derivatives, the firing rate $N(t)$ and the Dirac delta of the right hand side (RHS). The first derivative is approximated by a fifth order WENO scheme or a fifth order flux-splitting WENO scheme, as described below, the second derivative is approximated by standard second order finite differences, the firing rate by first order regressive finite diffences and the Dirac delta by a very concentrated maxwellian function. Notice that for a non-constant diffusion coefficient, $a(N) = a_0 + a_1 N$, the approximations of the derivatives could also have been performed using the Chang-Cooper method [14], as done in [15]. Here we have not applied this method, since it presents difficulties when the firing rate N is large and the diffusion coeficient is constant.

After approximating the derivatives, we define the funcional L as the sum of all the approximations,

getting thus something like this

$$\begin{cases} \frac{\partial \rho}{\partial t}(v,t) = L(t,\rho(v,t)), & \forall t \geq t^0, \quad \forall v \in I \\ \rho(v,t_0) = \rho^0(v), & \forall v \in I, \end{cases}$$

Finally, the time evolution of ρ is approximated using a third order TVD Runge-Kutta method, as described later. The time step is adapted dinamically via a CFL condition.

A.1   WENO scheme

For the numerical simulations, the advection term of the NNLIF models considered, has been approximated by a fifth order WENO method. This scheme has been widely analyzed in [27, 28, 57, 90] and is formulated as follows for model (A.1). (The formulation for the two population models is the same, it only has to be taken into account that for this case there will be two different fluxes: $f_\alpha(\rho_\alpha(v,t)) = h^\alpha(v, N_E(t-D_E^\alpha), N_I(t-D_I^\alpha))\rho_\alpha(v,t) \; \forall \alpha = E, I).$

Given the space mesh defined before, consider the middle node mesh defined by $v_{i+\frac{1}{2}} = v_0 + (i+\frac{1}{2})dv$. Then, denoting $f(\rho(v,t)) = h(v, N(t-D))\rho(v,t)$, approximate the first derivative of the advection term by centered finite differences using that middle nodes, obtaining

$$\frac{\partial}{\partial v} f(\rho(v_i,t)) \approx \frac{f(\rho(v_{i+\frac{1}{2}},t)) - f(\rho(v_{i-\frac{1}{2}},t))}{dv}, \qquad \forall i = 1, ..., n. \tag{A.2}$$

Notice that using the middle nodes instead of the regular nodes of the mesh improves the approximation done, since the space step considered for the approximation is smaller, specifically it is $dv/2$. Nevertheless, it appears a problem: the time evolution of the solution ρ will be calculated only over the initial mesh, and thus, we will not know the values of ρ on the middle nodes. This is solved by the WENO reconstruction. It permits to approximate the flux f on the middle nodes

$$\hat{f}_{i+\frac{1}{2}} \approx f(\rho(v_{i+\frac{1}{2}},t)), \tag{A.3}$$

$$\hat{f}_{i-\frac{1}{2}} \approx f(\rho(v_{i-\frac{1}{2}},t)), \tag{A.4}$$

using only the evaluations of the flux that are calculated using the values of ρ on the larger mesh: $\bar{f}_i = f(\rho(v_i,t))$, which can be easily obtained.
Moreover, depending on the direction of the "wind" or *Roe speed*

$$\bar{a}_{i+\frac{1}{2}} \equiv \frac{\bar{f}_{i+1} - \bar{f}_i}{\rho_{i+1} - \rho_i},$$

(A.3) is computed using the approximation on the right or the left of the flux on the middle node $v_{i+\frac{1}{2}}$. Specifically:

- If $\bar{a}_{i+\frac{1}{2}} \geq 0$ then the wind blows from the left to the right, and thus the approximation on the left is used: $\hat{f}_{i+\frac{1}{2}} = f^-_{i+\frac{1}{2}}$.

- If $\bar{a}_{i+\frac{1}{2}} < 0$ then the wind blows from the right to the left, and thus the approximation on the right is used: $\hat{f}_{i+\frac{1}{2}} = f^+_{i+\frac{1}{2}}$.

Finally, let us remember the concrete formulation of the fifth order WENO method [90]. Let us start with the approximation on the left

$$\hat{f}^-_{i+\frac{1}{2}} = \omega_0 f^{(0)}_{i+\frac{1}{2}} + \omega_1 f^{(1)}_{i+\frac{1}{2}} + \omega_2 f^{(2)}_{i+\frac{1}{2}}, \tag{A.5}$$

where the nonlinear weights ω_r and the linear weights α_s are given by

$$\omega_r = \frac{\alpha_r}{\sum_{s=0}^2 \alpha_s} \quad r = 0,1,2, \quad \alpha_s = \frac{d_s}{(\varepsilon + \beta_s)^2} \quad s = 0,1,2, \quad \epsilon = 10^{-6} \quad d_0 = \frac{3}{10}, \quad d_1 = \frac{3}{5}, \quad d_2 = \frac{1}{10},$$

where the smoothness indicators β_s are defined by

$$\begin{aligned}
\beta_0 &= \frac{13}{12}(\bar{f}_i - 2\bar{f}_{i+1} + \bar{f}_{i+2})^2 + \frac{1}{4}(3\bar{f}_i - 4\bar{f}_{i+1} + \bar{f}_{i+2})^2, \\
\beta_1 &= \frac{13}{12}(\bar{f}_{i-1} - 2\bar{f}_i + \bar{f}_{i+1})^2 + \frac{1}{4}(\bar{f}_{i-1} - \bar{f}_{i+1})^2, \\
\beta_2 &= \frac{13}{12}(\bar{f}_{i-2} - 2\bar{f}_{i-11} + \bar{f}_i)^2 + \frac{1}{4}(\bar{f}_{i-2} - 4\bar{f}_{i-1} + 3\bar{f}_i)^2,
\end{aligned} \tag{A.6}$$

and where the third order fluxes are given by

$$\begin{aligned}
f^{(0)}_{i+\frac{1}{2}} &= \frac{1}{3}\bar{f}_i + \frac{5}{6}\bar{f}_{i+1} - \frac{1}{6}\bar{f}_{i+2}, \\
f^{(1)}_{i+\frac{1}{2}} &= -\frac{1}{6}\bar{f}_{i-1} + \frac{5}{6}\bar{f}_i + \frac{1}{3}\bar{f}_{i+1}, \\
f^{(2)}_{i+\frac{1}{2}} &= \frac{1}{3}\bar{f}_{i-2} - \frac{7}{6}\bar{f}_{i-1} + \frac{11}{6}\bar{f}_i.
\end{aligned}$$

The approximation on the right reads

$$\hat{f}^+_{i+\frac{1}{2}} = \bar{\omega}_0 \bar{f}^{(0)}_{i+\frac{1}{2}} + \bar{\omega}_1 \bar{f}^{(1)}_{i+\frac{1}{2}} + \bar{\omega}_2 \bar{f}^{(2)}_{i+\frac{1}{2}}, \tag{A.7}$$

where the nonlinear weights $\bar{\omega}_r$ and the linear weights $\bar{\alpha}_s$ are given by

$$\bar{\omega}_r = \frac{\bar{\alpha}_r}{\sum_{s=0}^2 \bar{\alpha}_s} \quad r = 0,1,2, \quad \bar{\alpha}_s = \frac{\bar{d}_s}{(\epsilon + \beta_s)^2} \quad s = 0,1,2, \quad \varepsilon = 10^{-6} \quad \bar{d}_0 = \frac{1}{10}, \quad \bar{d}_1 = \frac{3}{5}, \quad \bar{d}_2 = \frac{3}{10},$$

where the smoothness indicators β_s are defined by (A.6) and the third order fluxes are given by

$$\begin{aligned}
\bar{f}^{(0)}_{i+\frac{1}{2}} &= \frac{11}{6}\bar{f}_{i+1} - \frac{7}{6}\bar{f}_{i+2} + \frac{1}{3}\bar{f}_{i+3}, \\
\bar{f}^{(1)}_{i+\frac{1}{2}} &= \frac{1}{3}\bar{f}_i + \frac{5}{6}\bar{f}_{i+1} - \frac{1}{6}\bar{f}_{i+2}, \\
\bar{f}^{(2)}_{i+\frac{1}{2}} &= -\frac{1}{6}\bar{f}_{i-1} + \frac{5}{6}\bar{f}_i + \frac{1}{3}\bar{f}_{i+1}.
\end{aligned}$$

A.2 Flux-splitting WENO scheme

Among others an inconvenient of the WENO-Roe approximation is, that sometimes it leads to solutions that violate the entropy, as explained in [90]. This can be fixed, using a global *flux splitting*. For that purpose, the flux is split using a suitable flux-splitting

$$f(\rho(v,t)) = f_{pos}(\rho(v,t)) + f_{neg}(\rho(v,t)),$$

which has to satisfy, among others [90], that

$$\frac{d}{d\rho} f_{pos}(\rho(v,t)) \geq 0, \quad \frac{d}{d\rho} f_{neg}(\rho(v,t)) \leq 0.$$

Remember that the flux splitting considered in this work is the Lax-Friedrich splitting, given by (3.39) [Chapter 3]. Then the first derivative of the flux is calculated without using the Roe speed as

$$\frac{\partial f}{\partial v}(\rho(v_i,t)) \approx \frac{\hat{f}_{i+\frac{1}{2}} - \hat{f}_{i-\frac{1}{2}}}{dv}, \qquad \forall i = 1,...,n, \tag{A.8}$$

where

$$\hat{f}_{i+\frac{1}{2}} = \hat{f}^{-}_{pos_{i+\frac{1}{2}}} + \hat{f}^{+}_{neg_{i+\frac{1}{2}}},$$

and where the approximations are defined as follows: $\hat{f}^{-}_{pos_{i+\frac{1}{2}}}$ is obtained applying (A.5) to the splitted flux f_{pos} and $\hat{f}^{+}_{neg_{i+\frac{1}{2}}}$ is calculated as (A.7) using f_{neg} as flux.

A.3 Second order finite differences

The second order derivative that is used in the NNLIF models considered, has been approximated by second order finite differences as follows

$$\frac{\partial^2 \rho}{\partial v^2}(v_i,t) \approx \frac{\rho(v_{i+1},t) - 2\rho(v_i,t) + \rho(v_{i-1},t)}{dv^2}, \qquad \forall i = 1,...,n. \tag{A.9}$$

A.4 TVD third order Runge-Kutta method

Given an interval $I \subseteq \mathbb{R}$ and an IVP

$$\begin{cases} \frac{\partial \rho}{\partial t}(v,t) = L(t,\rho(v,t)), & \forall t \geq t^0, \quad \forall v \in I \\ \rho(v,t_0) = \rho^0(v), & \forall v \in I, \end{cases}$$

the evolution in time of its solution, following a third order TVD Runge-Kutta method as in [16, 91], is numerically aproximated by the scheme

$$\rho^{(1)} = \rho^n + dtL(t_n, \rho^n),$$
$$\rho^{(2)} = \frac{3}{4}\rho^n + \frac{1}{4}\rho^{(1)} + \frac{1}{4}dtL(t_n + dt, \rho^{(1)}),$$
$$\rho^{n+1} = \frac{1}{3}\rho^n + \frac{2}{3}\rho^{(2)} + \frac{2}{3}dtL(t_n + 1/2dt, \rho^{(2)}),$$

where dt denotes the amplitude of the time step, $\rho^n \equiv \rho(v, t_n)$ for $n = 0, 1, 2, 3...$ and $t_n = t_0 + ndt$. For our simulations on the NNLIF models, the function L is the approximation to the advection, diffusion and RHS terms. For example, for model (A.1), it comes from adding (A.2) or (A.8), to (A.9) and the RHS. Thus, for non-flux splitting WENO it reads for $i = 1, ..., n$

$$L(t, \rho(v_i, t)) \approx a \frac{\rho(v_{i+1}, t) - 2\rho(v_i, t) + \rho(v_{i-1}, t)}{dv^2} - \frac{\hat{f}_{i+\frac{1}{2}}(t) - \hat{f}_{i-\frac{1}{2}}(t)}{dv} + N(t)\delta(v_i - V_R),$$

where the Dirac delta is approximated by a Maxwellian function that is very concentrated on V_R.

In all the simulations done in this work the time step has been adapted dynamically by the CFL condition, thus for one population models, for every time the next time step is given by

$$dt \leq \min \left\{ \frac{adv^2}{2}, \frac{CFL\ dv}{\max_i\{|h(v_i, N(t - D))|\}} \right\},$$

and for two population models by

$$dt \leq \min \left\{ \frac{a_E dv^2}{2}, \frac{a_I dv^2}{2}, \frac{CFL\ dv}{\max_i\{|h^E(v_i, N_E(t - D_E^\alpha), N_I(t - D_I^\alpha))|\}}, \frac{CFL\ dv}{\max_i\{|h^I(v_i, N_E(t - D_E^\alpha), N_I(t - D_I^\alpha))|\}} \right\}.$$

A.5   Improving the efficiency of the code using MPI

The simulations with delay, as done in the Chapter 3 are quite heavy, mainly due to the presence of the delay. This delay is saved in an array, that uses an important part of the memory. So, if we run this code sequentially in the case of one population or on two cores, in case of two populations, the computational times are improvable.

After doing the relevant simulations for Chapter 3, we started to work on the implementation of more efficient numerical solver using MPI. With that purpose, we divided the space mesh between the number of cores that are available, M, that is to say, if we have $n + 1$ points on the space mesh, each core handles $(n + 1)/M$ space points. Moreover, as we use a fifth order WENO scheme, that needs three ghost nodes on each side of the interval, the cores have to send to each other the missing nodes before calculating a WENO approximation. The firing rate N is calculated by only one of the cores, and then broadcasted to the rest. Also the recovery of the delayed firing rates is handled only by one of the cores.

With this strategy, the computational times improve significantly, as can be seen in the following table. This times were obtained for the delayed NNLIF model for one population with $D = 0.1$, saving

Number of cores	Computational time
1	874 seg
2	252 seg
4	138 seg

the firing rate every $dt = 0.000001$, the space mesh has $n = 2999$ points, the connectivity parameter is $b = 0.5$ ad the initial condition is a normalized maxwellian function centered at 1.83 with amplitude 0.003. The time step was adapted dynamically with the CFL condition, but with the restriction that is has to be smaller than 0.000001.

We are still working on this issue: on the one hand we aim to extend the code for the full NNLIF model (two populations, delays and refractory states) and, on the other hand, we are implementing a more parallel version of the code. This can be achieved, e.g., by distributing also the storage and recovery of the firing rate.

Bibliography

[1] L. F. ABBOTT AND C. V. VREESWIJK, *Asynchronous states in networks of pulse-coupled oscillators*, Phys. Rev. E, 48 (1993), pp. 1483–1490.

[2] J. ACEBRÓN, A. BULSARA, AND W.-J. RAPPEL, *Noisy fitzhugh-nagumo model: From single elements to globally coupled networks*, Physical Review E, 69 (2004), p. 026202.

[3] L. ALBANTAKIS AND G. DECO, *The encoding of alternatives in multiple-choice decision making*, Proc Natl Acad Sci U S A, 106 (2009), pp. 10308–10313.

[4] F. APFALTRER, C. LY, AND D. TRANCHINA, *Population density methods for stochastic neurons with realistic synaptic kinetics: Firing rate dynamics and fast computational methods*, Network: Computation in Neural Systems, 17 (2006), pp. 373–418.

[5] A. ARNOLD, J. CARRILLO, L. DESVILLETTES, J. DOLBEAULT, A. JÜNGEL, C. LEDERMAN, P. MARKOWICH, G. TOSCANI, AND C. VILLANI, *Entropies and equilibria of many-particle systems: an essay on recent research*, Springer, 2004.

[6] A. ARNOLD, P. MARKOWICH, G. TOSCANI, AND A. UNTERREITER, *On convex sobolev inequalities and the rate of convergence to equilibrium for fokker-planck type equations*, Comm. PDE, 26 (2001), pp. 43–100.

[7] G. BARNA, T. GROBLER, AND P. ERDI, *Statistical model of the hippocampal ca3 region, ii. the population framework: model of rhythmic activity in ca3 slice*, Biol. Cybern., 79 (1998), pp. 309–321.

[8] F. BARTHE AND C. ROBERTO, *Modified logarithmic sobolev inequalities on* $\mathbb{R}$, Potential Analysis, 29 (2008), pp. 167–193.

[9] A. BLANCHET, J. DOLBEAULT, AND B. PERTHAME, *Two-dimensional keller-segel model: Optimal critical mass and qualitative properties of the solutions.*, Electronic Journal of Differential Equations (EJDE)[electronic only], 2006 (2006), pp. Paper–No.

[10] R. BRETTE AND W. GERSTNER, *Adaptive exponential integrate-and-fire model as an effective description of neural activity*, Journal of neurophysiology, 94 (2005), pp. 3637–3642.

[11] N. BRUNEL, *Dynamics of sparsely connected networks of excitatory and inhibitory spiking networks*, J. Comp. Neurosci., 8 (2000), pp. 183–208.

[12] N. BRUNEL AND V. HAKIM, *Fast global oscillations in networks of integrate-and-fire neurons with long firing rates*, Neural Computation, 11 (1999), pp. 1621–1671.

[13] N. Brunel and X.-J. Wang, *What determines the frequency of fast network oscillations with irregular neural discharge? I. synaptic dynamics and excitation-inhibition balance*, J. Neurophysiol., 90 (2003), pp. 415–430.

[14] C. Buet, S. Cordier, and V. Dos Santos, *A conservative and entropy scheme for a simplified model of granular media*, Transp. Theory Statist. Phys., 33 (2004), pp. 125–155.

[15] M. J. Cáceres, J. A. Carrillo, and B. Perthame, *Analysis of nonlinear noisy integrate & fire neuron models: blow-up and steady states*, Journal of Mathematical Neuroscience, 1-7 (2011).

[16] M. J. Cáceres, J. A. Carrillo, and L. Tao, *A numerical solver for a nonlinear fokker-planck equation representation of neuronal network dynamics*, J. Comp. Phys., 230 (2011), pp. 1084–1099.

[17] M. J. Cáceres and B. Perthame, *Beyond blow-up in excitatory integrate and fire neuronal networks: refractory period and spontaneous activity*, Journal of theoretical Biology, 350 (2014), pp. 81–89.

[18] M. J. Cáceres, P. Roux, D. Salort, and R. Schneider, *Avoiding the blow-up: global-in-time classical solutions for the excitatory NNLIF model with delay*, Work in progress, (2017).

[19] M. J. Cáceres and R. Schneider, *Blow-up, steady states and long time behaviour of excitatory-inhibitory nonlinear neuron models*, Kinetic and Related Models, 10 (2017), pp. 587–612.

[20] ——, *Towards a realistic NNLIF model: Analysis and a numerical solver for excitatory-inhibitory networks with delay and refractory periods*, arXiv preprint arXiv:1705.02205, (2017).

[21] D. Cai, L. Tao, and D. W. McLaughlin, *An embedded network approach for scale-up of fluctuation-driven systems with preservation of spike information*, PNAS, 101 (2004), pp. 14288–14293.

[22] D. Cai, L. Tao, A. V. Rangan, D. W. McLaughlin, et al., *Kinetic theory for neuronal network dynamics*, Communications in Mathematical Sciences, 4 (2006), pp. 97–127.

[23] D. Cai, L. Tao, M. Shelley, and D. W. McLaughlin, *An effective kinetic representation of fluctuation-driven neuronal networks with application to simple and complex cells in visual cortex*, Proceedings of the National Academy of Sciences of the United States of America, 101 (2004), pp. 7757–7762.

[24] V. Calvez and L. Corrias, *Blow-up dynamics of self-attracting diffusive particles driven by competing convexities*, arXiv preprint arXiv:1301.7075, (2013).

[25] V. Calvez, L. Corrias, and M. A. Ebde, *Blow-up, concentration phenomenon and global existence for the keller–segel model in high dimension*, Communications in Partial Differential Equations, 37 (2012), pp. 561–584.

[26] J. Carrillo, B. Perthame, D. Salort, and D. Smets, *Qualitative properties of solutions for the noisy integrate & fire model in computational neuroscience*, Nonlinearity, 25 (2015), pp. 3365–3388.

[27] J. A. Carrillo, I. M. Gamba, A. Majorana, and C.-W. Shu, *A weno-solver for the transients of boltzmann–poisson system for semiconductor devices: performance and comparisons with monte carlo methods*, Journal of Computational Physics, 184 (2003), pp. 498–525.

[28] ——, *2d semiconductor device simulations by weno-boltzmann schemes: efficiency, boundary conditions and comparison to monte carlo methods*, Journal of Computational Physics, 214 (2006), pp. 55–80.

[29] J. A. Carrillo, M. d. M. González, M. P. Gualdani, and M. E. Schonbek, *Classical solutions for a nonlinear fokker-planck equation arising in computational neuroscience*, Comm. in Partial Differential Equations, 38 (2013), pp. 385–409.

[30] J. A. Carrillo and G. Toscani, *Asymptotic L^1-decay of solutions of the porous medium equation to self-similarity*, Indiana University Mathematics Journal, (2000), pp. 113–142.

[31] J. A. Carrillo and F. Vecil, *Nonoscillatory interpolation methods applied to Vlasov-based models*, SIAM J. Sci. Comput., 29 (2007), pp. 1179–1206 (electronic).

[32] T. Chawanya, A. Aoyagi, T. Nishikawa, K. Okuda, and Y. Kuramoto, *A model for feature linking via collective oscillations in the primary visual cortex*, Biol. Cybern., 68 (1993), pp. 483–90.

[33] J. Chevallier, *Mean-field limit of generalized hawkes processes*, arXiv preprint arXiv:1510.05620, (2015).

[34] J. Chevallier, M. J. Cáceres, M. Doumic, and P. Reynaud-Bouret, *Microscopic approach of a time elapsed neural model*, Mathematical Models and Methods in Applied Sciences, 25 (2015), pp. 2669–2719.

[35] L. Corrias, B. Perthame, and H. Zaag, *Global solutions of some chemotaxis and angiogenesis systems in high space dimensions*, Milan J. Math., 72 (2004), pp. 1–28.

[36] P. Dayan and L. F. Abbott, *Theoretical neuroscience*, vol. 806, Cambridge, MA: MIT Press, 2001.

[37] F. Delarue, J. Inglis, S. Rubenthaler, and E. Tanré, *Global solvability of a networked integrate-and-fire model of mckean–vlasov type*, The Annals of Applied Probability, 25 (2015), pp. 2096–2133.

[38] ——, *Particle systems with a singular mean-field self-excitation. Application to neuronal networks*, Stochastic Processes and their Applications, 125 (2015), pp. 2451–2492.

[39] G. Dumont and P. Gabriel, *The mean-field equation of a leaky integrate-and-fire neural network: measure solutions and steady states*, arXiv preprint arXiv:1710.05596, (2017).

[40] G. Dumont and J. Henry, *Population density models of integrate-and-fire neurons with jumps: well-posedness*, J. Math. Biol., (2012).

[41] ——, *Synchronization of an excitatory integrate-and-fire neural network*, Bull. Math. Biol., 75 (2013), pp. 629–648.

[42] G. Dumont, J. Henry, and C. O. Tarniceriu, *Noisy threshold in neuronal models: connections with the noisy leaky integrate-and-fire model*, arXiv preprint arXiv:1512.03785, (2015).

[43] L. C. Evans, *Partial differential equations*, American Mathematical Society, Providence, R.I., 2010.

[44] R. Fitzhugh, *Thresholds and plateaus in the hodgkin-huxley nerve equations*, The Journal of general physiology, 43 (1960), pp. 867–896.

[45] ———, *Impulses and physiological states in theoretical models of nerve membrane*, Biophysical journal, 1 (1961), pp. 445–466.

[46] N. Fourcaud and N. Brunel, *Dynamics of the firing probability of noisy integrate-and-fire neurons*, Neural Comp., 14 (2002), pp. 2057–2110.

[47] W. Gerstner, *Population dynamics of spiking neurons: Fast transients, asynchronous states, and locking*, Neural Comp., 12 (2000), pp. 43–89.

[48] W. Gerstner and W. Kistler, *Spiking neuron models*, Cambridge Univ. Press, Cambridge, 2002.

[49] M. d. M. González and M. P. Gualdani, *Asymptotics for a symmetric equation in price formation*, App. Math. Optim., 59 (2009), pp. 233–246.

[50] C. M. Gray and W. Singer, *Stimulus-specific neuronal oscillations in orientation columns of cat visual cortex*, Proc Natl Acad Sci U S A, 86 (1989), pp. 1698–1702.

[51] T. Guillamon, *An introduction to the mathematics of neural activity*, Butl. Soc. Catalana Mat., 19 (2004), pp. 25–45.

[52] E. Haskell, D. Nykamp, and D. Tranchina, *Population density methods for large-scale modeling of neuronal networks with realistic synaptic kinetics: cutting the dimension down to size*, Network: Compt. Neural. Syst, 12 (2001), pp. 141–174.

[53] J. A. Henrie and R. Shapley, *Lfp power spectra in v1 cortex: the graded effect of stimulus contrast*, J Neurophysiol, 94 (2005), pp. 479–490.

[54] A. L. Hodgkin and A. F. Huxley, *The components of membrane conductance in the giant axon of loligo*, The Journal of physiology, 116 (1952), pp. 473–496.

[55] ———, *A quantitative description of membrane current and its application to conduction and excitation in nerve*, The Journal of physiology, 117 (1952), pp. 500–544.

[56] E. M. Izhikevich and G. M. Edelman, *Large-scale model of mammalian thalamocortical systems*, Proc Natl Acad Sci U S A, 105 (2008), pp. 3593–3598.

[57] G.-S. Jiang and C.-W. Shu, *Efficient implementation of weighted ENO schemes*, J. Comput. Phys., 126 (1996), pp. 202–228.

[58] B. Knight, *Dynamics of encoding in a populaton neurons*, J. Gen. Physiol., 59 (1972), pp. 734–766.

[59] A. KOULAKOV, S. RAGHAVACHARI, A. KEPECS, AND J. LISMAN, *Model for a robust neural integrator*, Nat. Neurosci., 5 (2002), pp. 775–782.

[60] L. LAPICQUE, *Recherches quantitatives sur l'excitation électrique des nerfs traitée comme une polarisation*, J. Physiol. Pathol. Gen, 9 (1907), pp. 620–635.

[61] M. LEDOUX, *The concentration of measure phenomenon*, in AMS math. surveys and monographs, vol. 89, AMS, 2001.

[62] R. J. LEVEQUE, *Numerical methods for conservation laws (2. ed.).*, Lectures in mathematics, Birkhuser, 1992.

[63] J. MARINO, J. SCHUMMERS, D. C. LYON, L. SCHWABE, O. BECK, P. WIESING, K. OBERMAYER, AND M. SUR, *Invariant computations in local cortical networks with balanced excitation and inhibition*, Nature Neurosci., 8 (2005), pp. 194–201.

[64] P. A. MARKOWICH AND C. VILLANI, *On the trend to equilibrium for the fokker-planck equation: an interplay between physics and functional analysis*, Mat. Contemp, 19 (2000), pp. 1–29.

[65] M. MATTIA AND P. DEL GIUDICE, *Population dynamics of interacting spiking neurons*, Phys. Rev. E, 66 (2002), p. 051917.

[66] P. MICHEL, S. MISCHLER, AND B. PERTHAME, *General relative entropy inequality: an illustration on growth models*, J.Math.Pures Appl., 84 (2005), pp. 1235–1260.

[67] S. MISCHLER, C. QUININAO, AND J. TOUBOUL, *On a kinetic Fitzhugh–Nagumo model of neuronal network*, Communications in Mathematical Physics, 342 (2016), pp. 1001–1042.

[68] C. MORRIS AND H. LECAR, *Voltage oscillations in the barnacle giant muscle fiber*, Biophysical journal, 35 (1981), pp. 193–213.

[69] K. NEWHALL, G. KOVAČIČ, P. KRAMER, A. V. RANGAN, AND D. CAI, *Cascade-induced synchrony in stochastically driven neuronal networks*, Phys. Rev. E, 82 (2010), p. 041903.

[70] K. NEWHALL, G. KOVAČIČ, P. KRAMER, D. ZHOU, A. V. RANGAN, AND D. CAI, *Dynamics of current-based, poisson driven, integrate-and-fire neuronal networks*, Comm. in Math. Sci., 8 (2010), pp. 541–600.

[71] D. NYKAMP AND D. TRANCHINA, *A population density method that facilitates large-scale modeling of neural networks: Analysis and application to orientation tuning*, J. of Computational Neuroscience, 8 (2000), pp. 19–50.

[72] ——, *A population density method that facilitates large-scale modeling of neural networks: Extension to slow inhibitory synapses*, Neural Computation, 13 (2001), pp. 511–546.

[73] A. OMURTAG, K. B. W., AND L. SIROVICH, *On the simulation of large populations of neurons*, J. Comp. Neurosci., 8 (2000), pp. 51–63.

[74] K. PAKDAMAN, B. PERTHAME, AND D. SALORT, *Dynamics of a structured neuron population*, Nonlinearity, 23 (2010), pp. 55–75.

[75] ——, *Relaxation and self-sustained oscillations in the time elapsed neuron network model*, SIAM Journal on Applied Mathematics, 73 (2013), pp. 1260–1279.

[76] ——, *Adaptation and fatigue model for neuron networks and large time asymptotics in a nonlinear fragmentation equation*, The Journal of Mathematical Neuroscience (JMN), 4 (2014), pp. 1–26.

[77] B. PERTHAME, *Transport equations in biology*, Frontiers in Mathematics, Birkhäuser Verlag, Basel, 2007.

[78] B. PERTHAME AND D. SALORT, *On a voltage-conductance kinetic system for integrate and fire neural networks*, Kinetic and related models, AIMS, 6 (2013), pp. 841–864.

[79] C. POUZAT AND A. CHAFFIOL, *Automatic spike train analysis and report generation. an implementation with r, r2html and star*, Journal of neuroscience methods, 181 (2009), pp. 119–144.

[80] A. V. RANGAN AND D. CAI, *Fast numerical methods for simulating large-scale integrate-and-fire neuronal networks*, J. Comput. Neurosci., 22 (2007), pp. 81–100.

[81] A. V. RANGAN, D. CAI, AND D. W. MCLAUGHLIN, *Modeling the spatiotemporal cortical activity associated with the line-motion illusion in primary visual cortex*, PNAS, 102 (2005), pp. 18793–18800.

[82] ——, *Quantifying neuronal network dynamics through coarse-grained event trees*, PNAS, 105 (2008), pp. 10990–10995.

[83] A. V. RANGAN, D. CAI, AND L. TAO, *Numerical methods for solving moment equations in kinetic theory of neuronal network dynamics*, Journal of Computational Physics, 221 (2007), pp. 781–798.

[84] A. V. RANGAN, G. KOVAČIČ, AND D. CAI, *Kinetic theory for neuronal networks with fast and slow excitatory conductances driven by the same spike train*, Physical Review E, 77 (2008), pp. 1–13.

[85] A. RENART, N. BRUNEL, AND X.-J. WANG, *Mean-field theory of irregularly spiking neuronal populations and working memory in recurrent cortical networks*, in Computational Neuroscience: A comprehensive approach, J. Feng, ed., Chapman & Hall/CRC Mathematical Biology and Medicine Series, 2004.

[86] P. REYNAUD-BOURET, V. RIVOIRARD, F. GRAMMONT, AND C. TULEAU-MALOT, *Goodness-of-fit tests and nonparametric adaptive estimation for spike train analysis*, The Journal of Mathematical Neuroscience, 4 (2014), p. 3.

[87] H. RISKEN, *The Fokker-Planck Equation: Methods of solution and approximations*, 2nd. edn. Springer Series in Synergetics, vol 18. Springer-Verlag, Berlin, 1989.

[88] C. ROSSANT, D. F. M. GOODMAN, B. FONTAINE, J. PLATKIEWICZ, A. K. MAGNUSSON, AND R. BRETTE, *Fitting neuron models to spike trains*, Frontiers in Neuroscience, 5 (2011), pp. 1–8.

[89] M. SHELLEY AND L. TAO, *Efficient and accurate time-stepping schemes for integrate-and-fire neuronal networks*, J. Comp. Neurosci., 11 (2001), pp. 111–119.

[90] C.-W. Shu, *Essentially non-oscillatory and weighted esentially non-oscillatory schemes for hyperbolic conservation laws*, in Advanced Numerical Approximation of Nonlinear Hyperbolic Equations, B. Cockburn, C. Johnson, C.-W. Shu and E. Tadmor, A. Quarteroni, ed., vol. 1697, Springer, 1998, pp. 325–432.

[91] C.-W. Shu and S. Osher, *Efficient implementation of essentially non-oscillatory shock-capturing schemes*, Journal of Computational Physics, 77 (1988), pp. 439–471.

[92] D. C. Somers, S. B. Nelson, and M. Sur, *An emergent model of orientation selectivity in cat visual cortical simple cells*, J Neurosci, 15 (1995), pp. 5448–5465.

[93] L. Tao, M. Shelley, D. McLaughlin, and R. Shapley, *An egalitarian network model for the emergence of simple and complex cells in visual cortex*, Proc Natl Acad Sci U S A, 101 (2004), pp. 366–371.

[94] J. Touboul, *Bifurcation analysis of a general class of nonlinear integrate-and-fire neurons*, SIAM J. Appl. Math., 68 (2008), pp. 1045–1079.

[95] ——, *Importance of the cutoff value in the quadratic adaptive integrate-and-fire model*, Neural Computation, 21 (2009), pp. 2114–2122.

[96] ——, *Limits and dynamics of stochastic neuronal networks with random heterogeneous delays*, Journal of Statistical Physics, 149 (2012), pp. 569–597.

[97] ——, *Propagation of chaos in neural fields*, The Annals of Applied Probability, 24 (2014), pp. 1298–1328.

[98] ——, *Spatially extended networks with singular multi-scale connectivity patterns*, Journal of Statistical Physics, 156 (2014), pp. 546–573.

[99] A. Treves, *Mean field analysis of neuronal spike dynamics*, Network, 4 (1993), pp. 259–284.

[100] T. Troyer, A. Krukowski, N. Priebe, and K. Miller, *Contrast invariant orientation tuning in cat visual cortex with feedforward tuning and correlation based intracortical connectivity*, J. Neurosci., 18 (1998), pp. 5908–5927.

[101] H. Tuckwell, *Introduction to Theoretical Neurobiology*, Cambridge Univ. Press, Cambridge, 1988.

[102] C. Villani, *A review of mathematical topics in collisional kinetic theory*, Handbook of mathematical fluid dynamics, 1 (2002), pp. 71–305.

[103] ——, *Entropy production and convergence to equilibrium*, in Entropy methods for the Boltzmann equation, Springer, 2008, pp. 1–70.

[104] X. Wang, *Synaptic basis of cortical persistent activity: The importance of NMDA receptors to working memory*, J. Neurosci., 19 (1999), pp. 9587–9603.

[105] W. Wilbur and J. Rinzel, *A theoretical basis for large coefficient of variation and bimodality in neuronal interspike interval distributions*, J. Theor. Biol, 105 (1983), pp. 345–368.